AMERICAN UNIVERSITY OF BEIRUT

ADAPTATION TO SALTWATER INTRUSION ALONG HIGHLY URBANIZED COASTAL AREAS: A DSS-BASED SOCIOECONOMIC PERSPECTIVE

by
GRACE KAMAL RACHID

A dissertation
submitted in partial fulfillment of the requirements
for the degree of Doctor of Philosophy
to the Department of Civil and Environmental Engineering
of the Maroun Semaan Faculty of Engineering and Architecture
at the American University of Beirut

Beirut, Lebanon
May 2020

AMERICAN UNIVERSITY OF BEIRUT

ADAPTATION TO SALTWATER INTRUSION ALONG HIGHLY URBANIZED COASTAL AREAS: A DSS-BASED SOCIOECONOMIC PERSPECTIVE

by

GRACE KAMAL RACHID

Approved by:

Dr. Mutasem El-Fadel, Professor and Chairperson — Advisor
Civil and Environmental Engineering (AUB)

Rami Zurayk

Dr. Rami Zurayk, Professor and Chairperson — Member of Committee
Landscape Design and Ecosystem Management, AUB (Chair)

Dr. Ibrahim Alameddine, Assistant Professor — Member of Committee
Civil and Environmental Engineering, AUB

Dr. Majdi Abou Najm, Assistant Professor — Member of Committee
Land, Air and Water Resources, University of California – Davis (External)

Dr. Song Qian, Associate Professor — Member of Committee
Environmental Sciences, The University of Toledo (External)

Date of dissertation defense: May 13, 2020

AMERICAN UNIVERSITY OF BEIRUT

THESIS, DISSERTATION, PROJECT RELEASE FORM

Student Name: Rachid Grace Kamal
Last First Middle

○ Master's Thesis ○ Master's Project ● Doctoral Dissertation

[X] I authorize the American University of Beirut to: (a) reproduce hard or electronic copies of my thesis, dissertation, or project; (b) include such copies in the archives and digital repositories of the University; and (c) make freely available such copies to third parties for research or educational purposes.

[ ] I authorize the American University of Beirut, to: (a) reproduce hard or electronic copies of it; (b) include such copies in the archives and digital repositories of the University; and (c) make freely available such copies to third parties for research or educational purposes
after:
One ---- year from the date of submission of my thesis, dissertation, or project.
Two ---- years from the date of submission of my thesis, dissertation, or project.
Three ---- years from the date of submission of my thesis, dissertation, or project.

GRACE RACHID 22 MAY 2020

Signature Date

This form is signed when submitting the thesis, dissertation, or project to the University Libraries

ACKNOWLEDGEMENTS

A long journey towards the culmination of this research, which wouldnot have happened without the support, care, motivation and patience of many.

No words can define the gratitude to my advisor and mentor Prof. Mutasem El-Fadel for years and years of guidance and support as well as for multiple research opportunities and fulfilling work experiences. Special recognition and thanks to Assisant Prof. Ibrahim Alameddine for his invaluable guidance, follow-up, time and support throughout my research development and its implementation. A heartfelt thank you to all the members of my thesis committee namely Prof. Rami Zurayk, Associate Professor Majdi Abu Najm and Professor Song Qian for their enriching and constrctive feedback and suggestions. Thank you to Assistant Prof. Joanna Doummar, Dr. Elsy Ibrahim , Prof. Mahmoud Hindi and Prof. Salah Sadek for their invaluable contributions throughout the undertaking of this research.

Further, I would like to thank Dr. Lucy Semerjian and Mr. Joseph Daoud at the Environmental Engineering Research Center for facilitating laboratory analysis as well as fellow PhD students and MS students for their kind assistance and contributions in the field and lab work of this research. Special recognition to Mr. Assem Abou Ibrahim of the Lebanese Petroleum Administration for his support and understanding. A heartfelt thank you to my friends and loved ones for always being there for me.

I would like to acknowledge the International Development Research Center (IDRC) of Canada for funding this research (Grant No. 106706-001) at the American University of Beirut. Special thanks are extended to Dr. Charlotte Macalister at IDRC for her support.

Last but not least, I would like to thank my family and particularly my parents, Kamal and Lina, who patiently bear the ups and downs of this research while unconditionally supporting me throughout.

AN ABSTRACT OF THE DISSERTATION OF

Grace Kamal Rachid for Doctor of Philosophy
Major: Environmental and Water Resources Engineering

Title: Adaptation to saltwater intrusion along highly urbanized coastal areas: A DSS-based socioeconomic perspective

Saltwater intrusion (SWI) is a global coastal problem caused by aquifer over-pumping, land-use change, and potential climate change impacts. SWI is a threat to coastal aquifers worldwide by rendering groundwater quality not viable for its intended use. Understanding SWI and its impact is indispensable for informed decision-making on aquifer management. Despite advances in SWI research, it remains challenging to detect, quantify and manage. Given the complex pathways that lead to SWI, coastal urban areas with poorly monitored aquifers are in need of simple, robust, and probabilistic decision support models that can assist in better understanding and predicting SWI, while also exploring effective means for sustainable aquifer management.

This research targets the Eastern Mediterranean, an area highly vulnerable to increased saltwater intrusion into coastal fresh water aquifers. It examines the main drivers of SWI, assessing the relative impacts of local anthropogenic activities and projected global climate change. The research appraises the spatial and temporal dynamics of SWI and evaluates the associated socio-economic burden related to the degradation of groundwater resources used for domestic purposes. It attempts to estimate the risk of SWI through constructing the interplay of natural, anthropogenic and climatic drivers in view of adaptation and mitigation potentials as well as socio-economic and political conditions. This research further develops a Bayesian Belief Network (BBN) to account for the complex physical and geo-chemical processes leading to SWI while linking the severity of the SWI to the associated socioeconomic impacts. The BBN is further expanded into a dynamic Bayesian network (DBN), to assess the temporal progression of SWI and to accurately compound uncertainties over time. Pilot demonstrations mainly targeted a highly urbanized metropolitan as well as a densely populated city, a suburb and an agricultural area.

Results exhibited indications of advanced SWI in the pilot areas, albeit with spatial and temporal heterogeneity. Results also showed that the future impacts of climate change were largely secondary as compared to the persistent water deficits hinting towards the importance of demand management. Results highlighted the socioeconomic burden associated with the different scenarios including costs and benefits of adaptation strategies. It shows that while supply and demand management can pause the progression of salinity in the aquifer, the potential for reducing or reversing salinity is not apparent.

Through building a robust representation of drivers and impacts of SWI and the socioeconomic implications and policy options, the constructed DBN acts as an effective decision support tool to aid coastal managers towards sustainable aquifer management. While the research results provided valuable outcomes for the Eastern Mediterranean region, it equally conveyed to the global community lessons learnt on saltwater intrusion drivers, dynamics, implications and adaptation potential as well as a modular DBN-based decision support tool easily transferable to other aquifers.

Keywords: saltwater intrusion; dynamic Bayesian network; decision support tool; climate change; adaptation; socioeconomic burden;

CONTENTS

Appendices

ILLUSTRATIONS

Figure Page

TABLES

ABBREVIATIONS

AUB	American University of Beirut
BN	Bayesian Network
BDN	Bayesian Decision Network
CPT	Conditional Probability Tables
DAG	Direct Acyclic Graph
DBN	Dynamic Bayesian Network
GQI	Generalized Quality Index
MADM	Multi-attribute Decision Making
MAR	Managed Aquifer Recharge
PSS	Prediction Scaled Sensitivity
SWI	Saltwater intrusion
SWOT	Strengths, Weakenesses, Opportunities and Threats

To Beirut,

CHAPTER 1

INTRODUCTION

1.1 Background

Landward seawater intrusion into coastal aquifers, known as saltwater intrusion (SWI), is primarily caused by aquifer over-pumping and land-use change (Singh, 2014; Werner et al., 2013). SWI is governed by coastal hydrostatic pressures at the hydraulic interface between saline and freshwater. Under undisturbed conditions, a state of dynamic equilibrium between freshwater and seawater is maintained where the hydraulic gradient pushes freshwater towards the sea. As a result of prolonged changes in coastal groundwater levels due to pumping, land-use change, climate variations or sea-level fluctuations, this hydraulic gradient is reversed, resulting in seawater infringement into the aquifer (Bear, 1979; Simmons et al., 2001). Because saltwater is denser and has a higher water pressure, it can push inland beneath the freshwater, where a zone of transition between the lighter fresh aquifer water flowing to the sea and the heavier seawater forms (Bear 1979). As drivers of SWI persist, the transition zone rises, the interface moves landward, and wells located nearby become saline and unusable (Custodio, 1987).

SWI is a continuously increasing threat to urban coastal communities worldwide through contaminating freshwater aquifers and impairing their productive as well as consumptive value (Selmi, 2013; Fatoric & Chelleri, 2012; Park et al., 2012; Zhang et al., 2011; Standford & Pope, 2010; Sales, 2009; Conrad & Roehl, 2007; Bobba, 2002). Case studies documenting worldwide occurrence of SWI, albeit with varying intensity, in urban coastal areas are widely reported i.e. in New Zealand (EnviroLink, 2011), China (Zhang et al., 2011), Philippines (Sales, 2009), Korea (Park et al., 2012), US (Conrads & Roehl, 2007; Sanford & Pope, 2010), Bangladesh (Rahman, 2010), Taiwan (Lu, 2004), India (Bobba, 2002) and others. The Mediterranean Basin is no exception where freshwater aquifers along its northern, southern and eastern coasts are suffering from SWI that is affecting groundwater resources rendering them unfit for domestic, agricultural, recreational or industrial use i.e. in France (de Montety et al., 2008), Italy (Capaccionoi et al., 2005), Spain (Fatoric & Chelleri, 2012; Duque et al., 2008), Turkey (Alpar, 2009; Odemis et al., 2006; Demirel, 2004), Syria (Abu Zakhem et al., 2007), Lebanon (El-Fadel et al. 2017; El-Moujabber et al., 2006; Saadeh, 2008), Gaza (Selmi, 2013), Israel (Paster et al., 2006; Sivan et al., 2005), Egypt (El Shinnawy & Abayazid, 2011), Tunisia (Kouzana et al., 2010; Fedrigoni et al., 2001), Libya (El Hassadi, 2008) and Morocco (El Yaouti et al., 2009).

Research on SWI processes and biophysical characteristics relies on geochemical and geophysical methods as well as on laboratory experiments, hydrodynamic techniques and modeling (Werner et al., 2013; de Montetyet al., 2008; Boluda-Botella, et al., 2008; Duque et al., 2008). Geochemical techniques target the distinct difference in the chemical composition between freshwater and seawater to assess the occurrence, dynamics and intensity of SWI (Stuyfzund, 1989; Howard & LLoyd, 1983; Appolo & Postma, 2005; Piper, 1944). Distinctive indicators used include single parameter analysis of TDS, EC and chloride, symptomatic hydro-chemical ratios i.e. Na+/Cl-, Cl-/Br-, Ca2+/Mg2+ in addition to ionic deltas, base exchange and chloro-alkai indices and hydro-chemical facies that identify water types and represent SWI affected processes i.e. ion exchange, carbonate dissolution and sulfate reduction (Wang & Jiao, 2012; Seckin, et al., 2010; Kouzana, et al., 2009; de Montetyet al., 2008; Stuyfzund, 2008; Yaouti et al., 2009; Pulido-Lebeouf, 2004). Multivariate analysis, mainly principal component analysis (PCA) and hierarchical cluster analysis (HCA), geo-spatial analysis, particularly geo-statistical interpolation, and environmental tracers are often coupled with hydro-geochemical techniques (Zghibi et al., 2014; Batayneh et al., 2014; Tomaskiewicz et al., 2014; Villegas et al., 2013; Guler, et al., 2012; Mondal et al., 2010). The use of the GALDIT index, a geospatial numerical ranking tool based on the DRASTIC index, to assess and map aquifer vulnerability to SWI is common, relying on the aquifer type, hydraulic conductivity, depth of ground water level, distance from the shore, existing status of sea water intrusion, and thickness of the aquifer (Lobo Ferreira et al., 2005; Savariya & Bhatt, 2014; Sophiya & Syed, 2013).

Environmental tracers are relied upon to identify salinity sources and estimate the water age where the Br-/Cl- and 87Sr/86Sr ratios as well as the δ18O, δ2H, 3H, δ11B and 14C isotopes are most widely used (Alcala & Custodiao, 2008; Bouchaou, et al., 2008; Han, et al., 2011; Sivan, et al., 2005). Geophysical techniques rely on geo-electrical methods, primarily the electrical resistivity and the time domain electromagnetic induction (TEM) methods which measure resistivity, the inverse of electrical conductivity, to indicate areas of saline water based on the large electrical resistivity contrast between seawater (0.2 Ωm) and freshwater (> 5 Ωm) (Werner et al., 2013; Kirkegaard, et al., 2011; Yaouti et al., 2009; Gibnsberg & Levanon, 1976, Bear et al., 1999).

Hydrodynamic and modeling techniques aim to represent and understand SWI through mimicking the saline-freshwater interface, the multiple physical processes controlling SWI, the transport of salt and the general hydrological flow in aquifers. Modeling techniques generally consists of two main approaches: the interface models, predominantly solved through analytical solutions, and the variable density models, mainly resolved through numerical solutions (Ghyben, 1888; Herzberg, 1901; Cooper, 1959). However, 'only variable density models provide salinity predictions that can then be compared to field salinity measurements' (Werner et al., 2013); hence they are relied upon for understanding real world SWI cases as well as future predictions (Koussis et al., 2012; Abed-ElHamid & Javadi, 2012). Numerous codes, that capture the physical processes to varying degrees, have been developed combining variable density flow and solute transport equations where SEAWAT and SUTRA remain the most used codes (Cherubini & Pastore, 2011; Abdullah, et al., 2010; El-Bihery, 2009; Lin, et al., 2009; Nishikawaet al., 2009; Pool & Carrera, 2010; Praveena & Aris, 2010).

Nevertheless, the choice of technique(s) used to detect and study salinity is highly driven by the availability of data needed, the conditions required for reliable results, the tolerability of the associated uncertainty and error, as well as the objective of interest. Despite advances in SWI investigations, simulations and predictions, SWI remains difficult to monitor, examine and manage due to the complex influences of hydro-geochemical reactions, shoreline geomorphology and aquifer flow among others in addition to the uncertain effects of the interplay between SWI drivers (Melloul & Goldenberg 1997; Weneret al. 2013). Thus the need for simple, robust, and stochastic approaches and decision models that can assist in better understanding and predicting SWI under data-sparsity and compounded uncertainty. Accordingly, there is an increasing trend of using Bayesian Belief Networks (BBN) and similar influence diagrams i.e. neural networks, in the realm of water management and risk assessment, adaptation planning and management (Phan et al. 2016). Bayesian networks can model real-world decision problems using theoretically sound methods of probability theory and decision theory, able to handle uncertainty and lack of data in ecological modeling, natural resource management as well as water/groundwater management (Marcot et al. 2019; Alameddine et al., 2011; Ames, 2002; Borsuk et al., 2004; Bromley et al., 2003); however their use in cases of SWI and management as well as in climate change adaptation issues is still nascent (Sperretto et al. 2017; Catenacci & Giupponi, 2013; Molina et al. 2010; 2013; Hall & Twyman, 2005).

Understanding, managing, mitigating or adapting to SWI have become integral to sustainable coastal development and management with concerns mounting particularly in view of the synergy between the seemingly inevitable climate change impacts and the ever-increasing human-induced pressures (Nicholls et al., 2008). Climate change is expected to exacerbate SWI, induced by the projected sea level rise and aggravated, at times and locations, with increased temperatures (i.e. increased demand for water) and reduced precipitation (i.e. reduced surface water available for aquifer recharge) (Kumar et al. 2007; IPCC, 2007; 2014). The importance of planning to manage and adapt to SWI lies in protecting the biophysical elements (i.e. subsurface aquifers and groundwater quality) and curtailing associated socioeconomic burdens on coastal communities (i.e. the impairment of an important water source, damages to infrastructures, fixtures and water installations, the reduction in crop productivity and soil salinization as well as costs of groundwater treatment and alternative water sources and health problems). However, as coastal aquifer hydrodynamics and climate change impacts remain challenging to predict (Post VEA, 2005; Sanford & Pope, 2010; Werner et al., 2013) and as the interaction between impacts of global climate change and local environmental impacts (i.e. urbanization and land use and land cover remains ambiguous) remain difficult to quantify, coastal managers will need to plan and act under incomplete knowledge, complexity and uncertainty to cope with these impacts to protect the economic, social, and environmental security of coastal communities (Tribbia & Moser, 2008).

This research targets the assessment and management of saltwater intrusion along the Eastern Mediterranean region (Turkey, Syria, Lebanon, Occupied Palestinian Territories, Gaza, Cyprus and Egypt) with in-depth studies of drivers and the spatial and temporal distribution of SWI in aquifers under different land use and land cover patterns and water deficit conditions along the coast of Lebanon. It aims at estimating the risk of SWI in data-sparse aquifers through constructing the interplay of natural, anthropogenic and climatic drivers in view of adaptation and mitigation potentials as well as socio-economic and political conditions. The research builds a robust representation of the drivers and impacts of SWI and the associated socioeconomic implications as well as policy options. It develops a modular BBN to account for the complex physical and geo-chemical processes leading to SWI as well as link the severity of the SWI to the associated socioeconomic impacts. The BBN is further expanded into a dynamic Bayesian network (DBN) to assess the temporal progression of SWI and to accurately compound uncertainties over time which acts as an effective decision support tool to aid coastal managers towards sustainable aquifer management. The DBN is tested and validated in a pilot aquifer underlying the highly urbanized water-stressed coastal metropolitan area of Beirut.

1.2 Research Objectives

The overall objective of the research is to develop a platform that facilitates decision making towards SWI management and adaptation through socioeconomic evaluation of the impacts of SWI as well of potential policy options for adaptation under multiple SWI projections. The sub-objectives towards the realization of such a platform consist of:

1. Appraise the baseline groundwater quality in the study area, the occurrence of SWI and its spatial and temporal variability.
2. Evaluate the most effective methods and techniques for the assessment of SWI in data scarce and resource scarce aquifers.
3. Estimate the risk of SWI in data-sparse aquifers through re-constructing the interplay of natural, anthropogenic and climatic drivers in simple semi-quantitative models.
4. Evaluate the relative and synergistic impacts of climatic and anthropogenic drivers on SWI occurrence and intensification under different land use land cover patterns, seasonality and water deficit conditions.
5. Develop a Bayesian belief network that links the drivers, processes and impacts of SWI together with the associated socioeconomic implications as well as policy options towards probabilistic quantification of relationships and impacts while accounting for data-scarcity and associated uncertainties.
6. Synthesize the above functionalities into a decision support tool for decision making on the management of SWI and overall sustainable aquifer management based on a Dynamic Bayesian Belief network (DBN).

1.3 Research Innovation

While ongoing SWI research focuses on understanding the process of SWI and improving SWI simulation capabilities, decision makers, coastal planners and affected communities alike are left incapable of effective action due to the limited research on adaptation to and management of SWI. This is mainly due to the multiple layered processes involved as well as the multilayered associated uncertainties, which is further inflated in fractured media and data-scarce areas. The proposed research closes the gap between what scientists know and what coastal planners and decision makers need to know to plan to adapt to SWI, particularly in data scarce aquifers.

The proposed research constitutes a first attempt of decision making on SWI lifecycle including adaptation through a decision support tool. It is also a first attempt of using Bayesian networks, including dynamic BN, to construct, represent, assess and manage the SWI drivers, process and associated impacts. This research proved that a DBN can successfully represent the complex and challenging system of SWI multilayered drivers and impacts while catering for the dynamics and uncertainties associated with the data sparsity and imperfect knowledge while remaining a user-friendly tool.

The proposed research provides a comprehensive platform for decision makers to understand the process of SWI and the relative roles of its drivers, quantify and value the socioeconomic burden of SWI and evaluate the socioeconomic impacts of adaptation, all of which are fundamental for planning for effective adaptation. Addressing adaption by using a DBN improves the transparency and accountability of the decision-making process, which aids in providing an environment conducive to consensus building on adaptation policy and action plans. Evidently, the potential significance of the proposed research spreads across several beneficiary stakeholders including the decision maker (relevant governmental authorities, water establishments, and coastal planners), the end-user (coastal communities) and end-user/consumer advocates (relevant governmental units, consumer protection services, etc.). This research presents a tool, the DBN, that is easily transferable to other aquifers as the underlying conceptual model is developed as a global model.

1.4 Research Framework

The conceptual framework of the proposed research is summarized in Figure 1-1. The scope of work adopts a multi-disciplinary research methodology combining quantitative and qualitative approaches aiming to document the existing subsurface water quality conditions, analyse and interpret the anthropogenic and climatic factors that influence these conditions, quantify the associated socioeconomic burden under different conditions, identify and assess current and potential adaptation and mitigation measures towards the development of a decision support tool based on a dynamic Bayesian network for adaptation to saltwater intrusion.

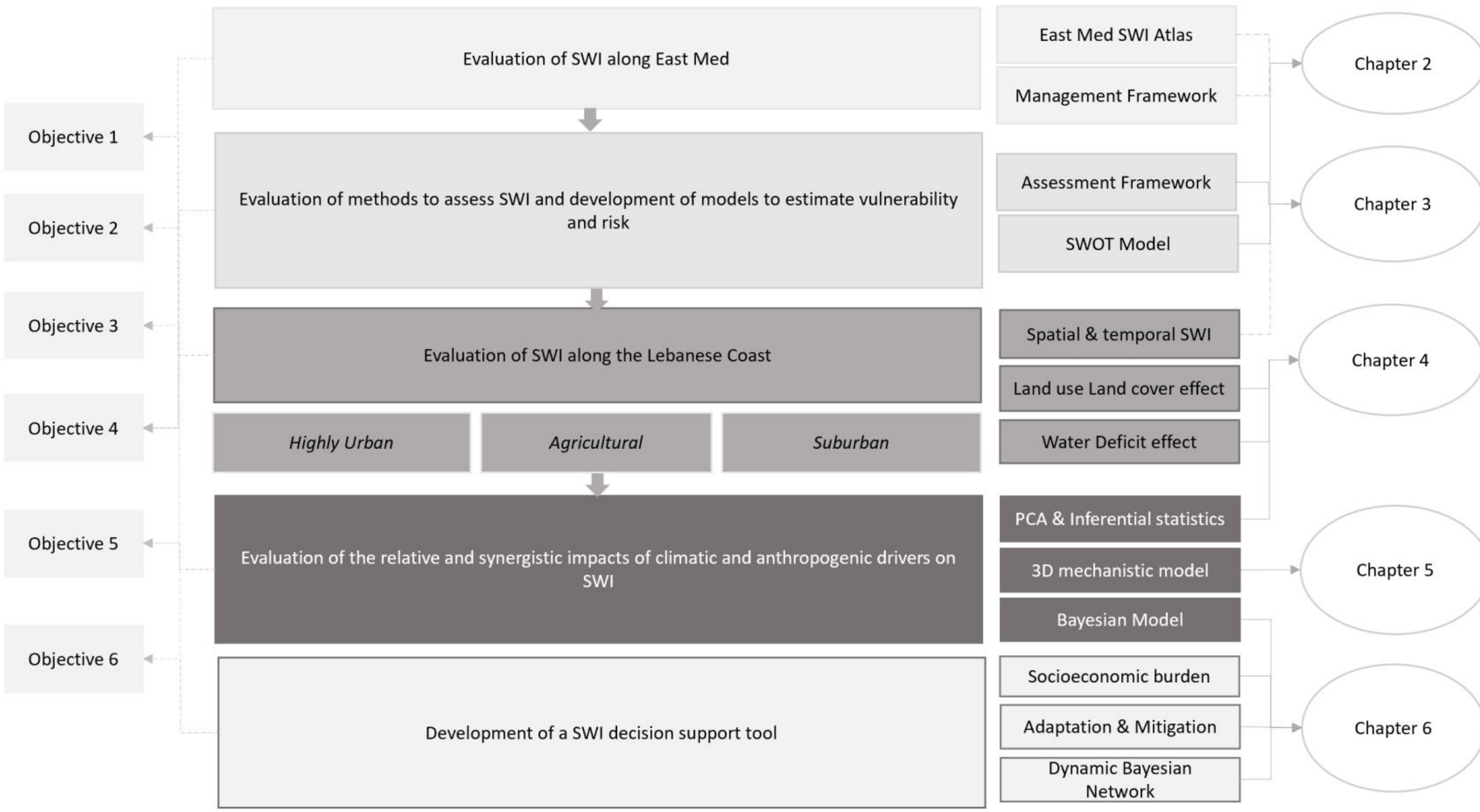

Figure 1-1 Conceptual Research Framework

1.5 Dissertation Structure

Chapter 2 explores the occurrence and intensity of SWI along the Eastern Mediterranean coastline to provide an overview of the current SWI conditions in the region and depicts findings through an indicative atlas. In addition, it scrutinizes the mitigation measures and adaptation strategies adopted by East Med countries to manage coastal aquifers and control SWI and proposes an inter-country adaptation and mitigation framework for the management of SWI. Chapter 2 also aims at estimating the risk of SWI in data-sparse aquifers through constructing the interplay of natural, anthropogenic and climatic drivers in view of adaptation and mitigation potentials as well as socio-economic and political conditions in a semi-quantitative Strengths, Weaknesses, Opportunities, and Threats (SWOT) model that was developed and validated using data from 26 aquifers in the East Med.

Chapter 3 examines commonly used methods to assess the SWI towards the development of a SWI assessment framework applicable in coastal data-sparse aquifers underlying urban areas. A matrix of complexity-functionality criteria was developed to evaluate the methods and then was validated at the pilot aquifer of the highly urbanized, highly populated metropolitan of Beirut, Lebanon.

Chapter 4 applies the assessment framework to other pilot aquifers along the Lebanese Coast to assess the impact of seasonality, water deficit and land use and land cover on SWI. Additionally, inferential statistics were used to identify principal components that explain salinity and quantify relations between drivers and impacts.

Chapter 5 examines the relative impacts of anthropogenic interventions and global climate change on the dynamics of saltwater intrusion (SWI) in highly urbanized coastal aquifers using a multi-objective 3D variable-density flow and solute transport model.

Chapter 6 presents the development of a modular Bayesian Belief Network (BBN) to account for the complex physical and geo-chemical processes leading to SWI while linking the severity of the SWI to associated socioeconomic impacts in data-sparse aquifers. The BBN is further expanded into a dynamic Bayesian network (DBN) to act as an effective decision support tool to aid coastal managers towards sustainable aquifer management. The DBN allows the assessment of the temporal progression of SWI and uncertainties over time as well as the estimation of socioeconomic burdens associated with SWI scenarios and adaptation interventions. It was tested and validated in a pilot aquifer underlying a highly urbanized water-stressed coastal metropolitan area along the Eastern Mediterranean coastline (Beirut, Lebanon).

Chapter 7 presents a synthesis of the research and concludes with challenges to address in future work.

Chapter 8 lists the bibliographic citations used throughout the dissertation.

CHAPTER 2

REGIONAL REVIEW OF THE STATUS AND RISK OF SEAWATER INTRUSION AND THE POTENTIAL FOR ADAPTATION ALONG THE CASE OF THE EASTERN MEDITERRANEAN: A SEMI QUANTATIVE SWOT MODEL

2.1 Introduction

Efforts towards the identification, assessment, and management of saltwater intrusion (SWI) into coastal aquifers have relied on multiple techniques and methods including geochemical and geophysical analysis, environmental tracers, laboratory experiments, hydrodynamic techniques, as well as physical modeling (Zghibi et al., 2014; Batayneh et al., 2013; Tomaskiewicz et al., 2014; Villegas et al., 2013; Guler, et al., 2012; Mondalet al., 2010; Rachid et al. 2017; Werner et al., 2013; de Montety et al., 2008; Boluda-Botella, et al., 2008; Duque et al., 2008; Sophiya & Syed, 2013; Cobaner et al., 2012; El Shinnawy & Abayazid, 2011; Harbor, 1994; Purandara, et al., 2010). In parallel, groundwater vulnerability assessment models e.g. GALDIT, DRASTIC and EPIC have been increasingly used to quantify, assess and map the vulnerability of aquifers to SWI based on data layers covering hydrogeological and hydrochemical characteristics of the aquifers under study (Moazamnia et al., 2020; Elewa et al. 2013; Gogu et al. 2003; Milnes 2011; Li et al. 2018; Momejian et al. 2019; Fijani et al. 2013; Shirazi et al. 2012; Klassen & Allen 2017; Shirazi et al. 2012; Rangel-Medina et al. 2004). Yet, almost all of these techniques are data intensive and require significant resources aimed towards collecting the needed input data. Unfortunately, these resources are often not readily accessible in data scarce and under-studied aquifers, especially in developing countries. Due to the multiple factors, including the biophysical characteristics, the geology and aquifer characteristics, climatic factors and anthropogenic factors as well as the associated uncertainty and synergy, that define the scale of SWI at any specific site, the quantification of the risk in data scarce aquifers remains challenging.

This study proposes a semi-quantitative SWOT model to assess the risk of aquifers to SWI in data scarce and under-studied aquifers along the Eastern Mediterranean coastline. The model attempts to account for the interaction of the natural, anthropogenic, and climatic drivers, while also accounting for the potential impacts of the socio-economic and political conditions at the local or national levels, all of which define the vulnerabilities and threats at play at the aquifer level. The model was tested on 26 aquifers along the Eastern Mediterranean region, an area highly vulnerable to increased SWI due to its heavy reliance on groundwater resources and its limited adaptive capacity towards management of the consecutive impacts (WB 2010). The study concludes with a framework to inform decision making towards sustainable aquifer management and SWI control.

2.2 Methodology

2.2.1 SWI along the East Med: identification of drivers

A comprehensive review and synthesis of the accessible literature on SWI along the Eastern Mediterranean region was undertaken in order to identify some of the studied affected aquifers and to be able to characterize the main drivers of SWI (Figure 2-1). The study area covered the coastal region of Egypt, Israel, Palestine, Lebanon, Syria, Turkey and Cyprus. We targeted published data for the period between 2000 and 2019 in an attempt to represent the recent status and drivers of salinization in the study area. The occurrence and intensity of the reported SWI across the aquifers was assessed and synthesized into an atlas that provides a generalized comparative representation of salinity along the entire study area. Given the large variability in the type and quality of the reported salinity data between the aquifers and by country, we opted to use the widely recognized salinity indicators (TDS, Cl- and EC) to classify the groundwater quality of the coastal aquifers into slightly, moderately, highly or very highly saline (Table 2-1). Given the limited information on the aquifers' biophysical and geological characteristics such as domain, boundaries, type, and the location of the seawater-freshwater interface, the spatial representation of the aquifers was limited to their coastal boundary and as such the maps may not necessarily refect the exact spatial extent of the aquifer.

Table 2-1 Classification of water based on chloride, TDS, and EC concentrations (Konikow & Reilly 1999)

Class	**Cl (ppm)**	**TDS (ppm)**	**EC**
Fresh groundwater	<100	0-500	<700
Slightly saline groundwater	100 – 250	500-1500	700-2000
Moderately saline groundwater	250 - 500	1500-7000	2000-10000
Highly saline groundwater	500 – 1000	7000-15000	10000-25000
Very highly saline groundwater	1000 – 10000	15000-35000	25000-45000
Seawater	>10000	>35000	>45000

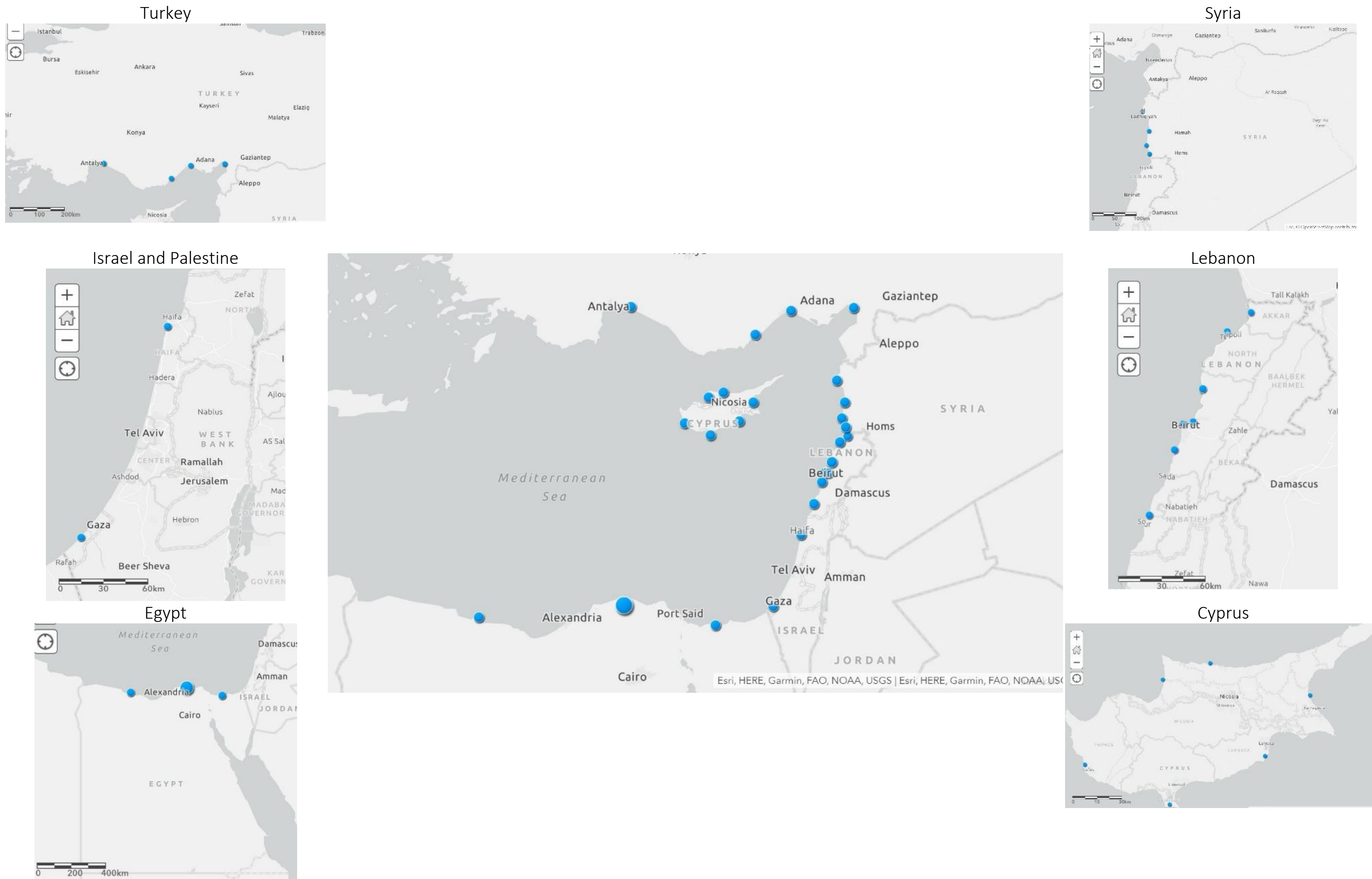

Figure 2-1 The study area: The East Mediterranean coastline (map not to scale) (maps to be replaced with esri base maps

Globally, research on the main drivers of SWI have identified a number of anthropogenic and climatic drivers (Safi et al. 2017; Selmi 2013; Cobaner et al. 2012; Ivkovic et al. 2012; Chang et al. 2011; Ranjan et al. 2006; Scanlon et al. 2005). Population growth and land development along the coastline are the two main facets of urbanization and constitute the main anthropogenic inducers of SWI (Safi et al. 2017; Cobaner et al. 2012; Ranjan et al. 2006; Scanlon et al. 2005). Population growth increases water demands and often intensifies the pressure placed on the available groundwater resources, while land development can reduce natural groundwater recharge due to land use and land cover (LULC) changes (Dawes et al. 2012; WB 2010; Ranjan et al. 2006; Doll & Florke 2005). Moreover, excessive groundwater abstraction can modify local subsurface hydrodynamics and promote saline water infringement into the freshwater aquifer when abstraction overcomes the rate at which the aquifer is being replenished (Selmi 2013; Koussis et al. 2012; Cobaner et al. 2012; Sherif et al. 2012; Ergil 2001). In parallel, climatic drivers also have a strong impact on SWI given their forcings on the water cycle. Note that their impacts on SWI are expected to be accentuated by climate change due to the projected changes in precipitation patterns, increase in temperatures, and the rise of sea levels (Bates et al., 2008; Jackson et al., 2011; Neukum & Azzam, 2012; Doll & Florke 2005). Future climatic predictions point towards a drier future in the Middle East with decreased runoff and increased frequency and intensity of drought (IPCC 2013) highlighting an “Extremely high” risk to climate change in the Eastern Mediterranean (Satta et al. 2017).

To overcome these anthropogenic and climatic drivers, countries worldwide have implemented a wide range of mitigation measures and adaptation strategies, either at the country or aquifer level, to halt or reverse SWI and potentially alleviating its impacts

(Abarca et al., 2006; Luyun et al., 2009; Pool & Carrera, 2010; UNFCCC, 2011; 2010; Masciopinto, 2013). The success of these measures and plans have been shown to be a function of the governance, policy making, socioeconomic, political, and water resources management capacities of each country (Saadeh, 2009; Giordana & Montginoul, 2006; El-Fadel et al. 2000). Accordingly, the identified drivers of SWI, for the purpose of this research, include the anthropogenic, climatic and natural drivers as well as the adopted or planned mitigation measures and adaptation strategies in light of the existing socioeconomic and political conditions within the study area.

2.2.2 SWOT analysis and definition of model parameters

SWOT analysis is a qualitative examination that aims to identify the main factors at play in a specific environment in order to improve our understanding of the process under study and to better formulate follow-up strategies (Kajanus et al., 2012; Chang and Huang, 2006). In this study, the evaluation criteria were determined and categorized into key internal (strengths and weaknesses) and external (threats and opportunities) factors that can promote or reduce SWI in coastal aquifers. Internal factors were defined as the efforts, measures and steps that are taken by the responsible authorities to recognize, prevent, manage, mitigate and adapt to SWI whereby their presence or absence signifies strengths or weaknesses, respectively. On the other hand, external factors represented the factors outside of the control of the responsible authorities but for which they can perceive either as an opportunity to benefit from in their pursuit for achieving sustainable aquifer management or as a threat that hinders their aspired management. To further enhance the SWOT analysis, a semi-quantitative approach was implemented by coupling SWOT with multi-attribute decision making (MADM) analysis. The use of MADM allows for the systematic evaluation of the SWOT factors and the commensuration of their intensities (Kajanus et al., 2012; Kurtilla et al., 2000). Coupling SWOT with MADM analysis has been increasingly being adopted and has been reported to provide more robust results as compared to the qualitative examinations of SWOT (Rachid et al. 2013; Svekli et al., 2012; Gao and Peng, 2011; Amin et al., 2011; Lee and Lin, 2008). In this work, the coupling of SWOT and MADM consisted of first qualitatively assessing the aquifers based on a set of defined evaluation criteria that were categorized into internal and external factors. This was then followed by scoring the aquifers based on a proposed standardized scale that was defined for each of the evaluation criteria.

2.2.2.1 SWOT Model Development

Based on the literature, the selected criteria for the semi-quantitative SWOT analysis included the physical, anthropogenic, and climatic drivers as well as the main socioeconomic indicators and governmental instruments related to the SWI mitigation and adaptation (Safi et al. 2017; Selmi 2013; Cobaner et al. 2012; Ivkovic et al. 2012; Chang et al. 2011; Ranjan et al. 2006; Scanlon et al. 2005; Dawes et al. 2012; WB 2010; Doll & Florke 2005; Sherif et al. 2012; Koussis et al. 2012; Ergil 2001; Bates et al., 2008; Jackson et al., 2011; Neukum & Azzam, 2012; Ferguson & Gleeson 2012; Payne 2010). These indicators were then defined as either internal or external factors. The internal factors (I) included (I1) physical drivers (geology, groundwater recharge; water stress); (I2) anthropogenic drivers (population growth and density, consumption rate, urbanization, land use); as well as (I3) government instruments for mitigation and adaptation (supply and demand management measures, nonconventional resources, integrated planning, regulations). The considered external (E) factors included (E1) climatic drivers (precipitation, temperature, sea level rise); and (E2) socioeconomic indicators (GDP per capita, stability, political will) (Table 2-2). The data for the external factors was only available at the country level (Table 2-2) due to the nature of the factor (e.g. political will) or due to limitations in data accessibility and availability (e.g. projected temperature increase per aquifer), as such aquifers of the same country reported the same score on the external factors.

For each of the selected indicators, a set of ordinal categories was defined with an emphasis on highlighting the differences between the aquifers in the study area (Table 2-2). The scores per indicator ranged between 5 and 20, with 5 representing 'good standing' and 20 representing major weaknesses and threats (Table 2-2). The definition of the categories per indicator and the assignment of scores were based on the literature and subjected to an expert elicitation process where five subject matter experts were consulted to validate the indicator categories and fine-tune the scoring system. The raw internal and external total scores for each aquifer were determined separately by summing the scores of their respective indicators (internal score alone and external score alone). These raw scores were then centered around the mean values of each of the internal and external factors calculated across all aquifers. The centered scores were then plotted on a SWOT numerical matrix, where the x-axis represents the internal assessment (strengths or weaknesses) and the y-axis represent the external assessment (opportunities or threats). The resultant axes form four quadrants, with the origin representing a hypothetical aquifer that has an average internal and external score for the study area. Quadrant I, top right, represents positive scores on both internal (strengths) and external (opportunities) factors, reflecting a positive sustainable environment that is less vulnerable to SWI, hence it is expected to correspond to fresh aquifers or those with a slight risk of SWI. Quadrant II, top left, reflects positive scores on the external (opportunities) factors, which is promising as it reflects an enabling environment if internal factors are also positive, however Quadrant II reflects negative scores on the internal (weaknesses) factors, which represent the major drivers of SWI that the country/aquifer has an ability to influence. Accordingly, aquifers in this quadrant are considered to represent a high risk of SWI due to the negative scores on the internal factors. Quadrant III, bottom left, reflects negative scores on both the internal and the external factors; hence these aquifers suffer from weak or lack of efforts, measures and steps to recognize, prevent, manage, mitigate and adapt to SWI and exist in environments that disable the sustainable management of SWI. Quadrant IV, bottom right, reflects positive scores on internal factors which indicates that efforts, measures and steps exist to recognize, prevent, manage, mitigate and adapt to SWI however due to the negative scores on the external factors, which limits the achievement of sustainable management of SWI, these aquifers are considered to have a moderate SWI risk. The risk is considered moderate relative to the risk associated with Quadrant II and III. A radar plot was used to illustrate the semi-quantitative SWOT results of all aquifers per country

2.2.3 Model Validation and Testing

The proposed semi-quantitative SWOT model was applied to 26 aquifers along the East Med coastline that are known to be experiencing different levels of SWI. The performance of the semi-quantitative SWOT model was then assessed by comparing the correspondence between the aquifer salinity level (Table 2-1) as reported in the reviewed literature versus the SWOT quadrant that each aquifer occupied (Table 2-3). Contingency table analysis was used to assess if the SWOT estimated risk of SWI showed a statistically significant association with the salinity-level classification (95% confidence level). This was assessed using both the Chi square and Fischer’s tests as well as the non-parametric Wilcoxon signed rank test. All statistical analyses were undertaken using XLSTAT (XLSTAT 2019).

Table 2-2 Alignment of water classification with SWOT quadrants for performance analysis

Class	Cl (ppm)	TDS (ppm)	EC	SWOT Quadrant	Numeric label [a]
Fresh groundwater	<100	0-500	<700	I	1
Slightly saline groundwater	100 – 250	500-1500	700-2000	I	
Moderately saline groundwater	250 - 500	1500-7000	2000-10000	IV	2
Highly saline groundwater	500 – 1000	7000-15000	10000-25000	II	3
Very highly saline groundwater	1000 – 10000	15000-35000	25000-45000	III	4
Seawater	>10000	>35000	>45000	III	

[a] Numeric Label for statistical analysis

2.2.4 Framework for sustainable aquifer and SWI management.

Currently practiced mitigation measures and adaptation strategies were examined both at the country and at the aquifer level along the Eastern Mediterranean coastline in order to propose a general framework for aquifer management and SWI control at the basin level. The proposed framework targets land use planning as well as water demand and supply management, while also highlighting the importance of an integrated approach for effective SWI control.

2.3 Results and Discussion

2.3.1 SWI status along the East Med

The synthesis of accessible literature revealed a discrepancy in the number of studies undertaken by countries (Table 2-4); yet it should be noted that other documents either in the native language of the country or not published online may be available but were not accessible. In Lebanon, the studies targeted mostly urban centers, with a focus on field sampling and saltwater detection (El Moujabber et al. 2006; Saadeh 2008; El Chami et al. 2009; Korfali & Jurdi 2010; Hdeib 2012; Zarour 2017; Rachid et al. 2017). Few studies targeted SWI modeling or adaptive management (Safi et al. 2017; Khadra & Stuyfzand 2014; Kalaoun et al. 2018). In Syria, studies that focused on water quality sampling and/or management were limited (Al Charideh 2007; Abou Zakhem & Hafez 2007; Allow 2012; Faour & Fayad 2014; Abou Zakhem & Katta 2017). Aquifers in Turkey were relatively well characterized with much work focusing on field sampling and modeling along the southern border (Demirel 2004; Motz et al. 2005; Seckin et al. 2010; Breheme et al. 2011; Kurunc et al. 2016; EEA, 2005). Similarly, in Egypt, aquifers were well studied, particularly in the Nile Delta and the Northwestern aquifers; these studies included field sampling, modeling, resistivity profiling as well as adaptive management (Negm 2019; Mabrouk et al. 2018; Eissa et al. 2018; Attwa et al. 2016; Nofal et al. 2015; Elewa et al. 2013; Salim, 2012). In Israel and Palestine, several studies were reported for the coastal aquifers, equally targeting field sampling, modeling and adaptive management (Vengosh et al. 2005; Mogheir et al. 2005; Baalousha 2006; Amir et al. 2013; Levi et al. 2018; Graber et al. 2008; Mushtaha et al. 2019). In Cyprus, most studies were generally based on old field data with a few that provided updates on the current situation (Ergil 2001; Milnes & Renard

2004; Elkiran & Ergil 2006; Mazi et al. 2014; Papadaskalopoulou 2015; Tzoraki et al. 2018). Note that in Turkey, Lebanon, Palestine, Israel and Egypt, multiple studies targeted the same aquifer at different time. This allowed for tracking the progression of SWI in these aquifers.

2.3.1.1 Spatial distribution and intensity of SWI

Based on the review and analysis of the available and accessible data, an atlas showing the most recent SWI status per site along the Eastern Mediterranean was developed (Figure 2-2). The northeastern and eastern coasts of the study area appear to suffer from moderately to highly saline groundwater, with pockets of very highly saline groundwater, such as in the Beirut-Lebanon and the Magosa, Cyprus aquifers. The southeastern section of the coastline suffers from well-advanced SWI as is observed in the Gaza aquifer and the Coastal Aquifer of Israel as well as in the Nile Delta aquifer and the northwestern aquifer along the Mediterranean coast of Egypt.

Table 2-3 Summary of literature review onthe status of SWI along the East Med

Reference	Sampling Year	No. Wells	Pilot Area	Land Use*	Formation*	Salinity
			Turkey			
Kurunc et al. 2016	2009 - 2010	211	Serik plain	A	Q, C, T	60 – 4170 (EC uS/cm)
Guler et al. 2012	2008	193	Tarsus, Mersin	A, I, R	C, T, Q	400 – 3000 (EC uS/cm)
Cobaner et al. 2012	2007-2008	23	Silifke - Gosku	A	Q	460 – 3300 (EC uS/cm)
Breheme et al. 2011	-	34	Hatay	A, R	Q, C	240 – 890 (EC uS/cm)
Demirel 2010	2006-2008	13	Gosku delta	A, R	Q, T	480 – 2800 (EC uS/cm)
Seckin et al. 2010	2007/2008	21	Silifke-Goksu	A	Q	400 – 3400 (EC uS/cm)
Motz et al. 2005	2001-2002	53	Silifke - Goksu		Q	100 – 2200 mg/l Cl
	2001-2003		Mersin		Q, mixed	380 – 6800 (EC uS/cm)
Demirel 2004	2001	8	Mersin-Kazanli	I	Q	700 mg/l Cl
EEA 2005	-	-	Southern Turkey			Affected aquifers
			Syria			
Faour & Fayad 2014	2001-2014		Latakia to Tartous	A, R	Q	Increase SWI
Abou Zakhem & Hafez 2007	1998/ 2003	23	Latakia	A, R	Q, C, T	1000 – 6700 uS/cm EC
			Tartous			600 – 2000 uS/cm EC
Al Charideh 2007	2002	21	Banyas to Amrit	Mixed	Q, C	380-640 uS/cm EC
Allow 2012	1966-2003	20	Damsarkho	A	Mixed	Active SWI
			Lebanon			
Zaarour 2017	2013	15	Akkar	A	Q	220 – 680 mg/l Cl
		6	Ghadir	R, I	C	415 – 3800 mg/l Cl
Momejian et al. 2019	2012/2013	29	Jal el Dib	Mixed	C, Q	400-8000 uS/cm EC
El-Fadel et al. 2017	2013/2014	60	Zahrani	A	C, Q	350-4000 uS/cm EC
Rachid et al. 2017	2012/2013	113	Beirut	R	C, T, Q	700-65000 uS/cm EC
Saadeh & Wakim 2017	2014	20	Beirut	R	C, T, Q	500 – 24000 mg/l TDS
El Fadel et al. 2015	2013	60	Hadath	R, I, A	C, T, Q	209 – 3460 mg/l TDS

Reference	Sampling Year	No. Wells	Pilot Area	Land Use*	Formation**	Salinity
Khadra & Stuyfzand 2014	2011	90	Damour	A	C, T, Q	350-2500 mg/l TDS
Tomaszkiewicz et al. 2014	2006/2007	60	Tripoli	R	C,Q	209 – 3460 mg/l TDS
Hdeib 2012	2012	75	Khalde	A, R, I	C, Q, J	1600 – 3000 uS/cm EC
			Dawha			1100 – 4000 uS/cm EC
			Jieh			600 – 2600 uS/cm EC
			Saadiyat			1500 – 7000 uS/cm EC
			Damour			500 – 3500 uS/cm EC
Korfali&Jurdi 2010	2005/2006	120	Beirut	R	U	900 – 5931 EC µS/cm
		30	Tripoli	R		500-3700 uS/cm EC
		21	Saida	R		450-4200 uS/cm EC
El Chami et al. 2009	2006	21	Byblos	A, R	Q	40 – 200 EC uS/cm
Saadeh 2008	2004/2005	22	Beirut	R	C, T, Q	260 – 2400 mg/l TDS
Korfali&Jurdi 2007	2005/2006	73	Beirut		U	110 - 3100 mg/l TDS
Masciopinto 2013	2003	44	Choueifat-Jieh	Mixed, A	U	1000 – 4000 mg/l TDS
El Moujabber et al. 2006	1999/2000	14	Hadath	I, R	Q	1000-2000uS/cm EC
			Rmyle	A	C	2000 – 5000 uS/cm EC
CAMP 2004	NA	9	Damour	A	U	500 – 1850 mg/l TDS
Palestine						
Abu AlNaeem et al. 2018	Unclear	219	Gaza	R, A	C, Q	597-30000 uS/cm EC
						370- 18000 mg/l TDS
Alagha et al. 2017	1999-2010	22	Gaza	R, A	C, Q	>2000mg/l CL
Dentoni et al 2015	2011 - 2020	Model	Gaza	R, A	C, Q	Increase average head
Mogheir et al. 2013	-	-	Gaza		C, Q	3700 – 6000 uS/cm EC
Vengosh et al 2005	2001	40	Gaza	R, A	C, Q	400 – 3600 mg/l TDS
Israel						
Yechieli et al. 2019	2014 - 2015	5	Yarkoun -Taninim		C	26000 – 40000 mg/l TDS

Reference	Sampling Year	No. Wells	Pilot Area	Land Use*	Formation**	Salinity
Tal et al. 2017	2014-2015	25	Yarkoun -Taninim		Q	1600-11000 mg/l Cl
Melloul & Collin, 2003	-	-	Tel Aviv	R	U	>1000 mg/l Cl; 20mg/l/yr
Yechieli et al. 2009	2002-2005	50	Coastal aquifer		Q	29- 20000 mg/l CL
			Egypt			
Eissa et al. 2018	2013	29	Ras el Hekmeh – northwestern coast	U	C, T	620-21000 uS/cm E
Eissa et al. 2016	2015	21	Bagoush - northwestern coast	A, R	Q, T	1000 – 23000 uS/cm EC
Attwa et al. 2016	2014	40	El Sharkia – Eastern Nile Delta	A	Q, C	370 – 26000 uS/cm EC
Salem et al. 2016	2012	20	Abu Madi area – Eastern Nile Delta	A	Q	4100 – 12300 uS/cm EC
Nofal et al. 2015	2013	-	Nile Delta	A	Q, fluvial	4900 – 20000 TDS
Gad & Khalaf 2015	2006	18	North Sinai	A, R	Q	1500 – 4500 mg/l TDS
Masoud, 2014	2011/2012	451	Western Nile Detla	R, I, A	U	2000-24000 mg/l TDS
Elewa et al. 2013	2010	46	Eastern Nile Delta	A	Q	390 – 32000 uS/cm EC
Salim 2012	2008	-	Nile Delta	A, R, I	Q	1000-5000 mg/l TDS
			Coastal aquifer		C	>2000 mg/l TDS
			Moghra aquifer		C	1000 – 15000 mg/l TDS
			Cyprus			
Tzoraki et al. 2018	2006 - 2011	9	Ezousa aquifer		Q, C	~ 1701 uS/cm EC; ~ 174 mg/l Cl
Ergil 2001	1997		Guzelyurt		C, T	>5000 ppm salinity
Milnes et al. 2006	2003	66	Akrotiri		Q, C	1500 – 5000 EC uS/cm
EEA 2005	-	-	Cyprus			Affected aquifers
Milnes & Renard 2004	2001	78	Kiti		Q,C	2000 – 10000 EC uS/cm
Elkiran & Ergil 2006	-	-	Magosa	A		Very highly saline, not in use

*****Land Use = A: agriculture; R: residential; I: industrial; **Formation=Q: quaternary; C: cenomanian; J: Jurassic; M: Miocene; T: tertiary; U: unknown

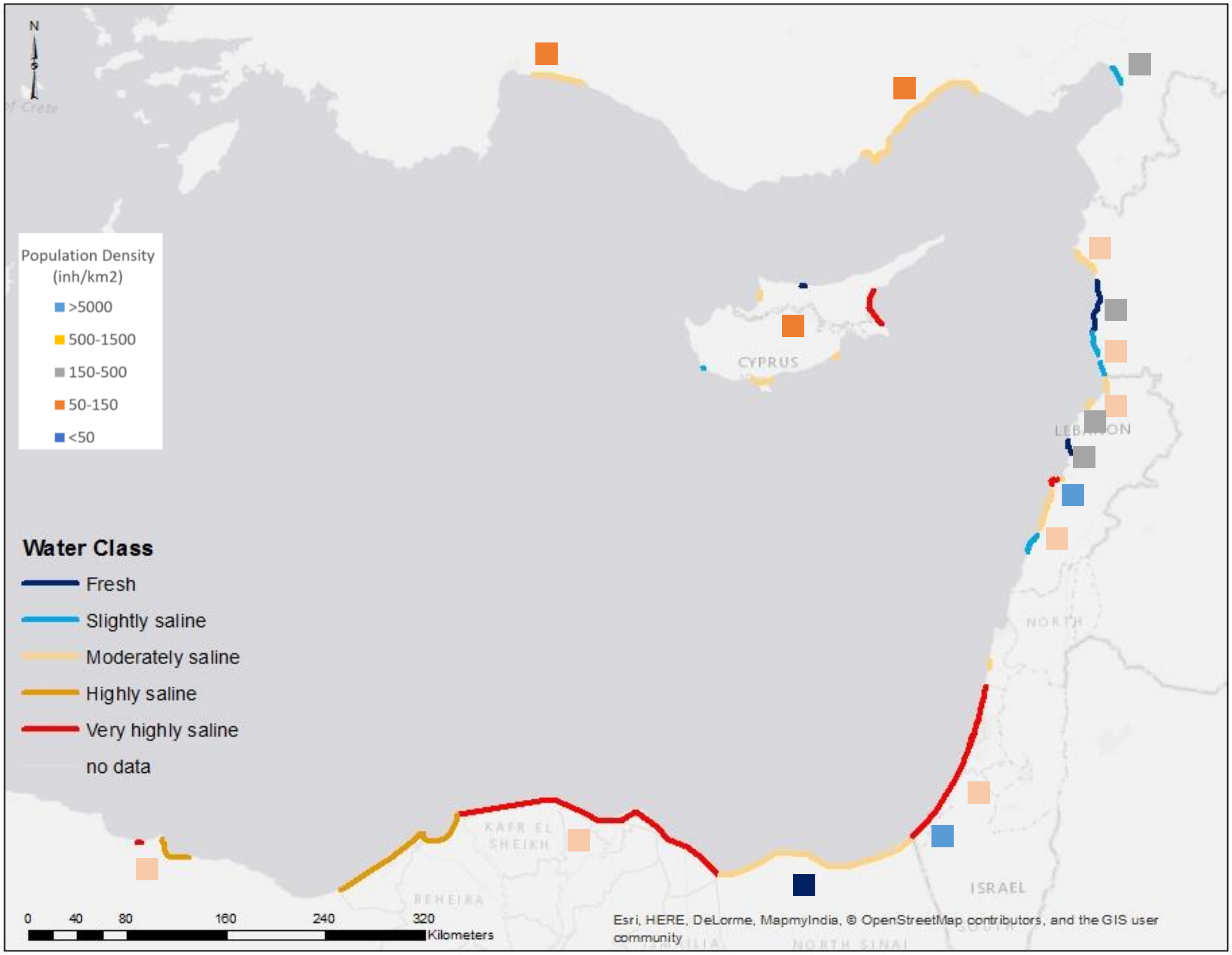

Figure 2-2 Atlas of status of SWI along the Easter Mediteranean

2.3.2 Management of SWI along the Eastern Mediterranean

Active attempts to adapt to SWI, through implementation of adaptation strategies and mitigation measures, were particularly observed in areas suffering most from advanced salinization or from limited water resources in general. In Turkey, aquifers were found to be periodically monitored (Gemici et al. 2006) with enforcement of demand and supply side measures to manage SWI including the use of water quotas and permits as well as an increased implementation of managed artificial recharge projects (Demirel 2010; Kurunc et al. 2016) and desalination (Giordana & Montginoul 2006; Kilickaplan et al. 2017). In Syria, the focus was largely on supply management (dams and occasional inter-basin transfers) rather than demand management (Wardeh et al. 2005). While several laws have been promulgated to regulate groundwater exploitation, well permitting and specifications, protection of recharge zones, pumping schemes, and water resources development, enforcement appear to be weak (SINC 2010). Similarly, in Lebanon, laws related to groundwater exploitation and well permitting exist but are not enforced. The most recent National Water Strategy targeted supply management through dams and promoted wastewater reuse and artificial recharge with limited emphasis on demand management (MOEW 2010). The plan is facing social challenges while small scale building-level RO units and an unregulated water tanker distribution system are proliferating (LTNC 2016). In Israel, a well-developed system of adaptation strategies and mitigation measures has been in place with a strong component focusing on demand management including water pricing, quotas, and taxes (scarcity rents, drought taxes) (Becker, 2015). Moreover a continuous hydrological monitoring system (Gilmont 2014) is in place and there are clear policies that aim towards reducing the demand on the natural water supply sources by shifting dependency to non-conventional sources like desalination (MIT 2015; ITNC 2018; Rosen et al. 2018), efficient systems, wastewater reuse (now at 85%) (ITNC 2018) as well as importing water intensive crops. In the Palestinian Gaza Strip, 90% of the population depends on desalinated water for drinking purposes (Mogheir et al. 2013) using public or privately-owned desalination units (Mogheir et al. 2013; Baalousha 2006). While existing hydrological monitoring systems are war-damaged (Abualtayef et al. 2016), adaptation strategies have been developed to reduce abstraction rates to promote aquifer recovery through wastewater reuse, artificial recharge, water transfer, and expansion of desalination capacities (Dentoni et al. 2015; Abualtayef et al. 2016). Adaptation strategies and mitigation measures have also evolved in Egypt (Batisha 2015), with monitoring systems installed in most vulnerable aquifers of the Nile delta (Elewa et al. 2013) and a positive trend towards increasing the reliance on solar powered desalination units (Salim 2012; El-Sadek 2010) and wastewater reuse in agriculture (Negm 2019). Yet, groundwater pumping remains unmonitored (Attwa et al. 2016). In Cyprus, a well-developed integrated water resources management system is in place targeting both supply management (dams and drainage canals, water transfer, the importation of water (from Greece particularly during the 2007-2008 drought), rainwater harvesting, wastewater reuse and a desalination program) and demand management (water metering, improved water networks as well as water pricing and quotas) (Papadaskalopoulou 2015; Tzoraki et al. 2018). Additional SWI- specific control measures have focused on artificial recharge such as in the Ezousa aquifer (Tzoraki et al. 2018) and terminating groundwater extraction as in the Magosa aquifer (Elkiran & Ergil 2006).

2.3.3 Compiling, testing and validation of SWOT model

Table 2-5 summarizes the data collected per aquifer with regards to the pre-defined internal and external factors for the semi-quantitative SWOT assessment. However, it is imperative to recognize the potential uncertainties associated with the reported data and the inconsistencies in the sampling methods used across studies. Limitations related to the availability of information also dictated whether data collation was undertaken at the aquifer or country level. Despite some similarities, each country has its unique loca context, which is a result of its governance framework, political and economic situation as well as its inherent natural and biophysical characteristics that affects how governments address SWI.

The results of the semi-quantitative SWOT assessment of the SWI risks in the Eastern Mediterranean aquifers are depicted in Figure 2-3. Aquifers' scores on internal and external factors are detailed in Appendix 1a. It is observed that the aquifers in Cyprus fall in Quadrant I with established strengths, despite some slight differences among the individual aquifers, as well as favorable opportunities. This combination of strengths and opportunities enable the reduction of risks and the proper management of SWI. Aquifers in Turkey seem to exhibit good strengths, that are comparable to the aquifers of Cyprus, however are subject to limited opportunities. As such, they appear to have a relatively low to moderate risk for SWI. This status is critical as the future vulnerability to SWI will be defined by how Turkey foster more opportunities and deals with threats to better enable sustainable aquifer management. In Egypt, all aquifers are faced by threats which play a hindering role in the proper management of SWI. Additionally, the Nile Delta and Ras El Hekmah aquifers also suffer from weaknesses. This combination of weaknesses and threats puts them at a very high risk of SWI. In particular, the North Sinai aquifer appears to enjoy better strengths and less weaknesses than the other aquifers, which infer a moderate risk of SWI. The opposite applies to the Coastal aquifer in Israel which suffers from considerable weaknesses that increases the risk of SWI; however enjoys strong opportunities which indicate an enabling environment to manage these risks, if weaknesses are overcome. Accordingly, the Coastal Aquifer suffers from high risk to SWI. Aquifers in Lebanon and Syria suffer from hindering threats, albeit at varying levels, in addition to weaknesses affecting some of these aquifers, hence aquifers are distributed over Quadrants III (very high risk) and IV (moderate risk). The aquifers of Beirut, Damour and Tripoli of Lebanon and Damsarkho of Syria are also observed to suffer from weaknesses relative to the other aquifers which represent an unhealthy environment that reflects an advanced risk for SWI. The combination of threats and weaknesses jeopardize the management of SWI and puts these aquifers at a very high risk of salinity. It is to be noted that the Beirut Aquifer is depicted to suffer from the most weaknesses amongst all aquifers in Lebanon and thus is the most at risk. The aquifers of Byblos, Akkar and Zahrani in Lebanon and the Banyas/Amrit in Syria appear to have good established strengths relative to the other aquifers and thus despite the threats they tend to suffer from a moderate risk to SWI. The Gaza aquifer is depicted to suffer the most of all studied aquifers. It has considerable internal weaknesses and is subject to hindering external threats. The aquifer is thus at a very high risk of SWI with a bleak future in the absence of proper actions to improve the enabling environment as well as manage the inherent aquifer/area characteristics.

Table 2-4 Aquifer/ Country data on SWI factors in the East Med

Aquifer	Pop growth per km^2	Pop. density (inh/km^2)	Water Consumption rate (l/c/d)	Urbanization trend (%)	Dominant land Use+	Water stress index[45]	Geology*	Recharge Pathway	Management measures	Projected precipitation reduction (%)	Projected Temp. increase (°c)	Projected sea level rise (m)	GDP per capita (USD)	Stability	Political will
Turkey															
Serik Plain [1]	4	96	190 [4]	2.04 [4]	urban; agriculture	high stress (overexploitation)	Q, C, T	rainfall; inflows	Monitoring [2]; Enforcement; Demand & Supply measures; Water quotas; Permits; MAR [1]; Desalination[3]	20[4]	3 - 4[4]	-	10500; 4.9% growth/ yr [4]	Stable	Strong (due to harmonization with EU)[46]
Mersin [5]	29	110			urban; agriculture; industrial		Q, C, T	rainfall							
Silifke – Goksu [7]	11	44			urban; agriculture		Q, C, T	rainfall; infiltration							
Hatay – Dortyol [6,8]	2	250			agriculture		Q, C	Rainfall; inflow							
Syria															
Tartous [9]	97	550 [10]	150 [10]	1.4 [10]	urban; agriculture	high stress [10] (16% GW deficit)	Q , C, T	rainfall; inflows	Supply management; Inter-basin transfers; Weak enforcement;	5 - 6[10]	1 - 2.2[10]	0.6 – 1.3[10]	2000; Neg. growth/yr [10]	War zone	Compromised (due to war)[47]
Banyas – Amrit [11]	4	300			urban; agriculture		Q, C	rainfall; inflows; infiltration							
Damsarkho [12]	195	550			urban; agriculture		Q, C, T	rainfall; infiltration							
Al Hamidiah coast [13]	370	500			urban; agriculture		Q, C, T	rainfall; inflows							
Lebanon															
Akkar [14]	41	419	200[15]	0.75	Medium agriculture	medium stress	Q, C	rainfall; inflow; infiltration	Weak enforcement; Regulations exist; No monitoring; No metering; Plan in place; Projects initiated; social opposition	4 - 11[16]	1 - 3[16]	0.3 -0,6[16]	8050; -4% growth/ yr[16]	Unstable	Weak[48]
Jal el Dib [17]	212	500			urban; agriculture; industrial	high stress	Q, C	rainfall; inflows							
Zahrani [18]	42	510			Medium agriculture	low to medium stress	Q, C	rainfall; infiltration; inflows							
Beirut [19]	510	20000[21]			urban	extremely high stress[20]	Q, C, T	Limited							
Damour [22]	17	990			urban; agriculture	high stress	Q, C, T	rainfall; infiltration							
Tripoli [23]	107	205			urban	extremely high stress	Q, C	rainfall; inflows							
Byblos [24]	1	370			urban; agriculture	low to medium stress	Q	rainfall; inflows							
Khalde to Jiyeh [25]	10	594			urban; agriculture	High stress	Q, C	rainfall; inflows							
Israel and Palestine															
Gaza [26]	142	4500[29]	90[27]	3[30]	urban	extremely high stress[27]	Q, C	rainfall	Regulations exist; damaged infrastructure[28]	15 – 20[27]	1.5 - 2.5[27]	-	3000	War zone	Compromised[27]
Coastal Aquifer [31]	19	1010	250	1.5	urban	extremely high stress	Q	rainfall; inflows MAR	Demand & Supply management; monitoring; Desalination[32]	10 – 20[33]	1.5[33]	-	40000; 4% growth/ yr[33]	Very stable	Strong[33]
Egypt															

Aquifer	Pop growth per km^2	Pop. density (inh/km^2)	Water Consumption rate (l/c/d)	Urbanization trend (%)	Dominant land Use+	Water stress index[45]	Geology*	Recharge Pathway	Management measures	Projected precipitation reduction (%)	Projected Temp. increase (°c)	Projected sea level rise (m)	GDP per capita (USD)	Stability	Political will
Ras el Hekmeh [34]	271				urban		C, T	rainfall							
Nile Delta [37]	9	1000	280[35,36]	2[30]	urban; agriculture	Medium	Q, C	rainfall; infiltration	Demand & Supply measures; Desalination	-20- 36[35]	1.3- 2.2[35]	0.59[35]	2400 – 6000; 1.8% growth/yr[35]	Stable[35]	Strong[49]
North Sinai [38]	50	15			urban		Q	rainfall							
Cyprus															
Ezousa [39]	37				urban; agriculture		Q, C	rainfall; inflows; MAR							
Akrotiri [41]	10				urban; agriculture		Q, C	rainfall; inflows; MAR							
Kiti [42]	10	130	200	0.75[30]	urban; agriculture	high stress[40]	Q,C	rainfall; inflows	Demand & Supply management; monitoring; Desalination	0 – 10[40]	1 – 2.5[40]	-	25000; 3% growth/ yr[40]	Very Stable	Strong[50]
Guzulyurt [43]	0.2				urban; agriculture		C, T	rainfall; inflows							
Girne [44]	2				urban; agriculture		C, T	rainfall; inflows							

[1]Kurunc et al 2016; [2] Gemici et al. 2006; [3] Kilickaplan et al. 2017; [4] TSNC 2018; [5] Guler et al. 2012; [6] Breheme et al. 2011; Demirel 2010; [7] Cobaner et al. 2012; [8] Breheme et al. 2011; [9] Fayad & Faour 2014; [10] SINC 2010; [11] Al Charideh, 2007; Fayad & Faour 2014;[12] Allow, 2012; 13 Abou Zakhem and Katta, 2017; [14] Zaarour 2017; [15] Amir et al. 2018; Kalaoun et al. 2016; [16] LTNC 2016; [17] Momejian et al. 2019; [18] El-Fadel et al. 2017; [19] Rachid et al. 2017; [20] MOEW 2010; [21] Ayash 2010; [22] Khadra & Stuyfzand 2014; [23] Kalaoun et al. 2016;2018); [24] El Chami et al. 2009; [25] Hdeib 2012; [26] Abu AlNaeem et al. 2018; Alagha et al. 2017; Dentoni et al 2015; Mogheir et al. 2013; Vengosh et al 2005; [27] PINC 2016; [28] Dentoni et al. 2015; Abualtayef et al. 2016; [29] WB 2018; [30] UN DESA 2018; [31] Yechieli et al. 2009; [32] MIT 2015; ITNC 2018; Rosen et al, 2018; [33] ITNC 2018; [34] Eissa et al. 2018; [35] ETNC 2016; [36] ETNC 2016; Mabrouk et al. 2018), [37] Attwa et al. 2016; Salem et al. 2016; Nofal et al. 2015; Masoud, 2014; Elewa et al. 2013; Salim 2012; [38] Gad & Khalaf 2015; [39] Tzoraki et al. 2018; [40] CSNC 2018; [41] Milnes et al. 2006; [42] Milnes & Renard 2004; [43] Ergil 2001; [44] Papadaskalopoulou 2015; [45] WRI 2013; [46]EC Report 2019; [47]Syria Report 2012; [48]SOER 2011;[49]Egypt Report 2016; [50]EC Report 2019a; +Refer to Table 4; * Refer to Table 4, Q: Quaternary, C: Cenomanian, T: Tertiary.

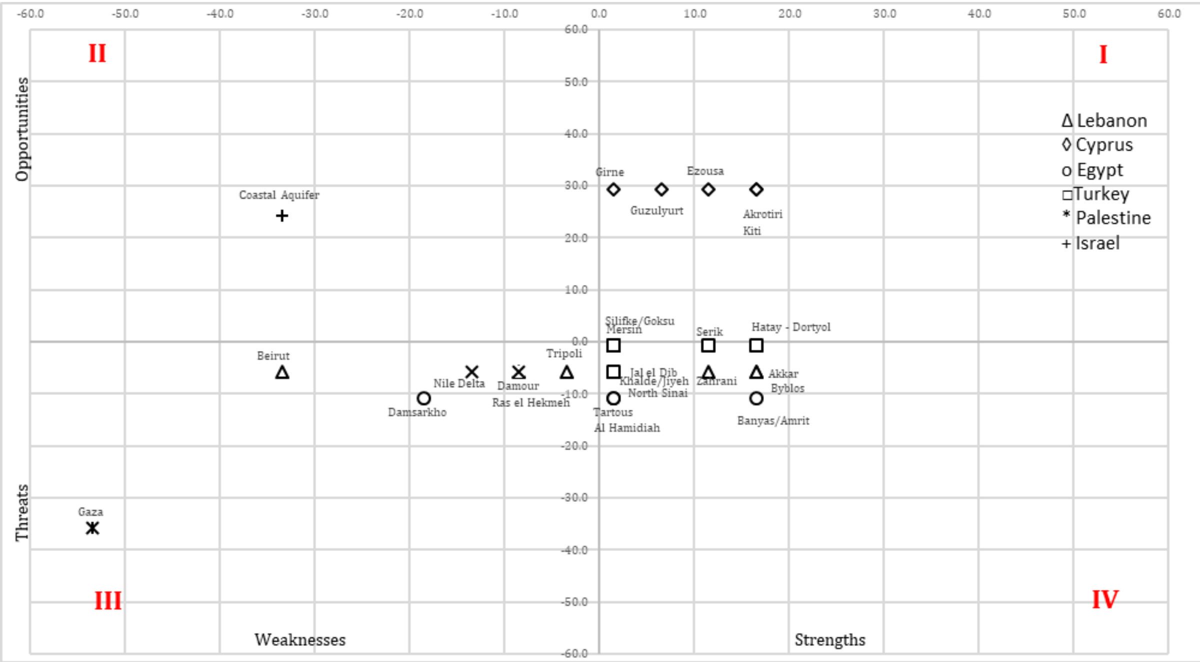

Figure 2-3 Semi- quantitative SWOT matrix of aquifers comparing the internal (x-axis) and external (y-axis) factors affecting risks towards SWI (same color icons represent aquifers of the same country)

Figure 2-4 shows the semi-quantitative individual SWOT analysis outcome at the country level. In Israel/Palestine, while the Coastal and Gaza aquifers suffer from weaknesses with high risk of SWI, the Gaza aquifer also suffer from severe threats that tend to make it much more sustainable to salinization conditions than the Coastal aquifer. In Syria, the Latakia/Damsarkho aquifer exhibited the most risk towards SWI given its relatively high weakness ac compared to the other aquifers. The remaining coastal aquifers in Syria are almost similar in conditions, with the Banyas-Amrit having the strongest internal factors and thus the least at risk of SWI. In Turkey, Silifke and Serik aquifers appear to have internal strengths that appear to reduce their risk towards SWI as compared to Hatay and Mersin, although the weaknesses in the latter are not alarming. Additionally, it is observed that the Hatay aquifer has a moderate risk towards SWI, similar to Mersin, but worse than Silifke and Serik, whereas in reality, it is slightly saline. In Cyprus, all aquifers seem to enjoy well established strengths as well as an enabling environment (opportunities) which highlights a relatively low risk to SWI in these aquifers. The case of the Girne aquifer shows well established strengths, as compared to the other aquifers, highlighting a lower risk towards SWI. In Egypt, the North Sinai conditions resemble those of the Silifke-Gosku aquifer in Turkey while the Nile delta conditions resemble those of the Coastal aquifer of Israel. In Lebanon, the case of the Beirut aquifer is alarming where strong weaknesses outweigh any internal strengths or opportunities and hint towards a very high risk towards SWI. On the other hand, the Akkar and Byblos aquifers appear to share similar good conditions, with the most established strengths relative to the other aquifers in Lebanon, which makes them less prone to SWI as compared to the rest of Lebanon aquifers.

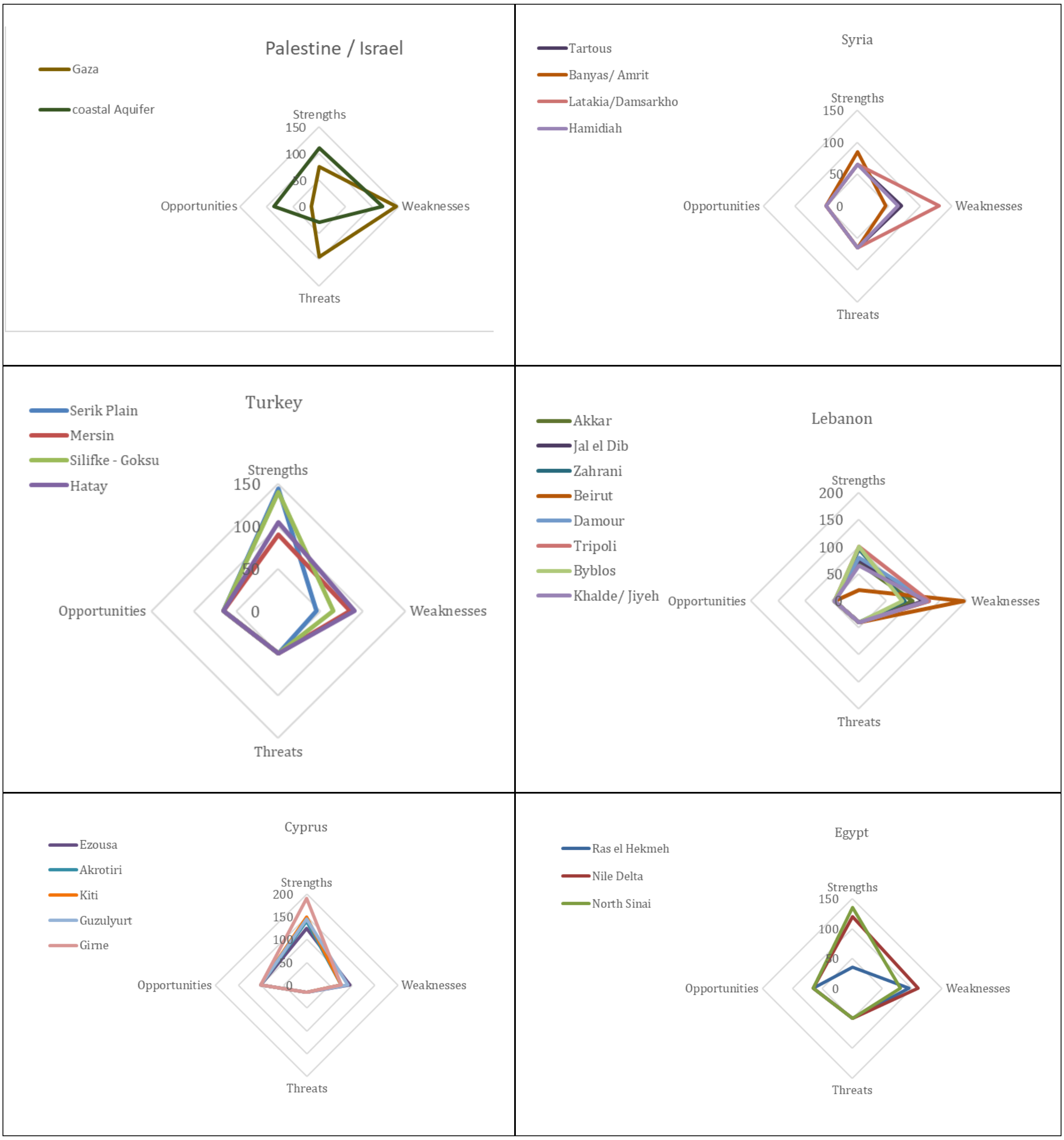

Figure 2-4 SWOT analysis per aquifer per country

The statistical tests conducted to assess the strength of the associations between the results of the semi-quantitative SWOT model on one hand and the reported SWI status showed that a strong statistically significant correlation (at $p<0.05$) existed between the two (Table 2-5). The results thus show that the semi-quantitative SWOT analysis was effective at predicting the status of SWI in the coastal aquifers.

Table 2-5 Significance of statistical tests of the SWI risk among the reported status and the modelled results

Reported SWI status /modeled	Chi square test (p<0.05)	Fischer test (p<0.05)	Wilcoxon (p<0.05)
Semi-quantitative SWOT	<0.016	0.018	0.04

2.3.4 Framework for aquifer management and SWI control

Similar to many locations worldwide, SWI is an evident threat along the Eastern Mediterranean with reported data stressing the need to control SWI towards sustainable aquifer management. Regional adaptation strategies and mitigation measures highlight a good adaptive capacity in Cyprus, Israel and Turkey that is still emerging in Egypt and weak in Lebanon, Syria, and Palestine. While national communications of all countries to the UNFCCC have included recommendations for adaptation and integrating potential climate change impacts in their water resources plans, albeit with heterogeneity in coverage and intensity (TSNC 2018; LTNC 2016; ETNC 2016; SINC 2010; PINC 2016), the actual implementation and integration within aquifer management, aside from Cyprus (CSNC 2018) and Israel (ITNC 2018) remains unclear.

Capitalizing on lessons learnt from regional experiences and recognizing the need for more systematic and holistic approaches towards the management of SWI, Figure 2-5 outlines a general framework for adaptation strategies and mitigation measures aimed towards sustainable aquifer exploitation to control SWI. The framework brings together measures that have proven to be successful in individual countries with an integrated approach that emphasizes the main pillars of water demand and supply management, while also attending to the importance of land use planning and interventions of SWI control. It recognizes awareness as a building block and highlights political will for achievement. While adaptation and mitigation are indispensable for aquifers vulnerable to or already affected by salinity, the framework also targets slightly saline and freshwater aquifers. In this context, protection efforts towards are equally important to delay and avoid salinization particularly that once salinization is well advanced, aquifer recovery becomes long and difficult (Safi et al. 2017; Cobaner et al. 2012; Selmi 2013

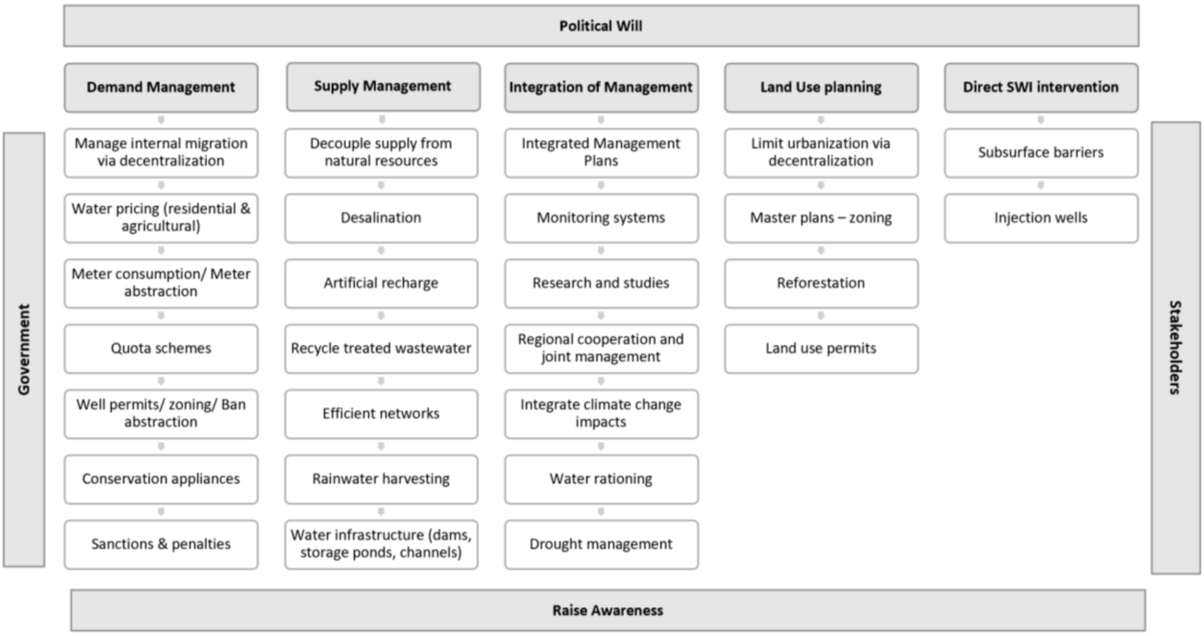

Figure 2-5 Synopsis of Management Framework for aquifer management and SWI risk control

2.4 Conclusion

This study presented a semi-quantitative model for the estimation of risk to seawater intrusion using a semi-quantitative SWOT (strengths, weaknesses, opportunities, threats) analysis. The model encompassed internal and external indicators that depicted the main drivers of seawater intrusion including the physical, anthropogenic, climatic as well as governance and political drivers. The model was tested with data collected from 26 aquifers along the East Med region. Its effectiveness in identifying aquifers at risk was verified with a statistically significant correlation with reported seawater intrusion levels. Limitations associated with the proposed semi-quantitative SWOT model include the availability and accessibility of information which led to the scoring of some elements at the country level rather than the aquifer level which might not be representative. Additionally, the assumption that elements sustain equal weights is arguable where the effect of weights per individual elements on the accuracy of the risk representation merits, further exploration.

Current knowledge on the intensity, spatial and temporal extent of SWI along the East Med was also illustrated through an indicative atlas. Aquifers in the region appear to be at different stages of SWI exhibiting signs of highly saline groundwater with alarming rates at dense population centers (Beirut, Magoza, Gaza and the Nile Delta). Adaptation strategies and mitigation measures highlighted a relatively strong adaptive capacity in Cyprus, Israel and Turkey, an emerging capacity in Egypt, while Lebanon, Syria, and Palestine exhibiting weak capabilities. Saltwater intrusion along the East Med is expected to increase under the synergistic effect of urbanization and climate change due to potential sea level rise, reduction in precipitation and aquifer recharge. In turn, increased SWI is expected to exacerbate the socio-economic burden to this area's vulnerable and fragile local livelihoods. Capitalizing on lessons learnt from the studied aquifers, a general framework for mitigation measures and adaptation strategies is presented towards SWI control and sustainable aquifer management. While adaptation and mitigation measures are indispensable for aquifers vulnerable to or already affected by salinity, the framework equally addresses slightly saline and freshwater aquifers.

CHAPTER 3

TOWARDS A FRAMEWORK FOR THE ASSESSMENT OF SALTWATER INTRUSION IN COASTAL AQUIFERS

3.1 Introduction

Saltwater intrusion (SWI) is a global coastal threat caused primarily by groundwater over-exploitation due to population growth, development, and urbanization. The extent of SWI is expected to exacerbate under potential impacts associated with future climate change such as sea level rise coupled with increased water demand due to temperature increase and precipitation decrease. When combined (Figure 3-1), these factors would reduce aquifer recharge with SWI manifesting itself in the mixing of freshwater with seawater, often rendering groundwater resources non-suitable for domestic, agricultural, industrial or recreational uses (Zhang *et al.*, 2011; Sales, 2009; Conrads & Roehl, 2007; Sanford & Pope, 2010, Bobba, 2002; de Montety *et al.*, 2008; Capaccionoi *et al.*, 2005; Fatoric & Chelleri, 2012; Duque *et al.*, 2008). The importance of understanding the dynamics and impacts of SWI lies in the need to plan, manage and adapt towards protecting the biophysical elements (i.e. subsurface aquifers and groundwater quality) from contamination and curtailing associated socioeconomic burdens on coastal communities (i.e. the impairment of an important water source, damages to water fixtures and infrastructure, soil salinization, treatment cost or alternative water sources, and potential health issues).

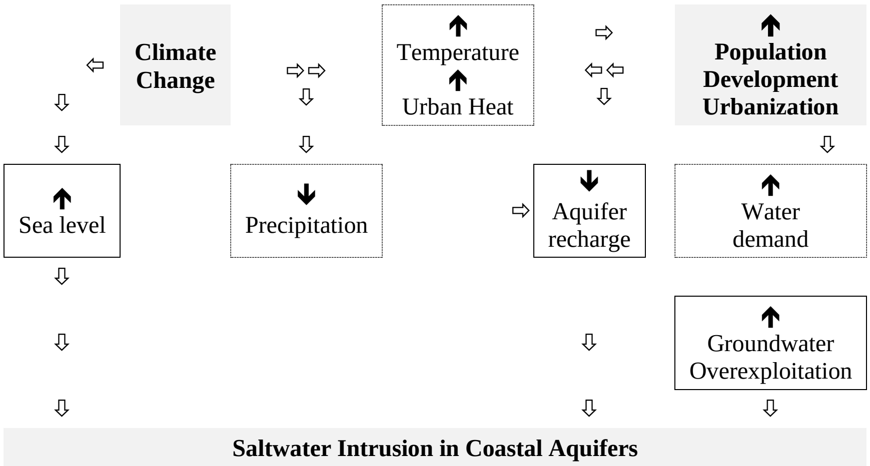

Figure 3-1General dynamics of saltwater intrusion driving processes
🡅=Increase; 🡇= Decrease
⇩ or ⇨ or ⇦ = Causal pathway

Efforts towards understanding the vulnerability to and the impact of SWI are widespread and rely on geochemical and geophysical characterization as well as on laboratory experiments, hydrodynamic techniques, and modeling often coupled with multivariate statistical analysis, geo-spatial analysis, and environmental tracers (Kumar *et al.* 2015; Werner *et al.* 2013; de Montety *et al*. 2008; Duque *et al*. 2008). Each SWI assessment method has its requirements, limitations, as well as advantages and disadvantages which frames its applicability, use, and implications of associated findings. Most methods are highly data-driven and prohibitively expensive to apply, affected by environmental noises, and vulnerable to interactions and interventions from processes that may mask their results (Werner et al., 2013).

Despite advances in SWI research, it remains challenging to assess and manage its impact due to influences of complex factors, including hydro-geochemical dynamics, shoreline geomorphology, biochemical reactions, and aquifer flow and transport processes among others (Werner *et al.*, 2013; 2012; Melloul & Goldenberg, 1997). This is particularly the case in fractured, karstic and semi-karstic media, which despite multiple attempts to characterize, remains poorly studied worldwide (Sebben et al., 2015; Werner et al., 2013; Cherubini & Pastore, 2011; Papadopoulou et al., 2005; Langevin, 2003). The understanding of the heterogeneity, discontinuities, fractures, conduits and faults' networks as well as the individual and synergistic effect of these complex features greatly shape how the aquifer allows and reacts to saltwater intrusion (Papadopoulou et al. 2005; Allen et al., 2002). It affects the pollutant flow, transport and concentration, here salinity, in the aquifer, hence defines how saltwater intrusion occurs and advances. This complexity is further aggravated in data-scarce regions where coastal managers need to plan and act under incomplete knowledge and uncertainty to delineate impacts and protect coastal communities (Cardenas & Halman, 2016; Werner et al., 2013; Tribbia & Moser, 2008).

In this study, we identify common techniques, methods and metrics used to assess the impact of SWI and analyze and appraise their characteristics and differences as well as their applicability in fractured media. These techniques were tested at a highly exploited but data-scarce, heterogeneous aquifer to understand the status and progression of saltwater intrusion in the aquifer. The study presents a first attempt at coupling a quantitative assessment of the outcomes of various methods with a qualitative comparison of their inherent characteristics resulting in the development of an assessment framework that provides a novel platform for informed impact assessment and sustainable exploitation of coastal aquifers reducing the gap between SWI knowledge on one side and management needs for practice and implementation on the other. The resulting framework is the first to apply SWOT and MADM analysis to SWI where 'fit for purpose' assessment techniques were identified based on functionality and simplicity. Such a framework, based on hydro-geochemical techniques coupling indicators and indices with geo-statistical analysis, is able to scrutinize the distribution and intensity of SWI and assess its impact on groundwater quality, applicable to heterogeneous systems.

3.2 Theory

Saltwater intrusion is governed by coastal hydrostatic pressures at the hydraulic interface between saline and freshwater. Under undisturbed conditions, a state of dynamic equilibrium between freshwater and seawater is maintained where the hydraulic gradient pushes freshwater towards the sea. As a result of prolonged changes in coastal groundwater levels due to pumping, land-use change, climate variations or sea-level fluctuations, this hydraulic gradient is reversed, resulting in seawater infringement into the aquifer (Bear, 1979). Studies on saltwater intrusion have focused on the process itself, the measurement of propagation and concentration, the prediction of intrusion as well as on the management of vulnerable aquifers (Werner et al., 2013). As the intrusion of saltwater is primarily a function of the hydrogeological characteristics of the aquifer and its hydrodynamics, and as uncertainty is always associated with aquifer characterization, there exists an 'inherent uniqueness of each case of intrusion' (Werner et al., 2013) which accentuates the need case-studies of aquifers to build the knowledge. Field data are often inadequate but indispensable for a proper characterization and assessment of saltwater intrusion. Concurrently, coastal aquifers worldwide are suffering from variable degrees of salinization, with a need for a better understanding of the process especially in complex aquifers. Capitalizing on accessible data in an integrated systematic framework can act as a preliminary assessment tool to inform decision makers and facilitate aquifer management.

3.3 Materials and Methods

The methodology consisted of a comprehensive analytical approach including: 1) review and selection of methods commonly used to asses SWI; 2) fieldwork for aquifer characterization and testing of methods; 3) evaluation of the effectiveness of tested methods based on predefined criteria; and 4) development of a SWI assessment framework towards informed planning and decision-making for improved groundwater management.

3.3.1 Review and Selection of methods for SWI assessment

The selection of methods for SWI assessment represents the first step towards decision-making whereby alternative methods are analyzed and assessed against clear criteria. For the purpose of this research, two levels of assessments were undertaken: a qualitative comparative assessment of families of methods (i.e. geochemical, geophysical, laboratory, modeling…etc.) followed by a semi-quantitative assessment of individual alternatives. The assessment of families of methods was based on a complexity-functionality assessment (CFA), adapted from Faludi *et al. (*2016) into a high-level qualitative evaluation because criteria to select methods for SWI assessment have not been reported (Table 3-1).

Table 3-1 Criteria for assessing complexity and functionality

Factor	Criteria	Explanation
Complexity	Level of input data	Relative level of input data required and specialization in the analysis and interpretation *(i.e. relatively specialized, specialized, highly specialized)*
	Accessibility and availability	Relative level of accessibility/ availability and feasibility in terms of requirements for sampling and analysis; challenges (*i.e. feasible/ expensive; readily accessible/ challenging*)
	Decision Makers friendly	Ease of use by decision makers *(i.e. easy, medium, complex)*
Functionality	Output of the method	Level of contribution to understanding the different aspects of SWI (spatial distribution, geochemical reactions, hydrochemical facies etc.) *(i.e. limited, varies, wide)*
	Use for monitoring	Potential to use the method in monitoring i.e. flexibility and feasibility for spatio-temporal analysis; *(Yes, No, not applicable)*
	Integration in framework	Potential to integrate method in a framework *(Yes, No)*

A wide variability in the complexity, feasibility and accessibility to the required input data as well as in the utility was observed (Table 3-2) amongst various methods used to assess the SWI impact. Geochemical techniques were selected for further analysis and field testing because of their inherent characteristics of being moderate in complexity, feasible in terms of data collection and analysis, cover a spectrum of SWI-related outputs, easy to replicate for monitoring, and popular with decision makers.

Table 3-2 Evaluation of methods' families against the selection criteria

Criteria **Method**	**Level of Data & analysis**	**Accessibility/ availability of data**	**Decision makers friendly**	**Output (coverage of SWI aspects)**	**Use for Monitoring**	**Integration in framework**
Geo-chemical (Fieldwork, lab analysis, geo-chemical analysis)	Relatively specialized	Sampling-based/ usually accessible/ relatively feasible	Relatively easy	Relatively wide	Yes/ continuous	Yes
Geophysical (Fieldwork, results interpretation)	Highly specialized	Noise interference in built-up areas/ technology-based/ not readily accessible/ expensive	Complex	Limited (only level and extent)	Not applicable	No
Laboratory experimental set-ups	Relatively specialized	Challenging in coastal heterogeneous aquifers/ not readily accessible/ relatively expensive	Relatively easy	Varies	No	No
Statistical analysis	Specialized	Accessible/ feasible	Level varies	Limited (Correlations; distribution)	Yes	Yes
Environmental tracers (Field work, sampling, lab analysis)	Specialized	Challenging in coastal heterogeneous aquifers/ tracers and analysis not readily accessible/ relatively expensive	Medium complexity	Limited (specialized use)	Not feasible	No
Modeling (model set-up, simulations)	Highly specialized	Challenging in coastal heterogeneous aquifers/ software-based/ expensive	Medium complexity	Limited (targeted use)	No	No

Commonly used hydro-geochemical techniques rely on the concentrations of chloride, total dissolved solids, and electrical conductivity which are the first and most common signs for detecting salinization (Table 3-3) as well as on indicative ratios such as Na^+/Cl^-, Ca^{2+}/Mg^{2+}, Br^-/Cl^-, SO_4^{2-}/Cl^-, Cl^-/HCO_3^- and $Ca^{2+}/(SO_4^{2-}+HCO_3^-)$, the seawater fraction, ionic deltas, the Base Exchange indices (BEX), the Chloro-Alkaline indicators ($CAI= [(Cl^- – (Na^+ +K^+)]/Cl^-$), and composite techniques that integrate multiple parameters into single metrics. Composite techniques in particular (Table 3-4) encompass the:

- Stuyfzand classification method, (Stuyfzand, 1989; 2008), which is used to characterize the water type and quality to assess the intensity of the SWI impact;
- Generalized groundwater quality index (GQI), that synthesizes water quality data by indexing them numerically relative to WHO standards, and then used to summarize water quality with and without indicators of pollution (nitrates and coliforms), and cross-check or complement aquifer vulnerability assessments (Babiker *et al.* 2007); and
- GQI specific to seawater intrusion (GQI_{SWI}), developed as a spatial mapping tool that couples the fresh-saline water mixing (sea fraction) with the piper diagram (Piper, 1953) analysis into a numerical indicator of the SWI polluting effect (Tomaszkiewicz *et al.* 2014).

Multivariate statistical analysis, geo-spatial analysis and geostatistical interpolation (i.e. Ordinary Kriging, indicator kriging, co-kriging…) are commonly coupled with the hydro-geochemical techniques (Zghibi *et al*. 2014; Tomaskiewicz *et al*. 2014; Villegas *et al*. 2013; Mondal *et al*. 2010; Abu Zakhem and Hafez, 2007). Geo-statistical analysis and interpolation is proving highly functional and informative in hydrogeological studies (Triki et al., 2014; Agoubi et al., 2013; Castrignano et al., 2007) as it allows the interpretation of spatial and temporal distributions of studied factors, as well as the extrapolation to areas where data is not available or cannot be collected, based on correlations among the available data. The inherent feature in geostatistical analysis to recognize and manage uncertainty in the domain and data through probabilistic approaches to correlations in data and interpolations through space and time is key in the assessment of SWI (Tomaskiewicz et al., 2014; Triki et al., 2014).

Given that aquifer analysis is usually constrained by the lack of data, which is more intricate in heterogeneous aquifers (De Filippis *et al*. 2016; Khadra and Stuyfzand 2014; Werner *et al.* 2013; Mascopianti, 2013), all identified geochemical methods for field application were tested for consideration in the assessment framework, coupled with geostatistical analysis and interpolation.

Table 3-3 Classification of water based on chloride, TDS, and EC concentrations (Konikow & Reilly, 1999; Rhoades *et al. 1992)*

Class	**Cl (ppm)**	**TDS (ppm)**	**EC**
Fresh groundwater	<100	0-500	<700
Slightly saline groundwater	100 – 250	500-1500	700-2000
Moderately saline groundwater	250 - 500	1500-7000	2000-10000
Highly saline groundwater	500 – 1000	7000-15000	10000-25000
Very highly saline groundwater	1000 – 10000	15000-35000	25000-45000
Seawater	>10000	>35000	>45000

Table 3-4 Stuyfzund's method and the generalized water quality indices (Stuyfzund, 1989; 2008; Babiker *et al*. 2007; Tomaskiewicz *et al.*, 2014)

	Code	Parameter	Description (chloride in mg/l)
Stuyfzund water type method		**Salinity**	
	g	Oligohaline	5-30
	F	Fresh	30-150
	f	Fresh-brackish	150-300
	B	Brackish	300-1000
	b	Brackish-salt	1000-10000
	S	Salt	10000-20000
	H	Hypersaline	>20000
		Alkalinity	**Alkalinity as HCO_3 (mg/l)**
	*	Very low	<31
	0	Low	31-61
	1	Moderately low	61-122
	2	Moderate	122-244
	3	Moderately high	244-488
	4	High	488-976
		Dominant cation and anion	**Most important cation and anion**
	Ca	Calcium	The most important cations and anions are placed in the appropriate fields inside two triangles constructed for this purpose
	Mg	Magnesium	
	Na	Sodium	
	HCO_3	Bicarbonate	
	Cl	Chloride	
	Mix	No anion > 50% sum of anions	
		Base exchange index (BEX) in meq/l	**BEX= Na + K+ Mg – 1.0716Cl** **BEX= Na+ K -0.8768Cl**
	e	Equilibrium	0 (zero) or no BEX (e)
	f	Freshened	>+(0.5 +0.02Cl) or positive BEX (+)
	s	Salinized	<-(0.5 +0.02Cl) or negative BEX (-)
Stuyfzund hydrochemical facies	***Code***	***Descriptor***	***Value***
	N	Neutral pH	>6.2
	a	Slightly acidic	5.0 – 6.2
	A	Acidic	<5.0
	M	Mixed Redox	-
	o	(Sub)oxic	1-3
	r	Reduced (anoxic)	4-5
	D	Deeply(anoxic)	6-7
Groundwater quality indices	**$GQI_{generalized}$**	$GQI = (100 – ((r_1w_1+r_2w_2+…+r_nw_n)/N)$ C= (X'-X)/(X'+X); X': sample concentration; X: WHO threshold r = is the rank value calculated as $0.5*C^2 + 4.5*C + 5$; N = is the total number of parameters; w= relative weight of the parameter	
	GQI_{SWI}	$GQI_{SWI} = (GQI_{piper} + GQI_{fsea})/2$	
	GQI_{piper}(%)= $[((Ca^{2+} + Mg^{2+})$/Total cations) + (HCO^{3-}/Total anions)]*50 (in molar mass)		$GQI_{fsea} = (1 – f_{sea})*100$

3.3.2 *Pilot aquifer characterization and testing of methods*

The pilot aquifer is located along the Eastern Mediterranean (Beirut, Lebanon) underlying a 20km^2 peninsula (Figure 3-2) with around 9 km of rocky coastline with patches of sandy shores and cliffs. The aquifer is overexploited by a large number[1] of unregulated residential wells (SOER, 2011; Saadeh 2008). The subsurface geology belongs to the Cretaceous (Cenomanian c4 (Sanine), Senonian c6 (Chekka), and Turonian (Maameltein) formations) and Quaternary (deposits of moving dunes and soils) periods with pockets of Tertiary (Miocene). The main geological units exposed are the Sannine Formation (C4) and the unconsolidated Quaternary deposits. The aquifer is heterogeneous and characterized by fractured and semi-karst systems (Masciopanti, 2013; Shaaban *et al.* 2006) and heavily jointed and faulted with at least two faults known to run in parallel along the NE to SW direction from the Eastern coast towards the center (Ukayli, 1971; Peltekian, 1980). The groundwater is stored in two principal aquifers of carbonate[2] and sandy[3] origins, making up one thick (~700m) and extensive formation consisting mainly of limestone and dolomite, as well as some intercalations of marl (Khair, 1992). The Cenomanian formation (c4) is characterized by a dual porosity matrix and by solution enlarged channels and cavities from joints and fractures. This high porosity enables groundwater to move laterally and vertically to great depths (Ukayli, 1971) however the Cenomanian- Quaternary formation is underlain by an aquiclude that separate it from deeper aquifers (Abdel Basit, 1971).

[1] Four to ten thousands
[2] Cenomanian limestone
[3] Quaternary with deposits directly overlaying the Cenomanian carbonates in many places

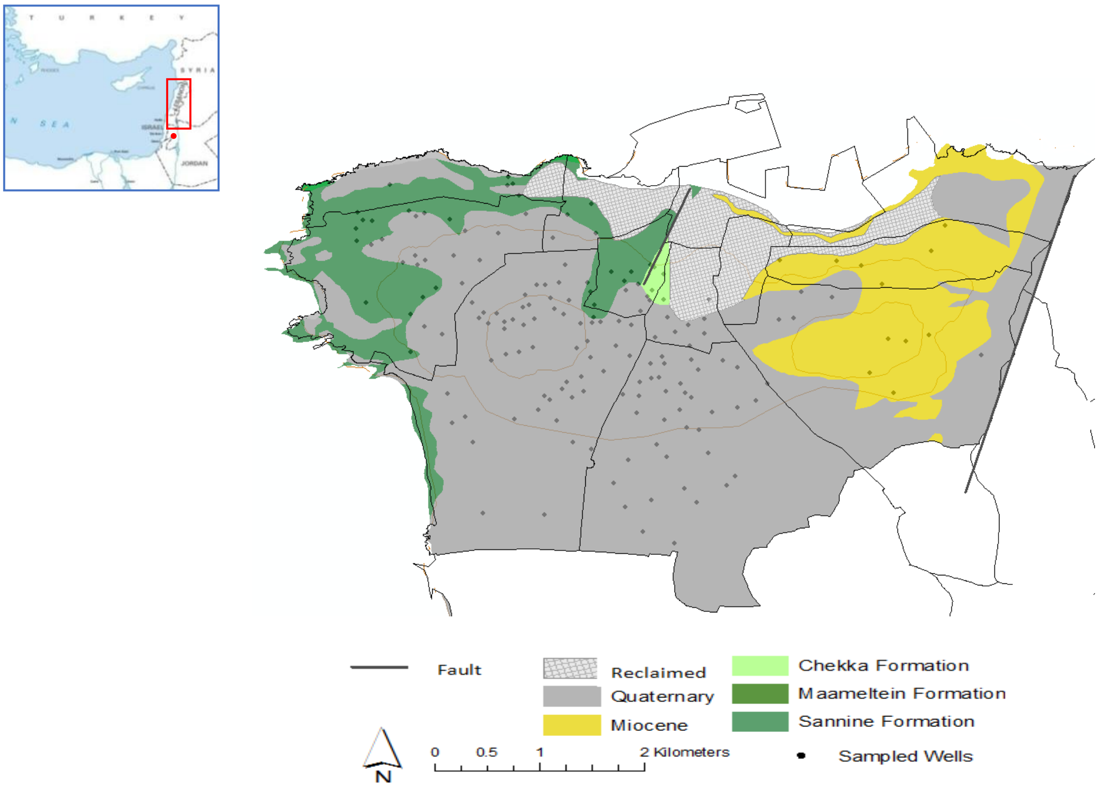

Figure 3-2 General location and layout of pilot aquifer with sampled wells

The aquifer is poorly studied, generally in terms of its characteristics and specifically in terms of groundwater quality. Little is reported on the nature of faults and dislocation conditions and implications on the compartmentalization of the aquifer with no lithostratigraphic cross-sections within the boundaries of the study area (El-Fadel *et al.* 2014). As such, information on the degree and spatial distribution of structural and physical heterogeneity of the aquifer, the underlying water table, the depth of wells, as well as extracted groundwater volumes are generally limited to non-existent. Additionally, wells are invariably cased and seldom accessible for water level measurements.

3.3.3 Groundwater Sampling and Quality Analysis

A spatial and temporal sampling and analysis program was implemented to characterize the groundwater quality and track seasonal changes. In total, 170 wells were targeted with three sampling rounds undertaken to capture both the dry (early dry - June 2013 and late dry - October 2013) and the wet (late wet - April 2014) seasons. Parameters analyzed included TDS, hardness and major ions (HCO_3^-, CO_3^{2-}, NO_3^-, SO_4^{2-}, Ca^{2+}, Mg^{2+}, Cl^-, Br^-, Na^+ and K^+) as well as microbiological indicators (fecal and total coliforms). The analyses were conducted in accordance with Standard Methods for the Examination of Water and Wastewater (APHA-AWWA-WEF, 2012) at the American University of Beirut.

The hydro-geochemical data were analyzed for descriptive statistics and correlations using the Statistical Package for Social Sciences (SPSS 16.0) software. Inferential statistical analysis, particularly 'Repeated Measures ANOVA', was used to assess the significance of the mean differences of sampled parameters between seasons, and to evaluate possible correlations amongst parameters. When needed, the parameters were transformed to comply with the normality condition and a Greenhouse-Geisser correction (i.e. when tests of sphericity failed). Post hoc tests using the Bonferroni correction were applied to identify the pairwise difference to boost confidence in the results and control of error rate.

3.3.4 Evaluation of techniques and development of SWI assessment Framework

The assessment of geochemical alternatives can be based on a Strengths, Weaknesses, Opportunities and Threats (SWOT) analysis, Multi-Criteria Decision Support (MCDS) or Multi-Attribute Decision Making (MADM) analyses, Analytical Network Process (ANP) or fuzzy analyses, a Life Cycle Assessment (LCA) approach, or a combination of methods to compare, weigh and select among alternatives (Faludi *et al.* 2016; Baycheva-Merger & Wolfslehner, 2016; Ruiz Padillo *et al*. 2016; Garing *et al.* 2013; Rachid & El-Fadel, 2013; Svekli *et al.* 2012; Yuksel & Dagdeviren, 2007). In this study, a semi-quantitative approach was adopted whereby a SWOT analysis is coupled with a CFA and MADM analysis.

3.3.4.1 Determination of evaluation criteria for SWOT coupled with CFA

As the objective is to develop a SWI assessment framework, the main measure of effectiveness is the contribution of a method to the comprehensiveness, reliability and feasibility of this framework and its responsiveness to interpretation by decision makers. However, since this effectiveness could come at a prohibitive cost, the complexity of the method is also considered. As such, criteria for the comparative assessment of the effectiveness of alternative methods focused on two levels: functionality and complexity. These are evaluated under the same performance areas defined above and categorized into internal (I) and external (E) factors (Table 3-5). Internal factors are intrinsic to the method and present a property or an integral element of the method. These were proposed to include input data (the scope of data needed to perform the method), interpretation (easiness of interpretation by decision makers), representativeness (the extent of coverage of SWI traits by the output), and distinctiveness (the extent of uniqueness of a method). On the other hand, external factors are those that influence the method or affect how it is interpreted and used. These were proposed to include independence (whether the method stands alone or requires supporting elements for proper interpretation), framework integration (the applicability of the method in a monitoring framework), and interference (the degree of misanalyses of the results due to interference).

Table 3-5 Scoring system for assessment of alternatives on pre-set criteria and factors

Scoring range	**3**	**2**	**1**	**0**
Internal Factors				
Input Data (C)	Limited	Low	Moderate	High
Interpretation (C)	Guidance	Need help	Need knowledge	Specialized
Representativeness (F)	Comprehensive	Rich	Fair	Limited
Distinctiveness (F)	Integrative	Unique	Share aspects	Redundant
External Factors				
Independence (C)	Standalone	Needs supplementary	Complementary	Dependent
Framework (F)	Basic block	Direct	Possible	Limited
Interference/Reliability (F)	None	Minimum	Possible	High

C: Complexity; F: Functionality

3.3.4.2 Definition of scores and scoring system

A weighing and scoring system is imperative for a semi-quantitative complexity-functionality assessment. While SWOT, MADM or any other assessment method that includes scoring of methods to evaluate SWI impacts has not been reported for benchmarking, a scoring system was proposed to reflect the functionality and complexity of alternatives (Table 3-5). The scoring ranged from 0 to 3 with 0 representing poor functionality and high complexity while 3 reflects high functionality and low complexity. The final score of each criterion was derived by summing the performance scores for each factor after a normalization process based on a benefit-criterion system (Chang and Huang, 2006). The average normalized score of each criterion was used as a benchmark value allowing a direct comparison among assessment alternatives over a complexity and functionality numerical scale.

3.3.5 Framework Development

Based on method effectiveness, a framework for the assessment of the impact of SWI was developed. It consists of several assessment methods to be undertaken in series and/or in parallel to provide an adequate understanding of the SWI extent towards informed aquifer management. The initial selection allows the identification of methods applicable to the aquifer of interest. Then, the testing of these methods allows the evaluation of the role and contribution of each method in assessing the impact of SWI. The semi-quantitative approach sheds light on advantages, disadvantages, limitations and effectiveness of each method and identify those that should define a framework with minimal complexity, highest functionality in terms of water quality characterization, spatially able to capture the aquifer heterogeneity, and easy to understand by decision makers.

3.4 Results and Discussion

3.4.1 Application and testing of metrics

3.4.1.1 Physiochemical Parameters: groundwater quality and spatiotemporal effects

Summary statistics of the physio-chemical characteristics of the groundwater (GW) in the pilot aquifer are presented in Table 3-6. Groundwater of neutral pH and (sub)oxic redox potential (having oxidation-reduction reactions at low oxygen levels) dominated during all seasons. High variability was observed for TDS in and between seasons ranging from 390 ppm (fresh GW) (June) to as high as 32,220 ppm (highly saline GW) (April), with only 21% of samples showing fresh to slightly saline water quality (<1500 ppm). A statistically significant increase in TDS values ($p<0.001$) reaching ~35% was observed in the late dry sampling (October) round in comparison with the early dry (June) sampling. Similarly, based on the Cl^- classification, only 14% of groundwater samples reported fresh to slightly saline quality (<250ppm), whereas the majority of samples exhibited saline to highly saline water quality.

Reduced recharge[4] coupled with continuous groundwater abstraction explains the increase in EC, TDS and Cl^- in April 2014, as compared to June 2013. A significant intra-variability was observed in samples collected in April 2014 where fresh and highly saline groundwater was reported to exist concurrently but spatially apart. This variability hints towards the possibility of having two major groundwater hydrosomes, where one has undergone freshening, probably due to a decrease in abstraction rates that balanced the reduced recharge driven by the drought, while the other suffered from increased SWI caused by continuous abstraction driven by the lack of water exacerbated by the drought (Figure 3-3).

Figure 3 was generated using the geostatistical analysis and interpolation tool within the GIS. Ordinary kriging was applied to present and analyze TDS and Chloride measurements at sampled locations and extrapolate concentrations based on correlations between neighboring observation points to non-sampled locations. The geostatistical analysis allowed the generation of predictive maps over the entire domain to visually emphasize hotspots spatially and temporally. An exponential semi-variogram model with nugget of 0.22 and RMSE of 1.2 was used for lognormal transformed TDS data while a spherical model with nugget of 0.28 and RMSE of 1.5 was used for lognormal transformed chloride data.

[4]due to an unusually dry 2013/2014 wet season (with total precipitation ~50% lower than the annual average)

Table 3-6 Summary of descriptive statistics of physio-chemical parameters, ionic ratios and indices for the pilot aquifer across the three sampling periods

Season	June 2013 (early dry)				October 2013 (late dry)				April 2014 (late wet)				*WHO*
Parameter*	*Min*	*Max*	*Mean*	*SD*	*Min*	*Max*	*Mean*	*SD*	*Min*	*Max*	*Mean*	*SD*	Threshold (2011)
pH	6.4	8.2	7	0.3	6.5	7.73	7.04	0.31	6.71	8.0	7.1	0.22	6.5-8.5
EC	908	47106	9504	10468	740.6	65047	12008	15905	1550	65565	16391	15666	
TDS	560	23320	4610	5088	425.7	31460	5943	7709	390	32220	8389	7838	600
Ca^{2+}	56	1362	282.7	212.7	32	1190	249	222	14.4	1126	270.7	196	300
Mg^{2+}	19.4	1297	229.9	213	14.8	1129.9	246.8	261	11.9	1883	431.7	430	300
TH	450	8740	1651.5	1267	336	7620	1637.6	1548.2	131	10200	2451.8	2136	
Na^{+}	2.27	7000	1132.5	1519	4.24	10561	1629	2472.5	8.83	9315	2103	2092	200
K^{+}	0.53	212	19.7	35	0.87	328.2	45.3	76	1.9	638	83.69	104.9	300
Cl^{-}	100	13080	2358	2818	105	17670	3203	4312	47.6	19030	4453.5	4422	300
CO_3^{2-}	0	1	0.019	0.13	0.13	25.6	0.98	4.44	0	0	0	0	
HCO_3^{-}	141.8	493	258.6	65	34.4	460	274.8	73.7	76.4	490	276.2	69.3	
NO_3^{-}	2	219	39.8	30.6	1.7	66.5	27	16.8	0.8	84.8	30.8	17.12	50
SO_4^{2-}	7	2200	391	477	7	2900	418.6	606	7	2750	583.8	592	250
*Ionic Ratios*** *(based on meq/l)*													Criteria***
Na^{+}/Cl^{-}	0.02	1.09	0.529	0.0227	0.044	0.99	0.617	0.273	0.068	1.65	0.78	0.30	≤0.86
Cl^{-}/HCO_3^{-}	0.778	122.17	18	1.92	0.508	163	24.38	38.25	0.281	178.5	31.76	36.8	20-50
Mg^{2+}/Ca^{2+}	0.078	4.65	1.47	0.88	0.147	5.3	1.74	1.08	0.1758	13	2.5	1.91	4.5-5.2
Cl^{-}/Br^{-}	0.017	0.00014	0.0027	0.0003	0.00445	0.00007	0.00117	0.0007	0.005	0.000018	0.0008	0.0009	0.0015
$Ca^{2+}/(HCO_3^{-}+SO_4^{2-})$	0.315	15.315	1.617	0.146	0.298	10.187	1.3	1.597	0.1778	4.369	0.908	0.638	>1
SO_4^{2-}/Cl^{-}	0	0.803	0.14	0.0009	0.0345	0.7	0.13	0.111	0.018	10.5	0.265	0.995	0.103
$GQI_{generalized}$	25.2	83.7	53.6	1.195	21.27	83.36	52.3	15.46	19.74	83.69	46.55	15.46	
GQI (w/o NO_3^{-},TC,FC)	20.2	89.6	61.3	1.61	17.79	91.74	60.1	21.53	18.2	91.2	51.36	22.02	
f_{sea}	0.005	0.652	0.118	0.011	0.0052	0.879	0.159	0.214	0.0024	0.947	0.222	0.22	
GQI_{SWI}	24.1	86	62.7	1.21	11.25	89.53	59	18.65	8.18	86.9	54	17.8	<75

*All values in mg/l except pH and EC (µs/cm); **Parameters in ratios expressed in meq/l; ***Indicators of salinity

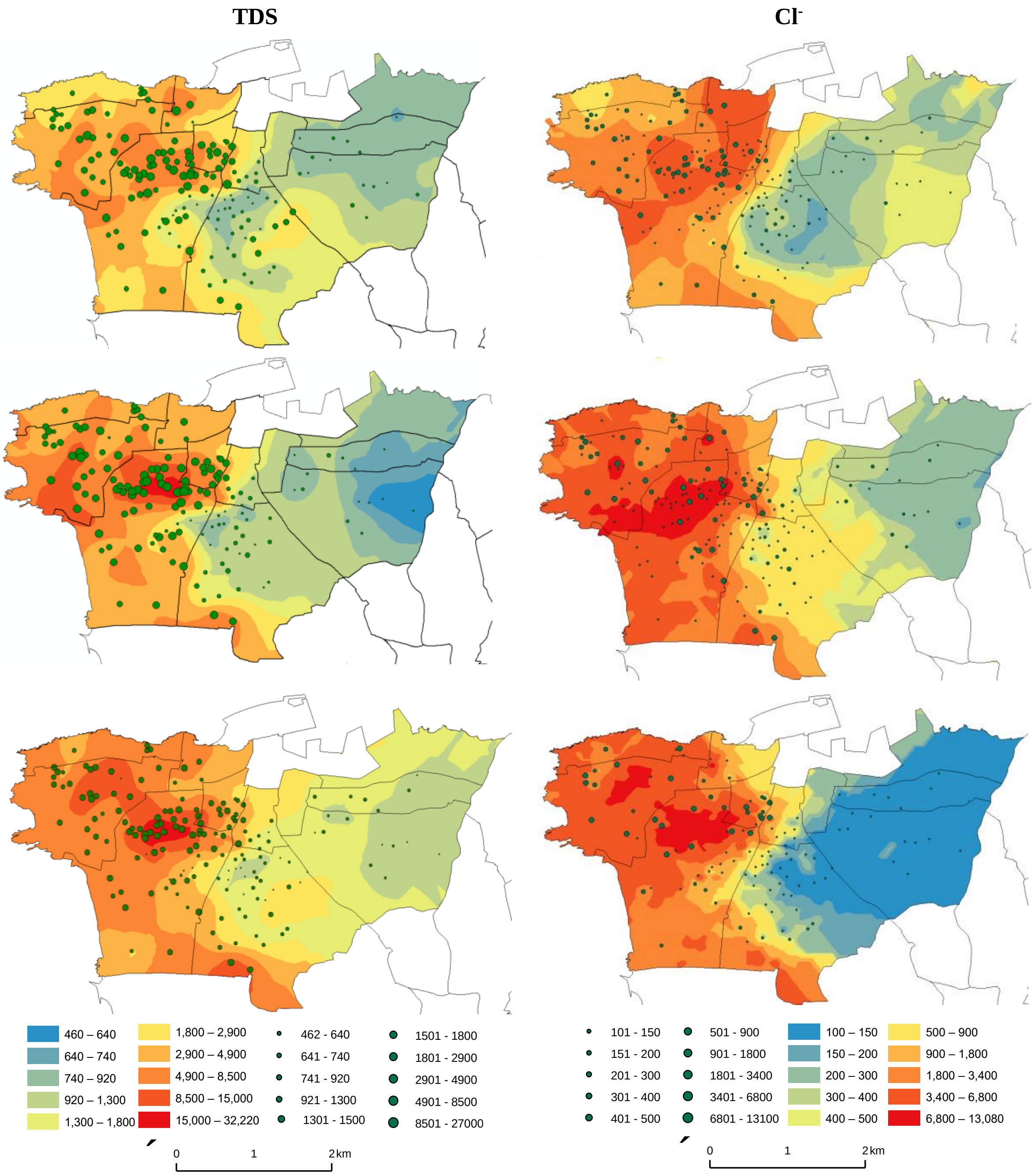

Figure 3-3 Spatial and temporal distribution of TDS (ppm) and Cl^-(mg/l) in the pilot aquifer
a) early dry season - June 2013, b) late dry season - October 2013 and c) late wet season - April 2014

3.4.1.2 Correlation analysis, indicator ratios and geochemical processes

The various ionic ratios indicated a wide variability within seasons, particularly in April, generally indicating an increasing trend of salinity from June to October to April (Table 3-6). The mean Na^+/Cl^- ratio, the symptomatic indicator of seawater intrusion, was at or below 0.86 for all seasons, suggesting well-developed SWI. Figure 4 shows that in June, samples with TDS <1,000mg/l generally had a Na^+/Cl^- ratio of <0.6 whereas samples with TDS >1,000mg/l were scattered around the 0.86 value. The October samples with TDS <1,000 mg/l migrated upwards on the plot. In April, the samples were divided in two envelopes: one saline and another fresh suggesting their concomitant existence.

The positive values of the seawater fraction and its wide range suggest considerable seawater-freshwater mixing within the aquifer (Table 3-6). It also indicates the coexistence of fresh and highly saline waters. Overall, the mixing rate increased ($p=0.001$ – Repeated Measures Anova) from June (11.8%) to October (15.9%), suggesting greater mixing along this timeline. Inter-elemental correlations showed that in June, TDS was highly correlated to Cl^-, Na^+, SO_4^{2-} and Mg^{2+}, suggesting signs of early salinization. In October and April, the TDS exhibited a stronger correlation with the same ions suggesting further salinization. The scatter of logTDS as a function of $\log Cl^-$ and of $\log Cl^-$ versus $\log Na^+$ (Appendix 2a) reveals a strong correlation in all sampling rounds, suggesting that Na^+ and Cl^- have the same seawater origin.

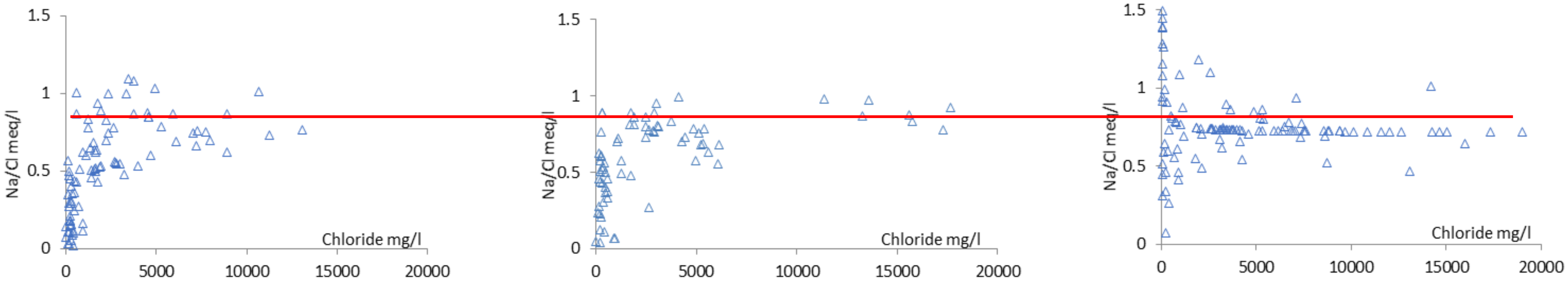

Figure 3-4 Na^+/Cl^- ratio versus Cl for a) June, b) October and c) April.

The redline represents the salinity indicator value of 0.86

The ionic changes/deltas for major ions also exhibited spatial and temporal variability indicating patterns of deficiency and surplus of the same ion over the entire study area and across seasons (Appendix 2b). While this reflects a groundwater experiencing mixing with seawater however the complexity of the hydrochemical changes such as the dissolution of gypsum and carbonate, de-dolomitization, direct and indirect cation exchange, as well as other potential sources limits clear conclusions from the observed changes in ionic deltas.

The piper diagram (Figure 3-5) reveals the presence of secondary saline water (hydrogeochemical domain V i.e. CaCl) as well as primary saline water (hydrogeochemical domain II i.e. NaCl) in June with the predominance of groundwater quality of the Cl^--SO_4^{2-}-Na^++K^+-Mg^{2+}-Ca^{2+} type. In October, the water was of the Cl^--Na^++K^+-Mg^{2+} type. Ion exchange and migration of samples from secondary saline water (domain V) to primary saline water (domain II) are observed when the mixed CaMgCl water type (domain IV) is detected. In April, three major water types were identified: freshwater (domain I, i.e. $CaHCO_3$), seawater (domain II, i.e. NaCl) in addition to domain IV (i.e. mixed CaMgCl). This highlights the occurrence of freshening processes in April and also confirms the occurrence of fresh and saline water concomitantly, albeit with spatial variability (Figures 3 and 6).

Water types as classified by the Stuyfzand method were mapped against the area's geology to explain potential relationships between spatial and temporal processes at play and the geological characteristics of the aquifer. Figure 3-6 shows that in October, fresh, fresh-brackish and brackish waters were observed in the Eastern districts within both the quaternary and tertiary geological formations, while brackish saline water was observed in the western districts with selected pockets of saline water. It also illustrates the spatial heterogeneity of the groundwater quality in April where two main phenomena are observed:

a) freshening processes occurring in the northeastern part (dilution of brackish and fresh-brackish water to fresh water) within the Miocene formations, and b) persisting salinization in the western districts with potential upconing of saline water particularly in the southwestern part within the Quaternary and Cenomanian formations. The disruption in the salinization in the eastern flanks of the aquifer coupled with the persistence of pumping in the 2014 late dry to early wet season, support either that 1) the pumping rates during this period dropped due to increased water supply from the public network, or 2) that groundwater recharge happens earlier and/or faster in that sector, potentially as a result of lateral flow from the north-northeastern highlands and/or the Beirut River, or 3) the impact of the degree of heterogeneity and complexity of fractured networks, or 4) the role of the geology particularly that the eastern flanks are characterized by an upper Miocene layer, or 5) that the study area consists of two aquifers responding differently and independently to similar stimulus. Further aquifer characterization and additional data on recharge, water level and water supply are needed to ascertain the interpretation of the results.

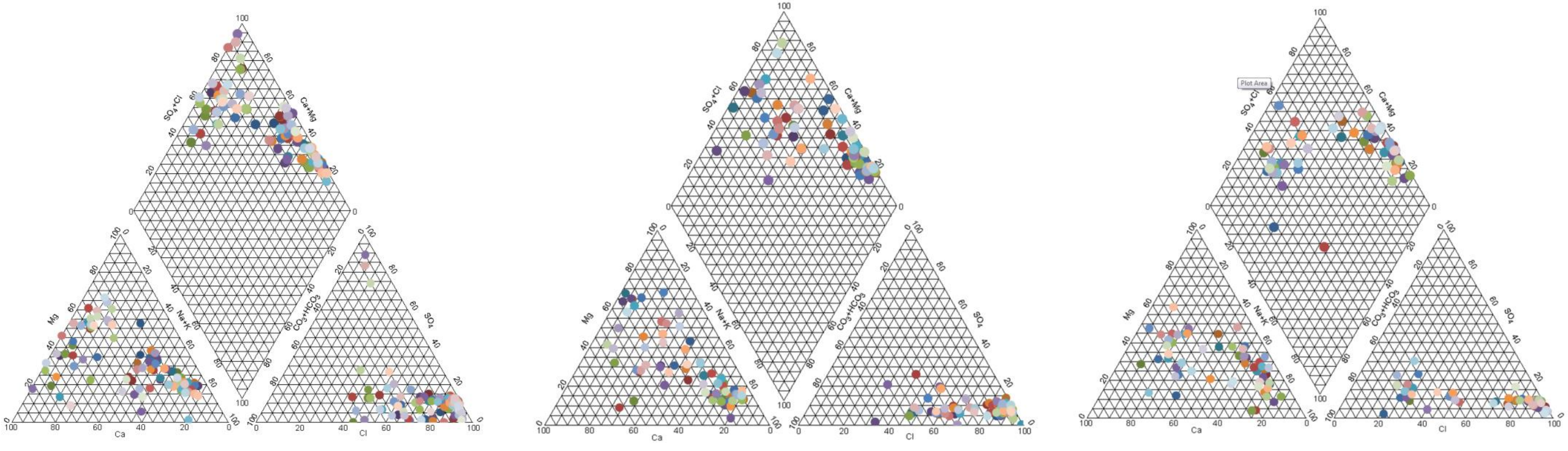

June 2013 **October 2013** **April 2014**

Figure 3-5 Piper diagram for thepilot aquifer
Each circle represents a well

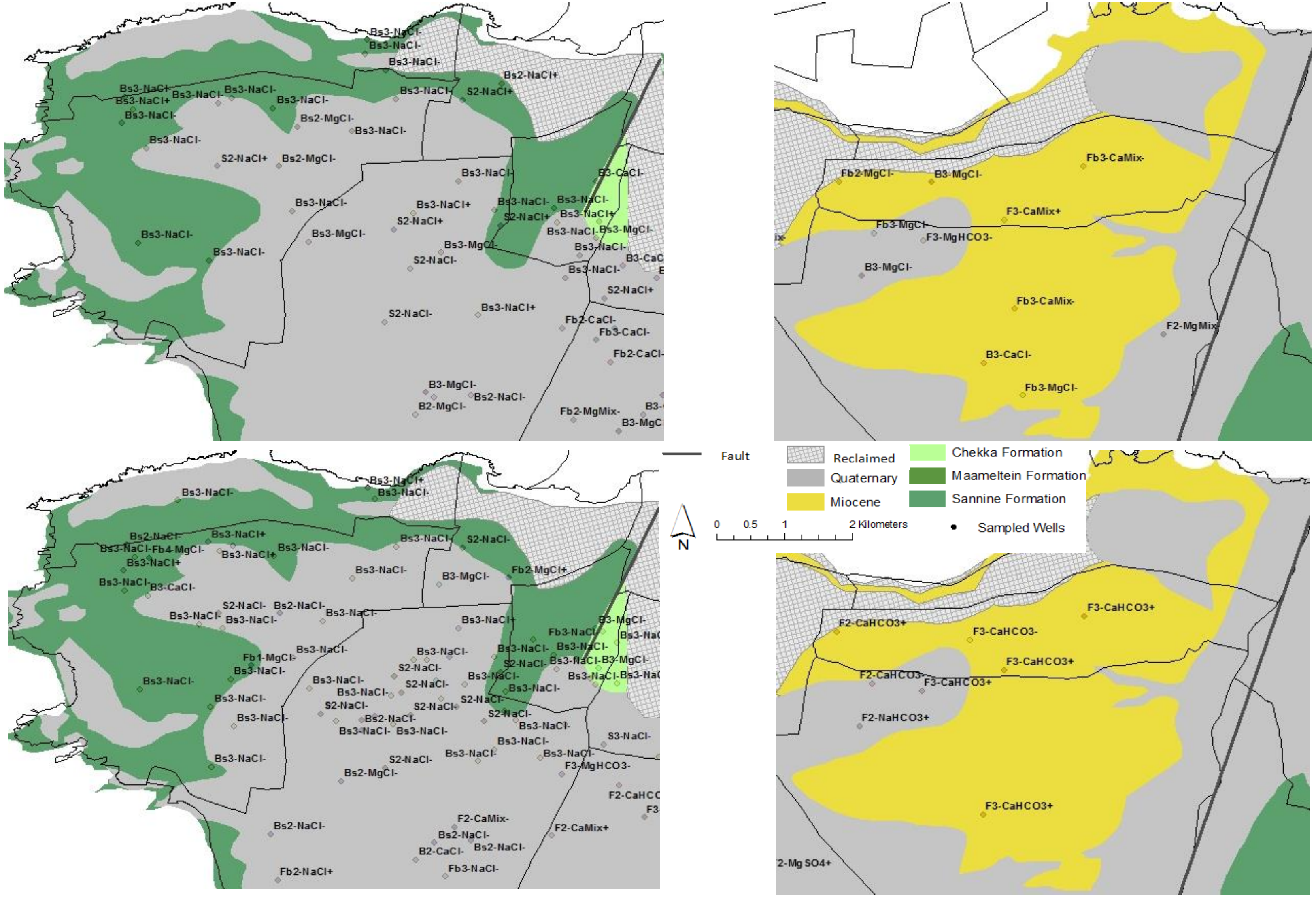

Figure 3-6 Water types based on Stuyfzund classification for the western (left) and northeastern(right) parts of the pilot aquifer for late dry - October (upper) and late wet -April (lower); *F:fresh; Fb: fresh-brackish; B:brackish; Bs: brackish-saline; S: saline - Table 3-4*

3.4.1.3 Groundwater quality indices

The generalized GQI (Table 3-6) exhibited average water quality for the three sampled seasons albeit with spatial heterogeneity. Figure 3-7 shows that the eastern zones tend to have better water quality under the three indices as compared to the western zones, with a general trend of degrading quality from June to October to April. This figure was generated using the geostatistical analysis and interpolation tool within the GIS where ordinary kriging was applied to the relevant water quality parameters and the GQI indices were calculated from the predicted concentrations in a multi-step process (Tomaskiewicz et al., 2014; Babiker et al., 2007) to generate predictive maps of pollution and salinity hotspots spatially and temporally. When removing the health-based water quality indicators (e.g. nitrates, total and fecal coliform) (Figure 3-7b), an improvement in water quality is observed in June suggesting that nitrates and fecal coliforms may be responsible for the low generalized GQI unlike October that showed no improvement (except in the eastern zones). This suggests that the reported minimum to average water quality in October under the generalized GQI is not due to direct anthropogenic pollution (nitrates, FC and TC) but more likely to SWI.

The GQI_{SWI} impact mapping (Figure 3-7c) demonstrates that the SWI is more developed in October and April, particularly in the western zones. Repeated measures ANOVA showed that the GQI_{SWI} values differed significantly between seasons whereby post hoc tests using the Bonferroni correction revealed a statistically highly significant decrease between June and October ($p<0.001$) and June and April ($p<0.001$). The GQI_{SWI} recaps and confirms the spatio-temporal impacts of SWI, particularly in terms of saline freshwater mixing dynamics and the hydro-geochemical domains.

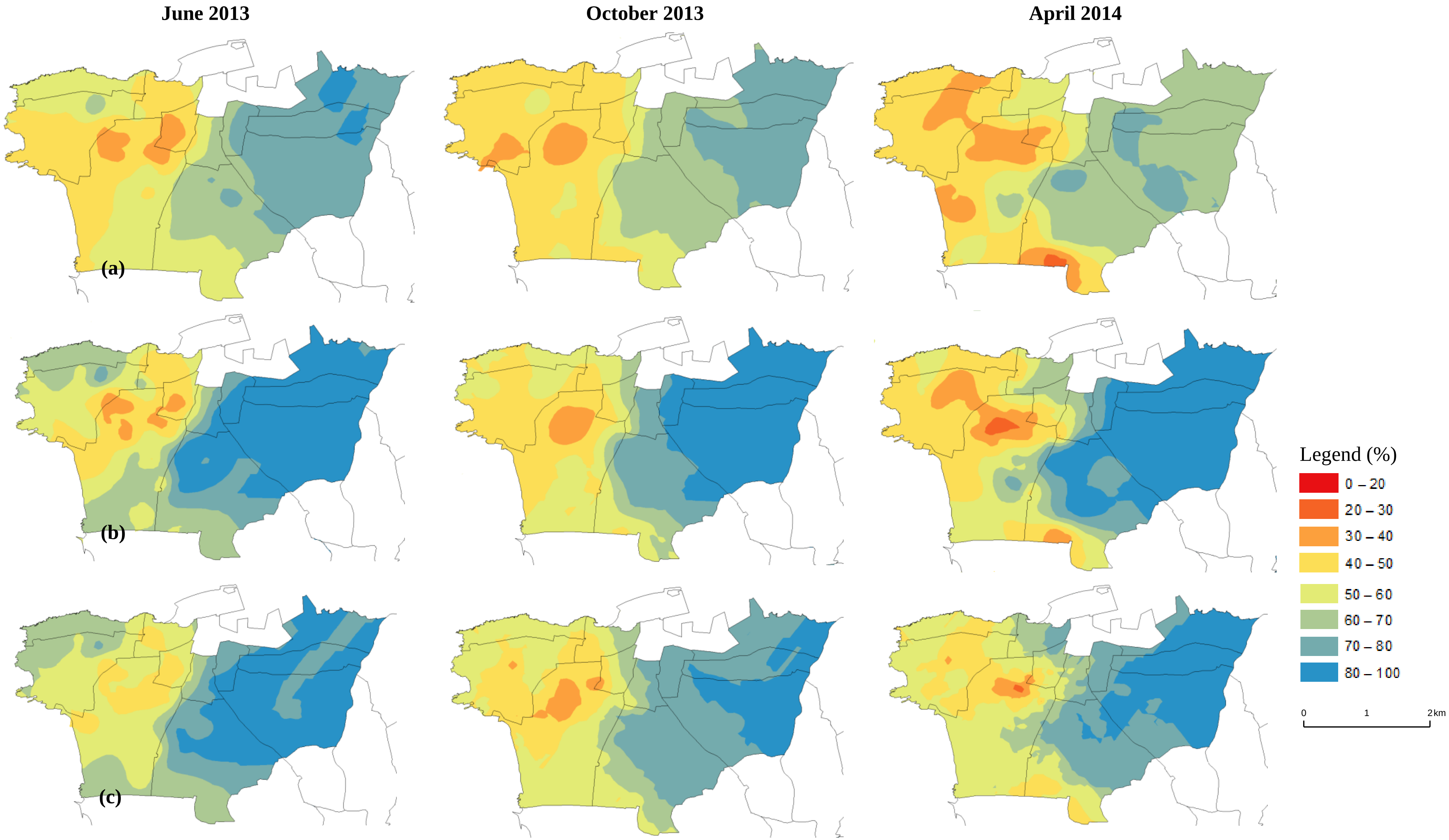

Figure 3-7 Groundwater quality indices (GQI)

a) Generalized GQI; b) Generalized GQI without NO_3^-, Fecal and Total Colifrom; c) Specific GQI_{SWI}

3.4.2 Evaluation of methods towards an assessment framework

Table 3-7 summarizes the qualitative SWOT analysis of the methods used to assess SWI. Table 3-8 summarizes the quantitative scoring of these methods based on their performance against set internal and external factors for SWOT and visually illustrates the evaluation on a numeric scale. While most parameters are good indicators of salinity, the type, scope and reliability of the results vary significantly. The variability was inherent among parametric versus composite methods in terms of complexity, feasibility, and ability to represent SWI impacts. However, the specificity of how each method is able to uniquely represent different aspects of SWI and the supplementary nature of outputs of the various parametric methods are also perceptible.

Simple indicators such as TDS, Cl^- and the seawater fraction act as a quick first screening of salinity while only hinting to its source. Nevertheless, being relatively easy to undertake, they form good candidates for monitoring and constitute a main building block in a SWI assessment framework. Hydrochemical ratios and the piper diagram add another layer of information to ascertain sources of salinity highlighting the impact of SWI, as well as interpret geochemical reactions to define water types and evolution. Ionic deltas, saturation and BEX/CAI indices provide input on geochemical reactions and their direction; however, they are data demanding requiring the knowledge of rock formations and on-going reactions to avoid misunderstandings due to interferences; hence, can only be useful if the aquifer is well characterized and understood particularly in terms of rock-water interactions.

The Piper diagram, acting here as a surrogate of hydrochemical diagrams, is also based on individual parameters and delivers multiple layers of information with a visual aspect that resonates with decision makers. The Stuyfzand hydrochemical classification, while comparable to the Piper diagram, is more data dependent yet also provide more layers of information. Being integrative, this composite index can also act as a standalone tool that encompasses most aspects of SWI. However, it is complex to undertake and also difficult to interpret. Nevertheless, its relative complexity is compensated for with a high functionality.

The generalized water quality indicators act as a final layer of confirmation of water quality serving as a one-stop shop that can be easily plotted to show spatio-temporal evolution of the quality in general (GQI) and of the impact of SWI in particular (GQI_{SWI}) for informed decision making. While both the GQI and the GQI_{SWI} are similar in their complexity, the GQI_{SWI} is a standalone robust and integrative tool for SWI assessment and monitoring. The embedded geo-statistical analysis offers the advantage of visual interpretation coupled with temporal and spatial representation of parameters and processes.

Based on input from the field application and results, the qualitative SWOT analysis coupled with the semi-quantitative overall assessment, a framework is suggested for the assessment of SWI impacts in less characterized heterogeneous aquifers. As adopting a suite of methods to assess the impact of SWI reduces the uncertainty that may obscure the interpretation of results (Garing *et al*. 2013; Vengosh, 2003), this framework is based on the concentrations of chloride, total dissolved solids (TDS) and electrical conductivity (EC), the seawater fraction (f_{sea}), the piper hydro-chemical diagram, the Stuyfzand's hydrochemical classification, and the SWI specific $GQI_{SWI.}$. It requires groundwater sampling and lab analysis of major ions (HCO_3^-, CO_3^{2-}, SO_4^{2-}, Ca^{2+}, Mg^{2+}, Cl^-, Na^+ and K^+) and TDS/EC. Measurements of Br^- and NO_3^- ions are optional, though recommended, particularly for eliminating other potential sources of pollution. TDS and EC are correlated and can be used interchangeably. They are also correlated with Cl^-. While a high Cl^- concentration can alone hint to salinity, this is not true for TDS and EC which represent a suite of all ions and charges. Nevertheless, Cl^- coupled with TDS or EC should be a starting point for a SWI assessment. The seawater fraction is also correlated to Cl^-; however, its unique representation of the freshwater-saline water mixing differentiates it from the mere measurement of Cl^-

concentration in groundwater, which might also point to other pollution sources. Here, the hydrochemical ratios become handy. Ratios will also consist part of this framework, capitalizing on their high score on simplicity despite their low score on functionality, as they can give insights on pollution sources and help understand interactions that confirm or invalidate conclusions of the TDS/EC and Cl^- concentrations.

Table 3-7 Contribution, advantages and disadvantages of indicators, indices and assessment methods

Method Factors	**Strengths**	**Weaknesses**	***Opportunities***	***Threats***
TDS, Cl^-, EC concentrations	- Limited input data - Quick first assessment - Common simple indicator of salinity	- No input on process, source or geochemical reactions	- Integral building block of framework - Useful for monitoring - Easy test	- Can be misinterpreted if not complemented by other detailed / advanced analysis
Hydrochemical ratios	- Low to moderate input data - Good indicators of reactions, direction of reactions and pollution source - Good indicators of salinity & SWI	- Weak but could be used in interpreting geochemical reactions - A suite of ratios is needed for complete representation	- Relies on conservative nature of Cl^-, Na^+, Br^- - Relatively easy to test - Useful for monitoring	- Due to overlapping ranges, values may mask or over-represent SWI - Can be misinterpreted if rock-water reactions are not understood
Seawater fraction	- Limited input data - Quick first assessment - Common simple indicator of salinity - Useful for monitoring	- Presents concentration only - Doesn't represent geochemical reactions	- Relies on conservative nature of Cl^- - Easy test	- Could be misinterpreted for SWI as it does not consider the effects of geochemical reactions - High sensitivity to Cl^- may overestimate SWI
Ionic deltas Saturation indices	- Presents geochemical reactions and changes	- Require input data and prior knowledge	- Useful for understanding rock-water interactions - Indicates paths of evolution of reactions	- High potential for interference due to multiple pathways for rock water interactions - Require aquifer understanding
Piper Hydrochemical diagrams	- Graphical representation - Represent water types reflecting intensity of salinity contamination - Indicates paths of evolution of water types	- Only generally indicates geochemical changes	- Visual aid for decision makers - Relatively easy to undertake	- Focus only on major parameters - Not readily spatially mapped - Could be misinterpreted
Stuyfzund hydrochemical classification	- Good indicators of reactions, direction of reactions, pollution source and water type - Comprehensive integrative standalone indicator	- Heavily relies on data - Not easy to interpret	- Comprehensive representation of water type - Can be easily plotted - Translate major parameters	- Could be misinterpreted with no specialized help

Method Factors	Strengths	Weaknesses	*Opportunities*	*Threats*
			into one indicator	
GQI generalized	- Good indicators of reactions, direction; pollution source - Test pollution by NO3, TC and FC	- Relies on concentrations of all major ions	- Easy to calculate and interpret - Translate major parameters into one indicator	- Presents general groundwater quality but not SWI - Needs to be complemented
GQI_{SWI}	- Good indicators of reactions, direction; pollution source - Comprehensive integrative standalone indicator - Specific to SWI	- Relies on concentrations of all major ions	- Easy to calculate and interpret - Translate major parameters into one indicator	- Presents general groundwater quality and SWI

Table 3-8 Summary of performance of methods against internal and external factors and corresponding scores

Method Criteria	Input data	Interpretation	Independence	Representativeness	Distinctiveness	Integration in framework	Interference
TDS, EC, Cl^-	Limited	Guidance	Needs supplementary	Limited	Share aspects	Basic block	Minimum
Hydrochemical ratios	Low	Need help	Needs supplementary	Fair	Share aspects	Direct	High
Seawater fraction	Limited	Guidance	Needs supplementary	Limited	Unique	Basic block	Minimum
Ionic deltas	Moderate	Need knowledge	Complementary	Fair	Share aspects	Possible	High
Saturation indices	Moderate	Need knowledge	Complementary	Fair	Unique	Possible	High
BEX and CAI	Low	Need help	Complementary	Fair	Share aspects	Direct	High
Hydro-chemical diagrams	Moderate	Need help	Standalone	Rich	Share aspects	Direct	Minimum
Stuyfzund method	High	Specialized	Standalone	Comprehensive	Integrative	Direct	None
GQI	Moderate	Guidance	Dependent	Comprehensive	Share aspects	Possible	Possible
GQISWI	Moderate	Guidance	Standalone	Comprehensive	Integrative	Direct	Possible
Inference statistics	Varies	Varies	Varies	Rich	Integrative	Limited	Possible
Geospatial analyst	Varies	Guidance	Dependent	Rich	Unique	Direct	Varies

Overall Scoring	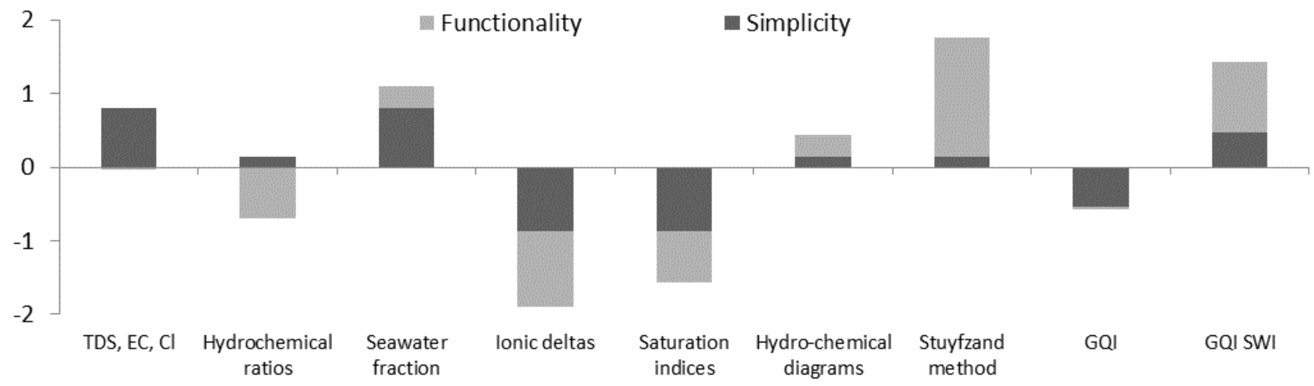

Plotting concentrations of major ions on the piper diagram allows direct inference on the water type and the hydrochemical reactions at each sampling point which is a very effective visual summary of concentrations, reactions, and water type. Coupling the piper diagram and the seawater fraction, the GQI_{SWI} further validates the salinization progress into the aquifer as well as allows a spatio-temporal representation of this progress. The framework's elements provide a good understanding of the freshwater-saline water mixing dynamics in the aquifer and can stand alone as a comprehensive assessment tool of the SWI impact (Figure 3-8). The metrics complement one another as each contributes different input layers to the analysis of processes, dynamics and impact of SWI within the aquifer. This ensures that results are double-checked against one another, while optimizing resources, input data and time. Further, interpretation through the Stuyfzand method, despite its relative complexity, can lead to additional detailed valuable knowledge about the aquifer of study. While this method does not necessarily have to be part of the assessment framework to be effective, it ensures a complete analysis cycle. Since it is a composite method, its main advantage is in summarizing levels of data and providing a profile of groundwater quality, and can be easily represented spatially and becomes handier if plotted temporally.

Put to test in a highly exploited heterogeneous coastal aquifer, this framework allowed the understanding of the spatio-temporal dynamics and impacts of SWI processes, provided a reliable baseline of the salinization status, and facilitated monitoring of the SWI impact over spatial and temporal domains while minimizing potential interferences by triangulating the results. As such, it aided in understanding that the occurrence and intensity of SWI in the pilot aquifer is shaped by multiple factors including the heterogeneous nature of the aquifer, the geologic characteristics (faults/flanks), and groundwater abstraction. Hence, the framework represents a starting point for planning and decision-making in strategic impact assessment towards improved groundwater management in coastal aquifers.

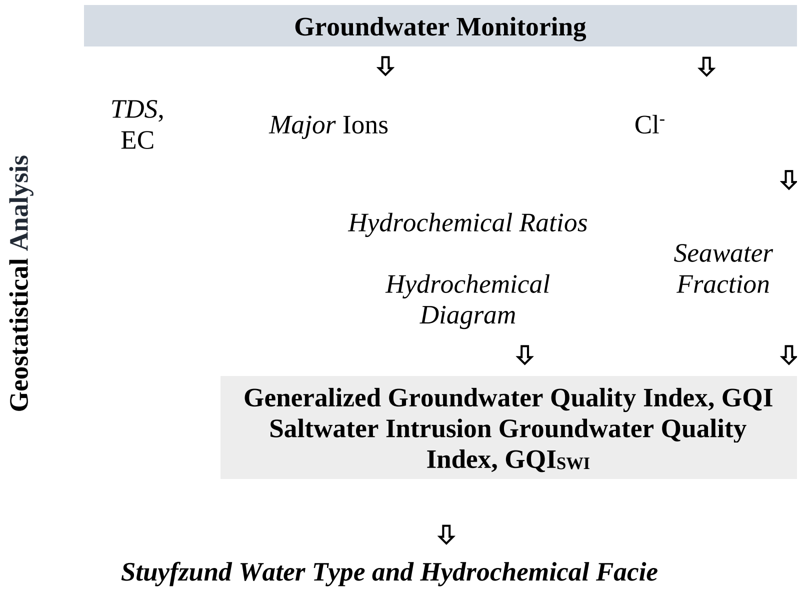

Figure 3-8 Elements of Proposed Framework

3.5 Conclusion

Common methods used in assessing the impact of SWI (saltwater intrusion) were examined to develop a novel effective assessment framework for managing coastal aquifers underlying densely populated urban areas. For this purpose, a qualitative assessment of complexity and functionality was first followed to select alternative methods that were tested and verified at an overexploited heterogeneous aquifer along the Eastern Mediterranean. A semi-quantitative CFA (complexity functionality assessment) coupling SWOT (strengths, weaknesses, opportunities and threats) and MADM (multi-attribute decision making) analyses was then developed and used to evaluate the effectiveness of various methods in scrutinizing the impact of SWI based on predefined criteria. Capitalizing on the characteristics of an indicator-index and its advantages, and complementing it with other indicators-indices to overcome associated uncertainties, provided a more reliable assessment framework of the intensity, ubiquity, persistence, and reversibility of SWI impacts. The framework of hydrogeochemical metrics (chloride, total dissolved solids (TDS) or electrical conductivity (EC) concentrations, the seawater fraction (f_{sea}), the piper hydro-chemical diagram, the SWI specific GQI_{SWI}, and the Stuyfzand's hydrochemical classification) coupled with geostatistical analysis was advanced to interpret complex groundwater quality data and examine the scale and magnitude of the impact of SWI and its dynamics in heterogeneous aquifers. Such a framework provides a platform for informed impact assessment and sustainable exploitation of coastal aquifers reducing the gap between SWI knowledge on one side and management needs for practice and implementation on the other. Efforts are on-going to further test this framework in other heterogeneous aquifers along the Eastern Mediterranean, to assess emerging saline aquifers moderately exploited for agricultural or domestic purposes.

Whilst utilizing well established and commonly used techniques to assess SWI, this study presented a first attempt at examining these techniques in a systematic, transferable, repeatable and verifiable process through the development and application of qualitative and semi-quantitative criteria. Similarly, it is the first to apply SWOT and MADM analysis to SWI where 'fit for purpose' assessment techniques were identified based on functionality and simplicity. In effect, this study has provided a systematic approach to the assessment of SWI and developed an effective assessment framework for managing coastal aquifers, including complex aquifers with data scarcity.

Future development of this work focuses on the management aquifers through identification and analysis of potential mitigation measures and adaptation strategies. Hydrogeochemical findings and the aquifer salinization status will be utilized to improve the characterization of the aquifer through building hydrogeological models, representing its heterogeneity, in an attempt to simulate and predict saltwater intrusion propagation under various anthropogenic stressors exacerbated by potential climate change impacts manifested through sea level rise.

CHAPTER 4

MANAGEMENT OF SALTWATER INTRUSION IN DATA-SCARCE COASTAL AQUIFERS: IMPACTS OF SEASONALITY, WATER DEFICITS, AND LAND USE

4.1 Introduction

Landward intrusion of seawater into coastal aquifers, known as saltwater intrusion (SWI), is primarily caused by aquifer over-pumping and land-use change (Singh 2014; Werner et al. 2013). The extent of SWI is governed by coastal hydrostatic pressures at the hydraulic interface between saline and freshwater. Under undisturbed conditions, a state of dynamic equilibrium is maintained between freshwater and seawater, where the hydraulic gradient pushes freshwater towards the sea. Aquifer over-pumping affects SWI by inducing a hydrostatic imbalance that reverses this hydraulic gradient resulting in seawater infringement into coastal aquifers (Bear 1979; Werner et al. 2013). Over-pumping is often a function of population density, water consumption rates, and available surface freshwater resources. Changes in Land use and land cover (LULC) affect SWI through increasing the intensity of abstraction from the aquifers (Safi et al. 2018; Cobaner et al. 2012; Sherif et al. 2012; Ferguson and Gleeson 2012; Ivkovic et al. 2012) or changing the recharge rates of these aquifers (Payne 2010; Ranjan et al. 2006; Scanlon et al. 2005). Climate change can further exacerbate the SWI process due to sea level rise aggravated at times and locations, with increased temperatures (i.e. increased evapotranspiration and water demand) and reduced precipitation (i.e. less surface water for aquifer recharge) (Kumar et al. 2007; IPCC 2007; 2014).

While general trends governing the interactions of these drivers are well established[5] worldwide, the direction and magnitude of these interactions remain area-specific (Werner et al., 2013). This complexity is aggravated in fractured, karstic and semi-karstic media (Sebben et al., 2015, Werner et al., 2013, Cherubini and Pastore, 2011, Papadopoulou et al., 2005) as well as in data-scarce regions, where coastal managers need to plan and act under incomplete knowledge and uncertainty to delineate impacts and protect coastal communities (Cardenas and Halman, 2016, Werner et al., 2013, Tribbia and Moser, 2008).

While many aquifers along the Eastern Mediterranean, particularly in urbanized settings are reported to suffer from SWI (Seckin et al. 2010; Cobaner et al. 2011; 2012; Allow 2012; Eissa 2016), they remain largely poorly characterized. Past efforts are often limited by their spatial extent, sampling frequency , methods of analysis, and a lack of focus on drivers, determinants and adaptation potentials (Tomaszkiewicz et al. 2014; Selmi 2013; Seckin et al. 2010; Alpar 2009; Abu Zakhem & Hafez 2007; Paster et al. 2006; Odemis et al. 2006; Sivan et al. 2005).

In this study, we examined the status and occurrence of SWI at four aquifers along the Lebanon coastline with different land uses and varying intensities of water deficits. The study aimed at understanding the contribution of land use and urbanization as well as water demand and deficit on the temporal distribution and intensity of SWI. For this purpose, field monitoring data coupled with hydro-geochemical techniques as well as multi-variate statistical analysis were undertaken to identify the main SWI determinants and to better understand their associated relationships in the aquifers. In light of the results, the study

[5] New Zealand (EnviroLink 2011), China (Zhang et al. 2011), Philippines (Sales 2009), Korea (Park et al. 2012), US (Conrads & Roehl 2007; Sanford & Pope 2010), Bangladesh (Rahman et al. 2011), India (Bobba 2002), France (de Montety et al. 2008), Spain (Fatoric & Chelleri 2012; Duque et al. 2008), Tunisia (Kouzana et al. 2010; Fedrigoni et al. 2001), Libya (El Hassadi 2008) among others.

discusses possible adaptation strategies and mitigation measures towards the sustainable management of the studied aquifers.

4.2 Methodology

4.2.1 Study Area

Four pilot aquifers located along the Eastern Mediterranean coast of Lebanon and overlain with different LULC patterns were monitored (Figure 4-1). Aquifer A (Tripoli) underlies a highly urbanized and densely populated city (Table 4-1). Aquifer B (Jal Eldib) is located below a moderately populated suburb of Beirut city. It is largely residential with few light to medium industries and a diminishing agricultural sector (Table 4-1). Aquifer C (Beirut) underlies a very highly urbanized and densely populated metropolitan with severe water shortages (Table 4-1). Aquifer D (Zahrani) underlies an agricultural plain with no urbanization (Table 4-1). All four aquifers are largely data-deficient, with little to no information on water levels, the location of the seawater-freshwater interface, pumping rates, well screen depths, and basic aquifer characteristics. In each of the four aquifers, operating wells were first identified through field visits. Then, a random sample of these wells were monitored at least once in the dry season and once in the wet season. The number of sampled wells ranged from 29 in Jal eldib up to 170 wells in Beirut (Table 4-1). All sampled wells are within 100 m from the ground surface and generally targeted the formations defined in Table 4-1.

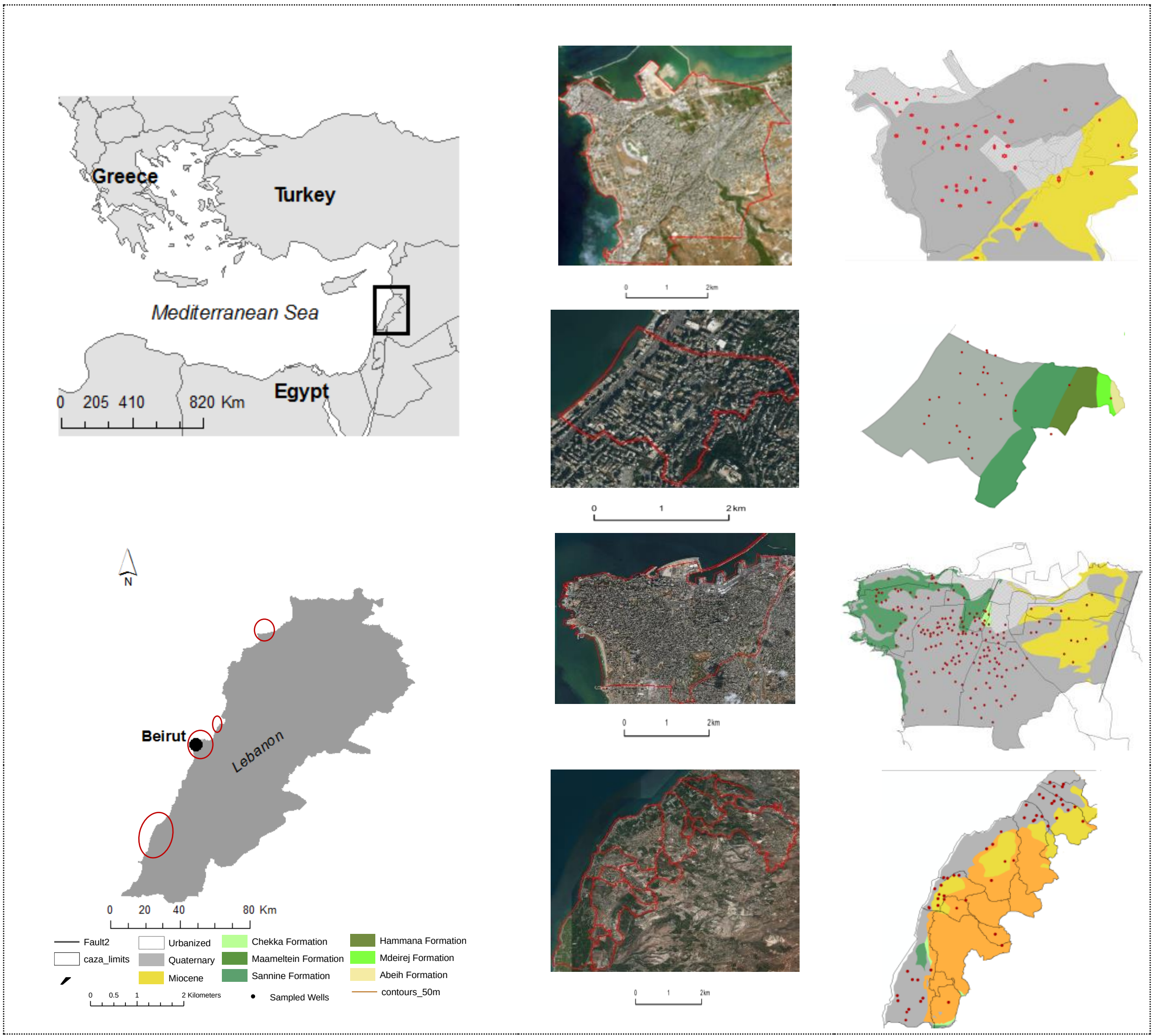

Figure 4-1 Pilot study areas along the Eastern Mediterranean
A: Tripoli city; B: Jal Eldib suburb; C: Beirut city; D: Zahrani Plain

Table 4-1 Pilot study areas with overall sampling program

Aquifer	Description	Land Use	Recharge potential[a]	Geology	Hydrogeology	Sampling season	Sampled Wells
Tripoli[b] (A)	– Area of 45 km^2 – Max elevation 200m asl – ~ 5km shoreline – Rocky coastline – Low rainfall (700mm) – Medium water deficit (limited to dry season)	– Highly urbanized – Residential – Limited agricultural parcels – Residents (> 80,000) – Estimate of 4000 lightly used small building scale wells	– Limited direct recharge – Aquifer replenishmen t through lateral flow	– Quaternary (alluvial deposits) – Cenomanian – Pockets of Tertiary (Miocene) – Semi karst – Faulted	– Miocene limestone aquifer – Shallow Quaternary clays – Eocene limestone aquiclude	– Dry – Septemb er 2006 – Wet – June 2007	0
Jal Eldib[c] (B)	– Area of 2 km^2 – Max elevation 100m – 1 km shoreline – Low rainfall (~800 mm) – Low water deficit (groundwater supplements network only in dry season)	– Moderately urbanized – Residential with light to medium industries – Estimate of 150 wells – Few wells supply water tankers for Beirut city	– Aquifer replenishmen t through direct recharge and lateral flow	– Quaternary deposits – Cretaceous (Cenomanian) – Multiple fractures	– Carbonate (Cenomanian limestone) – Quaternary	– Every 2 months between October 2012 and October 2013	29
Beirut[d] (C)	– Peninsula of 20 km^2 – Max elevation 250 m asl – 5 km shoreline – Cliffs, rocky and sandy coastline. – Low rainfall (~800mm) – High water deficit of ~35% & ~58% in winter & summer seasons respectively	– Very highly urbanized – Residential – Population density exceeding 20,000 person/Km^2 – Conservative estimate of >5000 heavily used small building scale wells	– Limited permeable pockets – Direct recharge is negligible – Lateral Flow is limited	– Cretaceous (Cenomanian C4 & Senonian S_6) – Quaternary (moving dunes and soils) – Pockets of the Tertiary (Miocene) – Semi-karst systems – Fractured, heavily jointed and faulted	– Carbonate - Cenomanian and Quaternary (sands depositing over the Cenomanian) forms one thick (~700m) extensive formation – Mainly limestone and dolomite, and some intercalations of marl	– Wet - June 2013 – Dry - October 2013	170
Zahrani[e] (D)	– Coastal area of 40 km^2, – Max elevation 250m asl – 20 km shoreline – Rocky and sandy coastline – Low rainfall (700 mm) – Low water deficit (groundwater supplements surface water in dry season)	– Not urbanized – Agricultural plain – Estimate of 150 wells – Major crop banana (*Musa ascuminata*). – Vegetables in greenhouses – Fruits in orchards. – Surface water for irrigation in wet season	– Aquifer replenishmen t through direct recharge and lateral flow	– Cretaceous (Cenomanian C4, Turonian C5, Senonian) – Tertiary (Miocene & Eocene outcrops) – Quaternary deposits – Semi-karst – Heavy fissures and faults	– Cenomanian -Turonian Limestone aquifer – Eocene Limestone – Quaternary aquifer.	– Wet – May 2014 – Dry - October 2014	61

[a] Due to lack of data, it was not possible to quantify and account for lateral flow in the analyses of the pilot sites. [b] MOEW/UNDP 2014; Kalaoun et al. 2016; Tomaskiecz et al. 2014
[c] Walley 1997; El Fadel et al. 2015; [d] Ukayli 1971; Peltekian 1980; Khair 1992; Rammal 2005; Shaaban et al. 2006; Saadeh 2008; Ayash, 2010; SOER 2011; Masciopanti 2013; [e] Dubertret 1961; Canaan 1992

4.2.2 Assessment of saltwater intrusion

The assessment of SWI at the four pilot aquifers followed a framework that combined field monitoring results with hydro-geochemical techniques with descriptive and inferential statistics (Rachid et al. 2017). The analysis targeted both the wet and dry seasons at each pilot area, with samples collected during the period of May/June to capture the wet season effect and in the month of October to capture the dry season effect. Identification and classification of salinity was based on the EC, TDS and Cl- levels (Table 4-2).

Table 4-2 Classification of water based on chloride, TDS, and EC concentrations (Konikow & Reilly 1999)

Class	**Cl^- (ppm)**	**TDS (ppm)**	**EC**
Fresh groundwater	<100	0-500	<700
Slightly saline groundwater	100 – 250	500-1500	700-2000
Moderately saline groundwater	250 - 500	1500-7000	2000-10000
Highly saline groundwater	500 – 1000	7000-15000	10000-25000
Very highly saline groundwater	1000 – 10000	15000-35000	25000-45000
Seawater	>10000	>35000	>45000

4.2.2.1 Hydrogeochemical methods

The Piper diagram (Figure 4-2), which is the standard hydro-geochemical diagram to graphically illustrate the chemistry of water, was constructed seasonally for each site. It consists of two triangles that represent the distribution of cations and anions of water samples, which are then projected onto a diamond that summarizes the geochemical processes and pathways, the dominant ions, hydro-chemical facies and the types of the water under study (Piper 1953). Additionally, the SWI Generalized groundwater quality index (GQI_{SWI}) (Table 4-3) was computed for each site. The GQI_{SWI} is an index that spatially maps SWI by coupling the fresh-saline water mixing (sea fraction) with the piper diagram (Tomaszkiewicz et al. 2014; Babiker et al., 2007). Note that the seawater fraction (fsea) depicts the direction and extent of saltwater-freshwater mixing (Table 4-3).

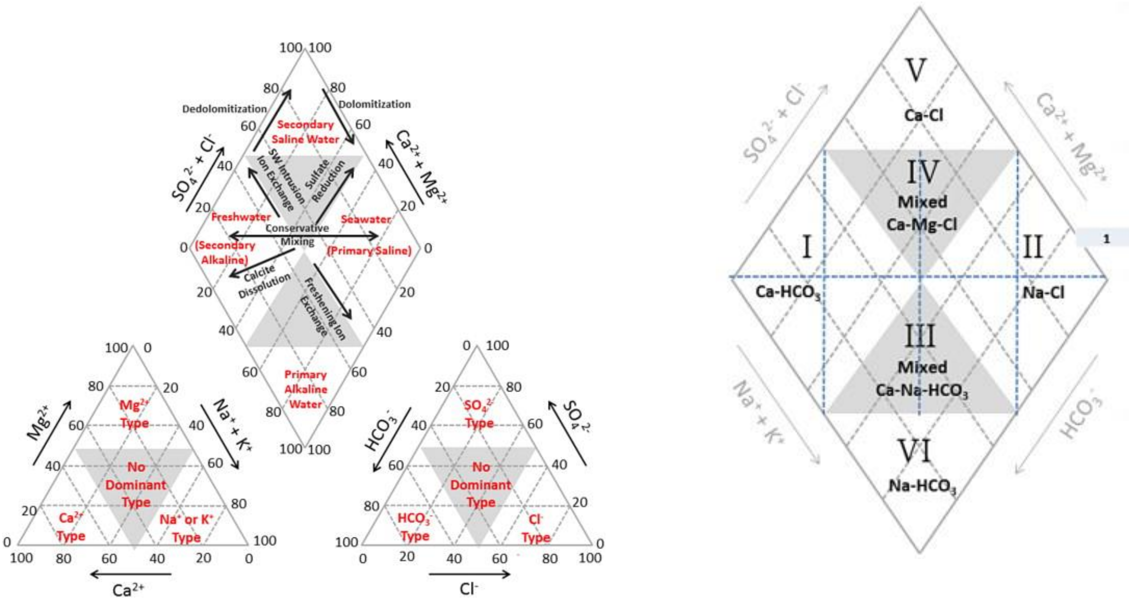

Figure 4-2 Water types and geochemical pathways as explained by the Piper hydrogeochemical diagram (adapted from Tomaskiewicz et al. 2014)

Table 4-3 Generalized water quality indices (adapted from Babiker et al. 2007; Tomaskiewicz et al. 2014)

Groundwater quality indices	**$GQI_{generalized}$**	GQI = (100 – (($r_1w_1+r_2w_2+\ldots+r_nw_n$)/N) C= (X’-X)/(X’+X); X’: sample concentration; X: WHO threshold r = is the rank value calculated as $0.5*C^2 + 4.5*C + 5$; N = is the total number of parameters; w= relative weight of the parameter
	GQI_{SWI}	GQI_{SWI}= (GQI_{piper} + GQI_{fsea})/2
	GQI_{piper}(%)= [((Ca^{2+} + Mg^{2+})/Total cations) + (HCO^{3-}/Total anions)]*50 (in molar mass)	
	f_{sea} = seawater fraction/ mixing ratio = (Cl^-sample − Cl^- freshwater) / (Cl^-seawater − Cl^-fresh)	

4.2.2.2 Statistical analysis

The principal component analysis (PCA), a multivariate technique, was performed to identify the most important components contributing to the data structure and to identify the inter-relationships between the different SWI variables (Mondal et al. 2010; Yaouti et al., 2009). It was used to reduce the dimensionality of the data and to check if the salinization processes were captured by the principal components (PCs). The logarithmically transformed hydro-geochemical data for the dry season at each pilot site were used in the PCA analysis as it is expected to represent the worst-case conditions. Rotation of PCs was carried out using the varimax method, where both Kaiser criterion (eigenvalues smaller than 1 are considered insignificant) and Cattell scree plot were used to determine the number of PCs that should be retained. In this study, if the first PC explained salinity, then it was concluded that it would be associated with the key salinity indicators i.e. Cl^-, TDS, Na^+, K^+, SO_4^{2-}. When the first PC did not capture the salinity related indicators, it was considered that the aquifer was less vulnerable to salinization. The variables used in the PCA included field measured parameters such as pH, EC, TH, Na^+, K^+, Ca^{2+}, Mg^{2+}, Cl^-, HCO_3^-, SO_4^{-2} and NO_3^-. Additionally, seasonal differences in TDS, Cl^-, and GQI_{SWI} levels, the main indicators of water quality and salinity, were assessed using inferential statistical analyses. Statistically significant (95% confidence level) seasonal changes were assessed using a paired t-test of the logarithmically transformed data collected for each well. All statistical analyses were undertaken using SPSS Statistics (IBM 2018).

4.2.3 Understanding the impact of LULC and water deficit on SWI

As described in Table 4-1, the four pilot aquifers are inherently different. Aquifer A (city of Tripoli) has different geological formations as compared to Beirut and Jal eldib (Aquifers B and C). While Aquifer A is highly urbanized as Aquifer C (Beirut); however, it is less dependent on groundwater resources due to the availability of surface water sources, hence Aquifer A suffers from medium water deficit mainly manifested in the dry season only (Table 4-1). Aquifers B (Jal eldib) and C (Beirut) share similar geological formations; however, Jal eldib is moderately urbanized and groundwater resources are only used to augment municipal water sources during the dry season, hence it suffers from a low water deficit (Momijian et al. 2019). In contrast to the uncontrolled spread of wells tapping into the Beirut aquifer (>5000 wells), about 150 wells only were estimated to operate in Jal eldib. Accordingly, Aquifer C (underlying the Beirut metropolitan) is heavily used to supply water to bridge the gap of the high-water deficit in the very highly urbanized overlaying surface with large imbalances between abstraction and recharge. The aquifer has a limited recharge capacity due to the high urbanization that curtails rainfall infiltration and limited lateral inflow from surrounding areas due to the aquifer hydrogeology. In Aquifer D, on the other hand, the use of groundwater is mainly for agricultural purposes with conjunctive use of surface water for irrigation. Few farmers depend completely on wells throughout the year with most relying on an irrigation surface canal throughout the year and only a few relies on wells occasionally during the dry season or when flow in the canal is low (El-Fadel et al. 2017). In addition, the absence of urbanization in the plain allows for direct aquifer recharge during the winter, keeping the seawater freshwater mixing in balance.

Accordingly, the direct quantification of the LULC impact and groundwater abstraction on SWI is challenging due to this interplay of hydrological, climatological, and anthropogenic forcings along with seasonal changes. Faced with this challenge, the relationship between LULC and water deficit coupled with the groundwater quality data during the dry season was assessed using Analysis of Variance (ANOVA) on the salinity indicators TDS, Cl and GQI_{SWI}. Samples from the four pilot sites were compiled in one set for which the water quality variables were log-transformed. The land use at each site was categorized into 4 classes: very highly, highly, or moderately urbanized and non-urbanized agricultural area (Table 4-1). The water deficit[6] was classified into three categories: low, medium, high based on the reliance of each area on groundwater to meet its existing deficit in water supply (Table 4-1). Post hoc t-tests with the Bonferroni and Tukey corrections were conducted in the event that the null hypothesis was rejected to identify the groups with statistically significant difference in their means.

4.2.4 Sustainable management of aquifers

Based on the results of the research, possible management measures for implementation at the studied sites are discussed. A series of site-specific adaptation strategies and mitigation measures are explored towards sustainable aquifer management.

[6] Low, medium and high deficit represent deficits of 5-15%, 15-25% and 25-55% of demand, respectively.

4.3 Results and Discussion

4.3.1 Occurrence and intensity of salinity in pilot aquifers – impact of seasonality

The overall assessment of SWI showed that the four pilot areas exhibited signs of salinization, albeit with great heterogeneity between seasons and among locations. Table 4-4 presents the physiochemical analysis of samples collected during the wet and dry sampling campaigns for comparative assessment. The results indicate that Aquifer A (urbanized Tripoli) showed early signs of salinization particularly along the western coastline during the dry season (Table 4-4). The physiochemical analyses of the aquifer are synthesized in the Appendix 3a. TDS levels ranged from 200 ppm (fresh GW) to as high as 3,460 ppm (moderately saline GW), with less than 6% of samples exhibiting saline water quality (>1500 ppm). The average Cl- concentration across both seasons was indicative of “slightly saline” water (Table 4-2). The Piper diagram for the dry season showed that groundwater was mostly of the CaHCO3 type (Domain I, freshwater), with a few samples exhibiting the CaMgCl type (Domain IV, mixed waters) as well as the limited NaCl type (Domain II, primary saline seawater). This indicates the concurrent presence of freshwater, mixed, and primary saline waters within the aquifer. In the wet season, the water type shifted and was dominated by the freshwater type (Domain I), whilst maintaining the mixed CaMgCl type (Domain IV) in some areas (Figure 4-3). These results point to slight salinization as confirmed with the GQISWI (Table 4-4), which predicted that the area has freshwater in the dry (mean GQISWI=79.5) and wet seasons (mean GQISWI=82.8). The change in TDS concentrations between the dry and wet seasons was not significant ($p=0.420$) (Table 4-5), however seasonal changes in Cl- and GQISWI values were statistically significant, pointing towards slight salinization in the dry season.

Table 4-4 Comparative assessment of the mean values of the physiochemical parameters in the four pilot sites in simultaneous sampling campaigns

Season / *Parameter	Wet season (June)				Dry season (October)				Drinking water Threshold WHO (2011)
	Tripoli[a] (2007)	*Jal el Dib[b] (2013)*	*Beirut[c] (2013)*	*Zahrani[d] (2014)*	*Tripoli (2006)*	*Jal el Dib (2013)*	*Beirut (2013)*	*Zahrani (2013)*	
pH	NA	6.9	7	6.95	NA	6.85	7.0	6.9	6.5-8.5
Electric Conductivity EC	NA	1905	9504	1159	NA	1823	12008	1005	
Total Dissolved Solids	631	1427	4610	903	657	1367	5944	1075.6	600
Ca^{2+}	121	169.5	282.7	126.1	140	136.8	249.3	158.3	300
Mg^{2+}	43	101.5	229.9	53.5	16.8	98.1	246.8	71.9	300
Total Hardness TH	480	840.5	1651.5	535.2	419	745.1	1637.6	691.1	
Na^{+}	58	189.9	1132.5	73.2	115	520.4	1629.3	152.5	200
K^{+}	NA	5.5	19.7	5.0	NA	5.3	45.3	3.6	300
Cl^{-}	212	477.9	2358	156.3	225.5	546.5	3203	293.8	300
CO_3^{2-}	NA	0	0.019	0	NA	0	0.9	0.21	
HCO_3^{-}	NA	306.7	258.6	318	NA	293.2	274.8	282.3	
NO_3^{-}	34	19.2	39.8	38	34.8	18.4	27	80.6	50
SO_4^{2-}	50.7	98.6	391	89.2	65.2	123.8	418.6	100.1	250
Ionic Ratios									SWI Criteria
Na^{+}/Cl^{-}	0.5	0.6	0.5	0.9	1.14	1.49	0.6	1.0	$\leq$0.86
Cl^{-}/HCO_3^{-}	NA	2.7	18	0.8	NA	3.2	24.4	1.8	20-50
Mg^{2+}/Ca^{2+}	0.6	1.0	1.5	0.8	0.20	2.57	1.74	0.96	4.5-5.2
Br^{-}/Cl^{-}	NA	0.001	0.003	0.004	NA	0.001	0.001	0.002	0.0015
$Ca^{2+}/(HCO_3^{-}+SO_4^{2-})$	NA	1.2	1.62	0.9	NA	15.8	1.3	1.3	>1
SO_4^{2-}/Cl^{-}	0.2	0.1	0.1	0.4	0.3	0.19	0.13	0.3	0.103
$GQI_{generalized}$	88	61.7	53.6	67	87.2	57.5	52.3	62	
Seawater fraction f_{sea}	0.01	0.02	0.12	0.01	0.01	0.03	0.2	0.01	
$GQI_{Saltwater\ Intrusion}$	82.8	74.4	62.7	82.2	79.5	67.9	59	75.8	<75

[a] Highly urbanized city; [b] Suburb/ lightly urbanized; [c] Very highly urbanized city; [d] Agricultural plain/not urbanized;
All values in mg/l except pH and EC (µs/cm); Parameters in ratios expressed in meq/l;
See Appendix 3 for full results.

Water quality in Aquifer B (the suburb of Jal el Dib North of Beirut City) exhibited early signs of moderate salinization. The TDS levels ranged from a minimum of 380 ppm (fresh GW) to a maximum of ~4000 ppm (moderately saline GW). The Cl- concentrations ranged from a low of 115 ppm (fresh GW during the wet season) to ~2400 ppm (moderately saline GW in the dry season). Around 90% of the samples were experiencing moderate salinization year-round. Seasonal differences in the SWI indicators were statistically significant (Table 4-5). The hydro-geochemical analysis showed that water in the aquifer was mostly of the mixed CaMgCl type (Domain IV) in the wet season and shifted to the NaCl type (Domain II, primary saline seawater) in the dry season, whilst maintaining the mixed CaMgCl type in some areas (Figure 4-3). This salinization trend was further confirmed by the GQISWI (Table 4-4) that showed that while ~80% of the wells were freshwater during the wet season only 60% were still considered to be fresh in the dry season. This reflects the active intrusion of seawater into the relatively fresh aquifer with areas closer to the sea presenting higher salinization levels as compared to inland areas. Appendix 3b presents the results of the full physiochemical analysis for the aquifer underlying the suburb pilot area.

Table 4-5 Significance of paired t-test of the observed change in groundwater quality between the dry and wet seasons

Study areas	**Sampling Period**	**p-value TDS**	**p value GQI**	**p value Cl**	**p value GQI_{SWI}**
Urban city (Aquifer A)	Dry 2006 – Wet 2007	0.42	*<0.001*	*0.04*	*0.02*
Suburb (Aquifer B)	Wet - Dry 2013	< *0.0001*	*0.000*	*0.033*	< *0.0001*
Highly urbanized (Aquifer C)	Wet - Dry 2013	< *0.0001*	*0.006*	< *0.0001*	*0.026*
Agriculture (Aquifer D)	Wet - Dry 2014	0.583	*0.004*	*0.979*	*0.810*

*Paired sample t-test with significance level α = 0.05

The physiochemical characteristics of Aquifer C (underlying the very highly urbanized metropolitan of Beirut) showed significant SWI (Table 4-4) albeit with high variability within and between seasons. TDS levels ranged from as low as 390 ppm (fresh

GW) in the wet season to as high as >31,000 ppm (highly saline GW) in the dry season, with only 21% of samples indicating fresh to slightly saline water quality (<1500 ppm). Based on Cl- concentrations, the majority of the samples also exhibited saline to highly saline water quality. Statistically significant seasonal deterioration in the water quality was apparent (Table 4-5), where an increase in TDS and Cl- and a decrease in the GQISWI were observed between the wet and dry seasons (Table 4-4). Furthermore, the hydro-geochemical analysis revealed the presence of secondary (domain V of CaCl type) and primary saline water (domain II of NaCl type) in the wet season with the predominance of groundwater quality of the Cl--SO42--Na+-K+-Mg2+-Ca2+ type (Figure 4-3). The water type shifted to primary saline water i.e. seawater (domain II of NaCl type) in the dry season. During the wet season, fresh-brackish, brackish and saline water persisted along the western flank of the aquifer (Cenomanian and quaternary formations) whilst fresh water dominated in the eastern zones within the Miocene tertiary formations. The full analysis is presented in Appendix 3c.

Finally, in Aquifer D (underlying the agricultural plain of Zahrani) early signs of salinization were noted. The aquifer is reported to be generally fresh to slightly saline (Table 4-4). The TDS ranged from a low of 375 ppm (fresh GW) to a high of 3,110 ppm (moderately saline GW) in the dry season, with only 10% of samples exhibiting saline water quality (>1500 ppm). Chloride concentrations ranged from a low of 32 ppm (Fresh GW) to a high of 835 ppm (saline GW) (Table 4-2). Note that no statistically significant change was observed between the wet and dry season in terms of TDS, Cl^- or GQI_{SWI} (Table 4-5) hinting to limited freshening-salinization of groundwater. The seawater fraction (Table 4-4) confirmed a low seawater-freshwater mixing rate in the dry and wet seasons at ~1%. The full analysis is presented in Appendix 3d. The water types in the agricultural aquifer of the Zahrani plain (Aquifer D), consisted mainly of domain IV (mixed CaMgCl water type) and domain V (CaCl, secondary saline water type), with a couple of wells only showing domain II type

(NaCl, primary saline seawater) in the dry season. Water types shifted to domain I ($CaHCO_3$ freshwater) in addition to domains V (CaCl, secondary saline) and IV (CaMgCl, mixed) in the wet season ascertaining that groundwater is fluctuating from freshwater to secondary saline waters (Figure 4-3). The worst GQI_{SWI} in Zahrani was observed during the dry season with a mean GQI_{SWI} of 75% indicating signs of early mixing of fresh and saline water whilst during the wet season the GQI_{SWI} pointed towards less mixing and the dominance of freshwater in the aquifer (Table 4-4). This presents a dynamic aquifer slightly subject to SWI with signs of early intrusion in specific areas albeit with a potential seasonal flushing due to the low urbanization and moderate abstraction rates as a result of the concomitant use of surface water.

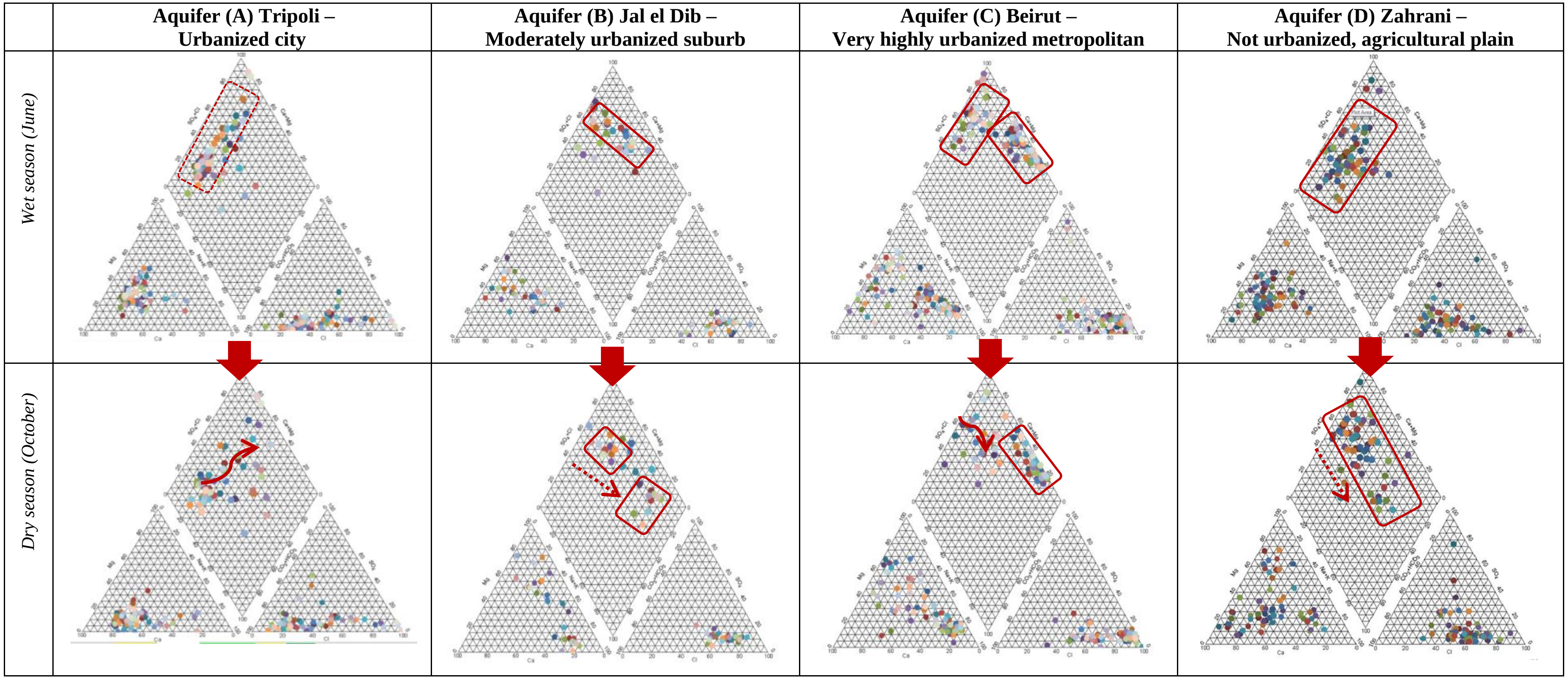

Figure 4-3 Piper Diagrams showing seasonal hydro-geochemical facies of pilot aquifers

4.3.2 Principal Components Analysis of salinity

The The PCA results are summarized in Table 4-6 in terms of the two main principal components (PCs) along with their associated eigenvalues, factor loadings, and the percent variability explained. In Aquifer A (Tripoli), three PCs with eigenvalues above 1 explained 79% of the total variability. The first PC (PC1) which explained 67% of the variability, exhibited a strong positive association with Cl^-, EC, TDS, Na^+ and SO_4^{2-} and a strong negative association with GQI_{SWI}. The presence of all variables associated with salinity in PC1 strongly indicates that this component represents the intrusion of saltwater in the aquifer. Similarly, in Aquifer B (Jal Eldib), three PCs with eigenvalues above 1 explained 79% of the total variability. Yet, the first PC was only able to explain 49.3% of the variability. It showed a strong positive association with Cl^-, TDS, EC, SO_4^{2-} and an equally strong negative association with GQI_{SWI}. This indicates that the first PC represents the intrusion of saltwater into the aquifer, however, it also hints that salinity is not the main factor responsible for the variability in the aquifer given its relatively low explaining power. In Aquifer C (Beirut), three PCs with eigenvalues above 1 represented 86.6% of the total variability. The first PC explained 56.8% of the variability and had a strong positive association with Cl^-, TDS, EC and Na^+ as well as a strong negative association with GQI_{SWI}. Accordingly, the first PC strongly represents the SWI into the aquifer. It also hints that salinity explains the majority of the variability in the aquifer, where SWI is well advanced. In Aquifer D (Zahrani), four factors with eigenvalues above 1 represented 74% of the total variability. The first PC which explained only 34.5% of the variability observed, was found to be only strongly associated with Total Hardness and TDS and to a lesser extent with Cl^-, Ca^{2+} and Mg^{2+}. This indicates active geochemical processes and ion exchange; yet there are no clear signs of salinization. Overall, the conclusions from the PCA concurred with those from the hydro-geochemical based approach, thus providing another layer of confirmation about SWI at the four pilot aquifers. It reaffirmed that while salinity was not a major process in Aquifer D (Zahrani), it was detected in Aquifer B (Jal ElDib) and was the dominant process in Aquifer C (Beirut) and Aquifer A (Tripoli).

Table 4-6 Principal component analysis (PCA) at the four pilot sites

Aquifer	**Aquifer (A) Tripoli Urbanized city**		**Aquifer (B) Jal elDib Moderately urbanized suburb**		**Aquifer (C) Beirut Very highly urbanized metropolitan**		**Aquifer (D) Zahrani Not urbanized, agricultural plain**	
*Loadings**	*PC1*	*PC2*	*PC1*	*PC2*	*PC1*	*PC2*	*PC1*	*PC2*
Cl	0.982		0.917	0.182	0.903		0.7	0.22
Ca	0.863		0.321	0.857	0.725	0.556	0.692	-0.136
Mg	0.855	-0.2	0.238	-0.908	0.453	0.508	0.618	0.271
TH	0.947		0.78	0.4	0.764	0.568	0.91	
HCO_3		0.897		0.118		0.347	-0.111	
EC	0.988		0.951	0.209	0.944	0.255	0.483	
TDS	0.988		0.951	0.209	0.944	0.255	0.812	0.411
NO_3			-0.337			0.794	0.135	-0.2
SO_4	0.952		0.923	-0.192	0.743	0.264	0.25	
Na	0.93	0.106	0.405	0.791	0.908		0.102	0.936
pH	-0.182	-0.563				0.196	0.163	-0.322
GQI_{SWI}	-0.959		-0.59	-0.7	-0.947	0.145	-0.294	-0.912
Eigenvalues	**8.071**	1.3	**5.9**	2.2	**6.8**	1.5	**4.1**	1.9
Variability	**67.3%**	10.9%	**49.3%**	18%	**56.75**	12.8%	**34.5%**	16.2%
Explains SWI	**Yes**		**Yes**		**Yes**		**No**	No

*loadings based on Rotated Component Matrix with Varimax rotation

4.3.3 Impact of land use and land cover (LULC) and water deficit on SWI

The ANOVA analysis revealed the impact of the LULC and the water deficit on salinity levels, measured as GQI_{SWI}, Cl^- and TDS. For GQI_{SWI}, both factors, LULC and water deficit, were found to be statistically significant ($F(3,216) = 40.2$, $p<0.000$ and $F(2,217) = 66.6$,

$p<0.000$, respectively). Post hoc paired-wise tests with the Bonferroni and Tukey corrections showed that the GQI_{SWI} differed between the various categories of land use (very highly, highly, moderately urbanized and agriculture). Only the GQI_{SWI} for the moderately urbanized (Aquifer B) and the agricultural aquifers (Aquifer D) were not statistically different. The post hoc tests also showed statistically significant differences (at $a=0.05$) in GQI_{SWI} between the high (Aquifer C) and low deficit (Aquifers B and D) regions as well as between moderate (Aquifer A) and low deficit (Aquifers B and D) areas but no statistically significant difference was observed between the aquifers with high (Aquifer C) or moderate (Aquifer A) water deficits. Similar deductions were reached when the analysis was repeated with Cl^- and TDS, as a measure of SWI instead of GQI_{SWI}. In terms of Cl^- analysis, ANOVA results showed that the land use and water deficit, were statistically significant ($F(3,217) = 64.3$, $p<0.000$ and $F(2,218) = 89.4$, $p<0.000$, respectively). Similarly for TDS, the ANOVA results showed the land use and water deficit, to be statistically significant ($F(3,217) = 45.3$, $p<0.000$ and $F(2,218) = 71.45$, $p<0.000$, respectively). Post hoc paired-wise tests with the Bonferroni and Tukey corrections showed that the TDS and Cl^- levels statistically differed between the various categories of land use (very highly, highly, moderately urbanized and agriculture) except for the moderately urbanized (Aquifer B) and the agricultural aquifers (Aquifer D) which were found to be not statistically different. The post hoc tests also showed statistically significant differences (at $a=0.05$) in TDS and Cl^- between the various categories of water deficit (high, low and moderate) except between the aquifers with high (Aquifer C) and moderate (Aquifer A) water deficits which was observed to be not statistically significant. Note that while the LULC and the state of the water deficit can interact, the assessment of the statistical significance of such an interaction was not possible because the limited number of pilot sites, which does not allow for all possible combinations between these two factors to be statistically observed.

The ANOVA results showed that the water deficit and the land use are the contributing factors in the occurrence and intensity of SWI. While water deficit directly drives groundwater abstraction, leading to seawater intrusion, establishing and quantifying a direct relationship between water deficit and SWI is challenging due to the multiple other factors at play including the availability of other water sources (i.e. tankers, bottled waters…etc.), abstraction rates, and the proliferation of wells. Similarly, while agricultural and non-urbanized areas are expected to allow more aquifer recharge, this relationship is also dependent on other factors including the level of urbanization, soil saturation, rainfall, aquifer characteristics, topography, as well as groundwater extraction. Nevertheless, urbanization played a surrogate for lower infiltration rates (land use) and higher pressures (water deficit) on groundwater aquifers as the factors associated with urbanization (i.e. less permeable areas with less recharge and more development with more pumping) tended to be associated with significant levels of salinity in the pilot areas.

4.3.4 Measures for Sustainable Management

The management of water deficits and seasonality requires a holistic understanding of the drivers of such deficits to enable decision making towards effective solutions. Management through increased water tariffs, metering, water quota as well as regulations on water uses (car washing, patio washing, smart water installations, well permits…etc.) targets the control of the demand on water, hence decreasing the gap between supply and demand through addressing the demand-driven water deficit. Management through water reuse and recycling (grey water systems), inter-basin transfer and rainwater harvesting projects, water storage, unconventional water resources (desalination) as well as groundwater recharge aim to supply additional water to meet the demand, hence decreasing the supply-driven water deficit. In Aquifers B and D, selective measures targeting demand only such as strict regulations on permits (well location, number, quotas), metering and water tariffs could be adequate as a long-term sustainable plan. Whereas in Aquifers A and C, both supply and demand measures are required to reinstate control on the water resources and manage aquifer usage.

Land use management is equally a core component of an aspired holistic approach to decrease the water deficit (e.g. recharge provides supply and less urbanized land uses induce less demand). In Aquifers B and D for instance, coastal planning and growing less water intensive crops could maintain the balance between the urbanized and non-urbanized areas whereas in Aquifers A and C, a full-fledged landscape approach to land use management is needed to integrate green infrastructure in urbanized areas to avoid further urbanization sprawl. Green infrastructure (green roofs, bioswale channels, planters and trenches, rainwater harvesting, sunken public spaces) boosts the resilience of urban centers by focusing on decentralized systems of intertwined green and gray infrastructure (Biswas et al., 2019). It slows runoff, captures rainfall and allow aquifer recharge while concomitantly decreasing the urban heat island effect (i.e. indirectly less stress on water demand).

Irrespective of the current status of salinity, a holistic approach to water management is imperative for decision making towards ensuring sustainable management of resources. While concerns and interests in managing SWI usually target aquifers already at risk (e.g. Aquifers A and C), protection of relatively freshwater or moderately saline aquifers (e.g. Aquifers D and B) is of equal priority. Beyond the selection of measures, monitoring of relevant indicators (e.g.

salinity levels, water table, water consumption, green cover, wells proliferation, urbanization rates …etc.) is key for continuous periodical evaluation.

4.4 Conclusion

In this study, the temporal dynamics of saltwater intrusion (SWI) under differing land use and land cover (LULC) patterns and water deficit conditions was assessed in four aquifers along the Eastern Mediterranean coast of Lebanon. While the aquifers exhibited signs of salinization, significant differences in the observed SWI were evident as a result of the interplay between various groundwater demand and supply factors operating under different LULC patterns. The current state of the aquifers ranged from being slightly saline (TDS < 1500 ppm) to highly saline (15,000 < TDS < 31,000 ppm). The overall assessment showed that the strength of the SWI signal was correlated to the dominant LULC at each aquifer and that the extent of the water deficit at each aquifer played a dominant role in explaining the occurrence and intensity of the observed SWI rates. Strong seasonal differences in SWI were observed, especially at the urbanized aquifers, which is believed to follow the water deficit dynamics between wet and dry seasons. The study suggests a synergistic effect of high water demands (water deficit) and increased urbanization (land use) on the SWI in aquifers. It also hints to a bleak future awaiting the aquifers underlying the suburbs of highly urbanized cities if water shortages are not alleviated and urbanization rates continue at the same rate. These findings reflect an increasing salinization challenge along the Eastern Mediterranean. Without proper mitigation measures, SWI is expected to further increase under the synergistic effect of climate change (i.e. sea level rise, reduction in precipitation, and increase in urbanization), exacerbating the associated socio-economic burdens to this region’s vulnerable and fragile communities. Consorted efforts towards the implementation of the proposed adaptation strategies are equally imperative for sustainable aquifer management that aim to alleviate the impacts of SWI.

CHAPTER 5

SYNERGY OF CLIMATE CHANGE AND LOCAL PRESSURES ON SALTWATER INTRUSION IN COASTAL URBAN AREAS: EFFECTIVE ADAPTATION FOR POLICY PLANNING

5.1 Introduction

Landward intrusion of seawater into coastal aquifers, known as saltwater intrusion (SWI), is primarily caused by aquifer over-pumping and land-use change (Singh, 2014; Werner *et al.*, 2013). SWI is invariably an increasing threat to urban coastal communities worldwide by contaminating groundwater and impairing its productive and consumptive value (Selmi, 2013; Fatoric & Chelleri, 2012; Park *et al.*, 2012; Zhang *et al*., 2011; Standford & Pope, 2010; Sales, 2009; Conrad & Roehl, 2007; Bobba, 2002). Climate change is expected to further exacerbate SWI due to potential sea level rise coupled with increased temperatures (that translates into an increase in water demand) and reduced precipitation (that translates into a decrease in surface water available for aquifer recharge). (Kumar *et al.* 2007; IPCC, 2007; 2014).

The importance of planning to adapt to SWI lies in protecting the biophysical elements (i.e. subsurface aquifers and groundwater quality) and curtailing associated socioeconomic burdens on coastal communities (i.e. the impairment of water resources, damages to soil, plants, and infrastructure, etc…). However, as coastal aquifer hydrodynamics and climate change impacts remain challenging to quantify and predict (Post VEA, 2005; Sanford & Pope, 2010; Werner *et al.*, 2013) and as the interaction between impacts of global climate change and local anthropogenic impacts remains ambiguous, coastal managers remain in dire need to plan and act under incomplete knowledge to cope with these impacts and protect the economic, social, and environmental security of coastal communities (Tribbia & Moser, 2008). In this context, drivers of saltwater intrusion have often been assessed using mathematical simulations that account for major hydrogeological inputs as well as temporal and spatial variations in groundwater recharge and discharge and sea level fluctuations, through mass balance, and numerical analysis (Sophiya & Syed, 2013; Cobaner *et al.*, 2012; El Shinnawy & Abayazid, 2011; Harbor, 1994; Purandara *et al*., 2010).

While groundwater overexploitation is strongly associated with lowering the water table and the advancement of the seawater front (Ergil, 2001; Cobaner *et al.* 2012; Koussis *et al.* 2012; Selmi, 2013; Sherif *et al*. 2012), the ability of flushing a saltwater contaminated aquifer by stopping or reducing pumping rates or managed aquifer recharge is not evident. Concurrently, the impact of sea level rise exhibits different responses in confined and unconfined aquifers with rising seas generally believed to first lift the entire aquifer, which would help alleviate the impacts of saltwater intrusion, before intrusion overrules again (Carretero *et al.* 2013; Chang *et al.* 2011; Werner *et al.* 2012). While the trends governing the physical, geological and chemical processes of the interaction between the drivers of SWI are generally similar, the rate and magnitude of these interactions remain highly context-specific (El Shinnawy & Aba Yazid, 2011; Melloul & Collin, 2006; Conrads *et al*. 2010; Dausman & Langevin, 2005; Niang *et al*. 2010; Oude Essink, 2001; Ranjan et al. 2006) confirming the need for local examination towards informed management and adaptation strategies. Similarly, studies that examined opportunities for adaptation, albeit limited, showed that their effectiveness is variable and site-specific (Abarca *et al.* 2006; Ergil, 2001; Fatoric & Chelleri, 2012; Frank & Boyer, 2014; Georgpoulou *et al.*2001; Kaleris & Ziogas, 2013; Masciopinto, 2013).

This study examines the additional factor of climate change impacts in comparison to local anthropogenic interventions on the occurrence and intensification of SWI along urban coastal aquifers using a multi-objective 3D hydrogeological model responsive to the dynamics of population growth, recharge and climatic stresses. In parallel, it assesses the potential role of planned adaptation strategies in alleviating saltwater intrusion in an attempt to inform policy making on sustainable management of urban coastal aquifers.

5.2 Methodology

The methodological framework consisted of three interrelated components: first, the characterization of the pilot aquifer study area; second, the identification of scenarios that account for local anthropogenic interventions, climate change, and planned adaptation strategies; and third, the assessment of these scenarios on saltwater intrusion dynamics using a multi-objective 3D variable-density flow and solute transport model.

5.2.1 Aquifer characterization

The pilot area consists of a fractured, heterogeneous aquifer underlying Beirut city and its suburbs, a highly urbanized metropolis recognized for water shortage challenges and high dependence on groundwater resources. The study area stretches midway along the Eastern Mediterranean with a 16.5 km of diverse shorelines including rocky beaches, sandy shores and cliffs over a total area of ~44 km^2 (Figure 5-1). Its hydrogeology belongs to the Cretaceous and Quaternary periods with restricted exposures of the Tertiary periods (Abdel Basit, 1971; Peltekian, 1980). The Cenomanian-Quaternary system (carbonate-sand) is considered as one thick aquifer, ~700m, consisting mainly of hard and compact limestone and dolomite interbedded with chert, and intercalations of marl (Khair, 1992) overlain by quaternary recent deposits. The aquifer is characterized by accessibility and relatively high transmissivity and low storativity, particularly in the Cenomanian formations, and high infiltration rates due to the presence of weak or partial cementation between the grains of sand in the quaternary deposits allowing for moderate permeability (Khair, 1992). It is characterized by fractured and karst systems (Masciopanti, 2013; Shaaban *et al.* 2006) and is heavily jointed and faulted (Ukayli 1971). Nearly 4500 small building scale wells are reportedly tapping into this aquifer (SOER, 2011; Saadeh 2008) complementing network water supply to nearly 1 million individuals (CAS 2008).

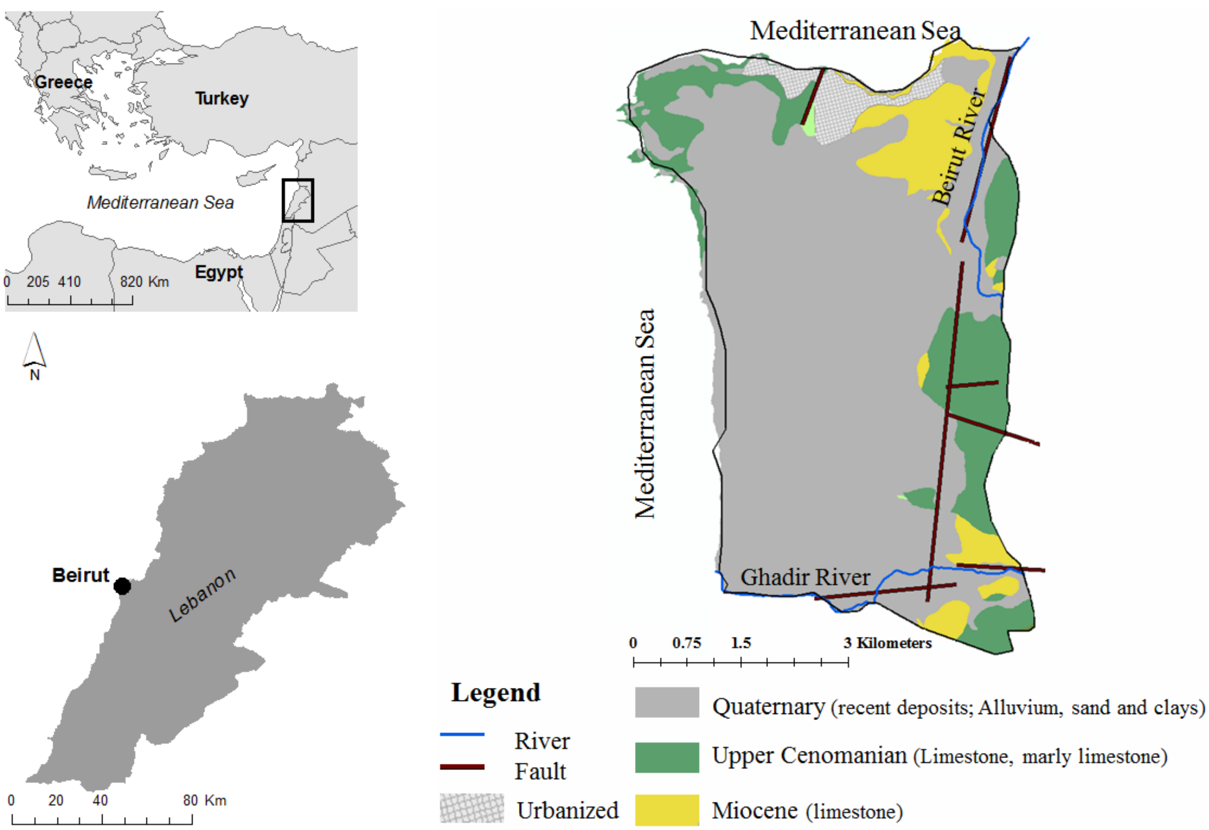

Figure 5-1 Location and surface geology of the pilot aquifer

5.2.2 Development of scenarios

Abstraction and sea level rise (SLR) scenarios were developed for the near future (2012-2032), as proxies for local anthropogenic interventions and global climate change. Groundwater abstraction was estimated based on domestic water demand rates using population growth and per capita consumption rates. Two growth rates were examined: an average of 1.75% (MoEW, 2010) and a high of 2.50% (WB, 2009). Total population estimates were based on the year 2010 with ~1.2 million inhabitants in the study area (CDR / DAR 2014). Similarly, a constant average consumption rate of 180 liters per capita per day (l/c/d) (MoEW, 2010) and a variable high rate of 200 l/c/d increasing linearly to 300 l/c/d (including network losses) were tested (El-Fadel et al., 2000; Korfali and Jurdi, 2010; Saadeh 2008).

Table 5-1 presents levels of input variables for scenario development with a total of 11 scenarios simulated over the period 2012 to 2032. Recognizing that water demand and availability vary between wet and dry seasons, this variation was considered in the scenario development, where fewer surface water supplies are expected to be available in dry seasons when the demand for water is at its highest. Assessment of the impact of sea level rise was based on estimations for the Eastern Mediterranean reported at 12 – 25 cm by 2030 and 22 – 45 cm by 2050 (Cazenave & Jaber, 2001) or 30 – 60 cm by 2040 (SNC 2011). Accordingly, both a low (20cm) and a high (65cm) SLR by 2032 were assumed using rates of 1.00 and 3.25 cm/yr, respectively. The cumulative impact of SLR and abstraction on the dynamics of saltwater intrusion was analyzed for the baseline scenario (S1) as well as the worst-case scenario (S4).

Table 5-1 Simulated scenarios with corresponding input parameters

Scenario	Population growth (%)	Consumption rate (l/c/d)	Description and details
S1	1.75	180	Baseline
S2	1.75	200 - 300	Most likely
S3	2.5	180	Modified baseline
S4	2.5	200 - 300	Worst case
S1A	1.75	180	Groundwater demand is reduced by 230,000 m^3/d as a result of adoption of adaptation/mitigation measures starting 2019
S2A	1.75	200 - 300	
S3A1	2.5	180	Groundwater demand is reduced by 350,000 m^3/d as a result of adoption of adaptation/mitigation measures starting 2019
S4A1	2.5	200 - 300	
S4A2	2.5	200-300	Abstraction is halted as demand is met as a result of adaptation/mitigation measures starting 2019
S1L	1.75	180	Sea level rise is included at 1 cm/yr i.e. rise of 20 cm by 2032
S4L	2.5	200 - 300	Sea level rise included at 3.2 cm/yr i.e. rise of 65 cm by 2032

Based on the understanding of the aquifer response to drivers, potential adaptation strategies for soothing the saltwater intrusion were analyzed under different scenarios. Given that the excessive spread of wells and the indiscriminate withdrawal of groundwater are necessitated by deficits between the water supply and demand, adaptation strategies focused on reducing abstraction by reducing the demand on groundwater in general as well as reducing the deficit between supply and demand. In line with the national plans (MoEW 2010), three levels of adaptation were evaluated to analyze for effectiveness and informed decision making towards sustainable aquifer management. The scenarios tested were based on the 10 year plan of the Ministry of Energy and Water (MOEW) which consisted of a) water conservation practices tailored towards reducing network losses, currently estimated at ~50% (MOEW 2010); b) the injection of treated wastewater for artificial aquifer recharge and c) a series of infrastructure projects including the conveyance of water from inland to the urban area under study through a phased dam-lake project (Beirut Awali Conveyor project) (MOEW 2010). In line with the methodology which is based on groundwater abstraction that is defined by demand, the selected adaptation strategies targeted the groundwater demand and adopted the projected additional supply to Beirut from several planned projects. Adaptation scenario (A) adopted an additional water supply of ~230,000 m^3/d projected under Phase I (2.5 - 3m^3/s) of the conveyor project (MOEW 2010) whereas scenario (A1) adopted an additional supply to Beirut of ~350,000 m^3/d projected under Phase II (4.5 - 6m^3/s) of the same project. Adaptation strategy A2 assumes the adoption of unconventional water supplies i.e. desalination so that the entire demand is met through desalinated water with no groundwater abstraction needed. All adaptation measures were assumed to start in 2019.

5.2.3 Model set-up and simulations

A multi-objective 3D variable-density flow and solute transport model using SEAWAT (Langevin *et al.,* 2008) was set for the target domain. Initial and boundary conditions, and sub-surface characteristics were assigned to the mesh following the digitization of the study area. The boundary to the north and west is a specified head boundary condition corresponding to the monthly stage of the sea level. Two rivers bound the domain from the northeast and the south (Figure 1). The southern river is dry with occasional flow from storm water runoff and groundwater influx, whereas the northeastern river acts as a drain downstream and a river upstream. The influx to the system is has been assumed to be primarily through recharge/runoff due to rainfall (Peltekian, 1980). During the last few decades, the rise in urban and suburban development in and around Beirut city resulted in a significant amount of impervious surfaces. Therefore, aquifer recharge from the surface runoff was considered nil in the model simulations.

A Dirichlet boundary condition was used to specify the average salinity level of the seaside boundary with a TDS concentration of 35 g/l (Figure 5-2). The complex hydrogeology of the subsurface environment is not well documented. Therefore, assumptions on the aquifer's hydrogeological characteristics were made in the design of the model. Spatial heterogeneity of groundwater abstraction and the number of supply wells (~2500 wells) tapping into the aquifer were assumed constant over time (from 2012 to 2032). The boundary to the east (between the two rivers) was set as a no-flow boundary due to its vicinity to the middle Cenomanian formation (C4b) which encompasses a low hydraulic conductivity. Nevertheless, the only opening in the Cenomanian formation in the eastern domain was characterized by a flux boundary condition with a low influx rate. Storativity was set at a constant of 0.3 for yield storage and 10E-6 for specific storage. The measurements of head and salinity field observations were considered reliable.

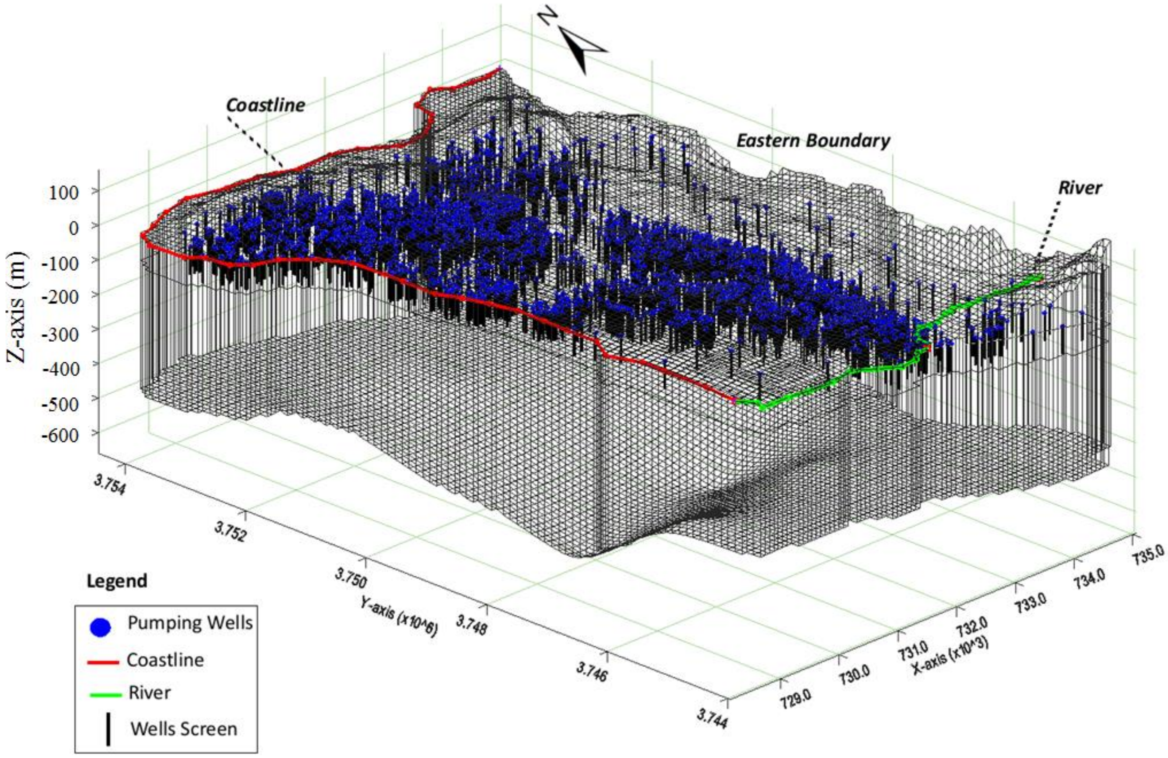

Figure 5-2 Model cells, boundary conditions and licensed wells in the Beirut aquifer (vertical magnification equals 4)

The model comprised a transient stress period (i.e. the computational time interval for a simulation, here taken at one month) of twenty-years subdivided into 240 sub-periods of one-month duration (from June 2012 to June 2032) that undergoes both steady state and transient conditions. The first stress period (June 2012) was specified as steady state with the aim of providing a stable head distribution at the beginning of the transient period. Monthly averaged head observations over the period of June 2012 to March 2014 were used in the transient model calibration within the Groundwater Modeling System (GMS-Version 10). The model used the advanced pilot-points parameterization coupled with PEST (Doherty, 2007) to characterize spatial heterogeneity of hydraulic conductivity. The final results of model calibration suggested a range of 8 to 81 m/day for the hydraulic conductivity in the first numerical layer containing the Quaternary, Cenomanian and Miocene formations. The value of hydraulic conductivity in the second and third layers varies between 5.02 to 182 m/day. Although the calibration results were generally satisfactory with a low level of model-to-measurement misfit error in terms of hydraulic head observations however, the existing geologic data were not sufficient to validate the model calibration results of hydraulic conductivity. Therefore, expected uncertainty in estimation of hydraulic conductivity values is recognized as a limitation of the model.

For model verification, salinity data collected during a 2013/2014 groundwater monitoring campaign were used (Rachid et al., 2015). A steady-state MT3D model coupled with the steady-state head results of MODFLOW for June 2012 was run using the standard finite difference method with central-in-space weighting scheme through SEAWAT. The purpose of this steady-state simulation was to adjust the salinity distribution with the hydraulic head to estimate the initial saltwater wedge profile that would exist in the system prior to stressors (Figure 5-3). The salinity distribution was derived through kriging interpolation using 91 salinity measurements (in the range of 416 to 21,485 mg/lit) collected during the groundwater monitoring program. However, the salinity data were not of sufficient number in depth to delineate a three-dimensional distribution within the aquifer. Since the knowledge of vertical distribution did not exist, the two-dimensional distribution was interpolated with the initial saltwater wedge profile (in 2012) produced by forecasting a historical model (which represents the water level in 1969) into 2012 (present water level). The saltwater-freshwater interface associated with the historical model was assumed to be under the non-intrusion condition when saltwater and freshwater were in balance.

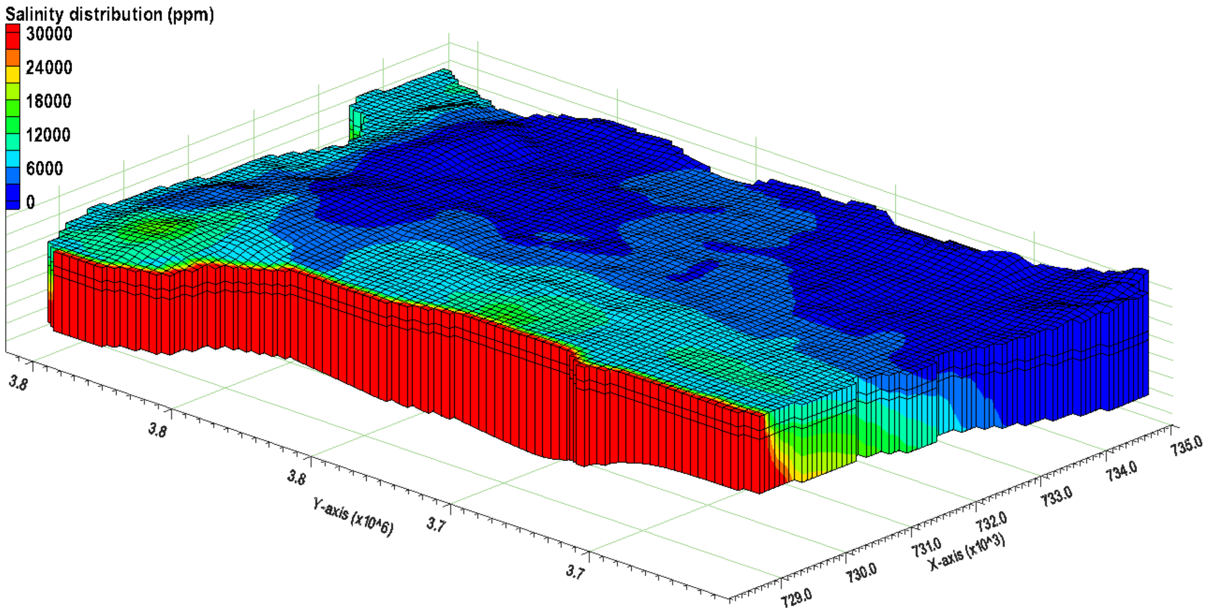

Figure 5-3 Salinity distribution in the pilot aquifer in June 2012

Analysis of saltwater intrusion dynamics under the various scenarios focused on the mass encroachment of saltwater into the fresh groundwater aquifer as well as the volumetric displacement of the saltwater-freshwater interface over the 20 years simulation. The volumetric extent of saltwater intrusion was computed using the areal extent of intrusion through vertically active cells overrun by salinity of greater than 7,000 mg/l equivalent to the threshold of brackish water. The volume of the interface with the iso-line ≥ 7,000 mg/L was estimated by multiplying the number of cells at a salinity ≥ 7,000 mg/L with the cells’ volumes (length*width*depth). The mass of salinity in the entire model domain was then calculated by multiplying the volume with the porosity and salinity ≥ 7,000 mg/L.

While two main mechanisms of saltwater intrusion are expected to take place[7], the geologic layer in the pilot aquifer was divided into two numerical zones to characterize the dominant mechanism of intrusion: an upper zone where supply wells are tapping and a lower zone where the toe of the interface is located.

As a measure of the relative impacts of model variables (i.e. water consumption rate, population growth and adaptation level) on the magnitude of intrusion, a Prediction Scaled Sensitivity (PSS) was conducted on scenarios of groundwater abstraction (s1A, s2, s2A, s3A1, s4 & s4A1). The PSS was defined as the percent change in the model prediction (i.e. mass of salinity and volumetric displacement of the interface) given a change in the rate of groundwater abstraction on the basis of the change in the water consumption rate, population growth and adaptation level as expressed in Equation 1 (Hill & Tiedeman, 2007):

$$PSS_{ij} = \left(\frac{\partial y_{ij}}{\partial b_{ij}}\right)(b_j/100)(100/y_j) \tag{1}$$

Where $\left(\frac{\partial y_{ij}}{\partial b_{ij}}\right)$ is the derivative of the mass encroachment or volumetric displacement to the derivative of abstraction rate evaluated at the i_{th} scenario from the j_{th} baseline scenario (mg/l/m^3/yr or m^3/m^3/yr); y_j is the magnitude of mass encroachment of salinity or volumetric displacement of the interface at the j_{th} baseline scenario (mg/l or m^3) ; ∂y_{ij} is the derivative of (change in) the mass encroachment or volumetric displacement in the i_{th} scenario from the j_{th}

[7] Lateral encroachment of recent seawater due to the high degree of heterogeneity in addition to upconing due to the high vertical velocity of water as a result of low storativity

baseline scenario; b_j is the abstraction rate at the j_{th} baseline scenario (m^3/yr); ∂b_{ij} is the derivative of (change in) the abstraction rate in the i_{th} scenario from the j_{th} baseline scenario; i corresponds to scenarios (s1A, s2, s2A, s3A1, s4 & s4A1) and j is the associated baseline scenarios (s1 & s3 for s2 & s4, respectively, and s1, s2, s3 & s4 for adaptation A & adaptation A1). For instance, if the abstraction rate increases from 10 to 12 Mm^3 (17% increase) and consequently the salinity mass increases from 2000 to 2200 tonnes (10% increase), the PSS value is estimated (200 tonnes / 2 Mm^3) * (10 Mm^3/100) (100/2000 tonnes) = 0.5. Note that the PSS values are dimensionless. The PSS was calculated for both the mass encroachment of salinity and the volumetric displacement of the interface under seasonal conditions.

5.3 Results and Discussion

5.3.1 Impact of abstraction

The model results indicate that under the baseline scenario (S1), the saltwater-freshwater interface moves landward, indicating increased salinization of the aquifer with ~15% mass encroachment of salinity and ~20% volumetric displacement of the interface occurring in the upper zone of the aquifer within a depth of 100 m below sea-level (where most wells are tapping). Concurrently, there is >80% encroachment occurring in the lower zone of the aquifer, where the toe of the interface is located. Figure 5-4 illustrates the estimated abstraction per year over the whole simulation period for all scenarios in the absence of any adaptation measure. The results show that higher water consumption per capita rates results in a greater increase in abstraction (S1 vs. S2 & S3 vs. S4) as compared to that associated with population growth rates (S1 vs. S3 & S2 vs. S4) (Figure 5-4). Increasing the rate of water consumption from 180l/c/d to

200-300 l/c/d under S2 (the most likely scenario) increases the total rate of abstraction by ~63% which is translated into ~60% increase in mass encroachment of SWI and a 70% additional displacement of the interface in 20 years (by October 2031) as compared to S1 (Figure 5-4).

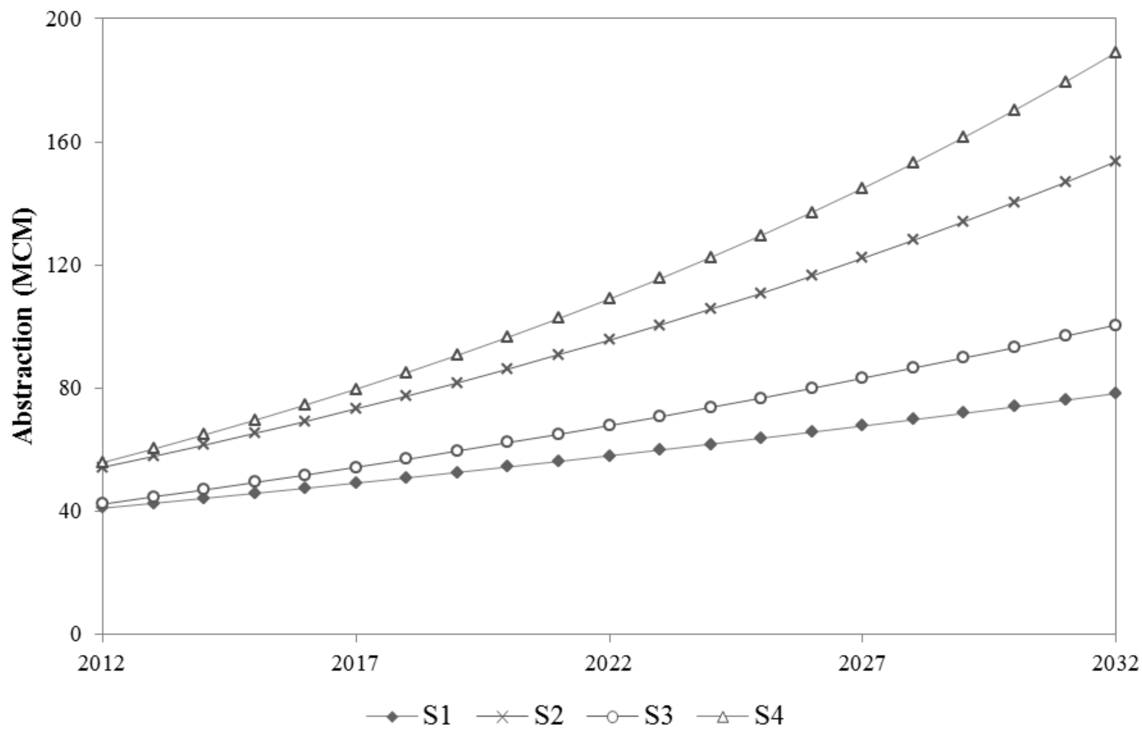

Figure 5-4 Groundwater abstraction in MCM: Variation under main simulated scenarios

The volumetric displacement of elevated concentrations at the end of the dry season for the current state of salinity (October 2015), the beginning of adaptation scenarios (October 2019) and the end of simulation period (October 2031) are displayed in Figure 5-5 across scenarios of groundwater abstraction. Simulations of the S3 scenario suggest that raising the rate of population growth from 1.75% (in S1) to 2.5% (in S3) increases the abstraction rate by 14.7% with ~12.8% exacerbation in salinity intrusion as compared to S1 suggesting that salinity encroachment is more sensitive to the existing rate of water consumption than the rate of population growth. The coupled impact of increasing both the population growth and the water consumption rates under S4 (the worst case scenario) led to a 78% increase in mass encroachment, which translated into a 90% increase in the landward displacement as compared to S1. Under the scenario S4, the simulated landward displacement is 5% more than the combined predicted impact of increased population growth (S3) and consumption rates (S2) due to the synergistic impact of both S2 and S3 scenarios on the dynamics of saltwater intrusion (Figure 5-6).

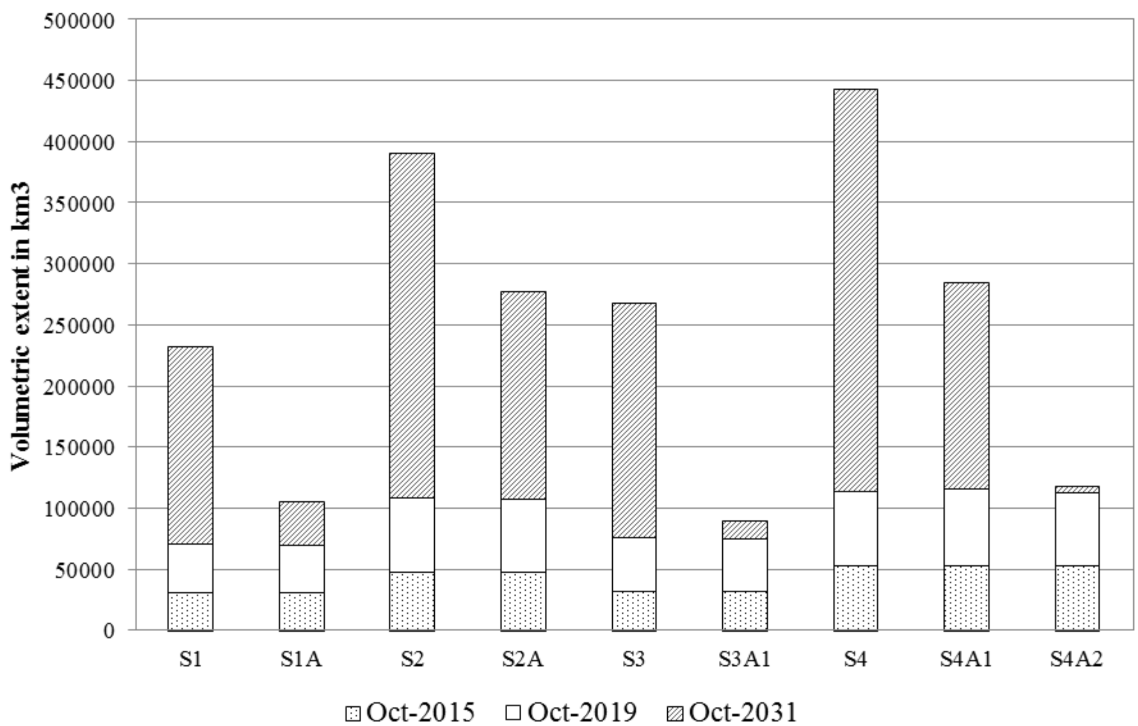

Figure 5-5 Volumetric extent of >7g/l salinity intrusion over the simulation period *(showing October 2015 (end of the dry season), October 2019 (beginning of adaptation scenarios) and October 2031 (end of simulation period)*

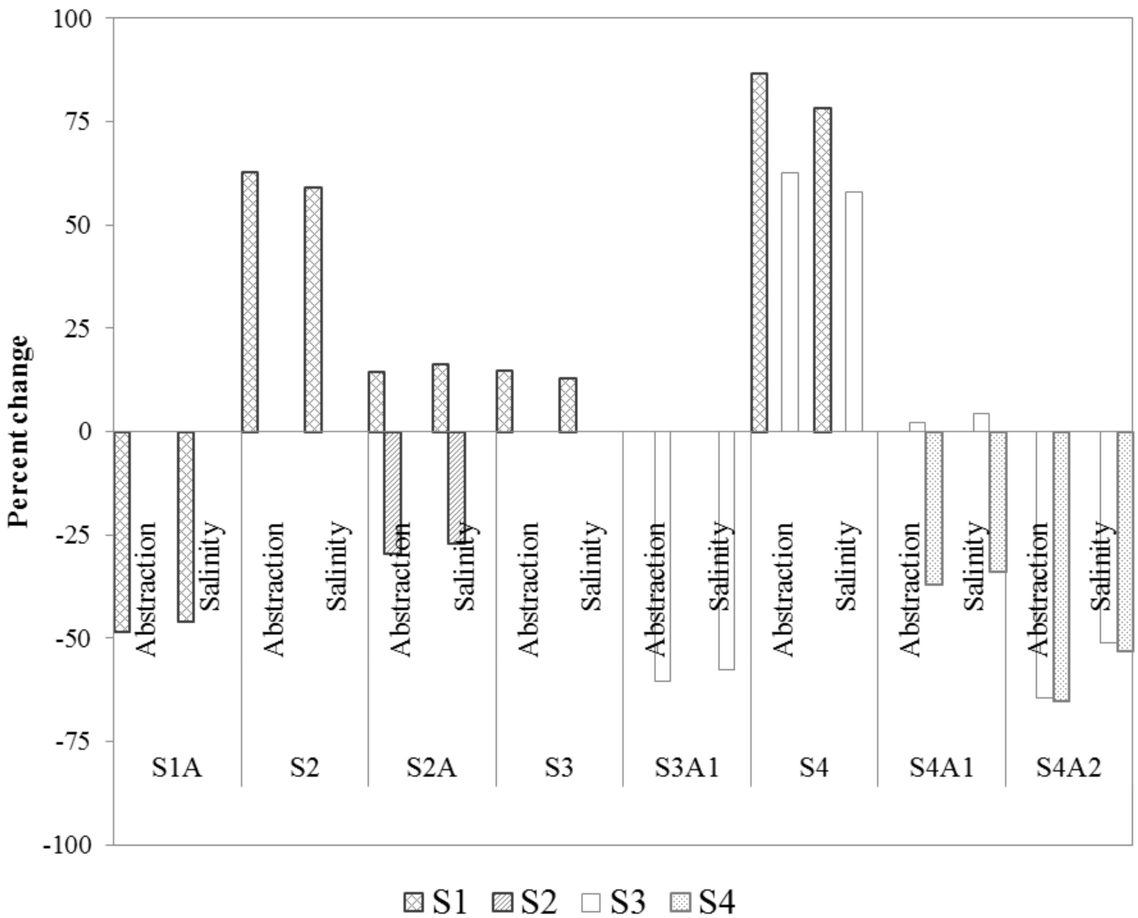

Figure 5-6 Percent change in abstraction and mass encroachment during 20 years simulation under various groundwater abstraction scenarios relative to the corresponding baseline scenarios

In the absence of adaptation measures (scenarios S1, S2, S3, and S4), it is expected that the upper zone now exhibiting saltwater intrusion with elevated salinity concentrations (>7000 mg/l) will experience a volumetric intrusion that is slightly reduced from the current rate of 20% (Figure 5-7). Since elevated concentrations are encountered mainly inside the transition zone, the diminishing volumetric percentage of intrusion in the upper zone suggests that the dominant mechanism of temporal intrusion is due to lateral encroachment in the lower zone. Since groundwater abstraction increases under scenarios S2 and S4 in comparison to S1 (baseline), the volumetric percent of intrusion in the upper zone further drops (Figure 5-7) while that of the lower zone increases thus demonstrating that the movement of the interface toe is sensitive to abstraction rates. Hence, managing the abstraction rates is imperative for managing the lateral encroachment and potentially reversing the intrusion of saltwater.

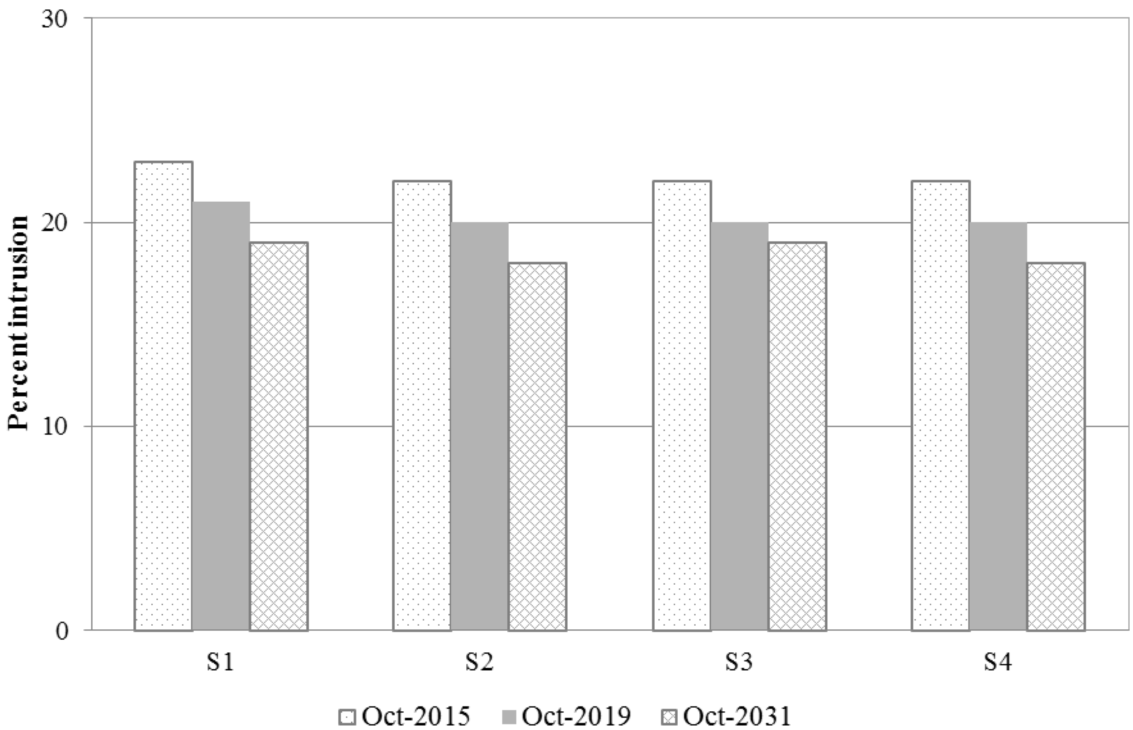

Figure 5-7 Percent volumetric extent of >7g/l salinity intrusion in upper layer of aquifer (100 m thickness)

5.3.2 Impact of Sea Level Rise

The simulation of a 1.00 cm/yr SLR (20 cm by 2032) (S1L) applied to the baseline scenario (S1) resulted in a slight increase in the mass encroachment of salinity, which is equivalent to the impact resulting from a 1% increase in groundwater abstraction over the simulation period (i.e. 20 years) under similar conditions. This suggests that a sea level rise of 20 cm by 2032 has a relatively insignificant impact on saltwater intrusion dynamics relative to groundwater abstraction in the study area. Similarly, a high SLR (S4L) of 3.2 cm/yr (65 cm by 2032) applied to the worst-case scenario (S4) resulted in an additional mass encroachment equivalent to the impact of only 1.7% increase in groundwater abstraction, reconfirming that the impact of a 65 cm SLR by 2032 will largely be masked by the overwhelming impact of over-abstraction. While under the analyzed scenarios of groundwater abstraction (S1, S2, S3 & S4), a SLR of 1.00 cm/yr seems to be of minimal concern due to lower magnitude of intrusion in S1 than other scenarios (S2, S3 & S4), the impact of an additional 2.20 cm/yr SLR (SLR of 3.20 cm/yr) on S1 is equivalent to the impact of a 2% increase in groundwater abstraction for the same scenario (S1). Accordingly, any adaptation strategy or management measure to alleviate saltwater intrusion must focus on controlling abstraction, which remains the main driver of saltwater intrusion. Note that SLR may cause potential changes to the shape of the interface, which may increase the possibility of upconing near the coastline.

5.3.3 Impact of adaptation scenarios

Figure 8 depicts the monthly change in the magnitude of saltwater intrusion upon considering adaptation scenarios throughout the simulation period (up to 2032). Both the mass and volumetric encroachment trends corresponding to scenarios 1A and 4A1 suggest that adaptation strategies under these scenarios helped reduce the demand for groundwater in the majority of years as compared to 3A and 6A1, where the demand for groundwater remained greater than that available supply defined in the adaptation strategies of those scenarios. For instance, S3A1 exhibited a 60% reduction in volumetric encroachment as compared to S3, suggesting that a reduction in demand of 350,000 m^3/d can reduce pumping rates to nil in the wet season (for a couple of years). Note however that while total abstraction rates decrease under various adaptation strategies (strategies A and A1), the salinity still exhibits an increasing trend, as expected, due to the higher rate of groundwater depletion as compared to the available replenishment particularly in the dry season. Nevertheless, adaptation strategies A and A1 proved to be effective in decreasing the total abstraction rates and simultaneously halt the intrusion for a significant duration before abstraction takes over again (S2A and S4A1). Across the scenarios S2A & S4A1, the largest reduction in mass encroachment of salinity occurred during the wet season (November to April) as the groundwater abstraction (in some years) decreased to almost nil. In contrast, the minimal reduction were as expected during dry season (mostly in October, the driest month of the year) because the adaptation strategies could not meet freshwater demands.

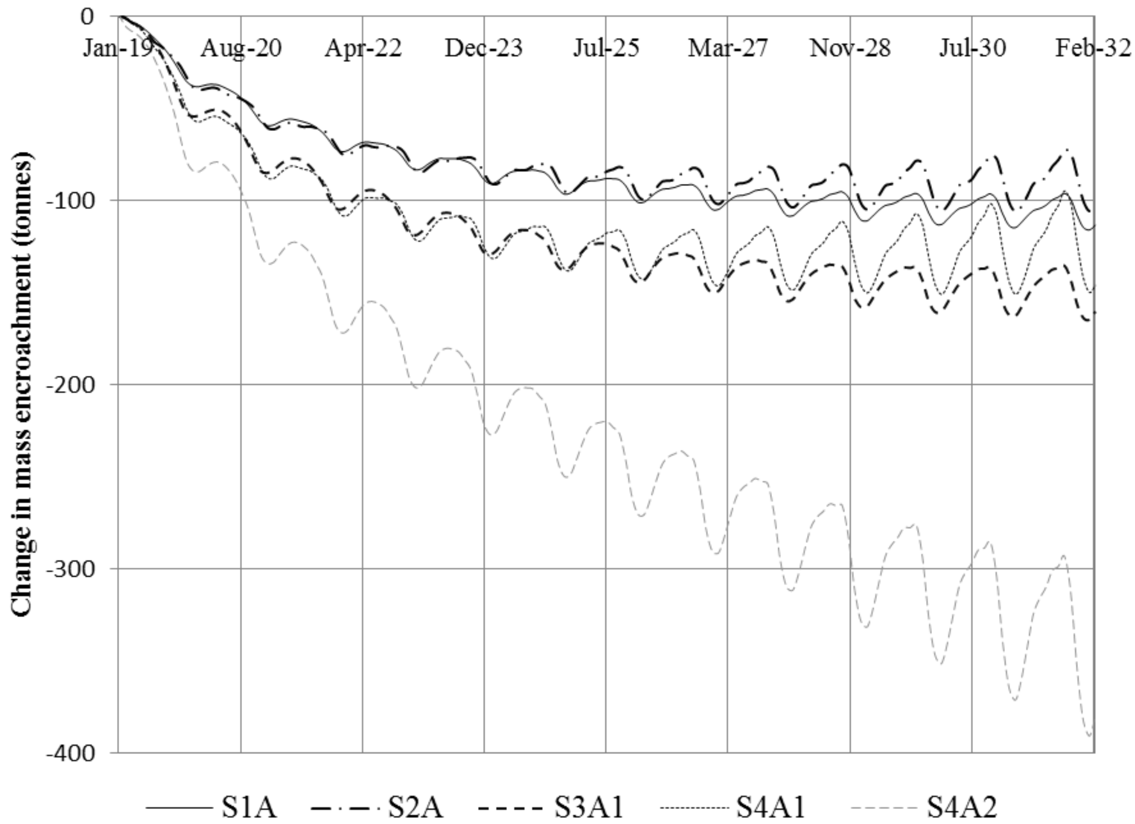

Figure 5-8 Changes in mass encroachment under adaptation scenarios
S1A & S2A: Reduction in groundwater abstraction by 230,000 m^3/d starting 2019;
S3A1 & S4A1: Reduction in groundwater abstraction by 350,000 m^3/d starting 2019.

The optimistic adaptation strategy whereby groundwater abstraction ceases by 2019 (with the demand being met through unconventional water resources - desalination) was tested under the worst-case scenario (S4) associated with assuming the highest abstraction rate and mass encroachment after 20 years (by 2032). While the simulation results showed that the mass encroachment of salinity decreased by 47% (from S4 to S4A2) over a period of 13 years (from 2019 to 2032) (Figure 5-8), the total mass of salinity in 2032 was still significantly higher (250%) than that in 2012. This asserts that while halting abstraction helps in freshening the aquifer system, a recovery period of 13 years did not revert the damage caused by 7 years of abstraction under the worst-case scenario (S4) since longer time is needed to aid the aquifer in recharge.

5.3.4 Sensitivity analysis

The sensitivity analysis suggests that the volumetric displacement of the interface, rather than the mass encroachment, is sensitive to changes in abstraction rates (Figure 9). Volumetric encroachment is only associated with landward displacement of elevated concentrations (> 7000 mg/l) while mass encroachment involves concentrations in the full TDS range of 0 – 35000 mg/l (seawater concentration), indicating that saltwater intrusion in the aquifer is governed by concentrations of greater than 7000 mg/l. Furthermore, the results show that salinity encroachment exhibits a higher sensitivity to water consumption rates in comparison to population growth rates (S2 & S1 (Volumetric PSS = 1.08, Mass PSS = 0.94) vs. S3 & S1 (Volumetric PSS = 1.04, Mass PSS = 0.87)) (Figure 5-9). In parallel, the baseline scenarios (S1 and S3) exhibited more sensitivity to adaptation strategies (S1A & S1 (Volumetric PSS = 1.13, Mass PSS = 0.95) vs. S3A1 & S3 (Volumetric PSS = 1.1, Mass PSS = 0.95)) than S2 and S4 (S2A & S2 (Volumetric PSS = 0.97, Mass PSS = 0.91) vs. S4A1 & S4 (Volumetric PSS = 0.98, Mass PSS = 0.92)), where S1A and S3A1 highlighted a large decrease in the magnitude of intrusion with reduced water abstraction, particularly during the wet season. Nevertheless, the response to adaptation strategy A1 (reduction of groundwater demand by 350,000 m^3/d) showed higher sensitivity than with adaptation A (reduction of groundwater demand by 230,000 m^3/), despite the fact that A1 is applied to scenario S3 which involves 15% more abstraction than S1. On the other hand, further increases in water consumption (under S2A and S4A1) reduced the impact of adaptation (S2A & S2 (Volumetric PSS = 0.97, Mass PSS = 0.91) vs. S4A1 & S4

(Volumetric PSS = 0.98, Mass PSS = 0.92), particularly after a period of time where the increase in groundwater demand dominates again.

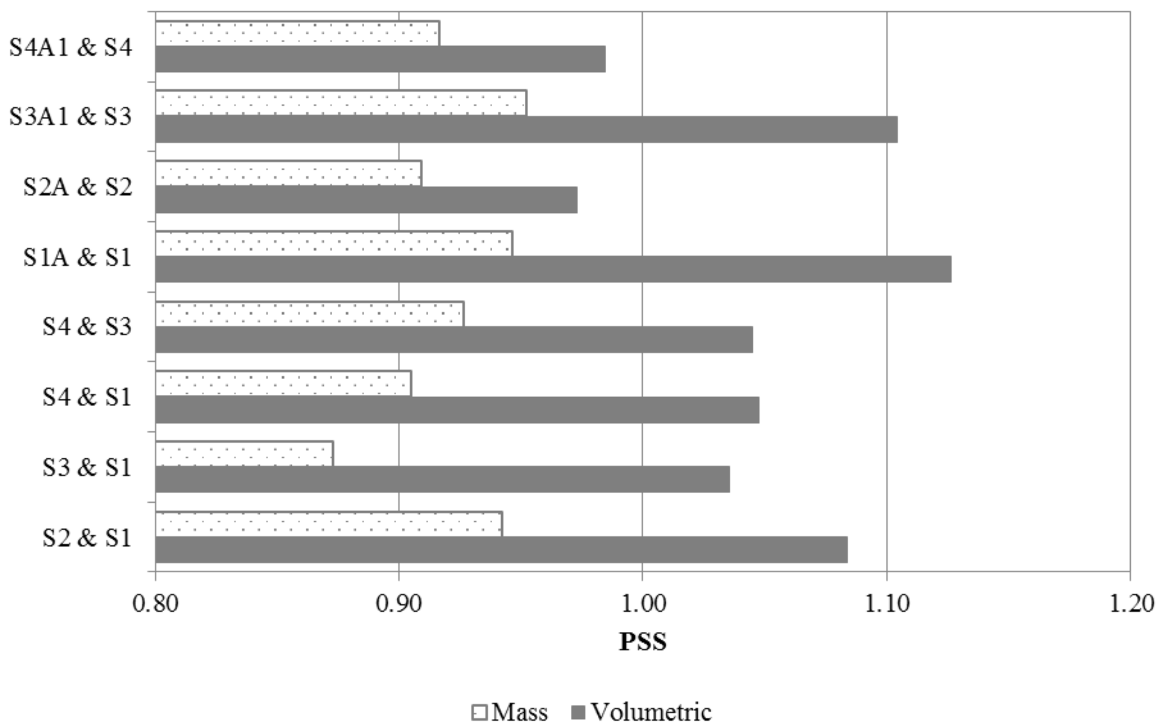

Figure 5-9 Simulated Scaled Sensitivity of various scenarios on mass and volumetric encroachment of intrusion

S1: Baseline scenario with 180 l/c/d water consumption rate and 1.75% population growth;
S2: Most likely scenario with 200 - 300 l/c/d water consumption rate and 1.75% population growth;
S3: Modified baseline scenario with 180 l/c/d water consumption rate and 2.5% population growth;
S4: Worst case scenario with 200 - 300 l/c/d water consumption rate and 2.5% population growth;
S1A & S2A: Reduction in groundwater abstraction by 230,000 m^3/d starting 2019;
S3A1 & S4A1: Reduction in groundwater abstraction by 350,000 m^3/d starting 2019;
S4A2: Abstraction in S4 is halted as demand is met as a result of adaptation/mitigation measures starting 2019;
S1L: Sea level rise is included at 1 cm/yr i.e. rise of 20 cm in S4 by 2032;
S4L: Sea level rise included at 3.2 cm/yr i.e. rise of 65 cm in S4 by 2032.

The seasonal sensitivity results indicated that the impact of adaptation strategies increased during the dry seasons when the aquifer undergoes maximum intrusion (Figure 5-10). Since the aquifer does not suffer from excessive intrusion during the wet season under the baseline scenario S1, the system exhibited the least sensitivity to the adaptation plan during the wet season (Wet PSS=0.56). This highlights the potential role of storing the excess water during the wet season for later usage during the dry season as a potential adaptation strategy to be further examined. However, the impact of adaptation on mass encroachment of salinity during the dry season was most effective under the baseline condition S1 when the PSS increased nearly four times from wet (0.56) to dry (1.73). The high sensitivity of the mass encroachment to the adaptation scenario S4A1 during the wet seasons indicates the vulnerability of the aquifer during the wet-season to increases in the population and water consumption rates (PSS=0.9). While this higher sensitivity to population growth (PSS=0.9) rather than water consumption (PSS=0.8) during the wet seasons (S3 vs. S2) is in contrast to the yearly sensitivity analysis results (where PSS is 0.87 for S3 & 0.94 for S2), it is due to the fact that water consumption varies per season but population growth mainly carries a constant ratio over a given year. This highlights the need for seasonal/monthly simulations to address the impact of seasonal change in the rates of groundwater abstraction on the seasonal state of SWI for proper analysis of the impact of adaptation or mitigation strategies aimed at halting the intrusion.

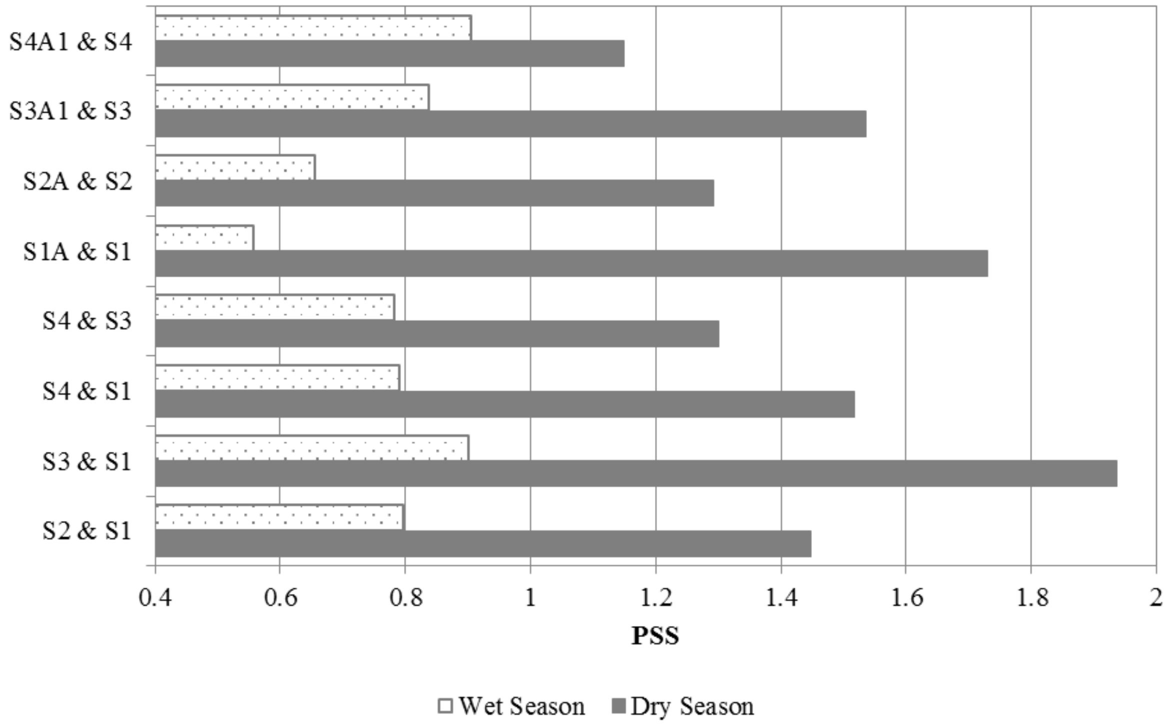

Figure 5-10 Seasonal PSS of simulated scenarios on the mass encroachment of intrusion

S1: Baseline scenario with 180 l/c/d water consumption rate and 1.75% population growth;
S2: Most likely scenario with 200 - 300 l/c/d water consumption rate and 1.75% population growth;
S3: Modified baseline scenario with 180 l/c/d water consumption rate and 2.5% population growth;
S4: Worst case scenario with 200 - 300 l/c/d water consumption rate and 2.5% population growth;
S1A & S2A: Reduction in groundwater abstraction by 230,000 m^3/d starting 2019;
S3A1 & S4A1: Reduction in groundwater abstraction by 350,000 m^3/d starting 2019;
S4A2: Abstraction in S4 is halted as demand is met as a result of adaptation/mitigation measures starting 2019;
S1L: Sea level rise is included at 1 cm/yr i.e. rise of 20 cm in S4 by 2032;
S4L: Sea level rise included at 3.2 cm/yr i.e. rise of 65 cm in S4 by 2032.

5.3.5 Adaptation / mitigation framework

While adaptation strategies can be very successful in slowing saltwater intrusion even under scenarios of high population growth rates, high water consumption rates must be controlled for this purpose. Scenarios of high consumption rates render adaptation strategies ineffective after an average period of 14 years as the increase in demand for groundwater masks the benefits of the adaptation. In this context, adaptation strategies should be planned together with mitigation measures in a comprehensive framework for effective saltwater intrusion control and sustainable aquifer management. While only three adaptation strategies were simulated, designing the adaptation framework necessitates examining all measures that can potentially reduce the water deficit, which is the main driver for groundwater abstraction, through targeting both demand and supply management options incorporated in national water plans in close coordination between relevant institutional and community stakeholders (Figure 5-11). In this context, the Ministry of Energy and Water (MoEW) and its Regional Water Establishments (RWE) are the main entity governing the water sector in coordination with other regulatory bodies such as the Ministries of Public Health (MoPH) and Environment (MoE) that are responsible for health and environmental protection and setting standards for water quality monitoring. The Ministry of Interior and Municipalities (MoIM) is involved in executing and monitoring of small-scale municipal works that relate to water infrastructure as well as enforcing regulations / penalties levied by other institutions. In practice, these ministries are also supported at times by the Council for Development and Reconstruction (CDR) through funding large-scale water supply projects such as dams from international organizations (MoE/UNDP/ECODIT 2011) and the Ministries of Finance (MoF) and Economy and Trade (MoET) through setting tariff structures and ensuring consumer protection.

Supply Side Management Strategies		Institutional Stakeholders		Demand Side Management Strategies
– Storm water collection along coastal areas – Dams (in or out of basin) – Desalination – Water harvesting (building level) – Water reuse (gray water and wastewater)	⇔	MoEW REW MoE MoPH MoIM CDR MoF MoTE ⇳ Consumer at the building level Commercial and Industrial NGOs	⇔	– Conservation appliances at the household level – Smart Metering – Tariff restructuring – Supply network efficiency (leaks / unaccounted for water)
		Community Stakeholders		

Figure 5-11 Adaptation framework

MoEW: Ministry of Energy & Water RWE: Regional Water Establishments
MoPH Ministry of Public Health MoE: Ministry of Environment (MoE)
MoIM Ministry of Interior & Municipalities CDR: Council for Development and Reconstruction
MoF: Ministry of Finance MoET Ministry of Economy and Trade

Smart metering, tariff restructuring, promotion of water conservation practices as well as incentives for water saving appliances are important demand side management measures indispensable for sustainable water consumption and proper resource management. On the other hand, reducing unaccounted-for-losses in the water supply network, currently estimated at 50% (MoEW, 2012), remains a priority supply management measure that can minimize groundwater abstraction as well as save invaluable surface water resources. Rainwater harvesting, benefiting from surface runoff (storm water) along coastal areas, as well as reuse of treated gray water and wastewater, despite associated sensitivity in terms of social acceptance, can also be incorporated in the framework. Other supply management methods, discussed in the national plans (MoEW, 2012), including the construction of a series of dams as well as conveying water from rural areas, could prove viable in the medium to long term when population growth and high consumption rates require boosting of available water resources. The latter should be considered in parallel to demand management strategies and other supply management measures such as unconventional sources (i.e. desalination, water harvesting, and water reuse etc.). This framework should be managed concomitantly with a monitoring program that continuously assesses the response of the aquifer system to groundwater extraction. Naturally, the framework needs to be implemented in a wise and timely manner where different measures are gradually undertaken at critical milestones to support and boost strategies that may grow ineffective and maintain aspired performance.

5.4 Conclusion and Way Forward

The impact of global environmental change and local anthropogenic interventions on the intrusion of saltwater in a coastal urban aquifer was analyzed using a multi-objective variable density model through analysis of groundwater abstraction and sea level rise scenarios. The results of annual simulations showed that while the aquifer system is highly sensitive to both water consumption rates and population growth rates, a ~50% increase in the rate of water consumption leads to at least four times more volumetric displacement of the interface than a similar increase in population growth rate after 20 years. Interestingly, coupling of both has a synergistic effect that aggravates the displacement beyond the sum of the individual impacts. On the other hand, the aquifer system revealed a relatively limited sensitivity to sea level rise (induced by climate change) whereby the impact on saltwater intrusion of a 65 cm rise by 2032 is masked by 2% increase in abstraction rates under the baseline scenario although other climate change impacts. Note however that the additionality factors associated with the decrease in precipitation and increase in temperature (hence increase in the net water demand) induced by climate change, is indirectly embedded in water consumption rates.

The analysis of adaptation strategies indicated considerable effectiveness in the ability to slow the rate of saltwater intrusion. While the adaptation strategy of halting abstraction could not cause system-recovery or reverse the saltwater intrusion damage, it succeeded in stopping the intrusion. The effectiveness of adaptation strategies to secure the aspired results is hinged on proper planning in terms of timing, duration, capacity and context. This underlines the importance of understanding the aquifer system and its seasonal response as well as its interaction with drivers, before selecting an adaptation strategy for successful and sustainable aquifer management.

This study contributed to the understanding of the response of coastal aquifer systems to local and global stresses as well as the role of adaptation strategies in alleviating saltwater intrusion. It forms a platform for effective local adaptation planning, providing informed policy and decision making for sustainable aquifer management.

CHAPTER 6

DYNAMIC BAYESIAN NETWORKS TO ASSESS ANTHROPOGENIC AND CLIMATIC DRIVERS OF SALTWATER INTRUSION: A DECISION SUPPORT TOOL TOWARDS IMPROVED MANAGEMENT

6.1 Introduction

Saltwater Intrusion (SWI) has been reported in various coastal zones around the world such as New Zealand (EnviroLink, 2011), China (Zhang et al., 2011), Philippines (Sales, 2009), Korea (Park et al., 2012), US (Conrads et al. 2010; Sanford and Pope, 2010), Bangladesh (Rahman et al. 2014), and India (Bobba, 2002). The Mediterranean basin is no exception, with SWI reported along its northern, southern and Eastern sections (e.g. France (de Montety et al., 2008), Italy (Capaccioni et al., 2005), Spain (Fatoric & Chelleri, 2012), Turkey (Cobaner et al. 2012), Syria (Allow 2012; Abu Zakhem & Katta 2017), Lebanon (Saadeh & Wakim, 2017; Rachid et al. 2017; Zaarour 2017), Israel (Levi et al. 2018; Mushtaha et al. 2019), Gaza (Selmi, 2013), Egypt (Eissa et al. 2016; Attwa et al. 2016), Tunisia (Kouzana et al., 2010), Libya (El Hassadi, 2008) and Morocco (El Yaouti et al., 2009)).

Complex coastal aquifer hydrodynamics and the uncertainties associated with future climate change limit our abilities to quantify and predict SWI (Sanford & Pope, 2010; Werner et al., 2013). Moreover, interactions between global climate change and local environmental drivers (e.g. urbanization with land use and land cover) remain poorly characterized. As such, the ability of coastal cities to manage and adapt to SWI is constrained by the complexity of the process, the limited data availability, and the associated high uncertainties (Tribbia & Moser, 2008). In this context, Bayesian networks (BNs) can be ab attractive decision support tool for risk analysis and management (Marcot & Penman, 2019; Li et al., 2018; Gonzalez-Redin et al. 2016; Fenton & Neil 2012; Barton et al. 2008). BNs are models that link variables of different states with probabilities in a directed acyclic graph and use probability theory, based on Bayes Theorem, to quantify interactions, calculate posterior probabilities of outcome states, and propagate uncertainties (Marcot, 2012; Pearl, 1986). They are effective in accommodating incomplete data, accounting for uncertainty, and integrating knowledge-based and expert-based information (Marcot & Penman, 2019; Eurie Forio et al. 2015; Aguilera et al., 2011). BNs also allow for forward and backward propagation of information as new information is made available (Aguilera et al., 2011). BNs are also attractive as decision support tools given their legible graphical interface that is user-friendly for the non-technical users. Additionally, they can incorporate both decision and utility nodes to form Bayesian decision networks. Traditionally, BNs have been run as standalone models that are static with respect to time. Recent developments have expanded the capabilities of traditional BN to allow them to be linked to other networks to produce Object-Oriented Bayesian Networks, while time slicing has permitted the development of Dynamic Bayesian Networks (DBNs) for temporal analysis and predictions of future states (Molina et al., 2013).

Given these advantages, bayesian decision networks have been successfully used to manage surface water resources and groundwater abstraction as well as to model catchments and irrigation needs (Keshtar et al. 2013; Molina et al. 2010; Sadoddin et al. 2005). BNs were also used in ecological modeling, natural resources management, water quality assessment, and water/groundwater management (Alameddine et al., 2011; Newton 2009; Borsuk et al., 2004; Bromley et al., 2003). However, their application in climate change related studies and adaptation management remains limited (Catenacci & Giupponi, 2013; Cuddy et al., 2007; Hall

& Twyman, 2005) and their use towards assessing saltwater intrusion is lacking. In this study, a conceptual DBN framework is developed and presented as an environmental management tool with applicability to semi-arid coastal areas affected by SWI with the aim of improving our understanding about the interaction between local anthropogenic drivers and global climatic determinants responsible for SWI in data-scarce and poorly monitored urbanized coastal aquifers. Additionally, we assess the socioeconomic implications of SWI that are associated with the projected changes in the physical environment and/or in the implementation of different policy drivers, while ensuring that the associated uncertainties in the data are accounted for and propagated transparently. The DBN is then used to compare between a set of proposed demand and supply management scenarios by assessing their abilities towards limiting/reversing SWI under projected climatic changes and socio-demographic transformations.

6.2 Material and Methods

6.2.1 Study area

The study area consists of the highly urbanized metropolitan (Beirut) located on a relatively flat triangular shaped-peninsula extending westward into the Mediterranean Sea (Figure 6-1). It has a surface area of 44 km2 with a 5 km shoreline and diverse features including rocky beaches, sandy shores and cliffs. Topographically, the study area starts at sea level then gains elevation along the south-west and north east directions to reach a maximum of 95m asl (Abdel Basit, 1971). Its population is nearly 1.2 million (CDR/ DAR 2014) residing in about 18,000 buildings (SOER, 2011) at a density of around 20,167 person/Km2 (Ayash, 2010). The population growth has been reported to range from 0.4 to 2.5% per year (CAS, 2008; WB 2009; MOEW, 2010; El Fadel et al., 2000). The study area has witnessed rapid urbanization, at a 111%

increase between 1963 and 2005 (Faour & Mhawej, 2014). With increased urbanization, the natural terrain of the study area was converted rapidly to impermeable surfaces; with an estimated 1 tree remaining for every 33 inhabitants as compared to 4 and 34 trees per inhabitant in Berlin and Abu Dhabi (ESCWA, 2005). The annual rainfall in the city ranges from 700 to 900 mm/yr (Peltekian, 1980; Atlas Climatique du Liban, 1977; El-Samra et al., 2016) with an average annual temperature of 20.9 °C (tu.tiempo, 2016; Atlas Climatique du Liban, 1977). Climatic predictions point towards a drier and warmer future as well as to a rising sea level at a rate of 20 mm/yr, which may reach up to 30-60 cm by 2040 (SNC 2011; TNC 2016).

The underlying geology of the study area belongs to the Cretaceous and Quaternary periods with pockets of the Tertiary periods (Figure 6-1). Groundwater occurs mainly in two principal aquifers of sand and carbonate (Abdel Basit, 1971). Available water resources to the city consist mainly of the water supplied through the public water network from nearby basins and groundwater wells (El Fadel et al., 2000; Acra et al., 1997; Saadeh, 2008; Nasr et al., 2012). The daily supplied volume is estimated at 183,000 and 283,000 m3/d for the summer and winter seasons respectively; whilst the demand is estimated to exceed 303,000 m3/d (Saadeh, 2008). As a result of this deficit, the residents rely heavily on tapping into subsurface aquifers to fulfill their unmet water needs (Ayash, 2010; Acra et al, 1997). According to CAS (2008), out of the 18,200 buildings in Beirut at least 5,000 operate a private well with a total yield of more than 14 MCM (million cubic meters) per year (MOEW 2010; SOER, 2011; Saadeh 2008; Peltekian, 1980).

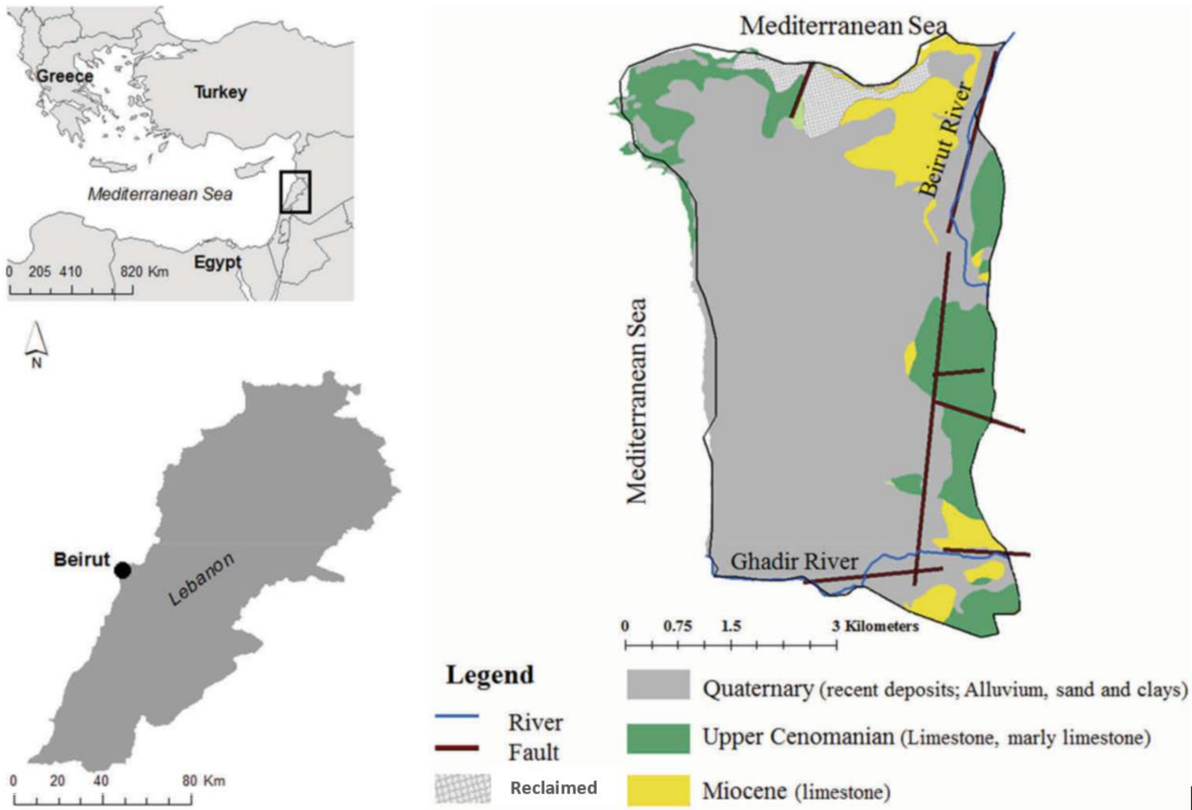

Figure 6-1 Location and geology of the study area

6.2.2 *SWI along the Beirut coastal aquifer*

Signs of SWI in Beirut were observed as early as 1969, through geo-electrical processing that confirmed SWI through tectonic fractures (FAO 1997). Since then chloride concentrations steadily rose from 340 mg/L in 1970 to over 4,200 mg/L in 1985 (Khair, 1992). In a more recent study, Rachid *et al*. (2017) analyzed 170 wells between 2012 and 2013 and reported that the aquifer suffers from advanced salinity (average chloride concentration = 4600mg/L) albeit with significant spatial and temporal heterogeneity. While these high levels of chloride are mostly driven by increased water demand and groundwater over extraction, they are expected to further intensify in the future under the synergy of climate change impacts and population growth.

6.2.3 Conceptual Model Development and parameterization

Anthropogenic and climatic drivers will influence the propensity of SWI in coastal aquifers. Studies have generally focused on three main drivers, namely groundwater abstraction, aquifer recharge, and sea level rise (SLR) (Safi et al., 2018; Sophiya & Syed, 2013; Cobaner et al., 2012; El Shinnawy & Abayazid, 2011; Purandara, et al., 2010; Harbor, 1994). Population growth and increased urbanization are the main anthropogenic inducers of SWI, as they increase water demands and reduce natural groundwater recharge (Selmi, 2013; Koussis et al. 2012; Cobaner et al. 2012). In addition, the daily water consumption rate plays an important role in determining the total water demand for a given area. The rate is known to differ geographically and temporally and as a function of affluence (Whitcomb, 2005). When the supply is short of the demand, groundwater extraction and SWI increase, especially when monitoring and enforcement are weak.

Climate change is another driver of SWI through multiple routes including the reduction in precipitation, the increase in ambient temperature and evapotranspiration, and the rise of sea level (Sherif et al. 2012; Abdel Hamid, 2010). A decrease in precipitation is expected to reduce the recharge and negatively affect available freshwater resources. On the other hand, an increase in ambient temperature is associated with a greater water demand (Jarboo & Al-Najar 2015; Goodchild, 2003) and evapo-transpiration (Bates et al., 2008; Jackson et al., 2011; Neukum & Azzam, 2012). The rise in sea level is expected to imbalance the saline-freshwater hydrostatic pressure and enhance the lateral seawater intrusion (Carretero et al., 2013; Werner et al., 2013; Conrads et al. 2010; Chang et al. 2011; Reilly & Goodman, 1985). While the general trends governing the physical, geological and chemical interactions between these drivers and the intensity of SWI are common, the direction and magnitude of these interactions are highly context-specific (Ferguson and Gleeson 2012; Ivkovic et al. 2012; Loáiciga et al. 2011).

As groundwater salinity levels increase, it becomes unusable for most purposes. Hence, salinization is associated with an economic burden in terms of incurring "avoidance costs" such as tapping into alternative resources, purchase of water, or the treatment of the salinized water to acceptable levels prior to use (Catenacci & Giupponi, 2013; Connor et al., 2012; Characklis et al. 2005). Moreover, consuming high salinity waters shortens the useful lives of piping systems, fixtures and appliances (water heaters, coolers, faucets, clothes washers, and dishwashers) and damages the infrastructure. These in turn result in increased expenditures on maintenance and repairs (Alameddine et al. 2018; Connor et al. 2012; Howitt et al. 2009; Ragan et al. 2000; Wilson, 2004). Additionally, the consumption of high salinity water has been associated with adverse health impacts (UrRahman et al. 2017; Talukder et al., 2016; Frank & Boyer, 2014). Overall, the scale of these damages is expected to intensify in view of the synergies between the seemingly inevitable impacts of climate change and the ever-increasing human-induced pressures (Nicholls et al., 2007).

For the study area, the available literature, exploratory data analysis and experts' judgment were used to formulate a conceptual framework for SWI (Phan et al. 2016; Kragt, 2009; Giordano et al. 2013; Keshtkar et al. 2013). Figure 6-2 depicts the framework of SWI along coastal aquifers representing the drivers, their effects or impacts, their potential interactions, and their implications.

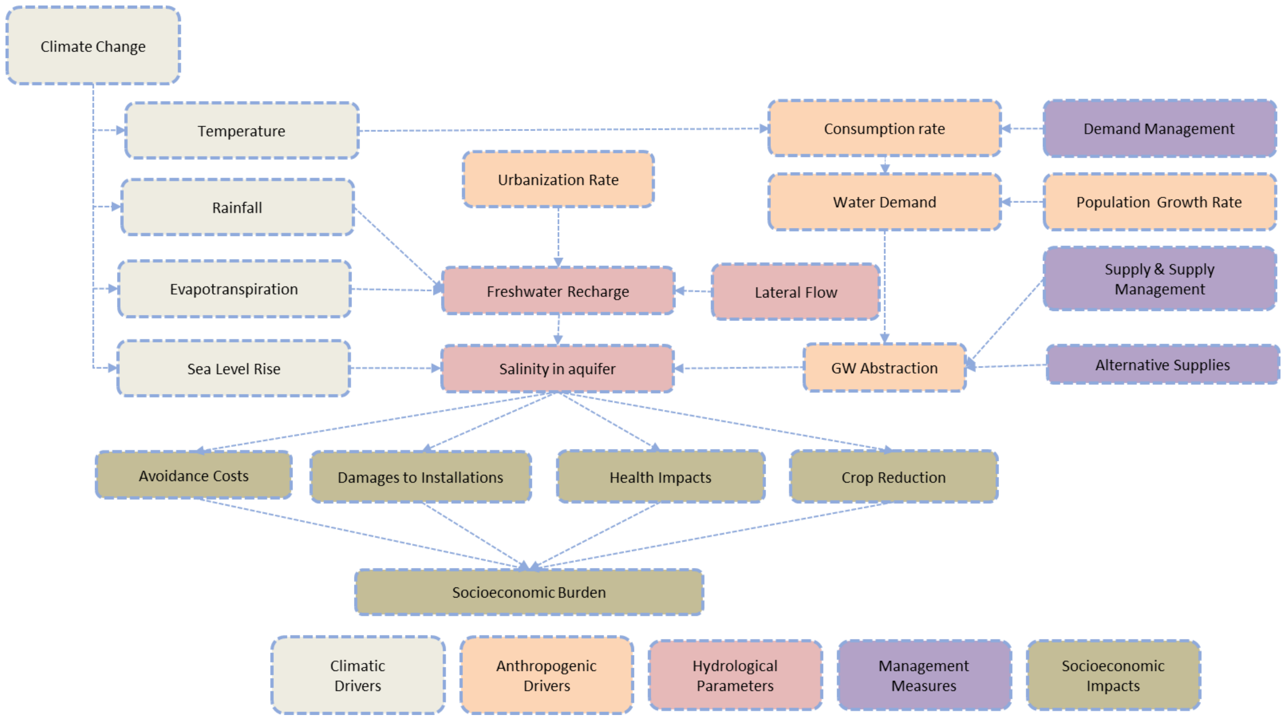

Figure 6-2 Conceptual framework for the main drivers of saltwater intrusion and their impacts

Transforming the conceptual framework into a BN model requires the identification of variables representing the parent and child nodes as well as establishing the conditional relationships between them (Phan et al. 2016; Catenacci et al. 2013; Keshtar et al. 2013; Kragt, 2009). Starting with the conceptual framework (Figure 6-2), the structure and variables of the SWI Directed Acyclic Graph (DAG) were developed in an iterative process involving reviews and feedback from domain experts. While most nodes in the conceptual framework were directly represented as variables in the SWI DAG (e.g. temperature, rainfall, population growth rate, consumption rate, aquifer salinity, freshwater recharge …etc.), others were captured by a set of variables (e.g. avoidance costs, lateral flow, etc.) as detailed below.

The final SWI DAG (Figure 6-3) consisted of multiple variables categorized into four components, namely a climate component, a hydro-geological component, a demographic component and a socio-economic component. The climate component accounts for the current conditions of temperature, rainfall and evapotranspiration as well as their projected future changes as defined by the RCP 4.5 and RCP 8.5 scenarios (IPCC 2014). Note that while the impact of SLR on aquifer salinity was initially included as a node in the conceptual framework, it was omitted due to the inconclusive nature in the direction and intensity of the relationship between SLR and salinity (Werner et al. 2013; Carretero et al. 2013; Chang et al. 2011; Reilly & Goodman 1985). The main route by which SLR affects salinity is through the advancement of the freshwater-seawater mixing zone and the interface toe, the dynamics of which can only be described through a spatially distributed numerical model specific for the aquifer. In this context, Safi et al. (2018) reported that the impact of SLR on salinity levels was negligible when compared to the magnitude of existing anthropogenic drivers. The demographic component of the model relates the current population and its potential growth over time along with the water consumption rates to estimate water demands. The hydrogeological component was divided into two sub-components, namely lateral flow and salinity. The lateral flow sub-component characterizes the recharge area outside the aquifer domain that contributes freshwater into the study area. It links the infiltration, pervious area and abstraction rates in the mountainous recharge area overlooking the city to the net freshwater recharge inflowing into the study area. Thus, it represents the total lateral flow. On the other hand, the salinity sub-component defines the relationships governing how the drivers of SWI (freshwater recharge, rainfall infiltration, pervious area, abstraction and safe yield) affect the salinity levels of the aquifer. Finally, the socioeconomic component relates the resulting salinity levels to the direct and indirect costs incurred by the targeted population as a function of avoidance costs that included the cost of treatment (e.g. reverse osmosis), damages to installations, or costs of using alternative sources (i.e. trucking water).

As the DBN is intended to be used as a decision support tool, a management component was included to explore the implications of potential or planned mitigation measures and adaptation strategies (i.e. demand and supply management options). Figure 6-3 illustrates the resultant DAG including the nodes and links associated with the multiple model components. Full details on the model set up and its components are presented in the Appendic 4a.

The definition of the states for each node was based on reported literature, empirical data, field surveys and stakeholders' elicitation (Sperotto et al. 2017; Phan et al. 2016; Keshtkar et al. 2013). The number of states was kept as low as possible to account for the need to populate the conditional probability tables (CPTs) (Eurie Forio et al. 2015; Chen & Pollino, 2012). As some nodes are continuous, discretization was necessary. Based on Fienen et al. (2013), natural thresholds evident from the physical environment were used first in addition to meaningful ranges reported in the literature. This was followed with an iterative process of fine-tuning the discretization process to ensure the generation of meaningful bins that are able to provide insights on the data and reflect changes. For example, the discretization of aquifer salinity followed the groundwater quality categorization into slightly, moderately, highly and very highly saline based on the six salinity bins of Konikow and Reilly (1999). These bins were then further examined where the first two very low and the last two very high extreme bins were compressed into 1 very low and 1 very high bin while the middle broad bins were each divided into two in order to capture the salinity changes within each category. The evaluation of the impact of the discretization method on the accuracy and computational efficacy, albeit recognized (Lucena–

Moya et al. 2015; Rahman et al. 2014; Nojavan, 2014; Alameddine et al. 2011; Aguilera et al. 2011; Uusitalo, 2007), was out of scope of this study.

Populating the prior probabilities of the parent nodes as well as the subsequent CPTs was based on available data, reported literature, official statistics, field surveys, outputs from other models, and expert elicitation and interviews (Table 6-1) (Nojovan et al. 2017; Rahman et al. 2014; Catenacci et al. 2013; Chen and Pollino, 2012; Kragt et al. 2009; Kjaerulff and Madsen, 2008; Pollino et al. 2007; Nyberg et al. 2006; Cain 2001). For example, the probabilities for the nodes on RO price, RO penetration rate, well penetration rate, and the water tanker prices were populated based on field surveys (El-Fadel et al. 2015; Constantine et al. 2017) and expert interviews. Elicitation was undertaken through the direct fixed value elicitation approach (Kashuba, 2010; Winkler, 2003; Morgan & Henrion, 1990; Clemen, 1991). Additionally, a set of CPTs were populated based on functions representing mass balances and regression equations (Table 6-1). Note that the time span of the DBN was defined between 2013 and 2034, with a time step of one year. The baseline year was set at2013/2014. While the states, prior probabilities and conditional probability tables were populated with data relevant to the pilot area, yet the model is easily transferable to other coastal cities with similar settings. Table 6-1 summarizes the developed DBN by highlighting the type of nodes used, their states and the basis for parameterization of their CPTs. The DBN was implemented in the HUGIN EXPERT 8.3 (HUGIN EXPERT 2019). Full information on the model parameters including the definition of the nodes' states and parameterization of CPTs are provided in the Appendix 4.

Table 6-1 DAG Parameterization: nodes, states and CPT references

	Node Name [a]	Unit [a]	States	Parameterization
Climatic Component	CC scenarios (P) (C)	RCP	4.5; 8.5	Output from global circulation models
	Temperature increase	˚c/yr	0 - $2.5x10^{-3}$; $2.5x10^{-3}$ -0.0208; 0.0208-0.037	Output from dynamic downscaling model (WRF [a] HiRAM [a] model) [b,c]
	Actual rainfall (C)	mm/yr	<350; 350 - 550; 550-750; 750 -950; 950 - 1100	Literature & data [b,c]
	Rainfall reduction	%/yr	0.006-0.01; 0.01-0.015; 0.015-0.02	Output from dynamic downscaling model (WRF HiRAM model) [b,c]
	Evapo-transpiration reduction	%/yr	0 - $4.97x10^{-4}$; $4.97x10^{-4}$ – $9.91x10^{-4}$; $9.91x10^{-4}$ – $3.85x10^{-4}$	Output from PRECIS model [c,n]
Hydrogeological Component - Lateral Flow	% pervious area in the lateral recharge zone (P)	%	1-10; 10-30; 30-50	Data & Literature [d]
	Infiltration volume in the lateral recharge zone	MCM/yr	0-1; 1-2; 2-3	Equation*
	Infiltration rate in the lateral recharge zone (P)	%/yr	10-20; 20-30; 30-60	Expert interviews
	Abstraction in the lateral recharge zone	MCM/yr	0-0.6; 0.6-1.6	Equation*
	Lateral flow into the study area	MCM/yr	0-1; 1-2; 2-3	Equation* – mass balance
Demographic Component	Population growth rate (P) (C)	%/yr	0.2-1.2; 1.2-2.2; 2.2-3.2	Data & Literature [e]
	Actual population (C)	Million	1-1.2; 1.2-1.4; 1.-1.6; 1.6-2.2	Data & Literature [f]
	Consumption rate (C)	l/c/d	<70; 70-100; 100-200; 200-300	Equation* Data & Literature [g]
	Water demand	MCM/yr	<10; 10-50; 50-100; 100-150; 150-250	Equation*
	Water Deficit	MCM/yr	0-1; 1-5; 5-10; 10-40; 40-140; 140-220	Equation*
Hydrogeological component - salinity	Effective infiltration in study area	MCM/yr	0-0.2; 0.2-0.4; 0.4-0.6	Equation* [Eq. 1]
	Pervious area decrease (P)	%/yr	0-0.2; 0.2-0.5; 0.5-1	Expert elicitation Literature [d,h]
	Freshwater recharge	MCM/yr	0-0.5; 0.5-2.5; 2.5-4.5; 4.5-8	Equation*
	Network supply	MCM/yr	30-50; 50-110; 110-180; 180-240	Official data [i]
	Groundwater abstraction	MCM/yr	0-1; 1-5; 5-10; 10-40; 40-140; 140-250	Equation*
	Safe yield	MCM/yr	0-1; 1-5; 5-10; 10-40; 40-140; 140-250	Equation*
	Groundwater abstraction rate (as a function of aquifer salinity)	% of previous year	10-50; 50-60; 60-75; 75-100	Expert elicitation
	Salinity in aquifer (C)	ppm	1000-4000; 4000-7000; 7000-10000; 10000-15000;15000-25000;25000-35000	Equation* - Mass balance [Eq. 2]
Socioeconomic Component	RO penetration	% of buildings	0-5; 5-10; 10-20; 20-40	Field survey + Expert elicitation
	RO price	$/m³	0-0.3; 0.3-0.5; 0.5-1; 1-2	Expert interviews
	RO cost (at the city level)	MUSD/yr	0 – 0.8; 0.8 – 10; 10-320	Equation*
	Installation damages (at the city level)	MUSD/yr	0-1; 1 – 2.5; 2.5 – 5	Equation* - Regression Model [Eq. 3]

	Node Name [a]	Unit [a]	States	Parameterization
	Water tankers (market penetration)	% of buildings	5-25; 25-35; 35-55; 55-80	Field survey
	Tanker price (price of water delivered by tankers)	$/m^3$	3-8; 8-12	Literature [j]
	Cost of tankers (annual cost of water delivery by tankers at the city level)	MUSD $/yr	0-5; 5-10; 10-60; 60-200; 200-900	Equation*
	Annual socioeconomic (SES) burden (at the city level)	MUSD $/yr	0-5; 5-10; 10-50; 50-100; 100-500; 500-1000; 1000-2400	Equation*
	Cumulative SES burden (C)	MUSD $	0-5; 5-2000; 2000-3000; 3000-4800; 4800-7000; 7000-10000; 10000-24000	Equation*
	Cumulative SES (over project life) per capita	$/capita	0-250; 250-500; 500-1500; 1500-2500; 2500-5000; 5000-10000; 10000-24000	Equation*
Management Component	GBWSP Phase I	MCM/yr	0 - 30 - 60	Official data [k]
	GBWSP Phase II	MCM/yr	0 - 30 - 60	Official data [k]
	Desalination	MCM/yr	0 - 60 - 120	Literature [l]
	Artificial recharge	MCM/yr	0 - 3.5	Official data [k]
	Demand Management (P) (increase in tariff)	%	0-50; 50-150; 150-300	Data & Literature [m]

* Equations detailed in Appendix 4b.

a (P) parent node; (C) temporal clone node; (RCP) Representative Concentration Pathways; (MUSD) Million US dollars; (MCM) Million Cubic Meters; (GBWSP) Greater Beirut Water Supply Project; (WRF) Weather Research and Forecasting model; (HiRAM) High Resolution Atmospheric Model

b El-Samra et al., 2016; c Atlas Climatique du Liban, 1977, SNC 2011, TNC 2016; d Faour & Mhawej, 2014; e CAS, 2008, WB 2009, MOEW, 2010, El Fadel et al., 2000; f CDR/DAR 2014, Ayash 2010, SOER 2011; g WB 2009, SOER, 2011, MOEW, 2010, Comair, 2010, Saadeh, 2008, Peltikian, 1980, El-Fadel et al. 2000; h El-Fadel et al. 2015; i MOEW 2010, Saadeh, 2008, SOER 2011; j Constantine et al. 2017; k MOEW 2010, WB 2017; l Saidy 2016; m MOEW 2010; n PRECIS Model, Met Office Hadley Center (2010)

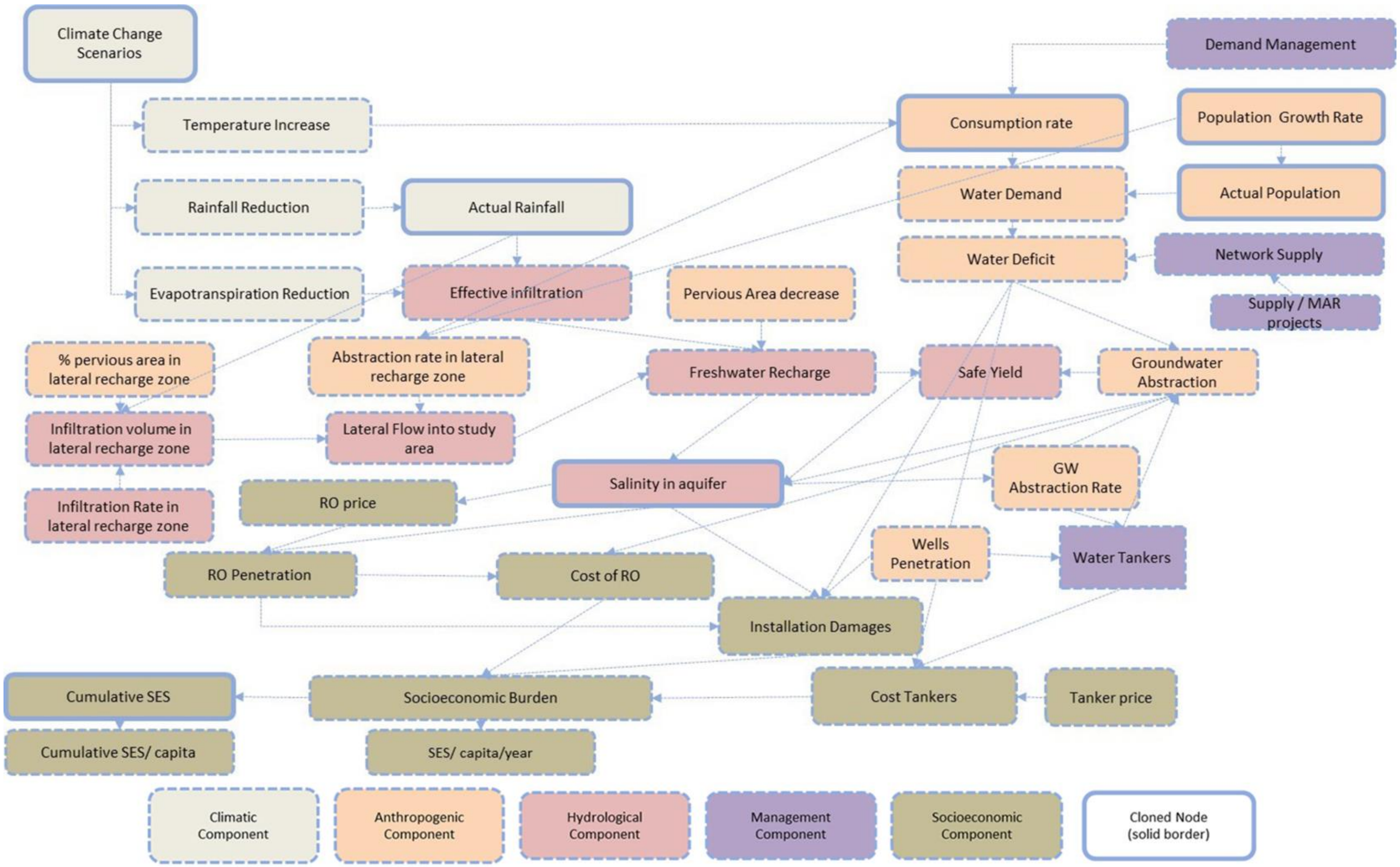

Figure 6-3 Proposed Directed Acyclic Graph for the Saltwater Intrusion Dynamic Bayesian Network. Cloned node: are select variables that represent the interface between two successive time slices in the DBN allowing for the modeling of time series

6.2.4 Dynamic Bayesian Network

While a BN is an effective decision support tool, it is limited in its capacities to propagate information through time. As such, the BN model was further developed into a DBN. The latter has been applied in various fields including clinical (Orphanou et al., 2014) and environmental studies (Uusitalo et al., 2018; Molina et al., 2013). DBNs allow for the modeling of time series by generating a BN for each time slice and allowing the realization of selected variables at a given time to be dependent on the state of the system at past times while maintaining the same DAG and node relationships throughout the time slices (Marcot & Penman, 2019; HUGIN EXPERT 2019). These select variables are known as temporal clones that represent the interface between two successive time slices in the model (HUGIN EXPERT 2019). As such, simulations of the BN at any time slice will result in updates to the probabilities of states for all nodes including the clone nodes at that time slice. These clone nodes will then communicate their updated states to their clone in the next time slice so that the BN of the next time slice will estimate the updated probabilities of all nodes accounting for the carried input from the previous time slice. In this study, 7 out of 37 nodes were designated as clone nodes (refer to Table 1). In total the DBN had 20-time steps (time step = 1 year) starting with the base year of 2014 and ending in 2034.

Several diagnostic metrics (e.g. receiver operating characteristic curves, k-fold cross-validation, confusion tables, and performance indices have been developed to assess the performance of BN models (Speretto et al. 2017; Marcot 2012; Farmani et al. 2009; Newton 2009; Ticehurst et al., 2007; Borsuk et al., 2004); yet their application to our model was constrained by the unavailability of cases or data against which to test and validate the model.

Accordingly, the accuracy of the model predictions was only assessed using the Area Under the Receiver Operating Characteristic (ROC) Curve (AUC) metric (Marcot 2012; Nojavan et al., 2014; Newton 2009). The ROC curve plots the percent true positives ("sensitivity") as a function of their complement percent false positives. The AUC, which represent the overall performance of the model, typically ranges between 0 and 1, whereby a model that consistently provides false predictions has an AUC of 0 while an AUC of 1 indicates a model with perfect predictions. For this purpose, the analysis wizard of HUGIN was used to simulate a total of 10,000 cases (with 5% missing values based on MCAR (missing completely random)) to test the model accuracy. Model diagnosis was assessed on the first time-slice of the model only as analysis is not possible on the DBN. In addition, the model results from the 20-year run of the DBN were compared with the results of a 3D variable-density flow and solute transport model developed by Safi et al. (2018) for the same aquifer. The results of the AUC (Appendix 4g) were found to be satisfactory.

6.2.5 Model simulations

The DBN was used to assess the relative importance of the projected changes in climatic forcing versus those associated with anthropogenic drivers on SWI, through a set of scenarios (Table 6-3) by comparing their marginal probabilities on the target nodes (i.e. the salinity of the aquifer and the ultimate socioeconomic burden). A base line scenario (S1) was defined under RCP 4.5 to represent the most probable situation in the study area. The impact of climatic variability was assessed in scenario (S2) under RCP 8.5. The worst-case scenario (S3) coupled RCP 8.5 with a higher consumption rate of 200-300 l/c/d (instead of 100-200 l/c/d). Note that for all three scenarios, no changes were considered to the existing demand and supply management.

Several supply management scenarios were then defined and run under RCP 4.5 and 8.5 (Table 6-3). Based on governmental plans (MOEW 2010), S1-Sa and S3-Sa use 60 MCM of additional water by year 2019 and scenarios S1-Sb and S3-Sb use another 60 MCM starting 2025. In an effort to capture the urgency of implementing the proposed governmental supply projects, two scenarios (S1-Sc and S3-Sc) were proposed to capture the impact of delaying project execution. These scenarios assumed that the 120 MCM additional supply volume will be only made available for use starting 2025 onwards. On the other hand, scenario S1-MAR was defined to quantify the potential of Managed Aquifer Recharge (MAR) to limit the salinity in the aquifer by examining the impact of injecting ~3.5 MCM/year of freshwater (MOEW/UNDP 2014)) into the Beirut aquifer under RCP 4.5. Finally, the impact of implementing demand management (S1-D and S3-D) was tested under both the Most Probable (S1) and the Worst Case (S3) scenarios by introducing a 150 % increase in the water tariff.

Table 6-2 Scenarios assessed including driver variabilities and management decisions

Scenario	**Scenario definition**		**RCP**	**Consumption rate l/c/d**	**Population growth rate %**	**Municipal Supply Projects**
	No management scenarios					
S1	Most probable		4.5	100-200	1.2-2.2	0
S2	Worsening climatic conditions		**8.5**	100-200	1.2-2.2	0
S3	Worst case		**8.5**	**200-300**	**2.2-3.2**	0
	Management scenarios					
Supply management		***Year*** [a]				
S1-S_a	Most probable	*2019*	4.5	100-200	1.2-2.2	**60 MCM**
S1-S_b		*2019* *2025*	4.5	100-200	1.2-2.2	**60 MCM** (2019) **+60 MCM** (2025)
S1-S_c		*2025*	4.5	100-200	1.2-2.2	**120 MCM**
S3-S_a	Worst case	*2019*	8.5	200-300	2.2-3.2	**60 MCM**
S3-S_b		*2019* *2025*	8.5	200-300	2.2-3.2	**60 MCM** (2019) **+60 MCM** (2025)
S3-S_c		*2025*	8.5	200-300	2.2-3.2	**120 MCM**
S1-MAR	Most probable + MAR of 3.5 MCM/yr	2025	4.5	100-200	1.2-2.2	0
	Demand management					
S1-D_a	Most probable + Demand Management *(150% tariff increase)*	*2019*	4.5	100-200 (rate at base year)	1.2-2.2	0
S1-D_b		*2025*				
S3-D_a	Worst case + Demand Management *(150% tariff increase)*	*2019*	8.5	200-300 (rate at base year)	2.2-3.2	0
S3-D_b		*2025*				

Year [a]: indicates the year at which the MAR, Demand Management or Supply Management projects will be initiated
RCP: Representative Concentration Pathways; MAR: managed aquifer recharge; MCM: million cubic meters

6.3 Results and discussion

6.3.1 Climatic forcing and anthropogenic drivers under the no-action scenarios

Simulation of the Most Probable Scenario (S1) showed that while in the base year (2014) there was a 99% probability that the aquifer's average salinity is in the slightly to moderately saline category (1000 -7000 ppm), the probability that the average salinity level by the end year (2034) will exceed the 10,000 ppm level exceeded 90%. This reflects a significant increase in the average salinity of the aquifer (Figure 6-4). Under RCP 8.5 climatic forcing (S2), the probability that the average salinity of the aquifer in 2034 will exceed 10,000 ppm (highly saline) increased to 96%, with a 75% chance that the salinity will even exceed the 15,000 ppm (very highly saline). On the other hand, the results from the Worst-Case Scenario (S3) showed that the probability that by 2034 the aquifer's salinity will exceed the 10,000 or 15,000 ppm was 99% and 89% respectively (Figure 6-4).

Naturally, this projected increase in aquifer salinity was associated with an increase in the socio-economic burden on the community. The model projected that the burden per year will not exceed 2500 USD/capita/year (around 18% of the current average annual income per capita in Lebanon, estimated at 14,000 USD (MOF/UNDP 2017)) at any given year over the whole simulation period and across all scenarios (Figure 6-4). Under S1, it was projected with 53% probability that the burden is <250 USD/capita/year (around 2% of the current average annual income per capita) at the end year, 2034 (initially 70% probability at the start year 2019) as compared to a 44% probability that the burden in 2034 is 500 to 1500 USD/capita/year (around 3.5 and 10% of the current average annual income per capita) under S3. In parallel, the model projected a probability of 94% that the cumulative cost burden from avoidance costs and damages to installations (over 20 years) will exceed 1500 USD per capita which represents about double the cost per capita at the end year of the implementation of mega supply projects, estimated at a 820 USD/capita. The probability that the cumulative costs will exceed 5000 USD per capita (around 35% of the current average annual income per capita) was 60% under S1 (Figure 6-4). The drastic increase in aquifer salinity projected under the Worst-Case scenario (S3) was also associated with an equally sharp increase in the cumulative socio-economic burden to the community projected at a 90% probability to exceed the 5000 $ per capita (around six times the estimated implementation cost of mega water supply projects at 820 USD/capita at end year) (Figure 6-4). Under the conditions defined for S2, this probability was estimated at 76% (Figure 6-4).

These findings indicate that even under RCP 4.5 conditions, the aquifer is heading towards unfavorable salinity conditions if no demand or supply management interventions are implemented. Interestingly, the major pathway through which the climatic drivers affected salinity was through the increase in the water consumption rate due to the rise of temperature. Note that the impact of the reduction in precipitation is diminished by the low infiltration potential due to urbanization in the area. The findings also show that under the Worst-Case Scenario (S3) there is a risk that the aquifer will become unusable within a period of 20 years.

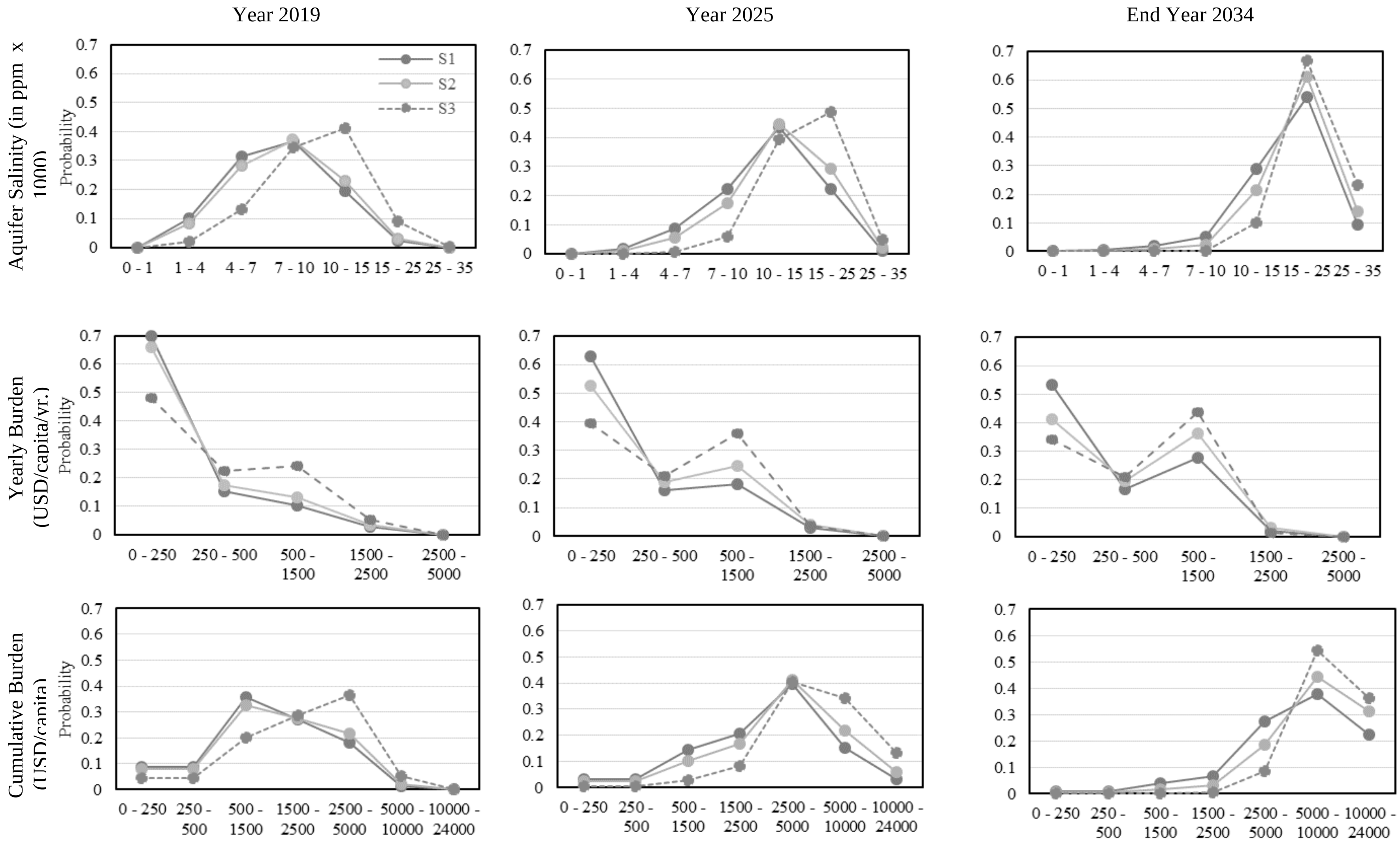

Figure 6-4 Probability of aquifer salinity (in ppm x1000) and socioeconomic burden (yearly in USD per capita/yr and cumulative in USD/capita) under S1: Most Probable; S2: Climatic forcing; S3: Worst Case scenarios

6.3.2 Projections with water management options

6.3.2.1 Managed aquifer recharge under the most probable conditions

Under the S1-MAR defined scenario, MAR exhibited little effect on reducing the probability that the aquifer salinity will exceed the 10,000 or 15,000 ppm marks by 2034. The drop in probability reached 8% and 4% respectively as compared to the probabilities estimated under S1 (Figure 6-5). Moreover, MAR did not reduce the socio-economic burden significantly (Figure 6-6). The effectiveness of MAR may improve under greater availability of recharge volumes albeit the karst nature of the aquifer remains a challenge.

6.3.2.2 Supply management scenarios

The S1-Sa simulations (Figure 6-5) show that the supply of an additional 60 MCM starting 2019 can reduce the probability that the aquifer salinity will exceed the 15,000 ppm (very highly saline) in 2034 from 63% (under S1) down to 32%. This also translates into a significant decrease in the associated socioeconomic burden. The probability that the cumulative socioeconomic burden will exceed the 5,000 USD per capita dropped from 60% under S1 to 25% under S1-Sa (Figure 6-6). Yet, this improvement comes with a significant investment cost (capital, maintenance and operation) adding a financial burden on the community equivalent to ~430 USD per capita (where the end year's (2034) population is estimated at 1,600,000 under the Most Probable Scenario for the calculation of cumulative cost per capita). Increasing the supply under the S1-Sb scenario, reduced the probability that the aquifer's salinity will be exceed the 15,000 ppm level from 63% under S1 down to 15% (Figure 6-5). Similarly, this reduction in salinity translates into a reduction in associated socio-economic burdens, whereby the probability that the cumulative burden by the end of the simulation period (i.e. by 2034) will exceed 5,000 USD per capita was reduced to 8% as compared to 60% under S1 (Figure 6-6). Nevertheless, these benefits come at the cost of implementing such mega projects, which has been estimated at a cumulative cost of around 820 USD per capita. This scenario seems to be very promising in terms of delaying the deterioration of the aquifer and alleviating the socio-economic burden. Comparing the actual cost of supply projects with the observed decrease in the projected salinity levels and the societal relief from salinity-induced burdens, highlights the cost effectiveness and worthiness of this project. The provision of additional water supply to reduce groundwater abstraction contributes also to the protection of the aquifer with ecological benefits.

Under worst-case conditions of climate and demand, supplying 60 MCM starting 2019 (S3-Sa) can reduce the probability that salinity will exceed the 15,000 ppm (very highly saline) by 15% as compared to the Worst-case Scenario (S3) without management actions. This slight improvement translates into a minor decrease in the cumulative socio-economic burden, with a 21% reduction in the probability that the burden will exceed 5,000 USD per capita (Figure 6-6). Under S3-Sb (Figure 6-5), the estimated probability that the average aquifer salinity in 2034 will exceed 15,000 ppm was 53%, which represents a 40% reduction in probability as compared to the no action Scenario under worst-case conditions (S3). The associated socio-economic burden was also reduced, whereby the probability that the cumulative burden per capita by the end of the simulation period will exceed 5,000 USD was around 40% as compared to 90% under S3 (a decrease of 55%) (Figure 6-6). These benefits however come with a high investment in supply projects, which translate into a cumulative cost per capita of 650 USD by 2034.

6.3.2.3 Demand management scenarios

Simulation of the impact of demand management in terms of increasing the water tariff by 150% under the conditions defined under the Most Probable scenario (S1) showed an 85% reduction in the probability that the average aquifer salinity exceeds 15,000 ppm as compared to S1 (Figure 6-5). The projected reductions in salinities minimized the socio-economic burden significantly (Figure 6-6). Even under worst-case conditions of climatic change and population increase, the increase in tariff resulted in a 66% reduction in the probability that the average aquifer salinity will exceed 15,000 ppm by 2034 as compared to S3 (Figure 6-5). Additionally, the probability that the cumulative cost burden (over 20 years) will exceed 5,000 USD per capita by 2034 was projected to decrease by 80% as compared to S3 (Figure 6-6). Increasing the tariff targets the water consumption rate in order to reduce the demand on water. However, while this directly affects the demand for both the network supply and groundwater abstraction, the caveat is that people might shift to other alternative sources (either recommended alternatives like greywater collection, rain harvesting …etc. or potentially unsustainable alternatives like water tankers, bottled water…etc. both associated with an additional cost) to meet the deficit. Hence, ensuring the success of demand management measures remains a challenge requiring awareness as well as cultural and behavioral shifts.

6.3.2.4 Value of time

The value of time was examined by delaying the implementation of supply and demand management projects by 5 years under the S1 (most probable) and S3 (worst case)scenarios. For the supply management scenarios, the S1-Sc scenario (supply of 120 MCM starting 2025) showed an increase in the aquifer salinity as compared to Scenario S1-Sb (supply of 60 MCM starting 2019, additional 60 MCM starting 2025) (Figure 6-5). As for the cumulative socioeconomic burden, it was estimated to exceed 5,000 USD per capita, at the end year, by a probability of17% as compared to the 60% probability projected under S1 and 8.5% under S1-Sb (Figure 6-6). These results reconfirm the benefits of an earlier intervention (Year 2019) and highlight the costs associated with these delays (Year 2025). Similar trends were observed under the worst-case conditions. The results from the S3-Sc scenario, reflected a 17% increase in the probability that the aquifer salinity will exceed 15,000 ppm (very highly saline) by 2034 as compared to the S3-Sb Scenario (Figure 6-5). On the other hand, the delay in project execution increased the probability that the cumulative socio-economic burden by 2034 will exceed the 5,000 USD per capita mark from 40% under S3-Sb to 51% (Figure 6-6).

Delaying the implementation of demand management by 5 years under the Most Probable scenario (S1-Db) increased the probability that the aquifer average salinity levels will exceed 15,000 ppm (very highly saline) from 38 % under S1-Da to 74 % (Figure 6-5). The delay also eroded the reductions in the socio-economic burden. The probability that the cumulative socio-economic burden per capita will not exceed the 5,000 USD mark dropped from 96 % if the project is initiated in 2019 to 76% if enforcement was delayed to 2025 (Figure 6-6). The delay of demand management under the worst-case conditions (S3-Db) resulted in even more significant losses. The probability that the salinity levels will exceed 15,000 ppm (very highly saline) by 2034 reached 67% as compared to the 30.5 % if the tariffs were reformed starting in early 2019. Additionally, the probability that the cumulative cost burden (over 20 years) will exceed 5,000 USD per capita by 2034 decreased by 34% as compared to S3, while the reduction reached 80% when the project was initiated in 2019. In short, time has a significant toll on the performance and success of both demand and supply initiatives.

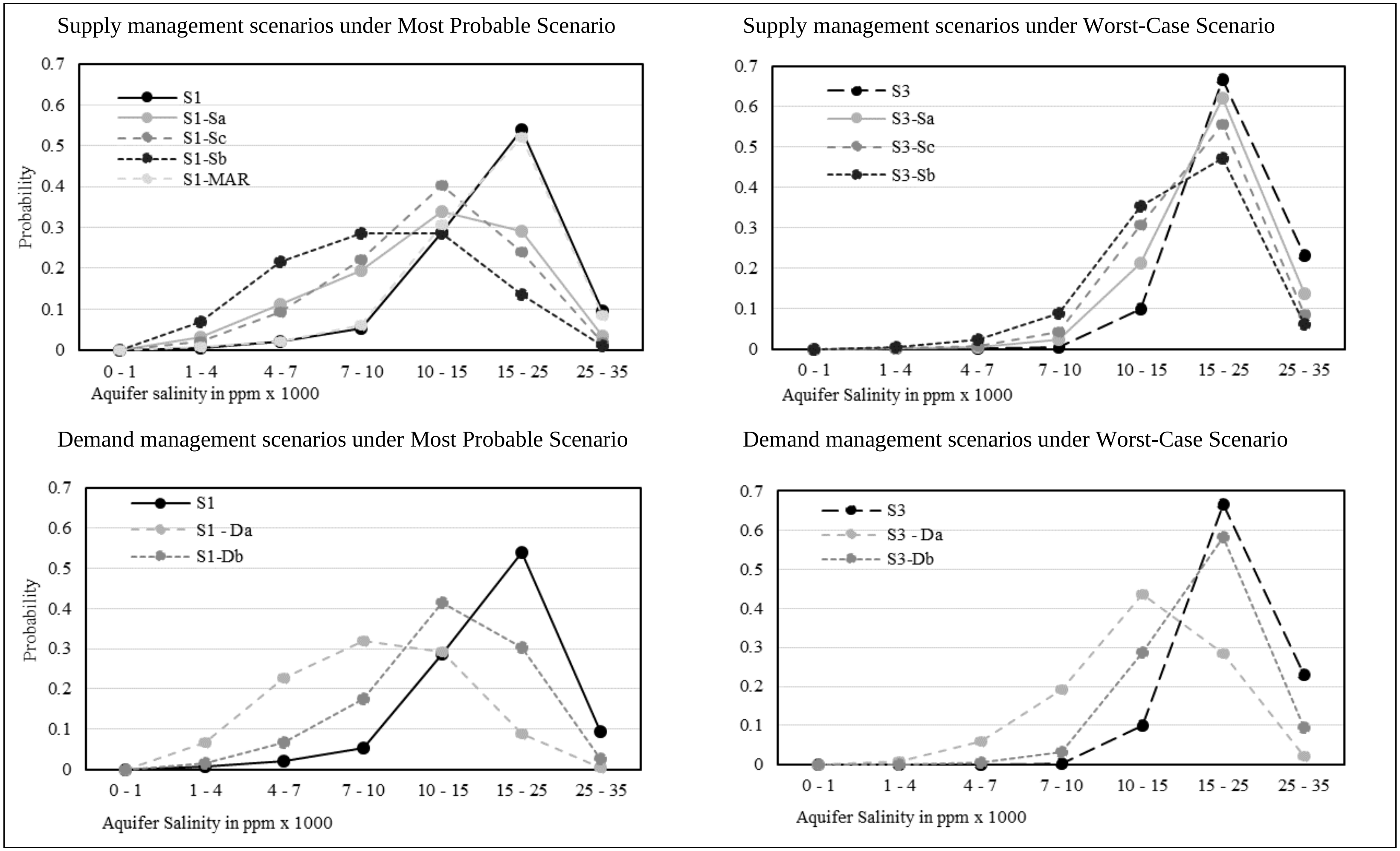

Figure 6-5 Probability of aquifer salinity (in ppm x 1000) at end year (2034) under base cases, MAR, demand and supply management scenarios; S1: Most Probable; S2: Climatic forcing; S3: Worst Case; Sa: 60MCM supplied in 2019; Sb: 60 MCM supplied in 2019 and additional 60 MCM supplied in 2025; Sc: 120 MCM supplied in 2025; MAR: Managed Aquifer Recharge in 2025; Da: demand management starts in 2019 ; Db: demand management starts in 2025

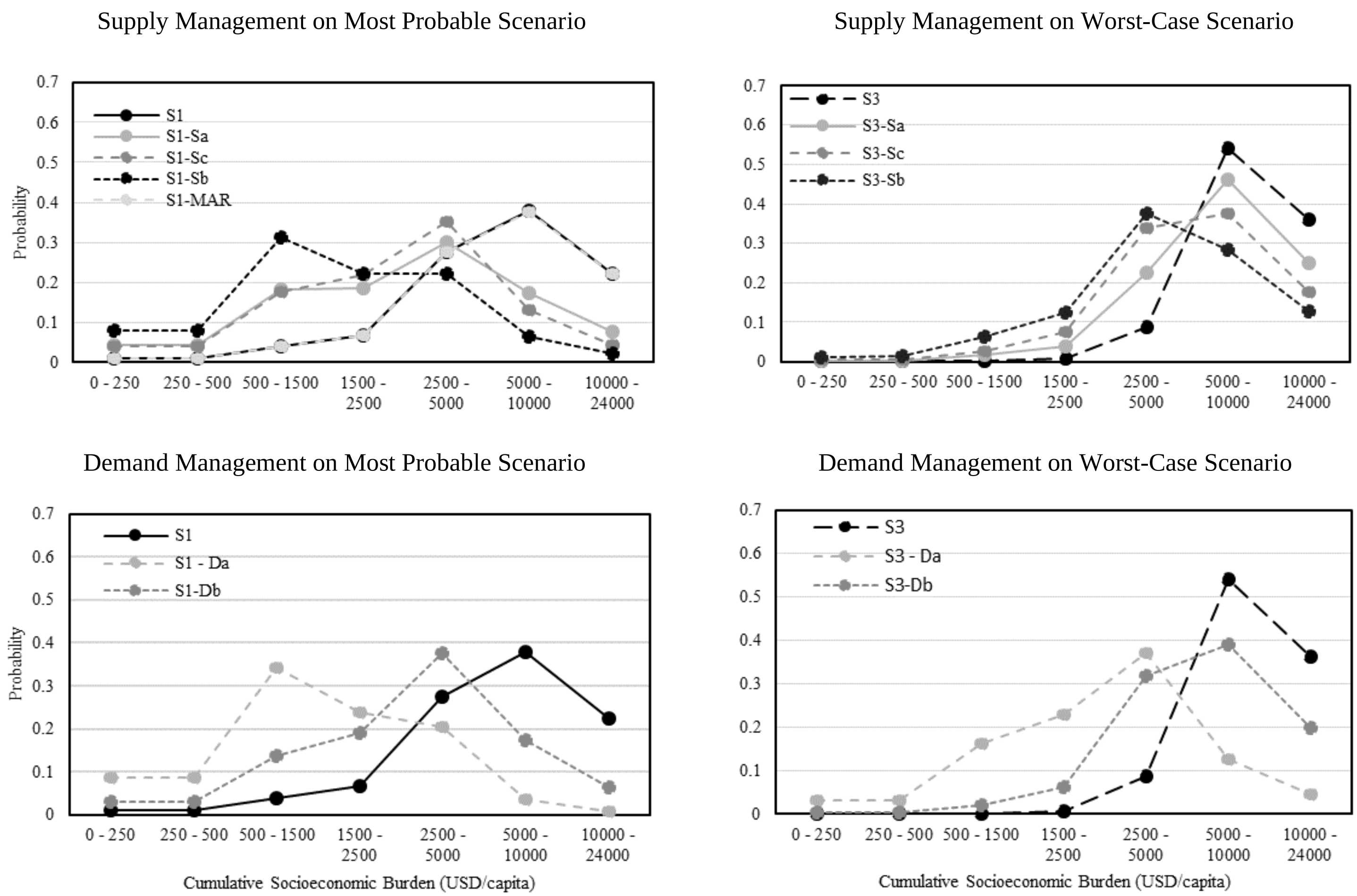

Figure 6-6 Probabilities of the cumulative socioeconomic burden (in USD per capita) at end year (2034) under MAR, demand and supply management scenarios; S1: Most Probable; S3: Worst Case; Sa: 60MCM supplied in 2019; Sb: 60 MCM supplied in 2019 and additional 60 MCM supplied in 2025; Sc: 120 MCM supplied in 2025; MAR: Managed Aquifer Recharge in 2025; Da: demand management starts in 2019 ; Db: demand management starts in 2025

6.4 Conclusion and way foreward

A first attempt at developing a decision support tool for the management of and adaptation to SWI using Bayesian networks is presented. The DBN proved effective in analyzing complex systems, while catering for the dynamics and uncertainties associated with data sparsity and imperfect knowledge. Its application on the lifecycle of SWI provided a valid representation of the interaction of multilayered factors and impacts with corresponding uncertainties and interdependence. It exhibited robustness in accommodating a series of scenarios with and without management options confirming its suitability as a decision support tool. Furthermore, its simulation results were consistent with those from a mechanistic 3D variable-density flow and solute transport model for the same aquifer (Safi et al. 2018) while offering the advantage of flexibility and transferability under an integrative platform able to compete with a data and simulation intensive 3D model to represent complex processes and reliably inform decision making in data-scarce aquifers.

The DBN results showed that while the impacts of the projected future climate change significantly increased aquifer salinity and socioeconomic burden, they proved to be secondary when compared to anthropogenic stressors (Figure 6 -7). While demand and supply management options exhibited promise in halting the progress of SWI, none could bring the system to full recovery. Demand management options promise better potential outcomes than supply scenarios but their implementation is challenging as they require much awareness as well as cultural and behavioral shifts to ensure that the poor are not disproportionately disadvantaged. Meanwhile, supply scenarios provide a faster engineered fix that often requires greater investments. As such, a combination of balanced supply and demand measures is inevitable to control SWI but in either case, implementation delays were shown to significantly reduce the cost-effectiveness of any intervention.

Future work will examine the sensitivity of the results to the discretization process with additional testing when new temporal data sets are available. Transfer to aquifers with no or early signs of salinization and/or under different use patterns (i.e. agricultural) cab also ensure wider applicability of the model.

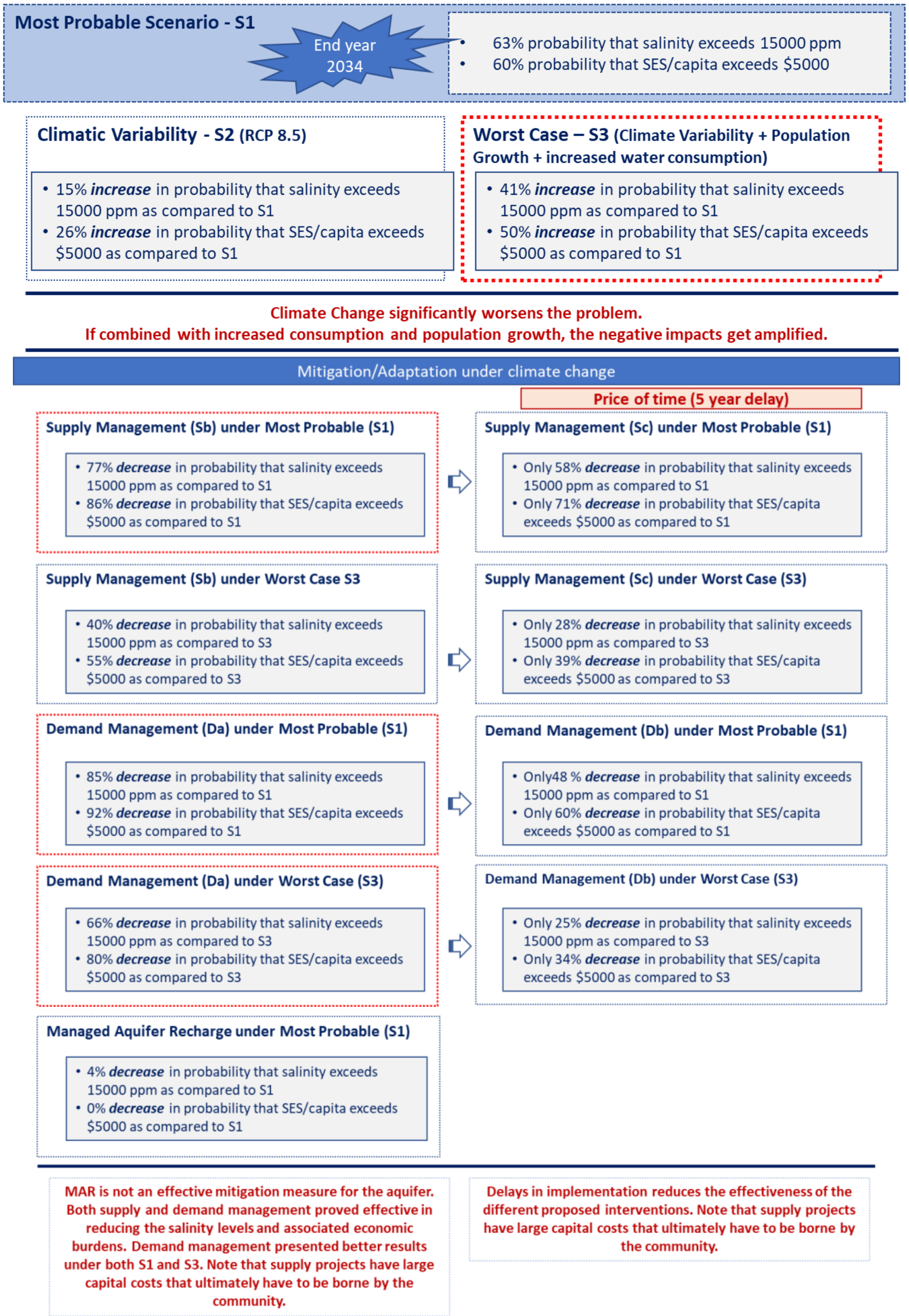

Figure 6-7 Summary findings of probability % change as compared to S1 (Most Probable Scenario)

CHAPTER 7

SUMMARY AND CONCLUSION

7.1 Summary and findings

This research is driven by the need to better understand, quantify, and predict the combined effect of climate change and anthropogenic impacts on SWI into freshwater coastal aquifers in semi-arid regions. It examines a) the quantification of the intensity, as well as the spatial and temporal extent, of SWI in aquifers along the Eastern Mediterranean, an area highly vulnerable to increased SWI, b) the evaluation of the risk of SWI due to anthropogenic drivers, taking into account current salinization rates caused by overexploitation, as well as the assessment of additional risks posed by climate induced SWI, c) the identification of currently practiced mitigation measures and adaptation strategies, d) the evaluation of the socio-economic burdens resulting from increased groundwater salinity, and e) the development of a decision support tool based on a Dynamic Bayesian Network to assess and project salinity based on anthropogenic and climatic drivers as well as to quantify the associated socioeconomic burden and evaluate potential management options.

The review of SWI along the East Med showed that aquifers are in different stages of SWI exhibiting signs of saline groundwater throughout the region with alarming rates in several eastern and south-eastern aquifers underlying dense population centers e.g. Beirut, Lebanon; Magoza, Cyprus; Gaza, Palestine and the Nile Delta, Egypt. The current status of SWI along the East Med was depicted in an illustrative atlas based on the readings of salinity indicators e.g. Cl^-, TDS and EC. In addition, the overview of adaptation strategies and mitigation measures to face SWI in the region highlighted a relatively strong adaptive capacity in Cyprus, Israel and Turkey, an emerging capacity in Egypt while Lebanon, Syria, and Palestine have weak capabilities.

A semi-quantitative Strengths, Weaknesses, Opportunities and Threats (SWOT) model was developed to estimate the risk of SWI in data scarce aquifers through characterizing the interplay of the main natural, anthropogenic, and climatic drivers in conjunction with the potential adaptation and mitigation measures and their socio-economic impacts. The model was tested with data collected from 26 coastal aquifers with varying degrees of SWI severity along the Eastern Mediterranean. The semi-quantitative SWOT model was effective in identifying aquifers at risk where the modelled results showed a statistically significant correlation with the reported seawater intrusion levels.

A framework for the assessment of SWI in coastal aquifers was developed based on the review and assessment of reported methods using a complexity-functionality matrix. The proposed framework was then applied at a pilot aquifer underlying the densely populated metropolitan of Beirut city (Lebanon) and tested by coupling the SWOT model with Multi-Attribute Decision Making (MADM) analyses to evaluate the effectiveness of the methods and identify elements of the framework. The latter consisted of hydrogeochemical metrics (Cl^-, TDS and EC levels, the seawater fraction, the piper hydro-chemical diagram, the SWI specific GQI_{SWI}, and the Stuyfzand's hydrochemical classification) coupled with geostatistical analysis to interpret complex groundwater quality data and examine the scale and magnitude of the impact of SWI and its dynamics in heterogeneous aquifers. It proved functional in synthesizing parametric results, assessing the dynamics of SWI and quantifying its potential impact, as well as providing an effective platform for informed impact assessment and planning for sustainable exploitation of coastal aquifers.

The framework was then applied at three pilot aquifer areas along the Lebanese coastline namely Tripoli, a highly urbanized and densely populated urban fabric with a small agricultural sector, Zahrani, an agricultural coastal plain and Jal elDib, a moderately urbanized suburb, besides the Beirut aquifer, where the temporal dynamics of SWI under the differing land use and land cover (LULC) patterns and water deficit conditions were assessed. While the aquifers exhibited signs of salinization, significant differences in the observed SWI were evident due to the interaction between various groundwater demand and supply factors operating under different LULC patterns. The strength of the SWI signal was correlated to the dominant LULC at each aquifer and the extent of the water deficit at each aquifer played a dominant role in explaining the occurrence and intensity of the observed SWI rates while a synergistic effect of high water demands (water deficit) and increased urbanization (land use) on the SWI was detected.

The relative impacts of anthropogenic interventions and global climate change on the dynamics of SWI were then assessed at the Beirut highly urbanized coastal aquifer for the near future using a multi-objective 3D variable-density flow and solute transport model. The results of annual simulations showed that while the aquifer system is highly sensitive to both water consumption rates and population growth rates, a ~50% increase in the rate of water consumption leads to at least four times more volumetric displacement of the freshwater-seawater interface than a similar increase in population growth rate after 20 years. Coupling of both, however, has a synergistic effect that aggravates the displacement of the freshwater-seawater interface beyond the sum of the individual impacts. Findings also showed that the sea level rise associated with climate change has less influence on the encroachment of salinity as compared to the anthropogenic abstraction. While the adaptation strategy of halting abstraction could not achieve a system-recovery or reverse the SWI damage, it succeeded in stopping the intrusion.

Placing all the puzzle pieces together, a Dynamic Bayesian Network (DBN) was then developed to account for the complex interaction of climatic and anthropogenic processes leading to SWI, while linking the severity of the SWI to the associated socioeconomic impacts and possible adaptation strategies. The objective of the DBN was to offer a simpler and reliable alternative to numerical distributive models for aquifers with data scarcity. The DBN, allowing the assessment of the temporal progression of SWI while accounting for the compounding associated uncertainties over time, was tested in the Beirut aquifer. The results show that the future impacts of climate change were largely secondary as compared to the persistent water deficit hinting towards the importance of demand management. The model shows that while both supply and demand management could halt the progression of salinity in the aquifer, the potential for reducing or reversing the salinity is still not apparent. The results also highlighted the indirect socioeconomic burden associated with adaptation strategies. Through building a robust representation of the main drivers of SWI and linking them to expected socioeconomic burdens as well as proposed management options, the developed DBN acts as an effective decision support tool that is fundamental for proper adaptation planning and can promote sustainable aquifer management. The developed DBN model also has the advantage of guaranteeing easy transferability to other similar aquifers with minimum, if any, modifications.

This research reflects an increasing salinization challenge along the Eastern Mediterranean. It hints to a bleak future awaiting the aquifers underlying the suburbs of highly urbanized cities if water shortages are not alleviated while urbanization rates continue to increase. Evidently, SWI along the Eastern Mediterranean is expected to increase under the synergistic effect of urbanization and climate change (due to potential sea level rise, reduction in precipitation and aquifer recharge). Increased SWI is expected to exacerbate the socio-economic burden to this area's vulnerable and fragile local livelihoods. Consorted efforts towards the implementation of adaptation strategies and mitigation measures are imperative for an integrated water resources management that alleviate the impacts of SWI towards sustainable aquifer management. This research contributed to the understanding of the response of coastal aquifer systems to local and global stresses as well as the role of adaptation strategies in alleviating SWI. It forms a platform for effective local adaptation planning, providing informed policy and decision making for sustainable aquifer management.

7.2 Limitations

The overarching limitation of this research is the data scarcity with limited knowledge about the complex hydrogeology, the aquifer characteristics, the saltwater-freshwater interface area, the depth of the water table, the abstraction rate…etc. This limitation, however, was turned into an incentive to ‘do more with less’ where realistic assumptions were drawn supported by literature and domain experts and where multiple approaches were undertaken to confirm and validate results. Specific limitations related to the data available, methodologies used, and models developed, include:

- Field work: field work was only limited to 3 sampling campaigns in Beirut and Zahrani aquifers targeting 2 seasons but included 7 sampling campaigns in Jal el Dib targeting all seasons. The sampling campaign in Beirut and Zahrani happened in year 2013/2014 when Lebanon was subject to a dry spell. This might have presented the SWI situation as more severe than it actually is. While such a snapshot of the SWI situation was sufficient for the purpose of this research, however it is not indicative of the long-term dynamics of the aquifer. In addition, fieldwork was limited by the accessibility to households and wells, where some well users prevented access in subsequent campaigns, as well as with the limited data that could be collected per well (depth, flow rate, year of operation…etc.).
- Data Assumptions: due to the absence of data or the inconsistency of data, assumptions were proposed and validated by domain experts at multiple instances including data related to geology and hydrogeology, water consumption rates, population and population growth rates, infiltration rates, number of wells, RO penetration rate… etc. while other parameters were recognized but scoped out of the research e.g. environmental externalities, costs associated with health impacts and agricultural impacts… etc.
- Impact of space and time: related to the limitation posed by the absence of data, it is also important to highlight that the work done on the East Med and on the Lebanese coastline, albeit with repeated sampling campaigns, represents a snapshot of the salinity status where the trend in salinity was not necessarily constructed over time and the aquifers' inherent distinctions were not considered.

- Discretization: As some nodes in the conceptual model are continuous, discretization was necessary. The evaluation of the impact of the discretization method on the results was recognized but scoped out of the study. To mitigate any shortcomings, discretization generally followed natural thresholds and thresholds reported in the literature which were later subject to an iterative process of fine-tuning so as to ensure the generation of meaningful bins able to provide insights on the data and reflect changes.
- The nomenclature of ‘Dynamic’ Bayesian Network used in the HUGIN software to refer to a Bayesian network with related variables over time slices is observed to be misleading. It can be mistakenly understood to infer that changes to CPTs and relationships are being undertaken through the time steps to predict the future while in fact these relationships and CPTs remain largely fixed. Accordingly, this is observed as a limitation of the HUGIN model where the use of the term ‘dynamic’ is to be revised to ensure a clearer distinction between the temporal progression in DBN and dynamic modeling.

7.3 Recommendations for future work

Recognizing the limitations and uncertainties associated with the assumptions put forward and the models used, and while all efforts were invested to fill the data gaps, overcome the limitations and validate the results through multiple approaches, future efforts to improve the current work and complement its findings include:

- Continuous aquifer Monitoring is indispensable along the East Med, in general, and in Lebanon, in particular, for spatial and temporal changes in groundwater quality and SWI status. Monitoring provides a better understanding of aquifers and sufficient data for model calibration, as well as analyses to inform and ensure effective management.

- Due to dynamic geochemical interactions that can be mis-interpreted in the absence of sufficient datasets, it is important to confirm the status of SWI through different means e.g. electro-sensitivity and resistivity analysis, environmental tracers i.e. isotopes, carbon source … etc.
- Better understanding of the hydrogeology is needed to guide and support future analysis of SWI. The understanding of the boundaries and the characteristics of aquifers, of the water flow within and in-between as well as the water bearing strata is indispensable to confirm our understanding and interpretation of the geology.
- The DBN could be updated to integrate the impact of sea level rise on SWI, when possible, as well as the associated impacts on community health and on the agricultural plains and produce.
- Future work could target the study of the sensitivity of the results of the Dynamic Bayesian Network to the discretization process used in order to confirm the robustness of the results in view of the selected discretization approach.
- Future work should consider backward propagation of input within the DBN, a limitation inherent to the current licenses of DBNs , which would assist in identifying the states to be targeted in order to manage salinity at an acceptable level in the future.

- The integration of decision nodes in the DBN, not possible under the current license of HUGIN, is important, once possible, to deliver an all-inclusive temporal decision support system for coastal managers.
- Future work could validate the flexibility and practicality of the transferability of this DBN to other aquifers.

Finally, the essence resides in the implementation. As this research was driven by the need to understand, quantify, and manage SWI in data scarce heterogeneous aquifers, embracing the DBN and using it to guide and inform potential decision making on coastal groundwater management puts it to the challenge and churns potential future amendments. A holistic approach to water resources management with integration of adaptation strategies and mitigation measures remains indispensable for a better future to vulnerable coastal communities.

APPENDICES

Appendix 1A .SWOT scoring

Factors	Internal									External							
Aquifer	Pop growth per km²	Pop. density (inh/km²)	Water Consumption rate (l/c/d)	Urbanization trend (%)	Dominant land Use+	Water stress index	Geology	Recharge Pathway	Management measures	Projected precipitation reduction (%)	Projected Temp. increase	Projected sea level rise (m)	GDP per capita (USD)	Stability	Political will	Internal score centered	External score centered
Turkey																	
Serik Plain	4	96	190	2.04	urban; agriculture	high stress (overexploitation)	Q,C,T	rainfall; inflows	Monitorg; Enforcemen; Demand & Supply measures; Desalination	20	3 - 4	-	10500	Stable	Strong		
	5	5	15	15	15	15	15	10	5	15	15	15	15	10	5	11.6	-0.9
Mersin	29	110	190	2.04	urban; agriculture; industrial	high stress (overexploitation)	Q, C,T	Rainfall; inflow	Monitorg; Enforcement Demand & Supply measures; Desalination	20	3 - 4	-	10500	Stable	Strong		
	10	5	15	20	15	15	15	10	5	15	15	15	15	10	5	1.6	-0.9
Silifke – Goksu	11	44	190	2.04	urban; agriculture	high stress (overexploitation)	Q, C,T	rainfall; infiltration	Monitorg; Enforcement Demand & Supply measures; Desalination	20	3 - 4	-	10500	Stable	Strong		
	10	5	15	20	15	15	15	10	5	15	15	15	15	10	5	1.6	-0.9
Hatay – Dortyol	2	250	190	2.04	agriculture	high stress (overexploitation)	Q, C	Rainfall, inflow	Monitorg; Enforcement Demand & Supply measures; Desalination	20	3 - 4	-	10500	Stable	Strong		
	5	10	15	15	10	15	10	10	5	15	15	15	15	10	5	16.6	-0.9
Syria																	
Tartous	9	500	150	1.4	urban; agriculture	high stress (16% GW deficit)	Q , C,T	rainfall; inflows	Supply management Weak enforcement	5 - 6	1 - 2.2	0.6 – 1.3	2000	War zone	Compromised		
	5	10	15	10	15	15	15	10	15	5	10	15	20	20	10	1.6	-10.9
Banyas – Amrit	4	300	150	1.4	urban; agriculture	high stress (16% GW deficit)	Q,C	rainfall; inflows; infiltration	Supply management Weak	5 - 6	1 - 2.2	0.6 – 1.3	2000	War zone	Compromised		

Factors	Internal									External							
Aquifer	Pop growth per km^2	Pop. density (inh/km^2)	Water Consumption rate (l/c/d)	Urbanization trend (%)	Dominant land Use+	Water stress index	Geology	Recharge Pathway	Management measures	Projected precipitation reduction (%)	Projected Temp. increase	Projected sea level rise (m)	GDP per capita (USD)	Stability	Political will	Internal score centered	External score centered
									enforcement								
	5	10	15	10	10	15	10	5	15	5	10	15	20	20	10	16.6	-10.9
Damsarkho	195	550	150	1.4	urban; agriculture	high stress (16% GW deficit)	Q,C,T	rainfall; infiltration	Supply management Weak enforcement	5 - 6	1 - 2.2	0.6 – 1.3	2000	War zone	Compromised		
	20	15	15	10	15	15	15	10	15	5	10	15	20	20	10	-18.4	-10.9
Al Hamidiah coast	370	500	150	1.4	urban; agriculture	high stress (16% GW deficit)	Q, C, T	rainfall; inflows	Supply management Weak enforcement	5 - 6	1 - 2.2	0.6 – 1.3	2000	War zone	Compromised		
	20	10	15	10	15	15	15	10	15	5	10	15	20	20	10	110 (1.6)	-10.9
Lebanon																	
Akkar	41	419	200	0.75	Medium agriculture	medium stress	Q, C	rainfall; inflow; infiltration	Weak enforcement Regulations exist; No monitoring; No metering; Plan in place;	4 - 11	1 - 3	0.3 - 0.6	8050	Unstable	Weak		
	10	10	15	5	15	10	10	5	15	10	15	10	15	15	15	95 (16.6)	-5.9
Jal el Dib	150	500	200	0.75	urban; agricultur; industrial	high stress	Q, C	rainfall; inflows	Weak enforcement Regulations exist; No monitoring; No metering; Plan in place;	4 - 11	1 - 3	0.3 - 0.6	8050	Unstable	Weak		
	15	10	15	5	15	15	10	10	15	10	15	10	15	15	15	110 (1.6)	-5.9
Zahrani	42	510	200	0.75	Medium agriculture	low to medium stress	Q, C	rainfall; infiltration; inflows	Weak enforcement Regulations exist; No monitoring; No metering; Plan in place;	4 - 11	1 - 3	0.3 - 0.6	8050	Unstable	Weak		
	10	15	15	5	15	10	10	5	15	10	15	10	15	15	15	100 (11.6)	-5.9
Beirut	510	20000	200	0.75	urban	extremely high stress[20]	Q, C, T	Limited	Weak enforcement Regulations exist; No monitoring; No metering; Plan in place;	4 - 11	1 - 3	0.3 - 0.6	8050	Unstable	Weak		

Factors	Internal									External							
Aquifer	Pop growth per km^2	Pop. density (inh/km^2)	Water Consumption rate (l/c/d)	Urbanization trend (%)	Dominant land Use+	Water stress index	Geology	Recharge Pathway	Management measures	Projected precipitation reduction (%)	Projected Temp. increase	Projected sea level rise (m)	GDP per capita (USD)	Stability	Political will	Internal score centered	External score centered
	20	20	15	5	20	20	15	20	15	10	15	10	15	15	15	145 (-33.4)	-5.9
Damour	17	990	200	0.75	urban; agriculture	high stress	Q, C,T	rainfall; infiltration	Weak enforcement Regulations exist; No monitoring; No metering; Plan in place;	4 - 11	1 - 3	0.3 - 0.6	8050	Unstable	Weak		
	10	15	15	5	15	15	15	10	15	10	15	10	15	15	15	120 (-8.4)	-5.9
Tripoli	107	205	200	0.75	urban	extremely high stress	Q, C	rainfall; inflows	Weak enforcement Regulations exist; No monitoring; No metering; Plan in place;	4 - 11	1 - 3	0.3 - 0.6	8050	Unstable	Weak		
	15	5	15	5	20	20	10	10	15	10	15	10	15	15	15	115 (-3.4)	-5.9
Byblos	1	370	200	0.75	urban; agriculture	low to medium stress	Q	rainfall; inflows	Weak enforcement Regulations exist; No monitoring; No metering; Plan in place;	4 - 11	1 - 3	0.3 - 0.6	8050	Unstable	Weak		
	5	10	15	5	15	10	10	10	15	10	15	10	15	15	15	95 (16.6)	-5.9
Khalde to Jiyeh	10	594	200	0.75	urban; agriculture	High stress	Q, C,T	rainfall; inflows	Weak enforcement Regulations exist; No monitoring; No metering; Plan in place;	4 - 11	1 - 3	0.3 - 0.6	8050	Unstable	Weak		
	5	15	15	5	15	15	15	10	15	10	15	10	15	15	15	110 (1.6)	-5.9
Israel and Palestine																	
Gaza	142	4500	90	3	urban	extremely high stress	Q, C	rainfall	Regulations exist; damaged infra	15 – 20	1.5 - 2.5	-	3000	War zone	Weak		
	15	20	5	15	20	20	10	15	15	10	10	15	20	20	15	165 (-53.4)	-35.9
Coastal Aquifer	19	1010	250	1.5	urban	extremely high stress	Q, C	rainfall; inflows MAR	Demand & Supply managemen; monitoring; Desalination	10 – 20	1.5	-	40000	Very stable	Strong		

Factors	Internal									External							
Aquifer	Pop growth per km^2	Pop. density (inh/km^2)	Water Consumption rate (l/c/d)	Urbanization trend (%)	Dominant land Use+	Water stress index	Geology	Recharge Pathway	Management measures	Projected precipitation reduction (%)	Projected Temp. increase	Projected sea level rise (m)	GDP per capita (USD)	Stability	Political will	Internal score centered	External score centered
	10	20	20	10	20	20	10	5	5	10	10	15	5	5	5	145 (-33.4)	24.1
Egypt																	
Ras el Hekmeh	271	109	280	2	urban	Medium	C, T	rainfall	Demand & Supply measures; Desalination	-20- 36	1.3-2.2	0.59	2400 – 6000	Stable	Strong		
	20	5	20	15	15	10	15	15	5	10	10	20	15	10	5	120 (-8.4)	-5.9
Nile Delta	50	1000	280	2	urban; agriculture	Medium	Q, C	rainfall; infiltration	Demand & Supply measures; Desalination	-20- 36	1.3-2.2	0.59	2400 – 6000	Stable	Strong		
	15	15	20	15	20	10	10	10	5	10	10	20	15	10	5	125 (-13.4)	-5.9
North Sinai	44	15	280	2	urban	Medium	Q	rainfall	Demand & Supply measures; Desalination	-20- 36	1.3-2.2	0.59	2400 – 6000	Stable	Strong		
	10	5	20	15	15	10	5	15	5	10	10	20	15	10	5	110 (1.6)	-5.9
Cyprus																	
Ezousa	37	130	200	0.75	urban; agriculture	high stress	Q,C	rainfall; inflows; MAR	Demand & Supply management monitoring; Desalination	0 – 10	1 – 2.5	-	25000	Very Stable	Strong		
	10	5	20	5	15	15	10	5	5	5	10	15	5	5	5	100 (11.6)	29.1
Akrotiri	10	130	200	0.75	urban; agriculture	high stress	Q, C	rainfall; inflows; MAR	Demand & Supply management monitoring; Desalination	0 – 10	1 – 2.5	-	25000	Very Stable	Strong		
	10	5	20	5	15	15	10	5	5	5	10	15	5	5	5	95 (16.6)	29.1
Kiti	10	130	200	0.75	urban; agriculture	high stress	Q,C	rainfall; inflows	Demand & Supply management monitoring; Desalination	0 – 10	1 – 2.5	-	25000	Very Stable	Strong		
	10	5	20	5	15	15	10	10	5	5	10	15	5	5	5	95 (16.6)	29.1
Guzulyurt	0.2	130	200	0.75	urban; agriculture	high stress	C,T	rainfall; inflows	Demand & Supply management monitoring; Desalination	0 – 10	1 – 2.5	-	25000	Very Stable	Strong		
	5	5	20	5	15	15	15	10	5	5	10	15	5	5	5	105 (6.6)	29.1

Factors	Internal									External							
Aquifer	Pop growth per km^2	Pop. density (inh/km^2)	Water Consumption rate (l/c/d)	Urbanization trend (%)	Dominant land Use+	Water stress index	Geology	Recharge Pathway	Management measures	Projected precipitation reduction (%)	Projected Temp. increase	Projected sea level rise (m)	GDP per capita (USD)	Stability	Political will	Internal score centered	External score centered
Girne	2	130	200	0.75	urban; agriculture	high stress	C, T	rainfall; inflows	Demand & Supply management monitoring; Desalination	0 – 10	1 – 2.5	-	25000	Very Stable	Strong		
	5	5	20	5	15	15	15	10	5	5	10	15	5	5	5	110 (1.6)	29.1
															Total Score	2901.8	1926.8
															Mean Score	111.607	74.1071

Appendix 2A. Statistics for Beirut Aquifer

Summary statistics for ionic changes and other indices

	June (early dry)			October (Late dry)			April (Late wet)		
	Min	*Max*	*Mean*	*Min*	*Max*	*Mean*	*Min*	*Max*	*Mean*
f_{sea}	0.005	0.652	0.118	0.0052	0.879	0.159	0.0024	0.947	0.222
ΔNa^{+}	-1632.0	723.6	-297.6	-1398.2	611.0	-271.2	-3744.9	957.3	-529.9
ΔMg^{2+}	-275.9	652.7	28.0	-289.9	334.1	-12.2	-368.7	1106.3	88.1
ΔCa^{2+}	-36.3	1126.3	155.4	-58.9	874.8	107.9	-103.1	893.2	108.4
ΔK^{+}	-276.9	9.0	-37.4	-157.0	27.5	-30.2	-183.3	310.0	-20.5
ΔSO_4^{2-}	-489.4	333.2	-64.8	-2606.9	915.4	-157.4	-1621.9	984.1	-151.7
ΔHCO_3^{-}	-197.3	155.2	-59.9	-295.8	143.2	-36.0	-255.8	153.6	-23.3
CAI	-0.114	1.2	-3.5	-0.424	0.947	0.368	-1.94556	0.8	0.18
BEX	-46.3	43.8	-3.5	-40.3	38.3	-4.2	-140	53.7	-5.3
BEX with dolomite	-62.4	46.4	-9.5	-53.3	43.1	-7.1	-139.6	70.1	-16.4

Appendix 2B. Scatter plot of log-relationships

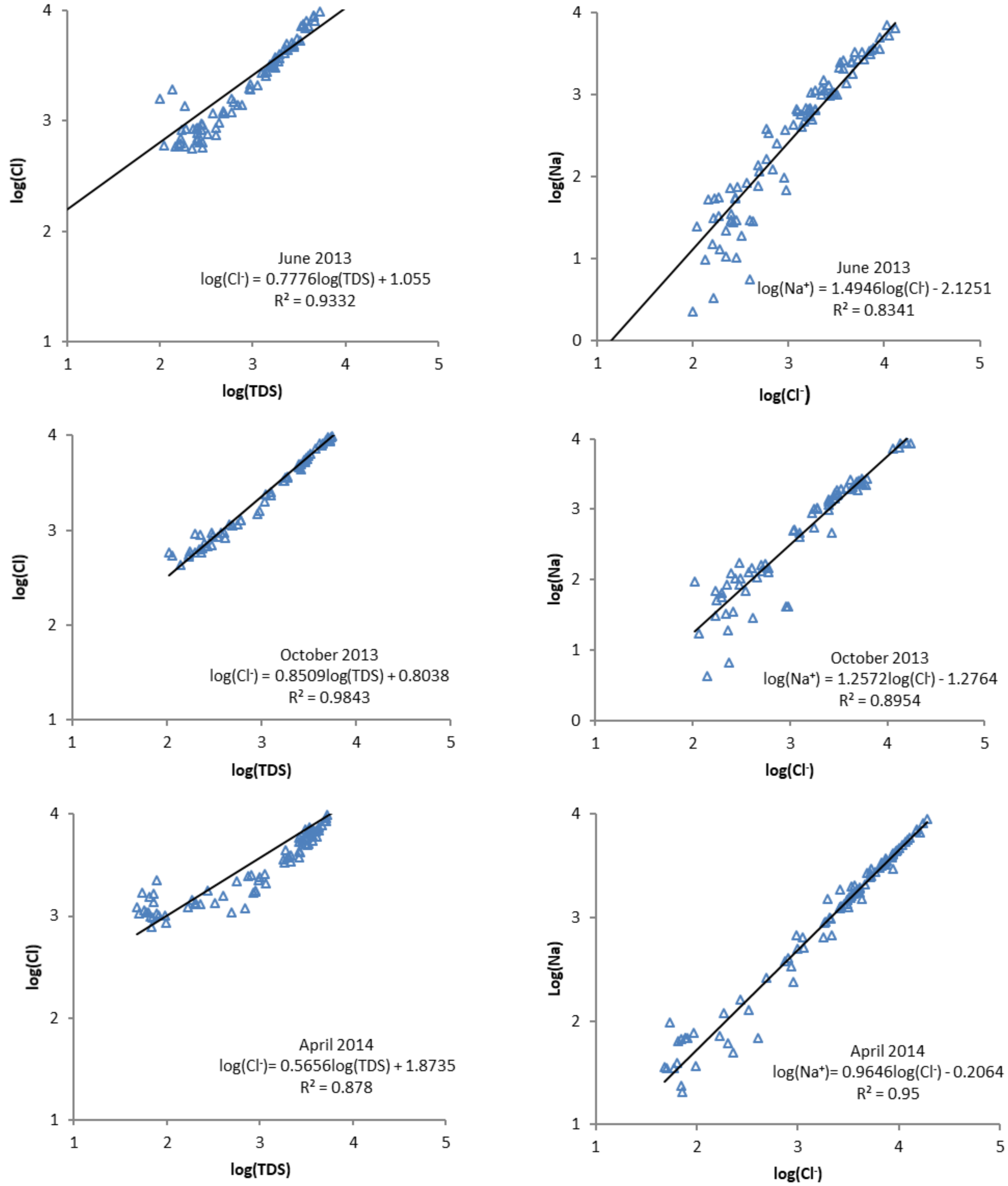

Appendix 3A. Descriptive statistics for the highly urbanized city – Tripoli Aquifer A

Season / *Parameter	Wet season (June) 2007 (n=60)				Dry season (October) 2007 *(n=60)*				Threshold (WHO 2011)
	Min	*Max*	*Mean*	*SD*	*Min*	*Max*	*Mean*	*SD*	
pH	NA	NA	NA	NA	NA	NA	NA	NA	6.5-8.5
Electric Conductivity EC	NA	NA	NA	NA	NA	NA	NA	NA	
Total dissolved Solids TDS	209	3420	631	517	270	3460	657.4	573.3	600
Ca^{2+}	47	425	121	65	47	471	140	86	300
Mg^{2+}	14	146	43	22.75	0	132	16.78	19.68	300
Total Hardness TH	224	1661	480	239	172	1720	419	277.4	
Na^{+}	17	166	58	44.3	25	1099	115	175.3	200
K^{+}	NA	NA	NA	NA	NA	NA	NA	NA	300
Cl^{-}	29	1610	212	244.5	33	1950	225.5	352	300
CO_3^{2-}	NA	NA	NA	NA	NA	NA	NA	NA	
HCO_3^{-}	NA	NA	NA	NA	NA	NA	NA	NA	
NO_3^{-}	6.4	87	34	16.8	9.9	98.4	34.8	19.26	50
SO_4^{2-}	0	370	50.7	67.8	1	580	65.2	87.82	250
Ionic ratios									*Criteria*
Na^{+}/Cl^{-}	0.159	2.84	0.52	0.37	0.1805	13.04	1.137	1.617	≤0.86
Cl^{-}/HCO_3^{-}	NA	NA	NA	NA	NA	NA	NA	NA	20-50
Mg^{2+}/Ca^{2+}	0.172	1.526	0.64	0.288	0	1.017	0.205	0.18	4.5-5.2
Br^{-}/Cl^{-}	NA	NA	NA	NA	NA	NA	NA	NA	0.0015
$Ca^{2+}/(HCO_3^{-}+SO_4^{2-})$	NA	NA	NA	NA	NA	NA	NA	NA	>1
SO_4^{2-}/Cl^{-}	0	0.82	0.173	0.153	0.0136	2.68	0.338	0.438	0.103
$GQI_{generalized}$	60.3	95.4	88	7.19	58.2	95	87.15	9	
GQI (w/o NO_3^{-},TC,FC)	57.57	87.57	74.7	8.35	44.6	86.99	67.5	9.78	
f_{sea}	0.00144	0.08	0.0105	0.0122	0.0016	0.097	0.0112	0.0175	
$GQI_{Saltwater\ Intrusion}$	70	95	82.8	2.67	60	90	79.5	3..88	<75

All values in mg/l except pH and EC (µs/cm); Parameters in ratios expressed in meq/l; (a)Misstear *et al.* 2006; (b) NA = Not available.

Appendix 3B. Descriptive statistics for the highly urbanized city – Jal Dib Aquifer B

*Parameter/Season	Dry season (October) 2012 (n=25)				Wet season (June) 2013 (n=29)				Dry season (October) 2013(n=27)				WHO Threshold (2011)
	Min	*Max*	*Mean*	*SD*	*Min*	*Max*	*Mean*	*SD*	*Min*	*Max*	*Mean*	*SD*	
pH	6.84	7.29	7	0.111	6.63	7.22	6.9	0.145	6.57	7.44	6.85	0.1788	6.5-8.5
Electric Conductivity EC	767	5370	2090	990.2	666	5820	1905	940	816	4970	1823.4	985.63	
Total Dissolved Solids TDS	384	2690	1044.5	496.36	545	4024	1427.3	637.196	659	3486	1369.59	676.39	600
Ca^{2+}	73.74	176.35	114.2	26.03	80.96	248.5	169.47	43.636	20.04	388.776	136.865	95.5	300
Mg^{2+}	18.94	98.17	50	20.9	26.97	245.43	101.48	40.132	9.23	177.39	98.082	41.125	300
Total Hardness TH	287	844	491.1	123.4	313	1630	840.45	219.57	500	1010	745.11	144.78	
Na^{+}	56.13	913.99	286.85	185.36	9.48	1034	189.95	212.89	8.15	1737.98	520.44	510.03	200
K^{+}	3.2352	18.525	6.795	3.021	1.4	24.13	5.53	3.999	1.4146	14.623	5.281	2.545	300
Cl^{-}	145	2442.5	630.7	439.65	115	182	477.9	324.09	180	1670	546.481	327.01	300
CO_3^{2-}	0	0	0	0	0	0	0	0	0	0	0	0	
HCO_3^{-}	239.8	339	310.35	20.34	238.4	3718	306.75	30.208	268.8	339.4	293.23	13.54	
NO_3^{-}	10.2	25.5	16.39	3.267	8	52.4	19.17	8.68	11.2	45	18.38	7.506	50
SO_4^{2-}	12	240	93.92	41.4	5	300	98.61	70.7118	32.5	330	123.79	59.9	250
Ionic Ratios													*Criteria*
Na^{+}/Cl^{-}	0.4935	1.2119	0.7137	0.2022	0.03	2.93	0.61	0.58	0.0393	5.922	1.493	1.4812	≤0.86
Cl^{-}/HCO_3^{-}	0.778	14.542	3.545	2.6302	0.65	9.83	2.67	1.759	1.0484	9.681	3.205	1.9219	20-50
Mg^{2+}/Ca^{2+}	0.3731	1.8481	0.7443	0.3444	0.38	2.13	1.04	0.4238	0.0296	13.743	2.5733	3.0272	4.5-5.2
Br^{-}/Cl^{-}	0	0.0156	0.00247	0.00291	0.0002	0.0027	0.0012	0.0005	0	0.00287	0.00143	0.00068	0.0015
$Ca^{2+}/(HCO_3^{-}+SO_4^{2-})$	0.543	1.088	0.8088	0.1487	0.74	2	1.22	0.3252	1.843	29.853	15.853	8.8317	>1
SO_4^{2-}/Cl^{-}	0.0612	0.1719	0.1183	0.03013	0.03	0.36	0.15	0.084	0.0843	0.5136	0.1873	0.0851	0.103
$GQI_{generalized}$	47.147	78.9	61.23	6.53	48.73	77.54	61.7	6.837	42.86	69.8	57.529	7.713	
GQI (w/o NO_3^{-},TC,FC)	56.365	91.27	76.21	7.068	51.12	91.44	76.28	8.195	56.31	85.93	73	9.193	
f_{sea}	0.0071	0.12	0.0314	0.02188	0.0057	0.0906	0.0238	0.0161	0.00895	0.0831	0.0271	0.0162	
$GQI_{Saltwater\ Intrusion}$	52.81	80.695	66.183	5.1087	58.02	85.93	74.39	6.834	55.869	81.76	67.895	7.763	<75

All values in mg/l except pH and EC (µs/cm); Parameters in ratios expressed in meq/l; [(a)]Misstear *et al.* 2006; [(b)] NA = Not available.

Appendix 3C. Descriptive statistics for the highly urbanized city – Beirut Aquifer C

Season / *Parameter/	Wet season (June) 2013 (n=92)				Dry season (October) 2013 *(n=71)*				Wet season (April) 2014 (n=113)				Threshold (WHO 2011)
	Min	*Max*	*Mean*	*SD*	*Min*	*Max*	*Mean*	*SD*	*Min*	*Max*	*Mean*	*SD*	
pH	6.4	8.2	7	0.3	6.5	7.73	7.045	0.313	6.71	8.03	7.11	0.223	6.5-8.5
Electric Conductivity EC	908	47106	9504	10468	740.6	65047	12008	15905	1550	65565	16391	15666	
Total Dissolved Solids TDS	560	23320	4610	5088	425.7	31460	5943.8	7709.9	390	32220	8389	7838.5	600
Ca^{2+}	56	1362	282.7	212.7	32	1190	249.3	222.2	14.4	1126.3	270.7	196.11	300
Mg^{2+}	19.4	1297.6	229.9	213.4	14.82	1129.95	246.8	261	11.9	1883.3	431.7	430.3	300
Total Hardness TH	450	8740	1651.5	1267	336	7620	1637.6	1548.2	131	10200	2451.8	2136	
Na^{+}	2.27	7000	1132.5	1519	4.24	10561	1629.3	2472.5	8.83	9315	2103.3	2092.4	200
K^{+}	0.534	212.3	19.7	35	0.877	328.2	45.3	76	1.9	638.3	83.69	104.9	300
Cl^{-}	100	13080	2358	2818.7	105	17670	3203	4312.3	47.65	19030	4453.5	4422.1	300
CO_3^{2-}	0	1.02	0.019	0.132	0.13	25.6	0.98	4.44	0	0	0	0	
HCO_3^{-}	141.8	493	258.6	65	34.4	460.4	274.8	73.7	76.4	490	276.15	69.3	
NO_3^{-}	2	219	39.8	30.6	1.7	66.5	27	16.85	0.8	84.8	30.8	17.12	50
SO_4^{2-}	7	2200	391	477	7	2900	418.6	606.2	7	2750	583.85	592	250
Ionic Ratios													Criteria
Na^{+}/Cl^{-}	0.02	1.09	0.529	0.0227	0.044	0.99	0.617	0.273	0.068	1.65	0.7875	0.30	≤0.86
Cl^{-}/HCO_3^{-}	0.778	122.17	18	1.92	0.508	162.8	24.38	38.25	0.281	178.5	31.76	36.8	20-50
Mg^{2+}/Ca^{2+}	0.078	4.65	1.47	0.886	0.147	5.3	1.74	1.08	0.1758	13	2.5	1.91	4.5-5.2
Br^{-}/Cl^{-}	0.017	0.00014	0.0027	0.0003	0.00445	0.00007	0.00117	0.0007	0.005	0.000018	0.0008	0.0009	0.0015
$Ca^{2+}/(HCO_3^{-}+SO_4^{2-})$	0.315	15.3153	1.6168	0.146	0.298	10.187	1.3	1.597	0.1778	4.369	0.908	0.638	>1
SO_4^{2-}/Cl^{-}	0	0.803	0.14	0.0009	0.0345	0.7	0.13	0.111	0.018	10.5	0.265	0.995	0.103
$GQI_{generalized}$	25.2	83.67	53.63	1.195	21.276	83.364	52.26	15.46	19.74	83.69	46.55	15.46	
GQI (w/o NO_3^{-},TC,FC)	20.24	89.63	61.27	1.61	17.794	91.747	60.1	21.53	18.2	91.18	51.36	22.02	
f_{sea}	0.005	0.652	0.118	0.011	0.0052	0.879	0.159	0.214	0.0024	0.947	0.222	0.22	
$GQI_{Saltwater\ Intrusion}$	24.13	86.084	62.74	1.212	11.252	89.526	59.01	18.65	8.184	86.9	54	17.82	<75

All values in mg/l except pH and EC (µs/cm); Parameters in ratios expressed in meq/l; [(a)]Misstear *et al.* 2006; [(b)] NA = Not available.

Appendix 3D. Descriptive statistics for the highly urbanized city – zahrani Aquifer D

Parameter / Season	Dry season (October) 2013 (n=59)				Wet season (May) 2014 (n=60)				Dry season (October) 2014 (n=55)				Irrigation Threshold[a]	WHO Threshold
	Min	*Max*	*Mean*	*SD*	*Min*	*Max*	*Mean*	*SD*	*Min*	*Max*	*Mean*	*SD*		
pH	6.58	7.55	6.93	0.2	6.37	7.38	6.95	0.183	6.8	7.67	7.11	0.19	6.5-8.4	6.5-8.5
Electric Conductivity EC_w	353	2510	1005	408.4	506	4288	1159	603	470	2506	1,054.6	469.0	700	
Total Dissolved Solid	552	3111	1075.65	416.84	375	2530	903	434.66	409	2250	789.5	304.6		600
Ca^{2+}	42.48	685.36	158.32	95.49	46.49	642.88	126.1	78.88	47.29	607	138.1	83.8	NA (b)	300
Mg^{2+}	8.505	303.75	71.96	55.64	19.2	376.65	53.52	47.84	7.53	103	37.8	15.9	NA	300
Total hardness TH	283	1990	691.1	336.83	279	1876	535.15	289.6	267	1726	500.3	223.3	NA	
Na^+	8.77	584.51	152.47	167.7	4.07	279.81	73.2	59.8	5.04	149.23	34.3	29.6	69	200
K^+	0.41	33.29	3.615	4.853	0.66	39.12	5.0	6.3	0.77	18.76	3.7	3.5	NA	300
Cl^-	82	835	293.86	159.2	82	820	156.3	140.5	32.5	667	168.2	142.9	107	300
CO3	0	12.4	0.210	1.614	0	0	0	0	0	0	0	0		
HCO_3	166.2	403.4	282.31	41.97	213.2	463.8	318	43	225.8	385.4	277.2	36.0	91.5	
NO_3^-	0.8	123.6	80.6	290.32	1.4	97	38	414.46	3.1	119.3	45.3	26.3	5	50
SO_4^{2-}	1	1800	100.14	238.64	3	1675	89.22	214.7	9	1200	81.5	158.2	NA	250
Br^-	0	3.9	1.13	0.804	0	3.35	0.9	0.536	0.18	27.14	2.9	3.8	Na	
Ionic ratios														*Criteria*
Na^+/Cl^-	0.0587	6.2	0.98	1.29	0.0348	4.7	0.91	0.69	0.1036	1.5776	0.4	0.32		≤0.86
Cl^-/HCO_3^-	0.445	5.545	1.81	0.992	0.1727	5.3	0.86	0.844	0.216	4.328	1.057	0.933		20-50
Mg^{2+}/Ca^{2+}	0.0963	5.507	0.965	0.975	0.17	4.84	0.81	0.654	0.0694	1.736	0.55	0.3128		4.5-5.2
Br^-/Cl^-	0	0.0078	0.0021	0.0017	0	0.0198	0.00374	0.00326	0.0012	0.082	0.00948	0.01217		0.0015
$Ca^{2+}/(HCO_3^-+SO_4^{2-})$	0.3069	3.928	1.31	0.71	0.3538	2.343	0.94	0.349	1.0723	13.4	7.236	3.657		>1
SO_4^{2-}/Cl^-	0.0027	5.53	0.3166	0.7469	0.029	2.41	0.445	0.4623	0.0353	13.813	0.666	1.8476		0.103
$GQI_{generalized}$	46.36	81.49	62.01	6.82	52.91	78.38	67.06	6.65	51	85.26	64.85	7.113		
GQI (w/o NO_3^-,TC,FC)	62.01	90.55	80.8	6.23	57	95.18	87.25	6.32	69.06	94.39	87.25	5.13		
f_{sea}	0.0041	0.0415	0.01462	0.0079	0.0014	0.04	0.01	0.0069	0.001617	0.0332	0.0083	0.00712		
$GQI_{Saltwater\ Intrusion}$	64.34	85.49	75.8	5.12	69.31	92.81	82.17	5.385	72.83	90.8	82.22	4.545		<75

All values in mg/l except pH and EC (µs/cm); Parameters in ratios expressed in meq/l; [(a)]Misstear *et al.* 2006; [(b)] NA = Not available.

Appendix 4A. DBN Model Components

Climate change component: Climatic change scenarios from global circulation models (IPCC 2013) particularly the RCP 4.5 (developed by MiniCAM modeling team (Clarke et al., 2007)) and the RCP 8.5 (developed by MESSAGE modeling team (Riahi et al., 2007)) were defined in this component. Data from downscaled climate change models, relevant to the study area, including the PRECIS (Providing Regional Climates for Impacts Studies) model (SNC 2011; TNC 2016) as well as the dynamically downscaled HiRAM-WRF model outputs (El-Samra et al. 2016) were used to populate the nodes for precipitation, temperature and evapotranspiration.

Demographic component: The relationships in this component are based on the direct associations between the population and its growth rate. These two nodes were used to estimate water demand as a function of the per capita consumption rate. The volume of water deficit per year was estimated by subtracting the demand from the available supply. The node representing the consumption rate was defined by two factors, namely demand management (i.e. tariff restructuring) and ambient temperature. The impact of each factor on the consumption rate was assumed to be independent. Changes in consumption as a function of the variations in both factors (tariff and temperature) was based on the available literature. Several studies have reported that the average elasticity of water consumption ranges between -0.39% to -0.1 for every 1% increase in tariff rate (Whitcomb, 2005, Herrington, 2006). We assumed an elasticity of -0.245% for every 1% increase in tariff. On the other hand, an average increase of 2% in water consumption was assumed for every 1°C increase in temperature (Jarboo & Al-Najar 2015; Goodchild 2007; Dowing et al. 2003; Herrington, 1996).

Hydrological component – freshwater recharge: This component represents the total recharge of freshwater incoming into the aquifer. Recharge can occur either through direct infiltration from the overlaying surface or from lateral flow from nearby aquifers. The direct infiltration was estimated by multiplying the 'effective infiltration' with the 'pervious area' of the study area. The 'effective infiltration' was thus estimated as the difference between the rainfall and the sum of the runoff and the evapotranspiration (assumed at 20% and 35% of rainfall respectively based on data concurred by expert interviews) (Eq. (1)).

$Re = Ra - Ev - Ru*PA$ (Eq. 1)

Where *Re* is the recharge in m^3/yr, *Ra* is the rainfall in mm/yr, *Ev* is the evapotranspiration in mm/yr, *Ru* is the runoff in mm/yr, and *PA* is the pervious area in m^2.

With regards to lateral flow, it was defined by the balance between the available stock, recharge, and abstraction at the aquifers that are hydrogeologically connected to the study area. Previous studies have reported that the lateral flow to the Beirut aquifer was limited to the Hazmieh aquifer, which is located along the south eastern boundary of the study area; yet the volume of recharge has not been quantified (Safi et al. 2018; El-Fadel et al. 2015). For this purpose, a mass balance model was constructed for the Hazmieh aquifer to quantify the volume of the lateral flow. The model accounted for population growth, changes in pervious areas, water consumption and demands as well as the abstraction rates in the contributing aquifer. The resultant lateral flow volume was assumed to be the difference between recharge to and abstraction from the Hazmieh aquifer. The related parameters were based on the work undertaken by El-Fadel et al. (2015). The lateral flow model was refined with feedback from expert interviews. Similarly, prior distributions on the contributing recharge area, infiltration rate, and the abstraction rate were based on expert interviews. The population growth rate and the consumption rates in the Hazmieh Aquifer were assumed to be similar to Beirut.

Hydrological component – salinity: The salinity in the aquifer was estimated based on a black box solute mass balance model constructed to represent the combined impacts of recharge, abstraction, and storage on the salinity of the Beirut aquifer. The mass balance equation is presented in Eq. (2).

$$C_t = (C_i * V_i + C_R * V_R - C_i * V_A + C_s * V_s)/(V_i * 1000) \quad \text{(Eq. 2)}$$

where C_t is the aquifer salinity at the end of a time step; C_i is aquifer salinity in the previous time step; C_R is the salinity of the recharged water (fixed at 6 mg/l); C_S is the salinity of seawater (fixed at 35,000 mg/l of TDS); V_i is the aquifer volume; V_R is the recharge volume; V_A is the abstracted volume of groundwater; and V_S is the volume of seawater inflow. All concentrations are in mg/l (ppm) of TDS and all volumes are in MCM. V_i was calculated based on the aquifer characteristics i.e. area of the aquifer, thickness (limited to the top 100 m, as this is the zone tapped by wells) and a porosity of 0.3 (Ukayli, 1971). V_a was estimated as the volume to meet the deficit in demand after accounting for alternative supplies (i.e. the volume of water provided through water tankers). Hence, V_A is calculated as the difference between the total water deficit and the volume of water being transported by water tankers. The volume delivered by water tankers was defined to be dynamic in time by allowing for changes in the "groundwater abstraction reduction" node. This node was defined to reduce pumping as the salinity in the aquifer increases. Abstraction reductions have been observed in the study area with people abandoning their wells and switching to the purchase of water tankers when the salinity of their wells increased above a certain threshold. Abstraction reduction was not allowed to reach 100%, as certain segments of the population maintain their pumping rates and invest in expensive treatment options. Note that the 'abstraction rate' node is presented as a function of the previous salinity of the aquifer based on field survey data and further validation. V_S was estimated as the difference between V_R and V_A; thus it assumes that any volumetric deficit in the water within the aquifer will be replenished by intruding seawater.

Socioeconomic component: The socioeconomic burden on the community was calculated as the sum of the costs associated with the use of advanced water treatment technologies (mainly reverse osmosis (RO)), the purchase of water through tankers as an alternative water source, and the damages incurred to installations due to the use of saline water. The socioeconomic burden was expressed both at the city level (cumulative burden in USD) and in terms of cumulative burden per capita (USD/capita). The cumulative socioeconomic burden per capita expresses the burden to the population by the end year (2034) over the whole simulation period. The cost (USD) of adopting RO in Beirut was assumed to be a function of the RO treatment cost (in USD/m^3) and the volume (m^3) of water being desalinated. Treatment cost was defined to be a function of salinity level, while the volume of water that is desalinated was defined as a function of the RO penetration rate in the city (i.e. % of buildings with RO) and the volume of groundwater abstracted. RO penetration itself was defined to be a function of the RO price and the salinity levels. This reflect that a household's decision to invest in RO will probably be a function of its ability to tolerate the elevated salinity and the affordability of treatment. The cost (USD) of water tankers was defined as a function of the tanker price (in USD/m^3) and the volume (m^3) of water supplied by tankers; the latter is a function of the water tankers' penetration rate and the existing water deficit. The probabilities on the RO price, RO penetration rate, well penetration rate, and the tanker price nodes were populated based on field surveys and expert interviews. The installation damages node was defined as a function of the aquifer salinity and the percentage of people using the saline water without RO treatment. The relationship between salinity and installation damages was based on a linear regression model developed by Alameddine et al. (2018) based on field data collected in the study area and modified for purpose of this BN to reflect the salinity interval between 1000-35000 ppm, Eq. (3). No damage was assumed to happen below 1000 ppm:

$DC = 23.5 * \log S - 140.4 \qquad 1000 < S < 35000\ ppm$ (Eq. 3)

Where *DC* is the damage cost in MUSD/yr, *S* is the salinity in ppm.

Management component: This component accounts for the adaptation strategies and mitigation measures that could be taken by the government to properly manage supply and demand in Beirut city. It also accounts for the associated costs of these interventions. We accounted for the adaptation strategies and mitigation measures that were proposed by the government (MOEW 2010). These include a set of supply management projects that aim to provide additional "new out of basin" water to the study area. These include the Greater Beirut Water Supply Project (GBWSP) (Phase I of expected to augment Beirut with 60 MCM starting 2019 and Phase II that will provide an additional 60 MCM starting 2025) and a managed aquifer recharge scheme through the injection of (3.5 MCM/yr) treated wastewater in the aquifer of interest. The demand management intervention was solely assessed in terms of increasing water tariffs in order to reduce consumption. In addition to these projects, we assessed the option of constructing a central desalination plant at the city-scale with an output equivalent to the 120 MCM supply expected by the GBWSP. Data (costs, capacities, timeline) on the planned infrastructure supply projects were collected from official reports by governmental and international institutions and published studies (WB, 2017, MOEW 2010; Ray 2005; Yamout & Fadel 2005). The costs include the annual and cumulative costs in USD/m^3 and the cumulative cost per capita of the construction, installation, operation and maintenance of the government proposed projects as detailed in Table 1 (Saidy 2016; Ray 2005). The cumulative cost per capita expresses the cumulative cost to the population at the end year (2034) from the cumulative costs of the project over the whole simulation period. All projects are associated with environmental externalities, which further increase their costs. Such externalities differ between desalination plants (brine disposal, land use, intensive energy use) and inter-basin infrastructure projects (social displacement, high capital investment costs, long execution period, lack of immediate benefits, potential negative impact on the survival and livelihoods of inhabitants in the affected area, cross-governate competition over available water resources, ecological modification of the river, obstructed development in downstream communities) (Dar Al Handasah, 2014). All adopted costs, except for desalination, excluded the cost of environmental externalities and were adjusted to year 2014, assuming a 3% annual inflation rate. As the cost per cubic meter of the construction and operation of the supply management projects are known as shown in Table 2, the projects' costs were directly quantified per scenario to calculate the cumulative cost and the cumulative cost per capita over the whole simulation period (Appendix 4a).

Management Component - Supply management projects

Project	Description	Cost (USD/m^3)
Greater Beirut Water Supply Project Phase I[1]	It is the Beirut Water Conveyor Project (BUWC) to transfer water from the Litani Basin to Beirut comprising a 24 km tunneled aqueduct and a treatment plant to supply 60 MCM/yr to Beirut	0.76[3]
Greater Beirut Water Supply project Phase II[1]	It is an extension of Phase I comprising of the construction of the Bisri Dam and lake to supply an additional 60 MCM/yr to Beirut	1.16[3]
Wastewater reuse and Managed Artificial recharge[1]	Treatment of sludge effluent and injection into coastal aquifers (estimated at 3.5 MCM/yr[2] for study area)	1.4[3]
Desalination	City level desalination plant with capacity of 120 MCM/yr	0.8[4] (including environmental externalities)
Demand Management	A 150% tariff increase	Not quantified

[1]MOEW 2010; [2]MOEW/UNDP, 2014; [3]WB 2017; Ray 2005; Yamout & Fadel 2005; [4] Saidy 2016; Ray 2005.

- **REFERENCES**

- Alameddine, I., Tarhini, R. & El-Fadel, M. 2018. Household economic burden from seawater intrusion in coastal urban areas, Water International, 43(2), 217-236.
- Clarke, L., Edmonds, J., Jacoby, H., Pitcher, H., Reilly, J. & Richels, R. 2007. Scenarios of Greenhouse Gas Emissions and Atmospheric Concentrations. Sub-report 2.1A of Synthesis and Assessment Product 2.1 by the U.S. Climate Change Science Program and the Subcommittee on Global Change Research. Department of Energy, Office of Biological & Environmental Research, Washington, 7 DC., USA.
- Dar Al Handasah Shair and Partners 2014. Greater Beirut Water Supply Augmentation Project Environmental and Social Impact Assessment. Beirut, Lebanon.
- Dowing, T.E., Butterfield, R.E., Edmonds, B., Knox, J.W., Moss, S., Piper, B.S. &Weatherhead, E.K. 2003. Climate change and demand for water. Final Report. Stockholm Environment Institute Oxford Office, Oxford.
- El-Fadel, M., Abu Najm, M., Alameddine, I., Momjian, N. & Bahnan, A. 2015. Managed aquifer recharge in the Hazmieh area to prevent seawater intrusion in Beirut – Lebanon. Published by Deutsche Gesellschaft fur Internationale Zusammenarbeir GIZ, Germany
- El-Samra, R., Bou-Zeid, E., Banalath, H.K., stenchikov, G. & El-Fadel, M. 2016. Future intensification of hydro-meteorological extremes: downscaling using the weather research and forecasting model. Climate Dynamics 49 (11-12), pp. 3765-3785
- Goodchild, C.W. 2007. Modelling the impact of climate change on domestic water demand. Water and Environment Journal 17, pp. 8 – 12.
- Herrington, P. (1996). Climate change and the demand for water. HMSO, London
- Herrington, P., 2006. Critical Review of Relevant Research Concerning the Effects of Charging and Collection Methods on Water Demand, Different Customer Groups and Debt. Report 05/CU/02/1 (London, UK Water Industry Research

- IPCC 2013. Climate Change: The Physical Science Basis. Contribution of WGI to the Fifth Assessment report of the Intergovernmental Panel on Climate Change [Stocker, T.F. et al., (eds)]. Cambridge University Press, Cambridge, United Kingdom and New York, USA
- Jarboo, M. & Al-Najar, H. 2015. Climate change and its impact on domestic water consumption in Sub-urban regions in the Gaza Strip. International Journal of Climate Change Strategies and Management 7(1), pp. 3-16.
- MoEW 2010. National Water Sector Strategy: Supply / Demand Forecasts, draft, Beirut: Ministry of Energy and Water, Beirut, Lebanon.
- MOEW/UNDP 2014. Assessment of Groundwater Resources of Lebanon. Report by Lebanese Ministry of Energy, Lebansese Center for Water Management and Conservation, Cooperzione Italiana, United Nations Development Program, Beirut, Lebanon.
- Ray, P. 2005. Least-cost optimization for water systems planning: An exploration of the potential applications of alternative technologies for water supply in Beirut, Lebanon. MS Thesis, Tufts University, Massachusetts, US.
- Riahi, K., Grübler, A. & Nakicenovic, N. 2007. Scenarios of long-term socioeconomic and environmental development under climate stabilization. Technological Forecasting and Social Change, 74(7), pp. 887 – 935. Greenhouse Gases - Integrated Assessment.
- Safi. A., Rachid, G., El-Fadel, M., Doummar, J., Abu Najm, M., & Alameddine, I. 2018. Synergy of climate change and local pressures on saltwater intrusion in coastal urban areas: effective adaptation for policy planning. Water International, 43 (2), 145-164.
- Saidy, M. 2016. Desalination for water shortage in the greater beirut area: a cost benefit comparative assessment with economy of scale and environmental externalities. MS Thesis, Deparment of Civil and Environmental Engineering, American University of Beirut, Beirut, Lebanon.
- SNC 2011. Second National Communication Report: Lebanon. Submitted to UNFCCC. Ministry of Environment/ UNDP.
- TNC 2016. Third National Communication Report: Lebanon. Submitted to UNFCCC. Ministry of Environment/ UNDP.
- Ukayli, M. 1971. Hydrogeology of Beirut and Vicinity, Master of Science Thesis, American University of Beirut, Lebanon.
- WB 2017. Greater Beirut Water Supply Project. Implementation Status & Results Report. Washington D.C.: The World Bank.
- Whitcomb, J.B. 2005. Florida Water Rates Evaluation of Single-Family Homes. Report prepared by the Florida Water Management Districts. Available from: https://www.researchgate.net/publication/237508244_Balancing_Urban_Water_Demand_and_Supply_in_Florida_Overview_of_Tools_Available_to_Water_Managers1 [accessed Apr 26 2019].
- Yamout, D & El-Fadel, M. 2005. An Optimization Approach for Multi-Sectoral Water Supply Management in the Greater Beirut Area. Water Resources Management 19, pp. 791–812.

Appendix 4B. DBN Relationships

Node Name [a]	**Equation (**Refer to Appendix 4a)
Infiltration volume in the lateral recharge zone	Recharge Area Infiltration (MCM/yr) = (Actual Rainfall (mm/yr) 0.001 (m/mm)* (Recharge Area Infiltration Rate/100)*8E+006* (Recharge Area Pervious/100)*1E-006)
Abstraction in the lateral recharge zone	Recharge Area Abstraction (MCM/yr) = (1400 + 1400 * (Population Growth Rate/100) * Consumption Rate (l/c/d) * 365 * 0.001/1E+006
Lateral Flow into the study area	Lateral Flow (MCM/yr) = Net Freshwater recharge (MCM/yr) = Recharge Area Infiltration (MCM/yr) – Recharge Area Abstraction (MCM/yr)
Water demand	Water Demand (MCM/yr) = Actual population * Consumption rate (l/c/d)* 365 * 0.001/1E+006
Water Deficit	Water Deficit (MCM/yr) = Network Demand (MCM/yr) – Water Supply (MCM/yr)
Effective infiltration	Recharge (m^3/yr) = ((Rainfall (mm/yr) - Evapotranspiration (mm/yr) - Runoff (mm/yr)) * 0.001 (m/mm) * pervious area (m^2)) *[Eq. 1]*
Freshwater Recharge	Fresh Water Recharge (MCM/yr) = 3.5 + Effective Infiltration (MCM/yr) * (2E+006 - 2E+006 * Pervious Area Decrease) * 1E-006 + Lateral Flow (MCM/yr)
Consumption rate	Consumption Rate (l/c/d) = If T (0 – 0.0025%) then (Previous Consumption Rate + Previous Consumption Rate * (-0.2345 * Demand Management)/100) * 1.005 If T (0.0025 – 0.0208%) then (Previous Consumption Rate + Previous Consumption Rate * (-0.2345 * Demand Management)/100) * 1.046 If T (0.0208 – 0.037%) then (Previous Consumption Rate + Previous Consumption Rate * (-0.2345 * Demand Management)/100) * 1.074
GW Abstraction	GW Abstraction (MCM/yr) = GW Abstraction Reduction Rate * (Water Deficit (MCM/yr) – Water Deficit (MCM/yr) *Water Tankers (%)
Safe Yield	Safe Yield (MCM/yr) = GW Abstraction (MCM/yr) – FW Recharge (MCM/yr)
Salinity in aquifer (C)	Salinity in Aquifer (ppm) = 1000 *Previous Aquifer Salinity *1386 + 6000 * FW Recharge – Previous Aquifer Salinity * 1000 * GW Abstraction + 3.5E+007 * Safe Yield)/ 1.386E+006 *Based on mass balance equation:* $Ct = (Ci * Vi + C_R * V_R - Ci * V_A + Cs * Vs)/(Vi * 1000)$ *[Eq.2]*
RO cost (at city level)	RO Cost (M USD) = 1.6 *GW Abstraction *RO Penetration *RO Price *10^6
Installation damages (at the city level)	Installation Damages (M USD) = (23.463 * $\log_{10}$ * Salinity Aquifer – 140.44) * (Wells Penetration (%) – Wells Penetration (%) * RO Penetration Rate (%)) * (Actual Population/ 4) *Based on regression model: Damage Cost =* $(23.462*\log_{10} Salinity-140.44)$ *[Eq. 3]*
Cost of Tankers (annual cost of water delivery by tankers at the city level)	Cost of Tankers (M USD) = Tanker Price ($) * Water Deficit (MCM/yr) * Water Tankers (%) * 10^6
Socioeconomic (SES) Burden (annual at the city level) (C)	SES (M USD) = RO Cost (M USD) + Installation Damages (M USD) + Cost of Tankers (M USD)
Cumulative SES (over project life) (C)	Cumulative SES (M USD) = SES (M USD) + Previous SES (M USD)
Cumulative SES USD/capita	Cumulative SES/capita (USD/c) = Cumulative SES over project duration (M USD) / Actual Population at end year
Supply Project Cost	Supply Project Cost (M USD) = (BWC Phase I (MCM/yr) * 0.76 ($/$m^3$) + BWC Phase II (MCM/yr) * 1.16 ($/$m^3$) + Desalination (MCM/yr) *0.8 ($/$m^3$) + 3.5 (MCM/yr) * 1.4 ($/m^3)) *1E+006
Cumulative supply cost (over project life) (C)	Cumulative SES (M USD) = SES (M USD) + Previous SES (M USD)
Cumulative Supply USD/capita	Cumulative Supply Cost/capita (USD/c) = Cumulative Supply Cost over project duration (M USD) / Actual Population at end year

Appendix 4C. Full DBN network with temporal clones

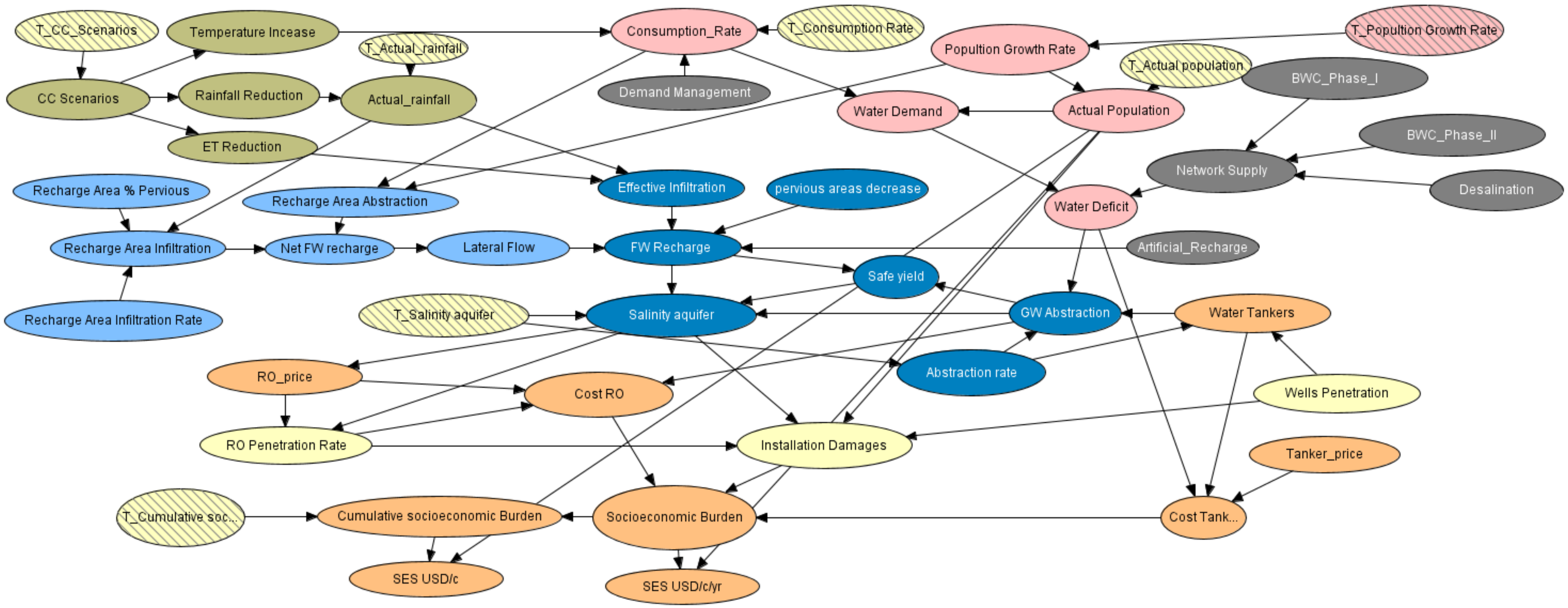

Appendix 4D. Full DBN in run mode (hugin Educational 8.6)

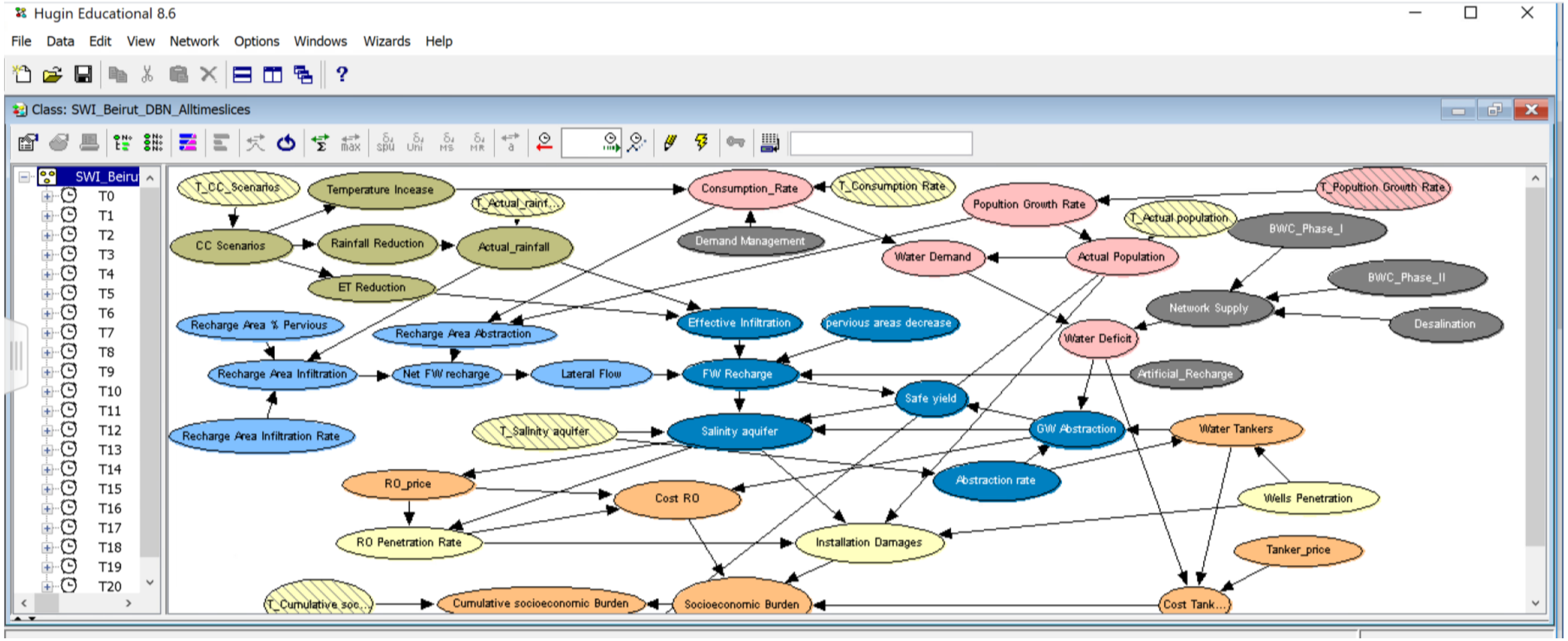

Appendix 4E. Full DBN in run mode with probability Tables

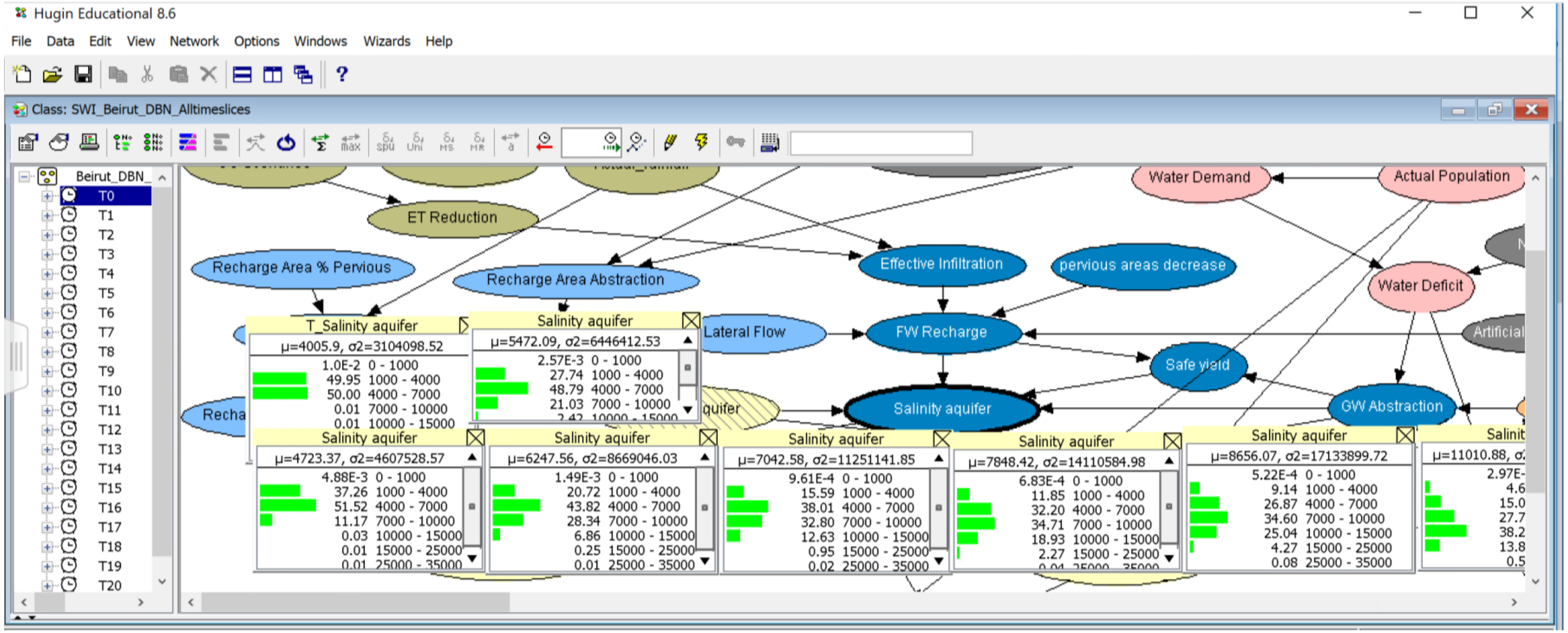

Appendix 4F. DBN conditional probability tables

Table 1 – Conditional Probability Table for Node – T CC Scenarios (clone) (T refers to clone node)

T CC Scenarios	
State	**Probability**
RCP 4.5	0.6
RCP 8.5	0.4

Table 2 – Conditional Probability Table for Node – CC Scenarios

CC Scenarios		
State	**Probability**	
T CC Scenarios	*RCP 4.5*	*RCP 8.5*
RCP 4.5	1	0
RCP 8.5	0	1

Table 3 – Conditional Probability Table for Node – ET Reduction

Evapotranspiration Reduction (%/yr)		
State	**Probability**	
CC Scenarios	*RCP 4.5*	*RCP 8.5*
0 – 0.000497	0.5	0.1
0.000497-0.000991	0.5	0.2
0.000991 – 0.003855	0	0.7

Table 4 – Conditional Probability Table for Node – Temperature Increase

Temperature Increase (˚c/yr)		
State	**Probability**	
CC Scenarios	*RCP 4.5*	*RCP 8.5*
0 – 0.0025	0.5	0
0.0025 – 0.0208	0.5	0.5
0.0208 – 0.037	0	0.5

Table 5 – Conditional Probability Table for Node – Rainfall Reduction

Rainfall Reduction (%/yr)		
State	**Probability**	
CC Scenarios	*RCP 4.5*	*RCP 8.5*
0.006 – 0.01	0.5	0
0.001 – 0.015	0.4	0.6
0.015 – 0.02	0.1	0.4

Table 6 – Conditional Probability Table for Node – T Actual Rainfall (clone) (T refers to clone node)

T Actual Rainfall (mm/yr)	
State	**Probability**
0 – 350	0.1
350 – 550	0.21
550 – 750	0.38
750 – 950	0.21
950 - 1100	0.1

Table 7 – Conditional Probability Table for Node – Actual Rainfall

Actual Rainfall (mm/yr)	
Expression	T_Actual_rainfall - T_Actual_rainfall * Rainfall_Reduction

Table 8 – Conditional Probability Table for Node – Effective Infiltration in the study area

Effective Infiltration in study area (MCM/yr)	
Expression	Actual_rainfall - (0.2 * Actual_rainfall - 0.2 * Actual_rainfall * ET_Reduction) - Actual_rainfall * 0.3) * 0.001

Table 9 – Conditional Probability Table for Node – Lateral Flow into the study area

Lateral Flow into the study area (MCM/yr)	
Expression	If (Infiltration Volume in lateral recharge zone – Abstraction in lateral recharge zone < 0, 0, Infiltration Volume in lateral recharge zone – Abstraction in lateral recharge zone)

Table 10 – Conditional Probability Table for Node – Freshwater Recharge

Freshwater Recharge (MCM/yr)		
Artificial Recharge	*Operational*	*Non- Operational*
Expression	3.5 + Effective_infiltration * (2E+006 - 2E+006 * pervious_area_decrease) * 1E-006 + Lateral_Flow	Effective_infiltration * (2E+006 - 2E+006 * pervious_area_decrease) * 1E-006 + Lateral_Flow

Table 11 - Conditional Probability Table for Node –Infiltration Rate in Lateral Recharge Zone

Infiltration Rate in Lateral Recharge Zone (%/yr)	
State	**Probability**
10-20	0.1
20 -30	0.6
30 – 60	0.3

Table 12 - Conditional Probability Table for Node – % pervious area in lateral recharge zone

% pervious area in lateral recharge zone (%/yr)	
State	**Probability**
1 - 10	0.05
10 -30	0.2
30 – 50	0.75

Table 13 - Conditional Probability Table for Node – Pervious Area Decrease

Pervious Area Decease (%/yr)	
State	**Probability**
0 – 0.2	0.99
0.2 – 0.5	0.005
0.5 - 1	0.005

Table 14 - Conditional Probability Table for Node –Abstraction in the Lateral Recharge Zone

Abstraction in the Lateral Recharge Zone (MCM/yr)	
Expression	(14000 + 14000 * (Population Growth Rate / 100)) * Consumption Rate * 365 * 0.001 / 1E+006)

Table 15 - Conditional Probability Table for Node –Infiltration volume in the lateral recharge zone

Infiltration Volume in the lateral recharge zone (MCM/yr)	
Expression	Actual Rainfall * (Infiltration Rate in lateral recharge zone / 100) * 0.001 * 8E+006 * (%Pervious in lateral recharge zone / 100) * 1E-006

Table 16 - Conditional Probability Table for Node – Population Growth Rate

Population Growth Rate (%/yr)			
State	**Probability**		
T_Population Growth Rate	*0.2 – 1.2*	*1.2 – 2.2*	*2.2 – 3.2*
0.2 – 1.2	1	0	0
1.2 – 2.2	0	1	0
2.2 – 3.2	0	0	1

Table 17 - Conditional Probability Table for Node – T Population Growth Rate (clone) (T refers to clone node)

T Population Growth Rate (%/yr)	
State	**Probability**
0.2 – 1.2	0.6
1.2 – 2.2	0.3
2.2 – 3.2	0.1

Table 18 - Conditional Probability Table for Node – T Actual Population (clone) (T refers to clone node)

T Actual Population

State	**Probability**		
T Population Growth Rate	*0.2 – 1.2*	*1.2 – 2.2*	*2.2 – 3.2*
1000000 – 1200000	0.7	0.05	0.05
1200000 – 1400000	0.2	0.7	0.05
1400000 – 1600000	0.05	0.2	0.2
1600000 - 2200000	0.05	0.05	0.7

Table 19 – Conditional Probability Table for Node – Actual Population

Actual Population

Expression	if (T_Actual_Population + T_Actual_Population * (Population_Growth_Rate / 100) > 2.2E+006, 2.2E+006, T_Actual_Population + T_Actual_Population * (Population_Growth_Rate / 100)

Table 20 – Conditional Probability Table for Node - Consumption Rate

Consumption Rate (l/capita/day)

State	**Probability**		
Temperature Increase (%)	*0 – 0.0025*	*0.0025 – 0.0208*	*0.0208 – 0.037*
Expression	If ((T_Consumption_Rate + T_Consumption_Rate * (-0.2345 * Demand_Management / 100)) * 1.005 > 300, 300, (T_Consumption + T_Consumption_Rate * (-0.2345 * Demand_Management / 100*1.005	If ((T_Consumption_Rate + T_Consumption_Rate * (-0.2345 * Demand_Management / 100)) * 1.046 > 300, 300, (T_Consumption + T_Consumption_Rate * (-0.2345 * Demand_Management / 100)) * 1.046	if ((T_Consumption_Rate + T_Consumption_Rate * (-0.2345 * Demand_Management / 100)) * 1.074 > 300, 300, (T_Consumption_Rate + T_Consumption_Rate * (-0.2345 * Demand_Management / 100)) * 1.074

Table 21 – Conditional Probability Table for Node – T Consumption Rate (clone) (T refers to clone node)

T Consumption Rate (l/capita/day)

State	**Probability**
<70	0.001
70 - 100	0.1
100 - 200	0.898
200 - 300	0.001

Table 22 – Conditional Probability Table for Node – Safe Yield

Safe Yield (MCM/yr)

Expression	if (GW_Abstraction - FW_Recharge < 0, 0, GW_Abstraction - FW_Recharge)

Table 23 - Conditional Probability Table for Node – Groundwater Abstraction

Groundwater Abstraction (MCM/yr)

Expression	Abstraction Rate * (Water Deficit – Water Deficit * Water Tankers

Table 24 – Conditional Probability Table for Node – T Aquifer Salinity (clone) (T refers to clone node)

T Salinity Aquifer (ppm)

State	**Probability**
<1000	0.0001
1000 – 4000	0.4995
4000 – 7000	0.5
7000 – 10000	0.0001
10000 – 15000	0.0001
15000 – 25000	0.0001
25000 - 35000	0.0001

Table 25 - Conditional Probability Table for Node – Salinity Aquifer

Salinity Aquifer (ppm)

Expression	If ((1000*T Salinity Aquifer *1386 + 6000*FW Recharge – T Salinity Aquifer*1000*GW Abstraction + 3.5E+007 *Safe Yield)/ 1.386E +006>= 35000, 35000, (1000 *T Salinity Aquifer *1386 + 6000*FW Recharge – T Salinity Aquifer*1000*GW Abstraction + 3.5E+007 *Safe Yield)/ 1.386E +006

Table 26 - Conditional Probability Table for Node – Groundwater Abstraction Rate

Groundwater Abstraction Rate (% of previous year)

State	**Probability**						
T_Salinity Aquifer	*<1000*	*1000-4000*	*4000-7000*	*7000-10000*	*10000-15000*	*15000-25000*	*25000-35000*
0.1 – 0.5	0.001	0.001	0.001	0.01	0.1	0.5	0.75
0.5 - 0.6	0.001	0.001	0.001	0.09	0.25	0.2	0.15
0.6 - 0.75	0.001	0.001	0.108	0.3	0.25	0.15	0.05
0.75 - 1	0.997	0.997	0.89	0.6	0.4	0.15	0.05

Table 27 - Conditional Probability Table for Node – Water Deficit

Water Deficit (MCM/yr)

Expression If (Water_Demand - Network_Supply < 0, 0, Water_Demand - Network_Supply)

Table 28 – Conditional Probability Table for Node – Water Demand

Water Demand (MCM/yr)

Expression Actual_Population * Consumption_Rate * 365 * 0.001 / 1E+006

Table 29 – Conditional Probability Table for Node – Wells Penetration

Wells Penetration Rate (%)

State	**Probability**
0.25 - 0.5	0.009
0.5 - 0.65	0.99
0.65 - 0.75	0.001

Table 30 – Conditional Probability Table for Node – Network Supply

Network Supply (MCM/yr)

Expression if (40 + Desalination + BWC_Phase_II + BWC_Phase_I > 239, 239, 40 + Desalination + BWC_Phase_II + BWC_Phase

Table 31 – Conditional Probability Table for Node – RO Price

RO Price (USD/m3)

State	**Probability**						
Salinity Aquifer	*<1000*	*1000-4000*	*4000-7000*	*7000-10000*	*10000-15000*	*15000-25000*	*25000-35000*
0 - 0.3	1	1	1	0.5	0.1	0	0
0.3 - 0.5	0	0	0	0.5	0.7	0.5	0
0.5 - 1	0	0	0	0	0.2	0.5	0
1 - 2	0	0	0	0	0	0	1

Table 32 – Conditional Probability Table for Node - RO Penetration Rate (% of buildings)

RO Penetration Rate (1)

State	**Probability**						
RO Price	0 – 0.3						
Salinity Aquifer	*<1000*	*1000-4000*	*4000-7000*	*7000-10000*	*10000-15000*	*15000-25000*	*25000-35000*
0 - 0.3	0.2	0.05	0.05	0.05	0.005	0.05	0.25
0.3 - 0.5	0.7	0.05	0.05	0.05	0.005	0.05	0.45
0.5 - 1	0.05	0.2	0.1	0.1	0.1	0.3	0.21
1 - 2	0.05	0.7	0.8	0.8	0.89	0.6	0.09

RO Penetration Rate (2)

State	**Probability**						
RO Price	0.3 - 0.5						
Salinity Aquifer	*<1000*	*1000-4000*	*4000-7000*	*7000-10000*	*10000-15000*	*15000-25000*	*25000-35000*
0 - 0.3	0.2	0.05	0.05	0.05	0.05	0.15	0.39
0.3 - 0.5	0.7	0.05	0.05	0.05	0.05	0.15	0.4
0.5 - 1	0.05	0.2	0.2	0.1	0.1	0.35	0.1
1 - 2	0.05	0.7	0.7	0.8	0.75	0.45	0.11

RO Penetration Rate (3)

State	**Probability**						
RO Price	0.5 - 1						
Salinity Aquifer	*<1000*	*1000-4000*	*4000-7000*	*7000-10000*	*10000-15000*	*15000-25000*	*25000-35000*
0 - 0.3	0.1	0.05	0.05	0.05	0.1	0.25	0.39
0.3 - 0.5	0.5	0.05	0.05	0.05	0.14	0.5	0.5
0.5 - 1	0.2	0.45	0.45	0.56	0.56	0.2	0.1
1 - 2	0.2	0.45	0.45	0.34	0.3	0.05	0.01

RO Penetration Rate (4)

State	**Probability**						
RO Price	1 - 2						
Salinity Aquifer	*<1000*	*1000-4000*	*4000-7000*	*7000-10000*	*10000-15000*	*15000-25000*	*25000-35000*
0 - 0.3	0.55	0.45	0.45	0.45	0.5	0.585	0.6
0.3 - 0.5	0.15	0.15	0.3	0.35	0.4	0.4	0.394
0.5 - 1	0.2	0.3	0.15	0.1	0.04	0.01	0.005
1 - 2	0.1	0.1	0.1	0.1	0.05	0.005	0.001

Table 33 – Conditional Probability Table for Node – Artificial Recharge

Artificial Recharge (MCM/yr)

State	**Probability**
Operational	0.0001
Non- Operational	0.9999

Table 34 - Conditional Probability Table for Node – BAWC Phase I

BAWC Phase I (MCM/yr)

State	**Probability**
0	0.9999
30	0.00005
60	0.00005

Table 35 – Conditional Probability Table for Node – BAWC Phase II

BAWC Phase II (MCM/yr)

State	**Probability**
0	0.9999
30	0.00005
60	0.00005

Table 36 – Conditional Probability Table for Node – Desalination

Desalination (MCM/yr)

State	**Probability**
0	0.9998
60	0.0001
120	0.0001

Table 37 - Conditional Probability Table for Node – Demand Management

Demand Management (% tariff increase)

State	**Probability**
0 - 1	0.95
1 - 50	0.025
50 - 150	0.02
150 – 300	0.005

Table 38 - Conditional Probability Table for Node – Socioeconomic Burden

Socioeconomic Burden (M USD/yr)

Expression	Cost RO + Installation Damages + Cost Tankers

Table 39 – Conditional Probability Table for Node - T_ Cumulative Socioeconomic Node (clone) (T refers to clone node)

T Cumulative Socioeconomic Burden (M USD)	
State	**Probability**
0 - 5000000	0.999
5000000 - 2000000000	0.0005
2000000000 - 3000000000	0.0001
3000000000 - 4800000000	0.0001
4800000000 - 7000000000	0.0001
7000000000 - 10000000000	0.0001
10000000000 - 24000000000	0.0001

Table 40 - Conditional Probability Table for Node - Cumulative Socioeconomic Node

Cumulative Socioeconomic Node (M USD)	
Expression	If (Socioeconomic Burden + T Cumulative Socioeconomic > 2.4E+010, 2.4E+010, Socioeconomic Burden + T Cumulative Socioeconomic)

Table 41 – Conditional Probability Table for Node – Socioeconomic Burden per Capita

Socioeconomic Burden per capita (USD/capita)	
Expression	Cumulative Socioeconomic Burden / Actual Population

Table 42 – Conditional Probability Table for Node – RO Cost

RO Cost (MUSD/ yr)	
Expression	1.6 * GW Abstraction * RO Penetration Rate * (RO_price * 10 ^ 6)

Table 43 - Conditional Probability Table for Node – Installation Damages

Installation Damages (MUSD/ yr)	
Expression	if (Salinity Aquifer < 1000, 0, (23.463 * log (Salinity Aquifer) - 140.44) * (Wells Penetration – Wells Penetration * RO Penetration)*Actual Population/40)

Table 44 - Conditional Probability Table for Node – Cost Tankers

Cost Tankers (MUSD/yr)	
Expression	If (10 ^ 6 * Tanker price * Water Deficit * Water Tankers > 1.9E+009, 1.9E+009, 10 ^ 6 * Tanker price * Water Deficit * Water Tankers)

Table 45 - Conditional Probability Table for Node – Water Tankers

Water Tankers (MCM/yr)	
Expression	0.8 – Abstraction Rate * Wells Penetration

Table 46 - Conditional Probability Table for Node – Tanker Price

Tanker Price (USD/m3)	
State	**Probability**
3 - 8	0.99
8 - 12	0.11

Appendix 4G. DBN Model Validation

Component	Node Name[a]	AUC
Climatic	CC scenario	0.99
	Temperature Increase	0.8
	Actual Rainfall	0.998
	Rainfall Reduction	0.8
	Evapo-transpiration Reduction	0.713
Hydrogeological Lateral Flow	% pervious area in the lateral recharge zone	0.59
	Infiltration volume in the lateral recharge zone	0.976
	Infiltration rate in the lateral recharge zone	0.58
	Abstraction in the lateral recharge zone	0.76
	Lateral flow into the study area	0.999
Demographic	Population Growth Rate	0.999
	Actual Population	0.99
	Consumption Rate	0.991
	Water demand	0.998
	Water Deficit	0.999
	Wells Penetration	0.927
Hydrogeological Salinity	Effective infiltration	0.974
	Pervious Area decrease	0.65
	Freshwater Recharge	0.87
	Network Supply	0.99
	Groundwater Abstraction	0.999
	Safe Yield	0.997
	Groundwater Abstraction rate	0.941
	Salinity in aquifer	0.7
Socioeconomic	RO penetration	0.878
	RO price	0.986
	RO cost	0.91
	Installation damages	0.95
	Water Tankers	0.76
	Tanker price	0.74
	Cost of Tankers	0.99
	Socioeconomic Burden	0.99

	Cumulative Socioeconomic burden	0.99
	SES USD/c	0.7
Management	BWC Phase I	0.99
	BWC Phase II	0.99
	Desalination	0.98
	Artificial Recharge	0.73
	Demand Management	0.64

PUBLICATIONS

Published papers

1. Rachid, G., El-Fadel, M., Abou Najm, M., Alameddine, I. 2017. Towards a framework for the assessment of saltwater intrusion in coastal aquifers. Environmental Impact Assessment Review 67, pp. 10-22
2. Safi, A., Rachid, G., El-Fadel, M., Doummar, J., Abou Najm, M., Alameddine, I. 2018. Synergy of climate change and local pressures on saltwater intrusion in coastal urban areas: effective adaptation for policy planning. Water International 43 (2), pp. 145-164.

Planned publications

1. Rachid, G., Alameddine, I., El Fadel, M. Management of saltwater intrusion in data-scarce coastal aquifers: Impacts of seasonality, water deficits, and land use. (*submitted to Water Resources Management Journal, in review)*
2. Rachid, G., Alameddine, I., El-Fadel, M. Risk of seawater intrusion and the potential for adaptation along the Eastern Mediterranean: A semi-quantitative SWOT model *(submitted to Journal of Environmental Management, in review)*
3. Rachid, G., Alameddine, I., Abu Najm, M., Qian, S., El-Fadel, M. Dynamic Bayesian Networks to assess anthropogenic and climatic drivers of saltwater intrusion: a decision support tool towards improved management *(submitted to the Integrated Environment Assessment and Management Journal, in review)*

Conference Papers

1. Rachid G., El Fadel, M., Alameddine, I. Developing a Dynamic Bayesian Network to Assess and Manage Saltwater Intrusion in a Data Sparse Urban Coastal Aquifer. In: proceedings of the 2019 European Geoscience Union (EGU), April 7 – 12, 2019, Vienna, Austria.
2. Rachid G., El Fadel, M., Alameddine, I., Abu Najm, M. and Doummar, J. Hydro-geochemical and geo-statistical analysis towards understanding the freshwater-saline water mixing dynamics. In: proceedings of the 42nd IAH Congress, September 13 – 18, 2015, Rome, Italy.
3. Rachid, G., El Fadel, M., Alameddine, I., Abu Najm, M. 2015. Vulnerability indices for SWI assessment. In Proceedings of IAIA Conference, April 26-29, 2015 Florence, Italy
4. El Fadel, M., Rachid, G., Alameddine, I., Abu Najm, M., 2014. Saltwater Intrusion in Karst Aquifers. In Proceedings of the 23rd Saltwater Intrusion Meeting, June 16 – 20, 2014, Husum, Germany

BIBLIOGRAPHY

Abarca, E., Carrera, J., Voss, C. & sanchez-Vila, X., 2002. Effect of aquifer bottom morphology on seawater intrusion. The Netherlands, SWIM.

Abarca, E., Vazquez-Sune, E., Carrera, J., Capino, B., Gamez, D., Batlle, F. 2006. Optimal design of measures to correct seawater. Water Resources Research, Vol. 42, W09415, doi:10.1029/2005WR004524.

Abdel Basit, S., 1971. Study of groundwater qualtiy in Beirut and suburbs, Beirut: American University of Beirut.

Abdel Hamid, H., 2010. A Simulation-Optimization Model to Study the Control of Seawater Intrusion in Coastal Aquifers, s.l.: University of Exter.

Abdullah, M., Praveena, S. & Aris, A., 2010. A numerical modelling of seawater intrusion into an oceanic island aquifer, Sipadan Island, Malaysia. Sains Malays, Volume 39, pp. 525-532.

Abed-ElHamid, H. & Javadi, A., 2012. A density dependent finite element model for analysis of saltwater intrusion in coastal aquifers. Journal of Hydrology, Volume 401, pp. 259-271.

Abou Zakhem, B. & Kattam, B. 2017. Overexploitation and cumulative drought trend effect on Ras El Ain karstic spring discharge (khabour Sub-basin, Syria). Journal of Earth System Sciences 126, pp.93 – 111.

Abou Zakhem, B., & Hafez, R. 2007. Environmental isotope study of seawater intrusion in the coastal aquifer (Syria). Environmental Geology 51, 1329 - 1339.

Abu-alnaeem, M., Yusoff, I., Fatt Ng, T., Alias, Y., & Raksmey, M. 2018. Assessment of groundwater slainity and quality in Gaza coastal aquifer, Gaza Strip, Palestine: An integrated statistical, geostatistical and hydrogeochemical approaches study. Science of the Total Environment 615, pp. 972-989.

Abultayef, M., Al-Najjar, H., Mogheir, Y., & Seif, A. 2016. Numerical modeling of brine disposal from Gaza central seawater desalination plant. Arab Journal of Geosciences 9, pp. 572 – 590

Acra, A., Milki, R., Karahagopian, Y. & Raffoul, Z., 1997. Supplementary water from private wells in Gretaer Beirut: a 1982 survey in retrospet. International Journal of Environmental Studies, 52(1/4), pp. 321-334.

Agoubi, B., Kharroubi, A., Abida, H., 2013. Saltwater intrusion modelling in Jorf coastal aquifer, Southeastern Tunisia: geochemical, geoelectrical and geostatistical application. Hydrological Processes 27, 1191-1199; http://dx.doi.org/10.1002/hyp.9207.

Aguilera., P., Fernandez. A., Fernandez, R. Runi, R. & Salmeron, A. 2011. Bayesian networks in environmental modelling. Environmental Modelling and Software, Volume 26, pp. 1376 - 1388.

Ahmadian S. 2013. Geostatistical based modelling of variations of groundwater quality during 2006 to 2009 (in Tehran-Karaj Plain). J. Basic Appl. Sci. Res., 3 (2s), pp. 264-272

Al Charideh, A. R. 2007. Environmental isotopic and hydrochemical study of water in the karst aquifer and submarine springs of the Syrian Coast. Hydrogeology Journal 15, pp. 351-364.

Alagha, J., Seyam, M., Said, M.A.M. & Mogheir, Y. 2017. Integrating an artificial intelligence approach with k-means clustering to model groundwater salinity: the case of Gaza coastal aquifer (Palestine). Hydrogeology Journal 25, pp. 2347 – 2361

Alameddine, I., Cha, Y. & Reckhow, K., 2011. An evaluation of automated structure learning with Bayesian networks: an application to estuarine chlorophyll dynamics. Environmental Modelling and Software, 26(2), pp. 163-172.

Alameddine, I., Tarhini, R., El-Fadel, M. 2018. Household economic burden from seawater intrusion in coastal urban areas, Water International, 43(2), 217-236.

Alcala, F. & Custodiao, E., 2008. Using the Cl/Br ratio as a tracer to identify the origin of salinity in aquifers in Spain and Portugal. Journal of Hydrology, Volume 2008, pp. 189-207.

Allen, D. M., Abbey, D.G., Mackie, D.C., Luzitano, R. D. and Cleary, M. 2002. Investigation of Potential Saltwater Intrusion Pathways in a Fractured Aquifer using an Integrated Geophysical, Geological and Geochemical Approach. Journal of Environmental Engineering and Geophysics, 7(1), 19-36.

Allow, K. A. 2012. The use of injection wells and a subsurface barrier in the prevention of seawater intrusion: a modelling approach. Arab Journal of Geosciences, 5, 1151-1161.

Alpar, B., 2009. Vulnerability of Turkish coasts to accelerated sea-level rise. Geomorphology, 107, 58 – 63.

Ames, D., 2002. Bayesian decsion networks for watershed management, Utah: Utah State Univserity.

Amin S.H., Razmi J., & Zhang, G., 2011. Supplier selection and order allocation based on fuzzy SWOT analysis and fuzzy linear programming. Expert Systems with Applications 38, pp. 334–342

Amir, N., Kafri, U., Herut, B. & Shalev, E. 2013. Numerical Simulation of submarine groundwater flow in the coastal aquifer at the Oalmahim Area, the Mediterranean Coast of Israel. Water Resources Management 27, pp. 4005 – 4020.

APHA-AWWA-WEF. 2012. Standard Methods for the Examination of Water and Wastewater, 22nd edition American Public Health Association/American Water Works Association/ Water Environment Federation, Washington, DC.

Appolo, C. & Postma, D., 2005. geochemistry, groundwater and pollution. 2nd ed. Rotterdam: Balkema.

Atlas Climatique du Liban, 1977. Atlas Climatique du Liban, Ministry of Public Works and Transport, Republic of Lebanon, Beirut.

Attwa, M., Gemail, K., & Eleraki, M. 2016. Use of salinity and resistivity measurements to study the coastal aquifer salinization in a semi-arid region: a case study in the northeast Nile Delta, Egypt. Environment Earth Sciences 75, pp. 784 - 803

Ayash, B., 2010. Assessment of the quality of private wells used as complementary domestic water sources in Beirut. MS Thesis, Department of Environmental Health, Faculty of Health Sciences, American University of Beirut, Lebanon.

Baalousha, H. 2006. Desalination status in the Gaza Strip and its environmental impact. Desalination 196, pp. 1-12.

Babiker, I. S., Mohamed, M. A. and Hiyama, T. 2007. Assessing groundwater quality using GIS. Water Resources Management, 21, 699–715.

Barton, D.N., Saloranta, T., Moe, S.J., Eggestad, H.O. & Kuikka, S. 2008. Bayesian belief networks as a meta-modelling tool in integrated river basin management — pros and cons in evaluating nutrient abatement decisions under uncertainty in a Norwegian river basin. Ecol. Econ. 66, 91–104.

Batayneh, A., Zaman, H., Zumlot, T., Ghrefat, H., Mogren, S., Nazzal, Y., Elawadi, E., Qaisy, S., Bahkaly, I., & Al-Taani, A., 2013, Hydrochemical facies and ionic ratios of the coastal groundwater aquifer of Saudi Gulf of Aqaba: implication for seawater intrusion. Journal of Coastal Research 30, pp. 75–87.

Bates, B., Kunderzewicz, Z., Wu, S. & Palutikof, J., 2008. Climate change and water., Geneva: IPCC.

Batisha, A. 2015. Implementing fuzzy decision-making technique in analyzing the Nile Delta resilience to climate change. Alexandria Engineering Journal 54, pp. 1043-1056.

Baycheva-Merger, T. and Wolfslehner, B. 2016. Evaluating the implementation of the Pan-European Criteria and indicators for sustainable forest management – A SWOT analysis. Ecological Indicators, 60, 1192 – 1199.

Bear, J. 1979. Dynamics of Fluids in Porous Media. American Elsevier Publishing Company Inc., New York

Bear, J. 1999. Seawater intrusion in cpastal aquifers-concepts, methods and practices.. s.l.:Kluwer Academic Publishers.

Becker, N. 2015. Water Pricing in Israel: Various Waters, Various Neighbors, Chapter 10, In: A. Dinar et al. (eds.), Water Pricing Experiences and Innovations, Global Issues in Water Policy 9, DOI 10.1007/978-3-319-16465-6_10

Biswas, S.K., Raj, P., R S, L., Balaganesan, B., KP, S., 2019. The Sponge Handbook: Chennai - Using the Landscape Approach to transform the South Buckingham Canal Area. GIZ

Bobba, A.G. 2002. Numerical modeling of salt-water intrusion due to human activities and sea-level change in the Godavari Delta, India. Hydrological Sciences, 47(S), S67–S80.

Boluda-Botella, N., Gomis-Yagues, V. & Ruiz-Bevia, F., 2008. Influence of transport parameter and chemical properties of the sediment in experiments to measure reactive transport in seawater intrusion. Journal of Hydrology, Volume 357, pp. 29-41

Borsuk, M., Stow, C. & Reckhow, K., 2004. A Bayesian network of eutrophication models for synthesis, prediction and uncertaiintiy analysis.. Ecological Modelling, Volume 173, pp. 219-239.

Bouchaou, L. et al., 2008. Application of multiple isotopic and geochemical tracers for investigation of recharge, salinizaiton, and residence time of water in the Souss-Massa aquifer, southwest Morocco.. Journal of Hydrology, Volume 352, pp. 267-287.

Brauch, H.G. 2013 Security and environment linkages on the Mediterranean space: Three phases of research on human and environmental security and peace. In: Brauch HG, Liotta PH, Marquina A, Rogers PF, Selim ME-S (eds) Security and environment in the Mediterranean: Conceptualising security and environmental conflicts. Hexagon series on human and environmental security and peace (1). Springer, Netherlands, pp 35–143

Breheme, M., Scheytt, T., Celik, M., & Dokuz, U. 2011. Hydrochemical characterization of groundwater and surface water at Dortyol/Hatay/Turkey. Environment Earth Sciences 63, pp. 1395 – 1408.

Bromley, J., Jackson, N.A., Clymer, O.J., Giacomello, A.M. & Jensen, F.V. 2003. The use of Hugin to develop Bayesian networks as an aid to integrated water resource planning. Environmental Modelling and Software, Volume 20, pp. 231-242.

Cain, J. 2001. Planning Improvements in Natural Resources Management Guidelines for Using Bayesian Networks to Support the Planning and Management of Development Programmes in the Water Sector and Beyond, Centre for Ecology and Hydrology, Wallingford, UK (2001)

CAMP 2004. Coastal area management programme CAMP-Lebanon. United Nations Environment Programme, MAP; Ministry of Environment, Lebanon.

Canaan, G., 1992. The hydrogeology of western slopes and coastal plain of Zahrani-Awali region. MS Thesis, Department of Geology, Faculty of Arts and Sciences, American University of Beirut, Lebanon.

Capaccioni, B., Didero, M., Paletta, C. & Didero, L. 2005. Saline Intrusion and refreshening in a Multilayer Coastal Aquifer in the Catania Plain (Sicily, Southern Italy): Dynamics of Degradation Processes According to the Hydrochemical Characteristics of Groundwaters. Journal of Hydrology 307, pp. 1-16.

Cardenas, I.C. and Halman, J.I.M. 2016. Coping with uncertainty in environmental impact assessments: open techniques. Environmental Impact Assessment Review, 60, 24 – 39

Cardona, O. 2011. Disaster and vulnerability: Concepts and measurement of human and environmental insecurity. In: Brauch HG, Oswald Spring U, Mesjasz C, Grin J, Kameri-Mbote P, Chourou B, Dunay P, Birkmann J (eds) Coping with global environmental change, disasters and security. Hexagon series on human and environmental security and peace (5). Springer, Netherlands, pp. 107–121

Carmi, I., Kronfeld, J., Yechieli, Y., Yakir, D., Boaretto, E., & Stiller, M. (2009). Carbon isoptopes in pore water of the unsaturated zone and their relevance for initial C14 activity in groundwater in the coastal aquifer of Israel. Chemical geology 268, 189-196

Carretero, S., Rapaglia, J., Bokuniewicz, H. & Kruze, E., 2013. Impact of sea level rise on saltwater intrusion length int he coastal aquifer, Partido de La Costa, Argentina. Continental Shelf Research, 61/62, 62-70.

CAS, 2008. Statistical Yearbook 2007, Beirut: Central Administration for Statistics.

Castrignanò, A. Cherubini, C. Giasi C, I. Musci, F. Pastore, N. 2007. Multivariate geostatistical and natural attenuation model approach for remediation of chlorinated compounds, World Scientific and Engineering Academy and Society (WSEAS); Transaction on Environment and Development, 3 (5), 90-98.

Catenacci, M. & Giupponi, C., 2013. Integrated assessment of sea-level rise adaptation strategies using a bayesian decision netwrok approach. Environmental Modelling and Software, 44, 87-100.

Cazenave, A. & Jaber, B., 2001. Recent sea level change in the Mediterranean Sea revealed by topex/poseidon satellite altimetry. Geophysical Research Letters, 28(8), 4.

CDR / DAR.2014. Environmental and social impact analysis of the Greater Beirut Water Supply Project. Dar El Handasah / Council of Development and Reconstruction.

Chang, H.H. & Huang, W.C., 2006. Application of a quantificiation SWOT analytical method. Mathematical and Computer Modelling 43, pp. 158 – 169.

Chang, S., Clement, T., Simpson, M. & Lee, K., 2011. Does sea-level rise have an impact on saltwater intrusion?. Advances in Water Resources, 34, 1283-1291.

Characklis, G., Griffin, R. & Bedient, P., 2005. Measuring the long term regional benefits of salinity reduction. Journal of Agricultural and Resource Economics, 30(1), pp. 69-93.

Chen, S.H. & Pollino, C.A. 2012. Good practice in Bayesian network modelling. Environonmental Modelling and Software 37, 134–145.

Cherubini, C and Pastore, 2011. Critical stress scenarios for a coastal aquifer in southeastern Italy. Natural Hazards and Earth System Sciences, 11, 1381–1393

Clemen, R. T. 1991. Making Hard Decisions: An Introduction to Decision Analysis. PWSKent Publishing Company, Boston, MA.

Cobaner, M., Cakar, A., Yurtal, R. 2011. Investigation of some parameters of groundwater in the Goksu Plain with probabilistic and geostatistical techniques. Turkish Chamber Civil Engineers, Teknik Dergi 22 (1), 5259 – 5283.

Cobaner, M., Yurtal, R., Dogan, A. & Motz, L., 2012. Three dimensional simulation of seawater intrusion in coastal aquifers: a case study in the Goksu Detaic Plain. Journal of Hydrology, 464/465, 262-280.

Comair, F., 2010. Water Resources in Lebanon, Documentation provided from MoEW to ECODIT, Beirut: ECODIT.

Connor, J., Schwabe, K. & King, D., 2012. irrigated agriculture and climate change: the influence of water supply variability and salinity on adaptation. Ecological Economics, Volume 77, pp. 149-157.

Conrad, P. & Roehl, 2010. Estimating salinity intrusion effects due to climate change along the grand strand of the south carolina coast. Las vegas, Federal Interagency.

Conrad, P., Roehl, E., Sexton, C., Tufford, D., Carbone, G., Dow, K., & Cook, J., 2010. Estimating salinity intrusion effects due to climate change along the grand strand of the south carolina coast Retrieved from http://acwi.gov/sos/pubs/2ndJFIC/Contents/7E_Conrads_12_20_09_final.pdf

Conrads, P.A. & Roehl, E.A., Jr. 2007, Analysis of salinity intrusion in the Waccamaw River and the Atlantic Intracoastal Waterway near Myrtle Beach, South Carolina, 1995-2002: U.S. Geological Survey, Scientific Investigations Report 2007-5110.

Constantine, K., Massoud, M., Alameddine, I. & El-Fadel, M. 2017. The role of the water tankers market in water stressed semi-arid urban areas: implications n water quality and economic burden. Journal of Environmental Management 188, pp. 85 – 94.

Cooper, H., 1959. A hypothesis concerning the dynamic balance of freshwater and saltwater in a coastal aquifer. Journal of Geophysical Research, Volume 64.

CSNC 2018. Seventh National Communication & Third Biennial Report under UNFCCC. Department of Environment, Ministry of Agriculture, Nicosia 2018.

Cuddy, S., Pollino, C., Tighe, M., Jakeman, T., Andrews, A., Davis, R., Whitfield, S., Raine, C., Brown, J., 2007. Implications of climate change for natural resource management in Central West catchment. Project description, ICAM Centre, The Australian National University.Custodio GE and Bruggeman GA 1987, ‘Groundwater problems in coastal areas’, Studies and Reports in Hydrology, Volume 45, UNESCO, Paris.

Custodio, E.M. 1987. Studying, monitoring and controlling saltwater intrusion in coastal aquifers. In: Guidelines for study, monitoring and control. FAO.

Dar Al Handasah Shair and Partners. 2014. Greater Beirut Water Supply Augmentation Project Environmental and Social Impact Assessment. Beirut, Lebanon.

Dausman, A. & Langevin, C., 2005. Movement of the saltwater interface in the Surficial Aquifer System in response to hydrologic stresses and water manageemnt practices, Broward, County, Florida, Florida: USGS Scientific Investigration Report.

Dawes, W. et al., 2012. Modeling the effects of climate change and land cover change on groundwater recharge in south-west Western Australia. Hydrological and Earth System Sciences, Volume 16, pp. 2709-2722.

De Filippis, G., Foglia, L., Guidici, M., Mehl, S., Margiotta, S., Luigi Negri, S. 2016. Seawater intrusion in karstic, coastal aquifers: Current challenges and future scenarios in the Taranto area (southern Italy). Science of the total Environment, 573, 1340–1351.

de Montety, V., Radakovitch, O., Vallet-Coulomb, C., Blavoux, B., Hermitte, D., & Valles, V. 2008. Origin of groundwater salinity and hydrogeochemical processes in a confined aquifer: case of the Rhone delta (Southern France). Applied Geochemistry 23, pp. 2337 - 2349.

Demirel, Z. 2004. The history and evaluation of saltwater intrusion into a coastal aquifer in Mersin, Turkey. Journal of Environmental Management 70, pp. 275- 282.

Demirel, Z. 2010. The influence of seawater on a coastal aquifer in an international protected area, Goksu Delta Turkey. Journal of Water Resource and Protection 2, pp. 651 – 659.

Dentoni, M., Deidda, R., Paniconi, C., Qahman, K., & Lecca, G. 2015. A simulation/optimization study to assess seawater intrusion management strategies for the Gaza Strip coastal aquifer (Palestine). Hydrogeol.ogy Journal 23, pp. 249–264.

Doherty, J., 2007. PEST user manual. 5th ed. Brisbane, Queensland, Australia: Watermark Numerical Computing.

Doll, P. & Florke, M., 2005. Global scale estimation of diffuse groundwater recharge: model tuning to local data for semi arid and arid regions and assessment of climate change impact. Frankfurt Hydrology Paper, August.

Dowing, T.E., Butterfield, R.E., Edmonds, B., Knox, J.W., Moss, S., Piper, B.S., Weatherhead, E.K. 2003. Climate change and demand for water. Final Report. Stockholm Environment Institute Oxford Office, Oxford.

Dubertret, L., 1961. Carte Geologique detaille, feuille de Tyre- Nabatiye et Naquora – Bennt Jbail, 1:50000. Ministere de Travauax Publics. Republique Lebanaise.

Duque, C., Calvache, M.L., Pedrera, A., martin-Rosales, W., & Lopex-Chicano, M.L. 2008. Combined time domain electromagnetic soundings and gravimetry to determine marine intrusion in a detrital coastal aquifer (Southern Spain). Journal of Hydrology 349, pp. 536-547

EC 2019. Country Report Cyprus 2019. Commission Staff Working Document. European Commission, Brussels

EC 2019a. Turkey Report. Commission Staff Working Document. European Commission, Brussels

EEA 2005. Groundwater quality and quantity in Europe. Environmental assessment report No 3. European Environment Agency. Copenhagen.

EEA 1999. Groundwater quality and quantity in Europe. Environmental assessment report No 3. European Environment Agency. Copenhagen.

Egypt 2016. National Voluntary Review on the Sustainable Development Goals. Egypt National Review Report. The Arab Republic of Egypt.

Eissa, M. 2016. Geophysical and geochemical studies to delineate seawater intrusion in Bagoush area, Northwestern Coast, Egypt. Journal of African Earth Sciences 121, pp. 365 - 381.

Eissa, M., de Dreuzy, J., & Parker, B. 2018. Integrative management of saltwater intrusion in poorly-constrained semi-arid coastal aquifer at Ras El-Hekma, Northwestern Coast, Egypt. Groundwater for Sustainable Development 6, pp. 57-70.

Eissa, M., Mahmoud, H.H., Shouakar-Stash, O., El-Shiekh, A. & Parker, B. 2016. Geophysical and geochemical studies to delineate seawater intrusion in Bagoush area, Northwestern Coast, Egypt. Journal of African Earth Sciences 121, 365 - 381.

El Chami, D., El Moujabber, M., & Scardigno, A. 2009. Regional water balance and economic assessment as tools for water management in coastal Lebanon. Water Resource Management 23, pp. 2361 – 2378

El Hassadi, A. 2008. Seawater intrusion in derna located in the Green Mountain region, Libya - a threatening recurrent phenomenon calling for desalination. Desalination, 220, 189-193.

El Shinnawy, I. & Abayazid, H., 2011. Vulnerability assessment of climate change impact on groundwater salinity in the Nile Delta coastal region, Egypt. s.l., ASCE, pp. 422-435.

El Yaouti, F.E., El Mandour, A., Khattach, D., Benavente, J., Kaufmann, O. 2009. Salinization processes in the unconfined aquifer of Bou-Areg (NE Morocco): a geostatistical, geochemical and tomographic study. Applied Geochemistry, 24, 16-31.

El-Bihery, M., 2009. Groundwater flow modeling of Quaternary aquifer Ras Sudr, Egypt. Environmental Geology, Volume 59, pp. 1095-1105.

Elewa, H., Shohaib, R., Qaddah, A. & Nousir, A. 2013. Determining groundwater protection zones for the quaternary aquifer of northeastern Nile Delta using GIS-based vulnerability mapping. Environment Earth Sciences 68, pp. 313 – 331.

El Fadel, M., Alamedine, I., Abu Najm, M., Zurayk, R., Doummar, J., Massoud, M., Chaaban, J., Jamali, D., Rachid, G., Maroun, R., Safi, A., Tomaskiewicz, M. et al., 2015. Climate change and saltwater intrusion along the Eastern Mediterranean: Socio-economic vulnerability and adaptation. Final Report. IDRC Grant No: 106706-001. American University of Beirut, Lebanon.

El Fadel, M., Deeb, T., Alameddine, I., Zurayk, R., Chaaban, J., 2017. Impact of groundwater salinity on agricultural productivity with climate change implications. Int. J. Sustain. Dev. Plann., 0, 1-11. ISSN: 1743-7601.

El-Fadel M., Alameddine I., Momjian N., Abou Najm M., Doummar J., Bahnan A., Majzoub A., Rachid G., and Maroun R. 2014. Managed Aquifer Recharge: IWRM for Preventing Seawater Intrusion. American University of Beirut, German Society for International Cooperation.

El-Fadel, M., Abu Najm, M., Alameddine, I., Momjian, N., & Bahnan, A. 2015. Managed aquifer recharge in the Hazmieh area to prevent seawater intrusion in Beirut – Lebanon. Published by Deutsche Gesellschaft fur Internationale Zusammenarbeir GIZ, Germany

El-Fadel, M., Alameddine, I., Abu Najm, M., Zurayk, R., Doumar, J., Massoud, M., Chaaban, J., Jamali, D., Maroun, R., Rachid, G., Safi, A. 2017. Climate Change and Saltwater Intrusion along the Eastern Mediterranean: Socioeconomic Vulnerability. IDRC Project ID 106706 Report.

El-Fadel, M., Massoud, M., and Kalinian, H. 2000. Screening groundwater quality in Lebanon: a preliminary assessment. USAID/AUB Report.

El-Fadel, M., Zeinati, M., & Jamali, D. 2000. Water resources in Lebanon: Characterization, water balance and constraints. International Journal of Water Resources Development, 16(4), pp. 615–638.

Elkiran, G. & Ergil, M. 2006. The assessment of a water budget of North Cyprus. Building and Environment 41, pp. 1671 – 1677.

Elkiran, G. & Turkman, A. 2008. Salinity problems in Northern Cyprus and desalination applications. Article available on Research Gate at: www.researchgate.net/publication/254882238_Salinity_Problems_in_Northern_Cyprus_and_Desalination_Applications

Elkiran, G., Aslanova, F. & Hizirogly, S. 2019. Effluent water reuse possibilities in Northern Cyprus. Water 11, pp. 191 – 214

El-Moujabber M., Darwish T., Atallah T., & Bou Samra B. 2006. Comparison of different indicators for Groundwater Contamination by Seawater Intrusion on the Lebanese Coast.Water Resources Management, 20, 1pp. 61-180.

El-Sadek, A. 2010. Water desalination: an imperative measure for water security in Egypt. Desalination 250 (3), pp. 876-884.

El-Samra, R., Bou-Zeid, E., Banalath, H.K., stenchikov, G., El-Fadel, M. 2016. Future intensification of hydro-meteorological extremes: downscaling using the weather research and forecasting model. Climate Dynamics 49 (11-12), pp. 3765-3785

El-Tahlawi, M., Farrag, A., & Ahmed, S. 2008. Groundwater of Egypt: "an environemntal overview". Environmental Geology 55, pp. 639-652.

EnviroLink 2011. New Zealand Guidelines for the Monitoring and Management of Seawater Intrusion Risks on Groundwater. Pattle Delamore Partners LTD.

Ergil, M. 2001. Estimation of saltwater intrusion through a salt balance equation and its economic impact with suggested rehabilitation scenarios: a case study. In Proceedings of: 1st International conference on Saltwater Intrusion and Coastal Aquifers Monitoring and Management, Essaouira, Morocco, April 23-25, 2001.

ESCWA, 2005. Urbanization and the changing character of the Arab city. UNESCWA Publication. GENERAL E/ESCWA/SDD/2005/1. United Nations, New York: April 2005

ETNC 2016. Egypt Third National Communication under the UNFCCC. Ministry of State for Environmental Affairs, Egyptian Environmental Affairs Agency, UNDP & GEF. Egypt 2016.

Eurie Forio, M., Landuyt, D., Bennetsen, E., Lock, K., Nguyen, T.H.T., Ambarita, M.N.D., Musinge, P.L.S., Boets, P., Everaert, G., Dominguez-Granda, L. & Goethals, P. 2015. Bayesian belief network models to analyse and predict ecological water quality in rivers. Ecological Modelling 312, pp. 222-238

Faludi, J., Hoang, T., Gorman, P., Mulvihill, M. 2016. Aiding alternatives assessment with an uncertainty-tolerant hazard scoring method. Journal of Environmental Management, 182, 111-125.

FAO, 1997. Food and Agriculture Organization of the United Nations Seawater Intrusion in Coastal Aquifers: Guidelines for Study, Monitoring and Control, pp. 119e122. Water Report 11, Rome.

Faour, G. & Mhawej, M. 2014. Mapping urban transitions in the Greater Beirut area using different space platforms. Land 3, pp. 941-956; doi:10.3390/lamd3030941

Faour, G., & Fayad, A. 2014. Water Environment in the coastal Basins of Syria - Assessing the impacts of War. Environmental Process 1, pp. 533-552.

Farmani, R., Henriksen, H.J., Savic, D. 2009. An evolutionary Bayesian belief network methodology for optimum management of groundwater contamination. Environmental Modeling and Software 24, pp. 303 – 310.

Fatoric, S. & Chelleri, L., 2012. Vulnerability to the effects of climate change and adaptation: the case of the Spanish Ebro Delta. Ocean and Coastal Management, 60, 1-10.

Fedrigoni, L., Krimissa, M., Zouari, K., Maliki, A., Zuppi, G.M. (2001). Origine de la mineralisation et comportement hydrogeochimique d'une nappe phreatique soumise a des contraintes naturelles er anthropiques severs: exemple de la nappe de Djebeniana (Tunisie). Earth and Planetart Sciences 332, 665 - 671.

Fenton, N. & Neil, M. 2012. Risk Assessment and Decision Analysis with Bayesian Networks. CRC Press, Boca Raton, FL 524 pp.

Ferguson, G. & Gleeson, T., 2012. Vulnerability of coastal aquifer to groundwater uses and climate change. Nature Climate Change, 2, pp. 342-345.

Fijani, E., Nadiri A.A., Asghari Moghaddam, A., Tsai, F.T.C, & Dixon, B. 2013. Optimization of DRASTIC method by supervised committee machine artificial intelligence to assess groundwater vulnerability for Maragheh–Bonab plain aquifer, Iran. J. Hydrol., 503 2013, pp. 89-100

Forio, M.A.E., Landuyt, D., Bennetsen, E., Lock, K., Nguyen, T.H.T., Ambarita, M.N.D., Musonge, P.L.S., Boets, P., Everaert, G., Dominguez-Granda, L., Goethals, P.L.M., 2015. Bayesian belief network models to analyse and predict ecological water quality in rivers. Ecol. Model. 312, 222e238. http://dx.doi.org/10.1016/j.ecolmodel.2015.05.025 .

Frank, K. & Boyer, T., 2014. Coastal utilities' response to saltwater intrusion. Florida, UF Water Institute.

Gad, M. & Khalaf, S. 2015. Management of groundwater resources in arid areas case study: North Sinai, Egypt. Water Resources 42(4), pp. 535 – 552.

Gao C.Y. & Peng D.H. 2011. Consolidating SWOT analysis with nonhomogenuous uncertain preference information. Knowledge-Based Systems 24, pp. 796 – 808.

Garing, C., Luquot, L., Pezard, P.A., Gouze, P. 2013. Geochemical investigations of saltwater intrusion into the coastal carbonate aquifer of Mallorca, Spain. Applied Geochemistry, 39, 1-10.

Gemici, U., Ak, M., & Turkman, A. 2006. Salinity problems and desalination applications in Turkey. Tenth International Water Technology Conference (pp. 745 - 755). Alexandria, Egypt: IWTC 10.

Georgpoulou, E. et al., 2001. A methodology to investigate brackish groundwater desalination coupled with aquifer recharge by treated wastewater as an alternative strategy for water supply in Mediterranean countries. Desalination, 136, 307-315.

Ghyben, W., 1888. Nota in verband met de voorgenomen putboring nabij Amsterdam. Tijdschrift van het Kononklijk, The Hague, The Netherlands, 9, 8-22.

Gibnsberg, A. & Levanon, A., 1976. Determination of a saltwater interface be electrical resisitivity soundings.. Hydrology Science Bulletin, 21, 561-568.

Gilmont, M. 2014. Decoupling dependence on natural water: reflexivity in regulation and allocation of water in Israel. Water Policy 16, pp. 79 – 101.

Giordana, G.A. & Montginoul, M. 2010. Policy instruments to fight against seawater intrusion in coastal aquifers: an overview. Vie et Milieu, Laboratoire Arago 56(4), pp. 287 – 294.

Giordano, R., D'Agostino, D., Apollonio, C., Lamaddalena, N., Vurro, M., 2013. Bayesian belief network to support conflict analysis for groundwater protection: the case of the Apulia region. J. Environ. Manage. 115, 136-146.

Gogu, C., Hallet, V., & Dssargues, A. 2003. Comparison of aquifer vulnerability assessment techniques. Application to the Neblon river basin (Begium). Environ. Geol., 44, pp. 881-892

Gonzalez-Redin, J., Luque, S., Poggio, L., Smith, R. & Gimona, A. 2016. Spatial Bayesian belief networks as a planning decision tool for mapping ecosystem services trade-offs on forested landscapes. Environ. Res. 144 (Part B), 15–26.

Goodchild, C.W. 2007. Modelling the impact of climate change on domestic water demand. Water and Environment Journal 17, pp. 8 – 12.

Graber, E.R., Laor, Y. & Ronen, D. 2008. Aquifer contamination by chlorinated – VOCs: the case of an urban metropolis megasite overlying the Coastal Plain in Israel. Hydrogeology Journal 16, pp. 1615 – 1623.

Guler, C., Kurt, M. A., Alpasalan, M., & Akbulut, C. 2011. Assessment of the impact of anthropogenic activities on the groundwater hyrology and chemistry in Tarsus

Coastal Plain (mersin, Turkey) using fuzzy clustering, mutivariate statistics and GIS technologies. Journal of Hydrology 414-415, pp. 435 - 451.

Guler, C., Kurt, M., Alpaslan, M. & Akbulut, C., 2012. Assessment of the impact of anthropogenic activities on the groundwater hydrology and chemistry in Tasrus coastal plain (Mersin, SE Turkey) using fuzzy clustering, multivariate statistics and GIS techniques. Journal of Hydrology, 414/415, 435-451.

Gunay G. 2003. Seawater intrusion in coastal aquifers of the Mediterranean coast of turkey.

Hall, J. & Twyman, C. K. A., 2005. Influence diagrams for representing uncertainty in climate related propositions. Climate Change, 69(2/3), 343-365.

Han, D. et al., 2011. Geochemical and isotopic evidence for palaeo-seawater intrusion into the south coast aquifer of Laizhou Bay, China. Applied geochemistry, 26, 863-883.

Harbor, J., 1994. A Practical Method for Estimating the Impact of Land-Use Change onSurface Runoff, Groundwater Recharge and Wetland Hydrology. Journal of the American Planning Association, pp. 95-108

Hdeib, R. 2012. Seawater intrusion at the Lebanese coastal aquifers Khalde – Jiyeh case study. Master’s Thesis. Lebanese University, Lebanon.

Herrington, P. 1996. Climate change and the demand for water. HMSO, London

Herrington, P., 2006. Critical Review of Relevant Research Concerning the Effects of Charging and Collection Methods on Water Demand, Different Customer Groups and Debt. Report 05/CU/02/1 (London, UK Water Industry Research

Herzberg, A., 1901. Die Wasserversorgung einiger Nordseebader.. Journal für Gasbeleuchtung und Wasserversorgung, 44, 815-819.

Hill, C. M., & Tiedeman, C. R., 2007. Effective Groundwater Model Calibration: With Analysis of Data, Sensitivities, Predictions, and Uncertainty, John Wiley and Sons, Inc., Hoboken, New Jersey. 454 pp.

Howitt, R., Kaplan, J., Larson, D., MacEwan, D., Medellin-Azuara, J., Horner, G., 2009. The Economic Impacts of Central Valley Salinity, California: University of California Davis.

Howitt, R., Medellín-Azuara, J., & MacEwan, D. 2009. Estimating the economic impacts of agricultural yield related changes for California. Sacramento, CA: California Climate Change Center

IBM, 2018. IBM SPSS Statistics for Windows, Version 25.0. Armonk, NY: IBM Corp IBM Corp.

IPCC, 2007. Fourth Assessment Report. Intergovernmental Panel on Climate Change Secretariat. Geneva, Switzerland. [online] Available at: http://www.ipcc.chwww.ipcc.ch

IPCC 2013. Climate Change: The Physical Science Basis. Contribution of WGI to the Fifth Assessment report of the Intergovernmental Panel on Climate Change [Stocker, T.F. et al., (eds)]. Cambridge University Press, Cambridge, United Kingdom and New York, USA

IPCC 2014. Climate Change: The Physical Science Basis. Contribution of WGI to the Fifth Assessment report of the Intergovernmental Panel on Climate Change [Stocker, T.F. et al., (eds)]. Cambridge University Press, Cambridge, United Kingdom and New York, USA

IPCC, 2014a. Climate Change 2014: Impacts, Adaptation, and Vulnerability. Part A: Global and Sectoral Aspects. Contribution of Working Group II to the Fifth Assessment Report of the Intergovernmental Panel on Climate Change [Field, C.B. et al. (eds.)]. Cambridge University Press, Cambridge, United Kingdom and New York, NY, USA.

ITNC 2018. Israel’s Third National Communication on Climate Change. EcoTraders Ltd on behalf of Ministry of Environmental Protection.

Ivkovic, K., Marshall, S., Carey, H., Morgan, L., Sundaram, B., Dicon-Jain, P., Caruana, L., Garlapati, N., & Werner, A.D. 2012. A national scale vulnerability assessment of seawater intusion: coastal aquifer typology. Summary report, Record 2013/04. Canberra: National Water Commission. Australian Government.

Jackson, C., Meister, R. & Prudhomme, C., 2011. Modelling the effects of climate change and its uncertainity on UK Chalk groundwater resources from an ensemble of global climate model predictions. Journal of Hydrology399, pp. 12-28

Jarboo, M. & Al-Najar, H. 2015. Climate change and its impact on domestic water consumption in Sub-urban regions in the Gaza Strip. International Journal of Climate Change Strategies and Management 7(1), pp. 3-16.

Kajanus, M., Leskinen, P., Kurttila, M., & Kangas, J. 2012. Making use of MCDS methods in SWOT analysis: Lessons learnt in strategic natural resource management. Forest Policy and Economics 20, pp. 1-9.

Kalaoun, O., Al Bitar, A., Gastellu-Etchegorry, J.P. & Jazar, M. 2016. Impact of demographics growth on seawater intrusion: case of the Tripoli aquifer, Lebanon. Water 8, pp. 104- 122.

Kalaoun, O., Jazar, M. & Al Bitar, A. 2018. Assessing the contribution of demographic growth, climate change and the refugee crisis on seawater intrusion in the Tripoli aquifer. Water 10, pp. 973 – 991.

Kaleris, V. & Ziogas, A., 2013. The effect if cutoff walls on saltwater intrusion and groundwater extraction in coastal aquifers. Journal of Hydrology, Volume 47, pp. 370-383.

Karaca, M., & Nicholls, R. (2008). Potential implications of accelerated sea level rise for Turkey. Journal of Coastal Research 24, 288-298.

Kashuba, R.O., 2010. Bayesian Methods to Characterize Uncertainty (Doctoral dissertation). Duke University

Keshtkar, A.R., Salajegheh, A., Sadoddin, A., Allan, M.G., 2013. Application of Bayesian networks for sustainability assessment in catchment modeling and management (Case study: the Hablehrood river catchment). Ecol. Modell. 268, pp. 48-54.

Khadra, W. 2003. Hydrogeology of the Damour Upper Sanine-Maameltain Aquifer. MS Thesis. Beirut, Lebanon: American University of Beirut.

Khadra, W. and Stuyfzand, P. 2014. Separating baseline conditions from anthropogenic impacts: example of the Damour coastal aquifer. Hydrological Sciences Journal, 59(10), 1872 - 1893.

Khair, K. 1992. The Effects of Overexploitation on Coastal Aquifers in Lebanon, International Association of Hydrogeologists, 3, 349 - 362.

Kilickaplan, A., Bogdanov, D., Peker, O., Caldera, U., Aghahosseine, A., & Breyer, C. 2017. An energy transition pathway for Turkey to achieve 100% renewable energy powered electricity, desalination and non-energetic industrial gas demand sectors by 2050. Solar Energy 158, pp. 218-235.

Kirkegaard, C., Sonnenborg, T., Auken, E. & Jorgensen, F., 2011. Salinity distribution in heterogeneous coastal aquifers mapped by airborne electromagnetics.. Vadoze Zone Journal, 10, 125 - 135.

Kjaerulff, U.B & Madsen, A.L. 2008. Bayesian Networks and Influence Diagrams, a guide to construction and analysis. Springer Science + business Media, LLC, New York, USA

Klassen, J. & Allen, D. 2017. Assessing the risk of saltwater intrusion in coastal aquifers. Journal of Hydrology 551, pp. 730 – 745.

Konikow, L., & Reilly, T. 1999. Seawater Intrusion in the United States Seawater Intrusion in Coastal Aquifers: Concepts, Methods and Practices, Springer (1999), pp. 463-506

Korfali, S. I. & Jurdi, M. 2007. Assessment of domestic water quality: case study, Beirut, Lebanon. Environmental Monitoring Systems 135, pp. 241-251.

Korfali, S. I. & Jurdi, M. 2010. Deterioration of Coastal Water Aquifers: Causes and Impacts. European Water 29, pp. 3-10.

Koussis, A., Mazi, K. & Destouni, G., 2012. Analytical single potential sharp interface solutions for regional saltwater intrusion in sloping unconfined coastal aquifers, with pumping and recharge. Journal of Hydrology, 416/417, pp. 1-11.

Kouzana, L., Mammou, A. & Felfoul, M., 2009. Seawater intrusion and associated processes: case of the Korba aquifer (Cap-Bon, tunisia). C.R. Geoscience, 341, 21-35.

Kragt, M.E., 2009. A Beginners Guide to Bayesian Network Modelling for Integrated Catchment Management. Landscape Logic. Landis, W.G., Durda, J.L., Brooks, M.L., Chapman, P.M., Menzie, C.A., Stahl, R.G.,

Kragt, M.E., Newham, L.T.H., Jakeman, A.J., 2009. A Bayesian network approach to integrating economic and biophysical modelling. In: 18th World IMACS/MODSIM Congress, Cairns, Australia, 13–17 July.

Kumar C. P., Chacahadi A. G., Purandara B. K., Kumar S., and Juyal R. 2007. Modelling of Seawater Intrusion in Coastal Area of North Goa. Water Digest 2(3):80-83.

Kumar, A.N., Carsten, S. and Keith, L.B. 2007. Modeling seawater intrusion in the Burdekin delta irrigation area, north Queensland, Australia. Agricultural Water Management 89, 217 - 228.

Kumar, P., Bansod, B., Debnath, S., Thukar, P. and Ghanshyam, C. 2015. Index-based groundwater vulnerability mapping models using hydrogeological settings: a critical evaluation. Environmental Impact Assessment Review, 51, 38 – 49.

Kurttila, M., Pesonen, M., Kangas, J., Kajanus, M., 2000. Utilizing the analytic hierarchy process (AHP) in SWOT analysis — a hybrid method and its application to a forest-certification case. Forest Policy and Economics 1, 41–52.

Kurunc, A., Ersahin, S., Sommez, N., Kaman, H., Uz, I., Uz, B. & Aslan, G. 2016. Seasonal changes of spatial variation of some groundwater quality variables in a large irrigated coastal Mediterranean region of Turkey. Science of the Total Environment 554-555, pp. 53 – 63.

Langevin, C. D. 2003. Simulation of Submarine Ground Water Discharge to a Marine Estuary: Biscayne Bay, Florida, Ground Water, 41, 6, 758–771, 2003.

Langevin, C. D., Thorne, D. T., Dausman, A. M., Sukop, M. C., & Guo, W., 2008. SEAWAT version 4 a computer program for simulation of multi-species solute and heat transport. Reston, Va.: U.S. Dept. of the Interior, U.S. Geological Survey.

Lee, K. & Lin, S., 2008.A fuzzy quantified SWOT procedure for environmental evaluation of an international distribution center. Information Sciences 178, pp. 531–549

Levi, E., Goldman, M., Tibor, G. & Herut, B. 2018. Delineation of subsea freshwater extension by marine geoelectromagnetic soundings (SE Mediterranean SEA). Water Resources Manageemnt 32, pp. 365 – 3779.

Li, X., Zhang, Y., Guo, F., Gao, X., & Wang, Y., 2018. Predicting the effect of land use and climate change on stream macroinvertebrates based on the linkage between structural equation modeling and Bayesian network. Ecol. Indicat. 85, pp. 820–831.

Lin, J., Snodsmith, J., Zheng, C. & Wu, J., 2009. A modeling study of seawater intrusion in Alabama Gulf coast, USA. Environmental Geology, 57, 119-130.

Loaiciga, H., Pingel, T. & Garcia, E., 2011. Seawater intrusion by sea-level rise: scenarios for the 21st century. Ground Water, 50(1), 37-47.

Lobo Ferreira, J., Chachadi, A., Diamantino, C. & Henriques, M., 2005. Assessing aquifer vulnerability to seawater intrusion using GALDIT method: Part I - Application to the Portuguese aquifer of Monte Gordo. Portugal, s.n., 1-12.

LTNC 2016. Lebanon’s Third National Communication to the UNFCCC. Ministry of Environment, UNDP & GEF, Lebanon 2016

Lucena-Moya, P.; Brawata, R.; Kath, J.; Harrison, E.; ElSawah, S.; Dyer, F. 2015. Discretization of continuous predictor variables in Bayesian networks: An ecological threshold approach. Environment Modeling and Software 66, pp. 36–45.

Luyun, R., Momii, K., & Nakagawa, K. 2009. Laboratory-scale saltwater behavior due to subsurface cutoff wall. J Hydrol 377, pp. 227–36

Mabrouk, M., Jonoski, A., Oude Essink, G. & Uhlenbrook, S. 2018. Impacts of sea level rise and groundwater extraction scenarios on fresh groundwater resources in the Nile Delta governorates, Egypt. Water 10, pp. 1690 – 1704.

MADforWATER 2018. Project on Development and application of integrated technological and management solutions for wastewater treatment and efficient reuse in agriculture tailored to the needs of Mediterranean African Countries. Deliverable 1: Review of the use of economic instruments in water management in Egypt, Morocco and Tunisia. Universidad Politecnia de Madrid. EU Contract No. 688320

Marcot, B. G. 2012. Metrics for evaluating performance and uncertainty of Bayesian network models. Ecological Modelling 230, pp. 50 – 62.

Marcot, B.G. & Penmann, T.D. 2019. Advances in Bayesian Network modeling: integration of modeling technologies. Environmental Modeling and Software 111, pp. 386-393.

Maroun R. and El Fadel M. 2002. Water Quality Monitoring Program for Jal Al-Dib/Bkennaya. Special Project for the Municipality of Jal Al-Dib, Department of Civil and Environmental Engineering, American University of Beirut.

Masciopinto, C. 2013. Management of aquifer recharge in Lebanon by removing seawater intrusion from coastal aquifers. Journal of Environmental Management, 130, pp. 306-312.

Masoud, A. 2014. Groundwater quality assessment of the shallow aquifers west of the Nile Delta (Egypt) using multivariate statistical and geostatistical techniques. Journal of African Earth Studies 95, pp. 123-137.

Mazi, K., Koussis, A.D., Destouni, G. 2014. Intensively exploited Mediterranean aquifers: resilience to seawater intrusion and proximity to critical thresholds. Hydrology and Earth System Sciences 18, pp. 1663-1677.

Melloul, A. & Collin, M., 2006. Hydrogeological changes in coastal aquifers due to seas level rise. Ocean and Coastal Management, 49, 281-297.

Melloul, A. and Goldenberg, L., 1997. Monitoring of seawater intrusion in coastal aquifers: Basics and Local Concerns. Journal of Environmental Management, 51, 73-86.

Melloul, A., & Collin, M. 2003. harmonizing water management and social needs: a necessary condition for sustainable development. The case of Israel's coastal aquifer. Journal of Environmental Management 67, pp. 385-394.

Michelsen, A., McGuckin, T., Sheng, Z., Lacewell, R., Creel, B., 2009. Rio Grande salinity management program: preliminary economic impact assessment. Rio Grande Salinity Management Coalition, El Paso, Texas.

Milnes, E. & Renard, P. 2004. The problem of salt recycling and seawater intrusion in coastal irrigated plains: an example from the Kiti aquifer (Southern Cyprus). Journal of Hydrology 288, pp. 327 – 343.

Milnes, E., Meilhac, C., Yeo, D., Renard, P., Hunkeler, D., Schnegg, P., & Bourret, F. 2006. Hydrogeochemical and hydrogeological investigation in the Akrotiri aquifer: identification of multiple salinization processes and implementation criteria for monitoring networks. European Community project SWIMED, contract ICA4-CT-2002-100004.

MIT 2015. Breakthrough Technologies 2015. MIT technological Review. March/April 2015 Issue.

MoEW, 2010. National Water Sector Strategy: Supply / Demand Forecasts, draft, Beirut: Ministry of Energy and Water, Beirut, Lebanon.

MOEW/UNDP, 2014. Assessment of the National groundwater resources of Lebanon. United Nations Development Program and Ministry of Energy and Water, Beirut, Lebanon.

MOF/UNDP 2017. Assessing labor income inequality in Lebanon’s private sector: findings, comparative analysis of determinants and recommendations. Ministry of Finance and United Nations Development Program Paper.

Mogheir, Y., De Lima, J.L.M.P., & Singh, V.P. 2005. Assessment of informativeness of groundwater monitoring in developing regions (Gaza Strip case study). Water Resour. Manag. 19, pp. 737–757.

Mogheir, Y., Foul, A., Abuhabib, A., & Mohamad, A. 2013. Assessment of large-scale brackish water desalination plants in Gaza strip. Desalination 314, pp. 96-100.

Molina, J., Pulido-Velazquez, D., Garcia-Arostegui, J. & Pulido-Velaszquez, M., 2013. Dynamic Bayesian networks as a decision support tool for assessing climate change impacts on highly stressed groundwater systems. Journal of Hydrology, 479, 113-129.

Molina, J.L., Bromley, J., Garcia-Arostegui, J.L., Sullivan, C. & Benavente, J. 2010. Integarted water resources management of overexploited hydrogeological systems using object-oriented batesian networks. Environmental Modelling and Software, 25, 383-397.

Momejian, N., Abu Najm, M., Alameddine, I., & El-Fadel, M. 2019. Can groundwater vulnerability models assess seawater intrusion? Environmental Impact Assessment Review 75, pp. 13-26.

Mondal, N.C., Singh, V.P., Singh, V.S. & Saxena, V.K. 2010. Determining the interaction between groundwater and saline water through groundwater major ions. Journal of Hydrology, 388, pp. 100 – 111

Morgan, M. G., & Henrion, M. 1990. Uncertainty: A Guide to Dealing with Uncertainty in Quantitative Risk and Policy Analysis. Cambridge, MA: Cambridge University Press

Motz, L., Hatipoglu, Z. & Yurtal, R. 2005. Seawater Intrusion in coastal aquifers at two sites in Turkey.

Mushtaha, A., Van Camp, M., & Walraevens, K. 2019. Evolution of runoff and groundwater recharge in the Gaza Strip over the last four decades. Environmental Earth Science 78, pp. 32.

Nasr, J., Jurdi, M., Chaaya, M. & El-Fadel, M., 2012. Actual and perceived water quality in one of Beirut's main settings: a comparative approach. IJWREM, 3(1), 47-54.

Negm, A. (Eds.) 2019. Groundwater in the Nile Delta. The Handbook of Environmental Chemistry 73, Springer International Publishing AG, Switzerland. ISSN 1867-979X.

Neukum, C. & Azzam, R., 2012. Impact of climate change on groundwater echarge in a small catchment in the Black Forest, Germany. Hydrogeology Journal, 20, pp. 547-560.

Newton, A.C., 2009. Bayesian Belief Networks in environmental modelling: a review of recent progress. In: Environ. Model. Res. Nov. Sci. Publ. Hauppauge, New York, USA, pp. 13-50.

Niang, I. et al., 2010. Impacts of climate change on the Senegalese coastal zones: examples of the Cap Vert peninsula and saloum estuary. Global and Planetart Change, 72, 294-301.

Nicholls, R., Wong, P., Burkett, V., Woodroffe, C., & Hay. J. 2008. Climate change and coastal vulnerability assessment: scenario for integrated assessment. Sustainable Science 3, pp. 89-102.

Nicholls, R.J., Hanson, S., Herweijer, C., Patmore, N, Hallegatte, S, Corfee-Morlot, J., Chaˆteau, J. & Muir-Wood, R . 2007. Ranking portcities with high exposure and vulnerability to climate extremes—exposure estimates. OECD environmental working paper No. 1, Organisation for Economic Co-operation and Development (OECD), Paris (PDF) Global sea-level rise and coastal vulnerability.

Nishikawa, T. et al., 2009. Stratigraphic controls on seawater intrusion and implications for groundwater management, Dominguez Gap area of Los Angeles, California, USA. Hydrogeology Journal, 17, 1699-1725.

Nofal, E., Amer, M., El-Didy, S., & Fekry, A. 2015. Delineation and modeling of seawater intrusion into the Nile Delta Aquifer: a new perspective. Water Science 29, pp. 156-166.

Nojavan, F.A., Qian, S., Paerl, H., Reckhow, K., Albright, E. 2014. A study of anthropogenic and climatic disturbance of the New River Estuary using a Bayesian Belief network. Marine Pollution Bulletin 83, pp. 107 – 115.

Nyberg, J.B.; Marcot, B.G.; Sulyma, R. 2006. Using Bayesian belief networks in adaptive management. Can. J. For. Res. 36, pp. 3104–3116

Odemis, B., Bozkurt, S., Agca, N. & Yalcin, M. (2006). Quality of shallow groundwater and drainage water in irrigated agricultural lands in a Mediterranean coastal region of Turkey. Environmental Monitoring and Assessment 115, 361 - 379.

Orphanou, K., Stassopoulou, A. & Keravnuo, E. 2014. Temporal abstraction and temporal Bayesian networks in clinical domains: a survey. Artif. Intell. Med. 60, 133–149.

Oude Essink, G., 2001. Saltwater intrusion in a three-dimensional groundwater system in The Netherlands: A numerical study.. Transport Porous Media, 43(1), 137-158.

Papadaskalopoulou, C., Katsou, E., Valta, K., Moustakas, K., Malamis, D. & Dodou, M. 2015. Review and assessment of the adaptive capacity of the water sector in Cyrpus against climate change impacts on water availability. Resources, Conservation and Recycling 105, pp. 95 – 112

Papadopoulou M. P., Karatzas, G. P., Koukadaki, M. A., and Trichakis, Y.2005. Modeling the saltwater intrusion phenomenon in coastal aquifers – A case study in the industrial zone of Herakleio in Crete Global Network of Environmental Science and Technology (NEST) Journal 7, Water Quality, 197–203

Park, H.Y., Jang, K., Ju, J.W. and Yeo, I.W. 2012. Hydrogeological characterization of seawater intrusion in tidally forced coastal fractured bedrock aquifer. Journal of Hydrology 446/447, 77-89

Paster, A., Dagan, G., Guttman, J. (2006). The salt-water body in the Northern part of Yarkon-Taninim aquifer: field data analysis, conceptual model and prediction. Journal of Hydrology 323, 154 - 167.

Payne, D., 2010. Effects of climate change on saltwater intrusion at Holton Head Island, SC USA (Conference Paper). In Proceedings of 21st Saltwater Intrusion Meeting, Azores, Portugal, 293-296.

PCBS (2017) Statistical Year book of Palestine, Palestinian Central Bureau of Statistics

Pearl, J., 1988. Probabilistic Reasoning in Intelligent Systems: Networks of Plausible Inference. Morgan Kaufmann.

Peltekian, A. 1980. Groundwater quality of Greater Beirut in relation to geologic structure and the extent of seawaterintrusion.MS thesis, American University of Beirut, Lebanon.

Phan, T.D., Smart, J.C.R., Capon, S.J., Hadwen, W.L., Sahin, O., 2016. Applications of Bayesian belief networks in water resource management: a systematic review. Environ. Model. Softw. 85, pp. 98-111.

PINC 2016. Initial National Communication Report to the United Nations Framework Convention on Climate Change. Environment Quality Authority & UNDP, State of Palestine, 2016

Piper, A., 1944. A graphic procedure in the geochemical interpretation of water analyses. Ann Trans Am Geophys Union, 25, 914-923.

Piper, A.M. 1953. A graphic procedure in geochemical interpretation of water analysis, U.S. Geology Survey. Groundwater Note, 12, 63.

Pollino, C.A., Woodberry, O., Nicholson, A., Korb, K., Hart, B.T., 2007. Parameterisation and evaluation of a Bayesian network for use in an ecological risk assessment. Environ. Model. Softw. 22, pp. 1140-1152.

Pool, M. & Carrera, J., 2010. Dynamics of negative hydraulic barriers to prevent seawater intrusion. Hydrogeology Journal, 18, 95-105.

Post VEA, 2005. Fresh and saline groundwater interaction in coastal aquifers: is our technology ready for the problems ahead. Hydrogeol Journal, 13, 120–3.

Praveena, S. & Aris, A., 2010. Groundwater resources assessment using numerical model: a case study in low-lying coastal area. International Journal of Environemntal Science and Technology, 7, 135-146.

Pulido-Lebeouf, P., 2004. Seawater intrusion and associated processes in a coastal complex aquifer (castell de Ferro, Spain). Applied Geochemistry, 19, 1517-1527.

Purandara, B., Venkatesh, B. & Choubey, V., 2010. Estimation of groundwater recharge under various land use and land covers in parts of Western ghat, Karnataka, India. RMZ-Materials and Geoenvironment, 57(2), 181-194.

Rachid G., Alameddine, I., El-Fadel, M. (n.a.). Dynamics of saltwater intrusion along the Eastern Mediterranean: Impacts of seasonality, water deficits, and a changing land cover. Submitted to the Environmental Monitoring and Assessment Journal, in review

Rachid, G., El-Fadel, M., Abou Najm, M. & Alameddine, I. 2017. Towards a framework for the assessment of saltwater intrusion in coastal aquifers. Environmental Impact Assessment Review, 67, pp. 10-22.

Rachid, G., El-Fadel, M., Alameddine, I. and Abu Najm, M. 2015.Vulnerability indices for SWI assessment. In Proceedings of: IAIA 2015: Impact Assessment in the Digital Era, 35th Annual Conference of the International Association for Impact Assessment, April 20 - 23, 2015, Florence, Italy.

Rachid. G. & El-Fadel, M. 2013. Comparative SWOT analysis of Strategic Environmental Assessment systems in the Middle East and North Africa region. Environmental Management, 125, pp. 85 – 93.

Ragan, G. E., Young, R. A., Makela, C. J., 2000. New evidence on the economic benefits of controlling salinity in domestic water supplies. Water Resour. Res., 36, 1087-1095.

Rahman, M.H., Lund, T., Bryceson, I., 2011. Salinity impacts on agro-biodiversity in three coastal, rural villages of Bangladesh. Ocean Coast. Manag., 54(6), 455-468.

Rahman, M.M., Hagare, D., Maheshwari, B., 2014. Framework to assess sources controlling soil salinity resulting from irrigation using recycled water: an application of Bayesian belief network. J. Clean. Prod. http://dx.doi.org/10.1016/j.jclepro.2014.04.068 .

Rammal H. 2005. Water in Greater Beirut, Personal Communication. In: Saadeh M. 2008. Influence of overexploitation and seawater intrusion on the quality of groundwater in Greater Beirut. Doctoral Thesis, Rheinisch-Westfalischen Technischen Hochschule Aachen.

Rangel-Medina, M., Rogelio Monreal, S., Mariano Morales, M., & Castillo Gurrola, J. 2004. Estimation of vulnerbaility to saline intrusion Geofis. Int., 43 (4), pp. 611-621

Ranjan, S., Kazama, S. & Sawamoto, M., 2006. Effects of climate and land use changes on groundwater resources in coastal aquifers. Journal of Environmental Management, 80, pp. 25-35.

Ray, P. 2005. Least-cost optimization for water systems planning: An exploration of the potential applications of alternative technologies for water supply in Beirut, Lebanon. MS Thesis, Tufts University, Massachusetts, US.

Reilly, T. & Goodman, A., 1985. Quantitative analysis of saltwater-freshwater relationships in groundwater systems- a historical perspective. Journal of Hydrology, 80, 125 - 160.

Rhoades, J.D., Kandiah, A., Mashali, A., 1992. The Use of Saline Waters for Crop Production. FAO.

Riahi, K., Grübler, A. and Nakicenovic, N. 2007. Scenarios of long-term socioeconomic and environmental development under climate stabilization. Technological Forecasting and Social Change, 74(7), pp. 887 – 935. Greenhouse Gases - Integrated Assessment.

Rosen, V., Garber, O.G., & Chen, Y. 2018. Magnesium deficiency in tap water in Israel: the desalination era. Desalination 426, pp. 88-96.

Ruiz-Padillo, A., Ruiz, D., Torija, A., Ramos-Ridao, A. 2016. Selection of suitable alternatives to reduce the environmental impact of road traffic noise using a fuzzy multi-criteria decision model. Environmental Impact Assessment Review, 61, 8 – 18.

Saadeh, M. & Wakim, E. 2017. Deterioration of groundwater in Beirut due to seawater intrusion. journal of Geoscience and Environment Protection 5, pp. 149 – 159.

Saadeh, M. 2008. Influence of overexploitation and seawater intrusion on the quality of groundwater in Greater Beirut. PhD Dissertation, RWTH Aachen, Germany.

Saadeh, M. 2009. Climate Change and environment in the Arab World. Researh and Policy Memo #4. Issam Fares Institute, American University of Beirut.

Sadoddin, A., Letcher, R.A., Jakeman, A.J., Newham, L.T.H., 2005. A Bayesian decision network approach for assessing the ecological impacts of salinity management. Math. Comput. Simul. 69 (1e2), 162e176. http://dx.doi.org/10.1016/j.matcom.2005.02.020 .

Safi. A., Rachid, G., El-Fadel, M., Doummar, J., Abu Najm, M., & Alameddine, I. 2018. Synergy of climate change and local pressures on saltwater intrusion in coastal urban areas: effective adaptation for policy planning. Water International, 43 (2), pp. 145-164.

Saidy, M. 2016. Desalination for water shortage in the greater beirut area: a cost benefit comparative assessment with economy of scale and environmental externalities.

MS Thesis, Deparment of Civil and Environmental Engineering, American University of Beirut, Beirut, Lebanon.

Salem, Z., Al Temamy, A., Salah, M & Kassab, M. 2016. Origin and characteristics of brackish groundwater in Abu Madi coastal area, Northern Nile Delta, Egypt. Estuarine, Coastal and Shelf Science 178, pp. 21 – 35.

Sales, R. J. 2009. Vulnerability and adaptation of coastal communities to climate variability and sea-level rise: their implications for integrated coastal zone management of Cavite City, Philippines. Ocean and Coastal Management, 52, 395-404.

Salim, M. 2012. Selection of groundwater sites in Egypt, using geographic information systems, for desalination by solar energy in order to reduce greenhouse gases. Journal of Advanced Research 3, pp. 11-19.

Sanford W.E. and Pope J.P. 2010. Current challenges using models to forecast seawater intrusion: lessons from the Eastern Shore of Virginia, USA. Hydrogeology Journal, 18, 73–93.

Satta, A., Puddu, M., Venturini, S. & Giupponi, C. 2017. Assessment of coastal risks to climate change related impacts at the regional scale: the case of the Mediterranean region. International Journal of Disaster Risk Reduction 24, pp. 284 – 296.

Savariya, P. & Bhatt, N., 2014. Groundwater vulnerability to seawater intrusion in Morbi-Maliya using GALDIT method. International Journal for Scientific Research & Development, 2(4), 595-600.

Scanlon, B., Reedy, R.C., Stonestrom, D.E., Prudic, D.E., Dennehy, K.F., 2005. Impact of land use and land cover change on groundwater recharge and quality in the southwestern US. Glob. Change Biol., 11, 1577-1593.

Sebben, M., Werner, A.D., Graf, T. 2015. Seawater intrusion in fractured coastal aquifers: A preliminary numerical investigation using a fractured Henry problem. Advances in Water Resources, 85, 93-108; DOI: 10.1016/j.advwatres.2015.09.013

Seckin, G., Yilmaz, T., & Ersu, C. 2010. Groundwater hydrochemistry at the Mediterranenan coastal plains - the case of Silifke, Turkey. Desalination 253, pp. 164-169.

Sefelnasr, A. & Sherif, M. (2014). Impacts of seawater rise on seawater intrusion in the Nile Delat aquifer, Egypt. Groundwater 52(2), pp. 264-276.

Selmi, A. 2013. Water management and modeling of a coastal aquifer - case study (Gaza Strip), Italy: University of Milan Bicocca.

Shaaban, A., Khawlie, M. and Abdallah, C. 2006. Use of remote sensing and GIS to determine recharge potential zones: the case of Occidental Lebanon. Hydrogeology Journal, 14, 433-443.

Shahin, M. 2009. Water scarcity in the Arab region-major problems and attempts to alleviate their impacts. Water Resources and Hydrometeorology of the Arab Region. Water Science Technology Library 59, pp. 519–547

Sherif, M., Kacimov, A., Javadi, A. & Ebraheem, A., 2012. Modeling groundwater flow and seaswater intrusion in the coastal aquifer of Wadi Ham, UAE. Water Resources Management, 26, pp. 751-774.

Simmons, C. T., T. R. Fenstemaker, and J. M. Sharp (2001), Variable-density groundwater flow and solute transport in heterogeneous porous media: approaches, resolutions and future challenges., J. Contam. Hydrol., 52(1-4), 245–75

SINC 2010. Climate Change: Initial National Communication Report. Syrian Arab Republic to UNFCCC. Ministry of State for Environmental Affairs in collaboration with UNDP and GEF. April 2010

Singh, A. 2014.Optimization modeling for seawater intrusion management. Journal of Hydrology 508, 43 – 52.

Sivan, D., Greenbaum, N., Cohenn-Seffer, R., Sisma-ventura, G., Almogi-Labin, A., Porat, N., Avnaim-Katav, S. 2016. Palaeo-environmental archive of groundwater-surface water intercation zone, the Kebara wetlands, Carmel coast, Israel. Quaternanry International, 138-149.

Sivan, O., Yechieli, Y., Herut, B. & Lazar, B., 2005. Geochemical evolution and timescale of seawater intrusion into the coastal aquifer of Israel.. Geochimestry Cosmochim Acta, 69, 579-592.

SNC 2011. Second National Communication Report: Lebanon. Submitted to UNFCCC. Ministry of Environment/ UNDP.

SOER, 2011. State of the Environment Lebanon, Beirut: Ministry of Environment andUnited Nations Development Program.

Sophiya, M. & Syed, T., 2013. Assessment of vulnerability to seawater intrusion and potenital remediation measures for coastal aquifers: a case study from eastern india. Environmental Earth Sciences, 70, pp. 1197-1209.

Speretto, A., Molina, J.L., Torresan, S., Critto, A. & Marcomini, A. 2017. Reviewing Bayesian Networks potentials for climate change impacts assessment and management: a multi-risk perspective. Journal of Environmental management 202, pp. 320-331

Spetzler, C.S. and von Holstein, C.S.S. 1975. Exceptional Paper: probability encoding in decision analysis. Management Science 22(3), pp. 340 – 358.

Stuyfzund, P., 1989. A New Hydrochemical Classification of Water Types. Baltimore, IAHS, pp. 89-98.

Stuyfzund, P., 2008. Base Exchange indices as indicators of salinization or freshening of coastal aquifers. In: Saltwater Intrusion Meeting (SWIM) 20th Proceedings, Naples, Florida, pp. 262-265.

Svekli, M., Oztekin, A., Uysal, O., Torlak, G., Turkyilmaz, A., & Delen, D., 2012. Development of a fuzzy ANP based SWOT analysis for airline industry in Turkey. Expert Systems with Applications 39, pp. 14 – 24.

Syria Report 2012. National Report of the Syrian Arab Republic on Sustainable Development Goals. Country National Report.

Tal, A., Weinstein, Y., Yechieli, Y., & Borisover, M. 2017. The influence of fish ponds and salinization on groundwater quality in the multi-layer coastal aquifer system in Israel. Journal of Hydrology 551, pp. 768-783.

Talukder, R.R., Rutherford, S., Phung, D., Islam, M.Z. & Chu, C. 2016. The effect of drinking water salinity on blood pressure in young adults of coastal Bangladesh. Environmental Pollution 214, pp. 248 – 254.

Ticehurst, J.L., Newham, L.T.H., Rissik, D., Letcher, R.A., Jakeman, A.J., 2007. A Bayesian network approach for assessing the sustainability of coastal lakes in New South Wales, Australia. Environ. Model. Softw. 22 (8), 1129e1139. http://dx.doi.org/10.1016/j.envsoft.2006.03.003 .

TNC 2016. Third National Communication Report: Lebanon. Submitted to UNFCCC. Ministry of Environment/ UNDP.

Tomaskiewicz, M., Abu Najm, M. & El Fadel, M. 2014. Development of a groundwater quality index for seawater intrusion in coastal aquifers. Environmental Modelling and Software 57, pp. 13 -26

Tribbia, J. and Moser, S. 2008. More than information: what coastal managers need to plan for climate change? Environmental Science & Policy, 11, 315-328.

Triki I., Trabelsi N., Zairi M., and Dhia H. B. 2014. Multivariate statistical and geostatistical techniques for assessing groundwater salinization in Sfax, a coastal region of eastern Tunisia. Desalination and Water Treatment, 52; 10-12

TSNC 2018. Seventh National Communication of Turkey under UNFCCC. Ministry of Environment and Urbanizaton, UNDP &GEF, Republic of Turkey 2018

tu.tiempo, 2016. World Weath. Available [online] at: https://en.tutiempo.net/

Tzoraki, O., Dokou, Z., Christodoulou, G., Gaganis, P. & Karatzas, G. 2018. Assessing the efficiency of a coastal managed aquifer recharge (MAR) system in Cyrpus. Science of the Total Environment 626, pp. 875-886.

Ukayli, M. 1971. Hydrogeology of Beirut and Vicinity, Master of Science Thesis, American University of Beirut, Lebanon.

UN DESA 2018. Revision of World Urbanization Prospects. Population Division of the UN Department of Economic and Social Affairs (UN DESA). https://population.un.org/wup/

UNDP 1970. Liban – Etude des eauxsouterraines. United Nations Development Programme, Department of Technical Cooperation for Development. New York

UNFCCC 2011. Assessing the costs and benefits of adaptation options: an overview of approaches, Germany: United Nations Framework Convention on Climate Change.

Ur Rahman, T., Rasheduzzaman, M., Habib, M.A., Ahmed, A., Tareq, S.M. & Muniruzzaman, S.M. 2017. Assessment of fresh water security in coastal Bangladesh: an insight from salinity, community perception and adaptation. Ocean and Coastal Management, 137, pp. 68-81.

USBR, 2003. Central Arizona Salinity study, Colorado: U.S. Department of the Interior.

Uusitalo, L., 2007. Advantages and challenges of Bayesian networks in environmental modelling. Ecol. Modell. 203, pp. 312-318

Uusitalo, L., Tomczak, M.T., Müller-Karulis, B., Putnis, I. & Trifonova, N. 2018. Hidden variables in a Dynamic Bayesian Network identify ecosystem level change. Ecol. Inf. 45, 9–15.

Vengosh, A., 2003. Salinization and saline environments. In: Sherwood Lollar, B. (Ed.), Environmental Geochemistry. Holland, H.D., Turekian, K.T. (Exec. Eds.), Treatise on Geochemistry, Elsevier.

Vengosh, A., Kloppmann, W., Marei, A., Livshitz, Y., Gutierrez, A., Banna, M., & Raanan, H. 2005. Sources of salinity and boron in the Gaza strip: natural contaminant flow in the southern Mediterranean coastal aquifer. Water Resoures Research 41 (1), pp.1-19.

Villegas, P., Paredes, V., Betancur, T. and Ribeirco, L. 2013. Assessing the hydrochemistry of the Uraba Aquifer, Colombia by principal component analysis. Journal of Geochemical Exploration, 134, 120 – 129.

Walley, C., 1997. The Lithostratigraphy of Lebanon. Lebanese Science Bulletin 10(1).

Wang, Y. & Jiao, J., 2012. Origin of groundwater salinity and hydrogeochemical processes in the confined Quaternary aquifer of the Pearl River Delta. Journal of Hydrology, 112-124.

Wardeh, S., Morvan, H.P., & Wright, N.G. 2005. Desalination for Syria. In Hamdy A. (ed.), Monti, R. (ed.). Food security under water scarcity in the Middle East: Problems and solutions. Bari: CIHEAM. Options Mediterraneennes: Serie A. Seminaires Mediterraneens; n. 65.

WB, 2009. Water Sector: Public Expenditure Report, Washington D.C.: The World Bank.

WB, 2010. Country Environmental Analysis. Washington D.C.: The World Bank Group.

WB, 2017. Greater Beirut Water Supply Project. Implementation Status & Results Report. Washington D.C.: The World Bank.

WB 2018. Economic Monitoring Report to the Adhoc Liason Committee. The World Bank.

Werner, A., Bakker, M., Post, V., Vandenbohede, A., Lu, C., Ataie-Ashtiani, B., Simmons, C. and Barry, D., 2013. Seawater intrusion processes, investigation and management: Recent advances. Advances in Water Resources, 51, 3-26.

Werner, A., Ward, J., Morgan, L., Simmons, C., Robinson, N., and Teubner, M. 2012. Vulnerability indicators of seawater intrusion. Groundwater, 50(1), pp. 48-58.

Whitcomb, J.B. 2005. Florida Water Rates Evaluation of Single-Family Homes. Report prepared by the Florida Water Management Districts. Available from: https://www.researchgate.net/publication/237508244_Balancing_Urban_Water_Demand_and_Supply_in_Florida_Overview_of_Tools_Available_to_Water_Managers1 [accessed Apr 26 2019].

WHO. 2011. WHO Guidelines for Drinking-water Quality third edition, Volume 1 Recommendations, World Health Organization Geneva, 2011.

Wilson, S., 2004. Dryland and urban salinity costs across the Murray-Darling basin: an overview and guidelines for identifying and valuing impacts., Canberra: Murray-Darling Basin Commission.

Winkler, R. L. 2003. An introduction to Bayesian inference and decision, Second edition. Gainesville, Fla: Probabilistic Publishing.

World Bank 2010. Water and climate change: impacts on groundwater resources and adaptation options, s.l.: Water Sector Board of the Sustainable Development Network of the World Bank.

World Bank, 2010a. Economic Evaluation of climate change adaptation projects: approaches for the agricultural sector and beyond, Washington D.C.: The International Bank for Reconstruction and Development; The World Bank.

XLSTAT 2019. Statistical Software for Excel. XLSTAT 2019.4.1. AddinSoft https://www.xlstat.com/en/

Yamout, D and El-Fadel, M. 2005. An Optimization Approach for Multi-Sectoral Water Supply Management in the Greater Beirut Area. Water Resources Management 19, pp. 791–812

Yaouti, F.E., El Mandour, A., Khattach, D., Benavente, J., Kaufmann, O., 2009. Salinization processes in the unconfined aquifer of Bou-Areg (NE Morocco): a geostatistical, geochemical and tomographic study. Appl. Geochem., 24, 16-31.

Yechieli, Y., KAfri, U. & Sivan, O. 2009. The inter-relationship between coastal sub-aquifers and the Mediterranean Sea, deduced from radioactive isotopes analysis. Hydrogeology Journal 17, pp. 265 – 274.

Yechieli, Y., Yokochi, R., Zilberland, M., Lu, Z.T., Purtschert, R., Sueltenfuss, J., Jiang, W., Zappala, J., Mueller, P., Bernier, R., Avrahamov, N., Adar, E., Talhami, F., Livshitz, Y. & Burg, A. 2019. Recent seawater intrusion into deep aquifer determined by radioactive noble-gas isotopes 81Kr and 39Ar. Earth and Planetary Science Letters 507, pp. 21-29.

Yuksel, I., Dagdeviren, M., 2007. Using the analytic network process (ANP) in a SWOT analysis – A case study for a textile firm. Information Sciences 177, 3364–3382.

Zaarour, T. 2017. Application of GALDIT index in the Mediterranean region to assess vulnerability to seawater intrusion. Lund University GEM Thesis Series No. 21. Lund, Sweden.

Zghibi, A., Merxougui, A., Zouhri, L. & Tarhouni, J. 2014. Understanding groundwater chemistry using multivariate statistics techniques to the study of contamination in the Korba unconfined aquifer system of Cap-Bon (North-east of Tunisia). Journal of African Earth Sciences, 89, pp. 1 – 15.

Zhang, E., Savenije, H., WU, H., Kong, Y. and Zhu J. 2011. Analytical solution for salt intrusion in the Yangtze Estuary, China. Estuarine, Coastal and Shelf Science, 91, 492 – 501

Zilberbrand, M., Rosenthal, E., Shachnai, E. (2001). Impact of urbanization on hydrogeochemical evolution of groundwater and on unsaturated-zone gas composition in the coastal city of Tel Aviv, Israel. J. Contam. Hydrol. 50 (3–4), 175–208.